

AD

AD 741384



AMMRC CTR 72-1

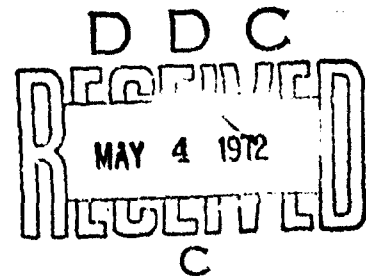
72SD2054

**ADVANCED HARDENED ANTENNA
WINDOW MATERIALS STUDY**

February 1972

edited by

James P. Brazel
General Electric Co., RESC
Philadelphia, Penna.



FINAL REPORT Contract Number: DAAG 46-71-C-0053

Reproduced by
NATIONAL TECHNICAL
INFORMATION SERVICE
Springfield, Va. 22151

Approved for public release; distribution unlimited.

Prepared for

**ARMY MATERIALS AND MECHANICS RESEARCH CENTER
Watertown, Massachusetts 02172**

177

| | |
|--------------------------------|---|
| ACCESSION NO. | |
| OPEN | WHITE SECTION <input checked="" type="checkbox"/> |
| BOC | COFF SECTION <input type="checkbox"/> |
| UNANNOUNCED | <input type="checkbox"/> |
| JUSTIFICATION | |
| BY | |
| DISPOSITION/AVAILABILITY CODES | |
| DISP. | AVAIL. AND/OR SPECIAL |
| A | |

The findings in this report are not to be construed as an official Department of the Army position, unless so designated by other authorized documents.

Mention of any trade names or manufacturers in this report shall not be construed as advertising nor as an official indorsement or approval of such products or companies by the United States Government.

DISPOSITION INSTRUCTIONS

Destroy this report when it is no longer needed.
Do not return it to the originator.

UNCLASSIFIED

Security Classification

| DOCUMENT CONTROL DATA - R&D | | |
|---|---|---|
| <i>(Security classification of title, body of abstract and indexing annotation must be entered when the overall report is classified.)</i> | | |
| 1 ORIGINATING ACTIVITY (Corporate author) General Electric Company Re-entry and Environmental Systems Division Philadelphia, Pennsylvania 19101 | | 2a REPORT SECURITY CLASSIFICATION UNCLASSIFIED |
| 3 REPORT TITLE Advanced Hardened Antenna Window Materials Study | | 2b GROUP |
| 4 DESCRIPTIVE NOTES (Type of report and inclusive dates) Final Report | | |
| 5 AUTHOR(S) (Last name, first name, initial) (edited by) James P. Brazel | | |
| 6 REPORT DATE February 1972 | 7a TOTAL NO. OF PAGES 184 | 7b NO. OF REFS 15 |
| 8a CONTRACT OR GRANT NO. XXXXX DAA G 46-71-C- 0053 | 9a ORIGINATOR'S REPORT NUMBER(S) AMMRC CTR 72-1 | |
| b. PROJECT NO. DA Project 1B062113A661 | 9b OTHER REPORT NO(S) (Any other numbers that may be assigned this report) 72SD2054 | |
| c AMCMS Code 502 N. 11. 0700 | d | |
| 10 AVAILABILITY/LIMITATION NOTICES Approved for public release; distribution unlimited | | |
| 11 SUPPLEMENTARY NOTES | | 12 SPONSORING MILITARY ACTIVITY Army Materials & Mechanics Research Center, Watertown, Mass. 02172 |
| 13 ABSTRACT A hardened composite antenna window material designated ADL-10 has been developed, based on GE-RESD's Omniweave multidirectional fiber reinforcement woven construction using pure silica fibers and GE SR-350 methyl silicone resin as the matrix. Process studies included the use of Teflon-coated silica fibers to achieve an increase in woven Omniweave density to 1.0 gm/cc as compared to earlier values ranging from 0.4 to 0.7 gm/cc. Also studied were the effects of hydrofluoric acid etching of the silica fibers, the use of a silicone coupling agent and a range of molding pressures. Used on an optimum fiber volume fraction of 68 percent, predicted minimum directional strength levels of 10,000 to 20,000 psi have been achieved with hardening capability as measured by flyer plate testing in excess of 4000 taps for nominal thickness of 1/4 to 3/8 inch. The material was verified to completely retain RF transparency up to heat flux levels of 100 Btu/ft ² sec. An inorganic silica/silica composite designated "Markite" and derived from multiple pyrolyses and reimpregnation of ADI -10 was studied for antenna window use at heat flux levels above 100 Btu/ft ² sec. Complete RF transparency was maintained up to the maximum test level of 457 Btu/ft ² sec. Only marginal improvements were achieved above earlier strength levels for Markite, to 2000-3000 psi, attributable to the improved Omniweave reinforcement fabric density. The effects of multiple reimpregnation and the fiber/matrix interaction mechanism are analyzed and recommendations made for new formulations. | | |

DD FORM 1 JAN 64 1473

UNCLASSIFIED

Security Classification

UNCLASSIFIED

Security Classification

| 14. KEY WORDS | LINK A | | LINK B | | LINK C | |
|--|--------|----|--------|----|--------|----|
| | ROLE | WT | ROLE | WT | ROLE | WT |
| Hardened Antenna Windows and Radomes Composite Fabrications Woven Fiber Composites Quartz (Fused Silica) Composite Characterization Thermal Conductivity Thermal Expansion Ablation Test Mechanical Properties Shock Resistance Ultrasonic Reaction Composite NDT | | | | | | |

INSTRUCTIONS

1. **ORIGINATING ACTIVITY:** Enter the name and address of the contractor, subcontractor, grantee, Department of Defense activity or other organization (*corporate author*) issuing the report.
- 2a. **REPORT SECURITY CLASSIFICATION:** Enter the overall security classification of the report. Indicate whether "Restricted Data" is included. Marking is to be in accordance with appropriate security regulations.
- 2b. **GROUP:** Automatic downgrading is specified in DoD Directive 5200.10 and Armed Forces Industrial Manual. Enter the group number. Also, when applicable, show that optional markings have been used for Group 3 and Group 4 as authorized.
3. **REPORT TITLE:** Enter the complete report title in all capital letters. Titles in all cases should be unclassified. If a meaningful title cannot be selected without classification, show title classification in all capitals in parentheses immediately following the title.
4. **DESCRIPTIVE NOTES:** If appropriate, enter the type of report, e.g., interim, progress, summary, annual, or final. Give the inclusive dates when a specific reporting period is covered.
5. **AUTHOR(S):** Enter the name(s) of author(s) as shown on or in the report. Enter last name, first name, middle initial. If military, show rank and branch of service. The name of the principal author is an absolute minimum requirement.
6. **REPORT DATE:** Enter the date of the report as day, month, year, or month, year. If more than one date appears on the report, use date of publication.
- 7a. **TOTAL NUMBER OF PAGES:** The total page count should follow normal pagination procedures, i.e., enter the number of pages containing information.
- 7b. **NUMBER OF REFERENCES:** Enter the total number of references cited in the report.
- 8a. **CONTRACT OR GRANT NUMBER:** If appropriate, enter the applicable number of the contract or grant under which the report was written.
- 8b, 8c, & 8d. **PROJECT NUMBER:** Enter the appropriate military department identification, such as project number, subproject number, system numbers, task number, etc.
- 9a. **ORIGINATOR'S REPORT NUMBER(S):** Enter the official report number by which the document will be identified and controlled by the originating activity. This number must be unique to this report.
- 9b. **OTHER REPORT NUMBER(S):** If the report has been assigned any other report numbers (*either by the originator or by the sponsor*), also enter this number(s).
10. **AVAILABILITY/LIMITATION NOTICES:** Enter any limitations on further dissemination of the report, other than those

imposed by security classification, using standard statements such as:

- (1) "Qualified requesters may obtain copies of this report from DDC."
- (2) "Foreign announcement and dissemination of this report by DDC is not authorized."
- (3) "U. S. Government agencies may obtain copies of this report directly from DDC. Other qualified DDC users shall request through _____."
- (4) "U. S. military agencies may obtain copies of this report directly from DDC. Other qualified users shall request through _____."
- (5) "All distribution of this report is controlled. Qualified DDC users shall request through _____."

If the report has been furnished to the Office of Technical Services, Department of Commerce, for sale to the public, indicate this fact and enter the price, if known.

11. **SUPPLEMENTARY NOTES:** Use for additional explanatory notes.
12. **SPONSORING MILITARY ACTIVITY:** Enter the name of the departmental project office or laboratory sponsoring (*paying for*) the research and development. Include address.
13. **ABSTRACT:** Enter an abstract giving a brief and factual summary of the document indicative of the report, even though it may also appear elsewhere in the body of the technical report. If additional space is required, a continuation sheet shall be attached.

It is highly desirable that the abstract of classified reports be unclassified. Each paragraph of the abstract shall end with an indication of the military security classification of the information in the paragraph, represented as (TS), (S), (C), or (U).

There is no limitation on the length of the abstract. However, the suggested length is from 150 to 225 words.
14. **KEY WORDS:** Key words are technically meaningful terms or short phrases that characterize a report and may be used as index entries for cataloging the report. Key words must be selected so that no security classification is required. Identifiers, such as equipment model designation, trade name, military project code name, geographic location, may be used as key words but will be followed by an indication of technical context. The assignment of links, rules, and weights is optional.

UNCLASSIFIED
Security Classification

AMMRC CTR 72-1 72SD2054

ADVANCED HARDENED ANTENNA WINDOW MATERIALS STUDY

edited by

James P. Brazel
General Electric Co., R2SD
Philadelphia, Penna.

February 1972

Final Report Contract Number DAAG 46-71-C-CJ53
D/A Project 1B062113A661
AMCMS Code 502N.11.0700
Title of Project: Reduction of Vulnerability, ABM Systems

This document has been approved for public release; its distribution is unlimited.

Prepared for

ARMY MATERIALS AND MECHANICS RESEARCH CENTER
Watertown, Massachusetts 02172

TABLE OF CONTENTS

| <u>Section</u> | | <u>Page</u> |
|----------------|---|-------------|
| FOREWORD | | xi |
| ABSTRACT | | xii |
| 1.0 | INTRODUCTION AND SUMMARY | 1-1 |
| 2.0 | COMPOSITE DESIGN AND FABRICATION | 2-1 |
| 2.1 | General Considerations | 2-1 |
| 2.2 | Materials Selection | 2-2 |
| 2.3 | Processing Considerations (Phase 1) | 2-5 |
| 2.4 | Processing of Test Specimens (Phase 1) | 2-8 |
| 2.5 | Processing of Test Specimens (Phase 2) | 2-28 |
| 2.6 | Preliminary Study of Silica Chemical Vapor Deposition for Densifying Markite | 2-42 |
| 3.0 | CHARACTERIZATION | 3-1 |
| 3.1 | The Sampling and Characterization Plan | 3-1 |
| 3.2 | Mechanical Characterization | 3-31 |
| 3.3 | Ultrasonic Measurements | 3-58 |
| 3.4 | Shock Testing | 3-65 |
| 3.5 | Electromagnetic Characterization | 3-71 |
| 3.6 | Thermal Characterization | 3-83 |
| 4.0 | CAPABILITY ANALYSIS OF ADL-10 AND MARKITE | 4-1 |
| 4.1 | Introduction | 4-1 |
| 4.2 | Material Geometry | 4-2 |
| 4.3 | Methods of Analysis | 4-10 |
| 4.4 | Test Specimen Geometry | 4-11 |
| 4.5 | Numerical Calculations | 4-14 |
| 4.6 | Parametric Material Studies | 4-15 |
| 4.7 | Analysis of "Markite" | 4-22 |
| 4.8 | Modes of Failure | 4-25 |
| 4.9 | Concluding Remarks | 4-26 |
| 5.0 | CONCLUSIONS AND RECOMMENDATIONS | 5-1 |
| 5.1 | Conclusions | 5-1 |
| 5.2 | Recommendations | 5-2 |
| 6.0 | REFERENCES | 6-1 |
| | APPENDIX: Index of Characterization Data | A-1 |
| | DISTRIBUTION LIST | DL-1 |
| | FD FORMS | DD-1 |

LIST OF ILLUSTRATIONS

| <u>Figure</u> | | <u>Page</u> |
|---------------|---|-------------|
| 1 | Multidimensional Reinforcement in Which the Fibers Follow Paths Parallel to the Diagonals of Intersecting Planes | 2-3 |
| 2 | Thermogravimetric Analysis of SR-350 Resin | 2-4 |
| 3 | Segmented Omniweave Scarf 290-Q3BA | 2-9 |
| 4 | Woven Omniweave Segment | 2-11 |
| 5 | Woven Omniweave Segment (4.5X) | 2-11 |
| 6 | Omniweave Strip Mold | 2-15 |
| 7 | Tensile Specimen | 2-17 |
| 8 | Scanning Electron Microscope Views of Astroquartz Fibers with A-1100 Scotchcast Coating | 2-19 |
| 9 | SEM Views of Astroquartz Fibers after Pyrolysis at 800° F | 2-21 |
| 10 | SEM Views of Etched, One and Ten Percent Silane - Treated Astroquartz Fibers | 2-23 |
| 11 | Schematic of Apparatus Used for Chemical Vapor Deposition Studies | 2-43 |
| 12 | Phase 1 Processing and Sampling Plan | 3-2 |
| 13 | Phase 2 Processing and Sampling Plan | 3-4 |
| 14 | Radiograph of Series 1 ADL-10 "Finger" (Specimens Molded at 300 PSI) | 3-6 |
| 15 | Radiograph of Series 1 ADL-10 "Finger" (Specimens Molded at 125 PSI) | 3-7 |
| 16 | Radiograph of Series 1 ADL-10 "Finger" (Specimens Molded at 1000 PSI) | 3-8 |
| 17 | Radiograph of Series 1 ADL-10 "Long Finger" (Flexure Specimens Molded at 1000 PSI) | 3-9 |
| 18 | Radiograph of Series 2 ADL-10 "Finger" Specimens, 125 PSI Molding Pressure, 10% HF Etch and High Silane Coupler Concentration | 3-10 |
| 19 | Radiograph of Series 2 ADL-10 "Finger" Specimens, 125 PSI Molding Pressure, 10% HF Etch and Low Silane Coupler Concentration | 3-11 |
| 20 | Radiograph of Series 2 ADL-10 "Finger" Specimens, 125 PSI Molding Pressure, 10% HF Etch; S1, S2, T1, T2 Containing "Cab-O-Sil" Colloidal Silica; U1, U2, V1, V2 with Low Silane Concentration | 3-12 |
| 21 | Radiograph of Filament-Wound Unidirectional ADL-10 Composites, Etched and Silane-Coupled | 3-13 |
| 22 | Sample Layout: ADL-10 Plate 331-1 | 3-15 |
| 23 | Radiograph of ADL-10 Plate 331-1 | 3-16 |

LIST OF ILLUSTRATIONS (Continued)

| <u>Figure</u> | | <u>Page</u> |
|---------------|--|-------------|
| 24 | Sample Layout: ADL-10 Plate 331-2 | 3-17 |
| 25 | Radiograph of ADL-10 Plate 331-2 | 3-18 |
| 26 | Radiograph of ADL-10 Plate 331-3 | 3-19 |
| 27 | Radiograph of Markite Plate 318-1 (Cast) | 3-21 |
| 28 | Sample Layout: Markite Plate 318-2 (Cast) | 3-22 |
| 29 | Radiograph of Markite Plate 318-2 (Cast) | 3-23 |
| 30 | Sample Layout: Markite Plate 318-3 (15PSI Molding Pressure)..... | 3-24 |
| 31 | Radiograph of Markite Plate 318-3 (Molded at 15 PSI)..... | 3-25 |
| 32 | Sample Layout: Markite Plate 318-4 (1000 PSI Molding Pressure).... | 3-26 |
| 33 | Radiograph of Markite Plate 318-4 (Molded at 1000 PSI) | 3-27 |
| 34 | Sample Layout: Markite Plate 319-1 | 3-28 |
| 35 | Sample Layout: Markite Plate 319-2 | 3-29 |
| 36 | Sample Layout: Markite Plate 209-3 | 3-30 |
| 37 | Series 1 Tensile Tests: Ultimate Tensile Strength vs. Surface Reinforcement Angle | 3-34 |
| 38 | Ultimate Tensile Strength vs. Surface Reinforcement Angle Series 2 Specimens | 3-37 |
| 39 | SEM's of Fracture Surface of Tensile Specimen A2 | 3-40 |
| 40 | Stereo SEM's of Fracture Surface of S1 (Cab-O-Sil Filled) Tensile Specimen | 3-41 |
| 41 | SEM's of Fracture Surface of Cab-O-Sil Loaded Tensile Specimen S1 | 3-42 |
| 42 | Thermal Expansion, Plates 331-1 and 331-2 | 3-45 |
| 43 | Thermal Expansion of Markite Silica/Pyrolyzed Silicone | 3-54 |
| 44 | Silica/Silicone Transformation, Short Peam Flexure; Tensile Stress at Failure as a Function of Processing Operations, Latest Values Superimposed on Data from Reference 1 | 3-55 |
| 45 | Top: Scanning Electron Micrographs of Fracture Surface from Markite Plate 209-3; Left: Electron Micrograph on Sample from Same Plate Taken at GE Space Sciences Laboratory | 3-57 |
| 46 | Effect of Process Parameters on Ultrasonic Velocity: Series 1 ADL-10 Specimens | 3-60 |
| 47 | Variation of Ultrasonic Wave Propagation Velocity with Density | 3-62 |
| 48 | Permittivity Measurement System Schematic | 3-72 |
| 49 | Block Diagram of Microwave Ablation Test Facility | 3-74 |
| 50 | Specimen 331-1 ADL-10 | 3-77 |
| 51 | Specimen 318-2 (Cast Markite) | 3-78 |
| 52 | Specimen 319-1 (Markite) | 3-79 |
| 53 | Specimen 319-2 (Markite) | 3-80 |

LIST OF ILLUSTRATIONS (Continued)

| <u>Figure</u> | | <u>Page</u> |
|---------------|--|-------------|
| 54 | Thermal Conductivity of Markite, C-Direction | 3-84 |
| 55 | Molded SR-350 Resin, Infrared Absorption | 3-85 |
| 56 | Model of Omniweave Showing Relative Orientation of Fiber Axes | 4-3 |
| 57 | Model of Rigid "Fibers" in Omniweave Pattern Showing High Volume Fraction for Straight Fibers | 4-3 |
| 58 | Omniweave Cross Section Showing Solid Circular Fibers in Maximum Packing Array | 4-4 |
| 59 | Omniweave Cross Section Showing Solid Hexagonal Fibers or Roving in Maximum Packing Array | 4-6 |
| 60 | Hexagonal Rod Packing Models | 4-7 |
| 61 | Deformed Shape of Individual Rovings Due to Molding Pressures | 4-8 |
| 62 | Typical Sections Through Model of Fig. 59 Showing Shape of Matrix Region Between Hexagonal Rovings | 4-9 |
| 63 | Variation of Through-the-Thickness Projected Angle with Axial Projected Angle for Series 1 Specimens | 4-12 |
| 64 | Variations of Through-the-Thickness Projected Angle with Axial Projected Angle for Series 2 Specimens | 4-13 |
| 65 | Variation of Estimated Fiber Volume Fraction with Axial Projected Angle | 4-14 |
| 66 | Computed and Experimental Extensional Moduli of ADL-10 Composites | 4-16 |
| 67 | Theoretical and Experimental Strength Values for ADL-10 Series 1 Specimens | 4-17 |
| 68 | Theoretical and Experimental Strength Values of ADL-10 Series 2 Specimens | 4-18 |
| 69 | Extensional Modulus as a Function of Angle Between Fibers and Load for Symmetric 4-D Configurations | 4-20 |
| 70 | Axial Strength as a Function of Angle Between Fibers and Load for Symmetric 4-D Configurations | 4-21 |
| 71 | Photomicrograph of Markite Fracture Surface Structure Showing Characteristic Fiber Spacing (Plate 209-3, 21X) | 4-23 |
| 72 | Frame Model | 4-24 |

LIST OF TABLES

| <u>Table</u> | | <u>Page</u> |
|--------------|--|-------------|
| 1 | Characteristics of Segmented Omniweave Scarf 290-Q3BA (Phase 1, Series 1 and 2) | 2-10 |
| 2 | Characteristics of Quartz Filaments and Roving | 2-10 |
| 3 | Characteristics of Series No. 1 Test Specimens | 2-12 |
| 4 | Measurements of Fiber Angle (Series 1 Test Specimens) | 2-20 |
| 5 | Characteristics of Series No. 2 Test Specimens (All Molded at 125 psi) | 2-22 |
| 6 | Processing Variables (Series 2 Test Specimens) | 2-25 |
| 7 | Measurement of Fiber Angle (Series 2 Test Specimens) | 2-26 |
| 8 | Characteristics of Omniweave Constructions, Phase 2 | 2-29 |
| 9 | Characteristics of ADL-10 Composite Panels 331' | 2-30 |
| 10 | Characteristics of Markite Silica/Silica 318 Composite Panels . . | 2-33 |
| 11 | Characteristics of 319 Pyrolyzed Composite Panels (Woven with Teflon Coated Fibers) | 2-37 |
| 12 | Characteristics of Markite Silica/Silica 320 Composite Panels. . . | 2-39 |
| 13 | Characteristics of Unidirectional Composite | 2-41 |
| 14 | Deposition Conditions | 2-44 |
| 15 | Results of Flexural Tests (Series 1 Test Specimens) | 3-32 |
| 16 | Results of Tensile Tests (Series 1 Test Specimens) | 3-33 |
| 17 | Results of Tensile Tests (Series 2 Test Specimens) | 3-36 |
| 18 | Tensile Test Data - Plates 331-1 and 331-2 (Improved Processing) | 3-43 |
| 19 | Flexure Test Data-Plates 331-1 and 331-2 (Improved Processing) | 3-43 |
| 20 | Flexure Data on Silicone Resin (Four Point) | 3-45 |
| 21 | Torsional Shear Data for Cured and Molded SR-350 Silicone Resin | 3-46 |
| 22 | Unidirectional Quartz - Silicone Tensile Test Data | 3-47 |
| 23 | Tensile Test Data on Markite Panels | 3-50 |
| 24 | Short Beam Flexure Tests, Markite Pyrolysis and Reimpreg- nation Study (Three Point Loading, 1" Span) | 3-51 |
| 25 | Short Beam Flexure Tests, Chemical Vapor Deposition Studies on Plate 209-3 Markite Molded at 1000 psi | 3-53 |
| 26 | Ultrasonic Velocity and Attenuation Data - Woven ADL-10 Strips | 3-59 |
| 27 | Ultrasonic Velocity and Attenuation Data-Specimens from Plates | 3-63 |
| 28 | Definition of Degree of Damage | 3-66 |
| 29 | Magnetic Flyer Plate Test Results | 3-68 |

LIST OF TABLES (Continued)

| <u>Table</u> | | <u>Page</u> |
|--------------|---|-------------|
| 30 | Pre Arc Test Dielectric Property Data (C-Band- 5470 MHz) | 3-76 |
| 31 | Change in Transmitted Signal in Tandem Gerdien Arc Test, Heat Flux = 460 Btu/(ft ² sec) (Cold Wall) | 3-81 |
| 32 | A Comparison of Sample Properties Before and After Ablation Tests, Heat Flux = 460 Btu/(ft ² sec) | 3-82 |
| 33 | Comparison of Predicted Strength of Low-Density Markite without and with the Addition of Horizontal Fibers | 4-25 |

FOREWORD

The work described in this report was carried out at General Electric Re-Entry and Environmental Systems Division (GE-RESD) Materials Laboratories, Valley Forge Space Technology Center, King of Prussia, Pennsylvania. Technical supervision was provided for the U. S. Army Materials and Mechanics Research Center by Dr. Nathaniel S. Schneider. The principal technical investigator for the General Electric Company was Mr. James P. Brazel. Consultation on the program goals was provided by Messrs. John Dignam and Lewis Aronson of AMMRC and Mr. Kenneth Hall of GE-RESD. A study of the potential capability of the omniweave composites was provided by Dr. B. Walter Rosen of Materials Sciences, Incorporated under a consulting subcontract.

The principal contributors to the technical effort and preparation of the report are listed below :

| | |
|--|----------------------------------|
| Omniweave Composite Design and Fabrication | Leonard Markowitz, Melvin Wexler |
| Silica Chemical Vapor Deposition Studies | Dr. Joseph Gebhardt |
| Characterization Plan, Thermal Characterization, Program Management and Final Report | James Brazel |
| Mechanical Testing | Wilfred Connell |
| Ultrasonic Characterization | John Roetling |
| Flyer Plate Testing | John Roetling, G. Sullivan |
| Electromagnetic/Ablation Testing | Jack Hanson, Charles Fehl |
| Omniweave Composite Capability Analysis | Dr. B. W. Rosen |

The authors also wish to acknowledge in particular the laboratory and experimental contributions of the following personnel: Vincent Archidiacono for impregnation, molding and heat treatments of the composites; Jordan Konell for mechanical testing; Arthur Oaks and Louis Sponar for radiography and Bryce S. Kennedy and Kenneth Bleiler for thermal measurements.

This project has been accomplished as part of the U.S. Army Manufacturing Methods and Technology Program, which has as its objective the timely establishment of manufacturing processes, techniques or equipment to insure the efficient production of current or future defense programs.

ABSTRACT

A hardened composite antenna window material designated ADL-10 has been developed, based on GE-RESD's Omniweave multidirectional fiber reinforcement woven construction using pure silica fibers and GE SR-350 methyl silicone resin as the matrix. Process studies included the use of Teflon-coated silica fibers to achieve an increase in woven Omniweave density to 1.0 gm/cc as compared to earlier values ranging from 0.4 to 0.7 gm/cc. Also studied were the effects of hydrofluoric acid etching of the silica fibers, the use of a silicone coupling agent and a range of molding pressures.

Based on an optimum fiber volume fraction of 68 percent, predicted minimum directional strength levels of 10,000 to 20,000 psi have been achieved with hardening capability as measured by flyer plate testing in excess of 4000 taps for nominal thickness of 1/4 to 3/8 inch. The material was verified to completely retain RF transparency up to heat flux levels of 100 Btu/ft² sec.

An inorganic silica/silica composite designated "Markite" and derived from multiple pyrolyses and reimpregnation of ADL-10 was studied for antenna window use at heat flux levels above 100 Btu/ft² sec. Complete RF transparency was maintained up to the maximum test level of 457 Btu/ft² sec. Only marginal improvements were achieved above earlier strength levels for Markite, to 2000-3000 psi, attributable to the improved Omniweave reinforcement fabric density. The effects of multiple reimpregnation and the fiber/matrix interaction mechanism are analyzed and recommendations made for new formulations.

1.0 INTRODUCTION AND SUMMARY

The purpose of this program is to develop hardened, radio frequency transparent multidimensionally reinforced heat shield materials for possible ABM applications using the General Electric Re-Entry and Environmental Systems Division's "Omni-weave" process. The work was performed in the Materials and Structures Laboratory of GE-RESA, from December 7, 1970 to November 7, 1971, mainly by personnel of the Plastics Technology and Materials Performance Assessment and Applications Laboratories.

The "Advanced Hardened Antenna Window" program is a continuation of the "Hardened Antenna Window Program" (July 1, 1969 to March 31, 1970). This earlier effort studied four variations of a high purity silica Omniweave/SR-350 silicone resin designated "ADL-10." As indicated in the final report of the prior study (Reference 1), ADL-10 showed excellent promise in the hardening and RF/ablation categories below 100 Btu/ft² sec, but the mechanical strength levels were disappointing, in the 2000 - 4000 psi range. An inorganic version of the material produced by multiple pyrolyses and reimpregnations and designated "Markite" was also studied. This silica-silica composite was produced and characterized principally as a result of development work on another, strategic systems program.

The present effort has had as its first goal the realization of higher strength levels for the resin-based ADL-10 material via specified improvements in Omniweave fabric densities and through the thickness fiber weaving angles. Additional process improvements to be investigated included variables such as fiber coating processes (using such plastics as Teflon TFE) and the effects of fiber etching and coupling agents. A second task was to investigate the transformation to an inorganic hardened antenna window for higher heat flux applications.

The first goal has been successfully met with the achievement of ADL-10 strength levels in the range of 10,000 - 20,000 psi and hardening capability as measured by flyer plate testing in excess of 4000 taps for nominal thicknesses of 1/4 to 3/8 inch. This high performance in the heat flux range below 100 Btu/ft² sec and the relative low cost of the ADL-10 series of composites make it an outstanding candidate for immediate application to several antenna window and radome applications.

The development effort on Markite was centered on use of the much improved weaving densities and process optimization achieved for the resin-based ADL-10 material. Although systematic improvements of about 20 percent in the strength of several versions of this material were evident at successive stages of pyrolysis and reimpregnation, the desired strength and hardening levels have not been achieved. An immediate alternative is a hybrid "slightly reimpregnated" Markite produced at higher pyrolysis temperatures. But, to meet ultimate performance goals, an inorganic composite

antenna window material such as silica-silica is definitely required. It is an analytic and experimental conclusion of this study that a fiber-matrix interaction fundamentally different from that of the Markites studied thus far is required for achievement of the structural strength and hardening goals.

This report has been written along the same format as Reference 1, the final report for the previous program. Ready comparisons can thus be made in analogous sections, and figures and sections in the previous report are frequently referenced. The basic Omniweave process, specimen characterization and measurement techniques, and photographs of facilities described in Reference 1 are not repeated in this report.

Section 2 covers the composite design and fabrication including a first investigation of chemical vapor deposition of silica. In Section 3.1, the detailed Sampling and Characterization Plan for the materials is repeated in the format of Reference 1 with reproduction of plate radiographs. Mechanical (3.2), Ultrasonic (3.3), Shock Testing (3.4), Electromagnetic (3.5) and Thermal Characterization (3.5) are covered in the balance of Section 3. In Section 4, a Capability Analysis of the ADL-10 and Markite Composite Systems is presented. In Section 5, Conclusions and Recommendations for further work are given.

An appendix is added to the report, after the conclusions, for convenient cross reference to processing, sampling and characterization of the various material formulations.

TABLE OF CONTENTS: SECTION 2

| | Page |
|---|------|
| 2.0 Composite Design and Fabrication | 2-1 |
| 2.1 General Considerations | 2-1 |
| 2.2 Materials Selection | 2-2 |
| 2.2.1 Omniweave | 2-2 |
| 2.2.2 Impregnating Resin | 2-3 |
| 2.3 Processing Considerations (Phase 1) | 2-5 |
| 2.3.1 Control of Fiber Notching (Pyrolysis of Woven Construction) | 2-5 |
| 2.3.2 Silane Coupling Agent | 2-5 |
| 2.3.3 Pyrolyzation Effects | 2-8 |
| 2.4 Processing of Test Specimens (Phase 1) | 2-8 |
| 2.4.1 Quartz Omniweave Reinforcement (Scarf 290-Q3BA-1) | 2-8 |
| 2.4.1.1 Pyrolyzation of Omniweave Specimens (Series No. 1) | 2-13 |
| 2.4.1.2 Hydrofluoric Acid Etching | 2-13 |
| 2.4.1.3 Application of Coupler | 2-13 |
| 2.4.1.4 Impregnation with SR-350 Resin | 2-13 |
| 2.4.1.5 Molding Procedure | 2-14 |
| 2.4.1.6 Preparation of Specimens for Test | 2-14 |
| 2.4.1.7 Fiber Angle Measurements | 2-16 |
| 2.4.2 Quartz Omniweave Reinforcement (Scarf 290-Q3BA-2, Series 2) | 2-16 |
| 2.4.2.1 Pyrolyzation of Omniweave Specimen (Series No. 2) | 2-18 |
| 2.4.2.2 Hydrofluoric Acid Etching | 2-18 |
| 2.4.2.3 Application of Coupler | 2-18 |
| 2.4.2.4 Impregnation with SR-350 Resin | 2-24 |
| 2.4.2.5 Molding Procedure | 2-24 |
| 2.4.2.6 Preparation of Specimens for Test | 2-24 |
| 2.5 Processing of Test Specimens (Phase 2) | 2-28 |
| 2.5.1 Quartz Omniweave Construction (Scarf 331-Q3BA) | 2-28 |
| 2.5.1.1 Pyrolyzation of Omniweave Construction | 2-28 |
| 2.5.1.2 Hydrofluoric Acid Etching | 2-28 |
| 2.5.1.3 Application of Coupler | 2-28 |
| 2.5.1.4 Impregnation with SR-350 Resin | 2-28 |
| 2.5.1.5 Molding Procedure | 2-28 |
| 2.5.1.6 Preparation of Specimens for Test | 2-31 |
| 2.5.2 Quartz Omniweave Construction (Scarf 318-Q3JA) | 2-32 |
| 2.5.2.1 Pyrolyzation of Omniweave Construction | 2-32 |
| 2.5.2.2 Hydrofluoric Acid Etching | 2-32 |
| 2.5.2.3 Application of Coupling Agent | 2-32 |
| 2.5.2.4 Impregnation with SR-350 Resin | 2-32 |
| 2.5.2.5 Casting and Molding Procedures | 2-34 |
| 2.5.2.6 Pyrolyzation and Reimpregnation Cycles | 2-35 |
| 2.5.2.7 Preparation of Specimens for Test | 2-35 |

TABLE OF CONTENTS: SECTION 2 (Continued)

| | Page |
|---|------|
| 2.5.3 Quartz Omniweave Construction (Scarf 319-Q35A) | 2-36 |
| 2.5.3.1 Pyrolyzation of Omniweave Construction 319-1 to Remove Teflon Coating | 2-36 |
| 2.5.3.2 Hydrofluoric Acid Etching | 2-36 |
| 2.5.3.3 Application of Coupling Agent | 2-36 |
| 2.5.3.4 Impregnation with SR-350 Resin | 2-36 |
| 2.5.3.5 Molding Procedure | 2-36 |
| 2.5.3.6 Pyrolyzation and Reimpregnation Cycles | 2-38 |
| 2.5.3.7 Preparation of Specimens for Test | 2-38 |
| 2.5.4 Quartz Omniweave Construction (Scarf 320-Q3JA) | 2-38 |
| 2.5.4.1 Pyrolyzation of Omniweave Construction 320-3, 4 | 2-38 |
| 2.5.4.2 Impregnation with SR-350 Resin | 2-38 |
| 2.5.4.3 Molding Procedure | 2-38 |
| 2.5.4.4 Pyrolyzation and Reimpregnation Cycles | 2-40 |
| 2.5.5 Unidirectional Quartz Construction | 2-40 |
| 2.5.5.1 Impregnation of Quartz Roving | 2-40 |
| 2.5.5.2 Molding Procedure | 2-40 |
| 2.5.5.3 Preparation of Tensile Test Specimens | 2-41 |
| 2.5.6 SR-350 Disc Molding Procedure | 2-41 |
| 2.6 Preliminary Study of Silica Chemical Vapor Deposition for Densifying Markite | 2-42 |
| 2.6.1 Introduction | 2-42 |
| 2.6.2 Experimental | 2-42 |
| 2.6.3 Prognosis | 2-44 |

2.0 COMPOSITE DESIGN AND FABRICATION

2.1 GENERAL CONSIDERATIONS

Assessment of the performance and capabilities of thermal shield materials for re-entry and ABM vehicles are always predicated on a series of trade-off considerations. These include, but are not limited to: ^{2,3}

| <u>Performance Category</u> | <u>Related Test Parameters</u> |
|-----------------------------|---|
| Ablation | recession, heat of ablation, mass loss, surface temperature |
| Insulation | thermal conductivity, specific heat, thermal diffusivity |
| Thermo-Structural | mechanical strength and thermal expansion as a function of temperature, notch sensitivity |
| Producibility | fabrication cost analysis |
| Weapons Effects | resistance to high impulse loading |

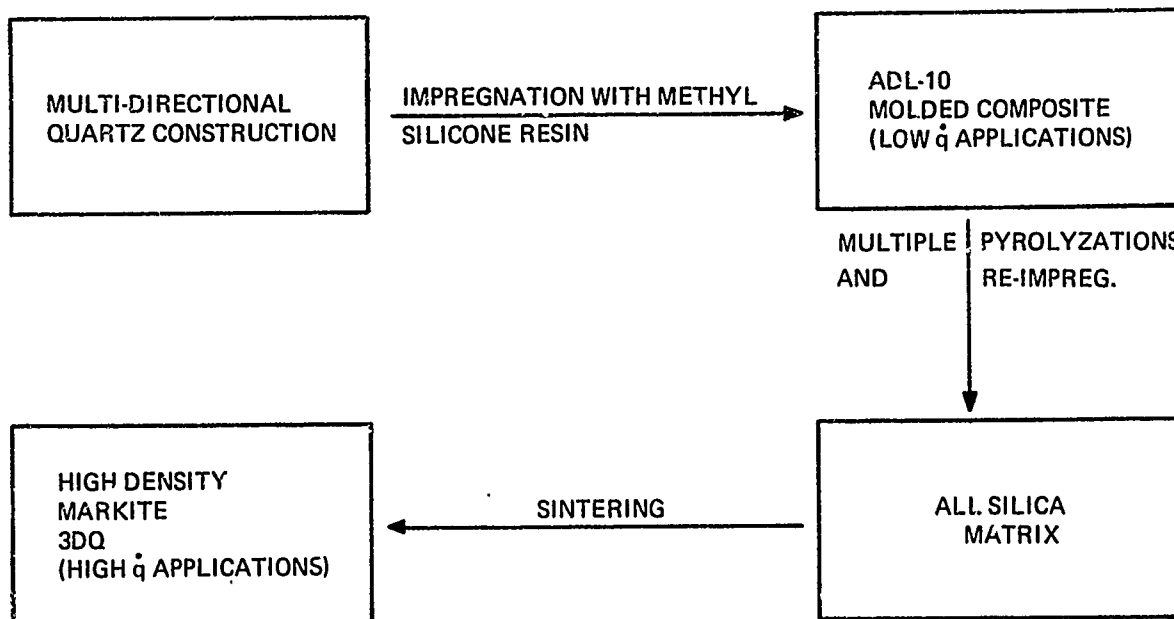
In addition to these parameters, an antenna window, which forms a part of the thermo-structural shell, must have and maintain RF transparency at specific frequencies before and during the ablation environment experienced during re-entry.

Monolithic transparent and slip cast fused silica have been used extensively as antenna window materials on re-entry vehicles. While flight performance of these materials have proven adequate, they do exhibit a number of limitations. Perhaps the most important limitation resulting from the brittle nature of fused silica is its relatively low performance capability with respect to high impulse loading.

One of the approaches which has proven successful, with respect to meeting many of the aforementioned performance requirements, involves the utilization of multidirectionally reinforced composites. This type of material exhibits greater resistance to the deleterious effects of high impulse loading in comparison to either monolithic ceramic materials or conventional laminates. Superior resistance to weapons effects environments is attained by the more efficient dissipation of energy by the multidirectional reinforcement.

Also, under proper fiber-matrix interaction conditions, superior tensile properties may be achieved, approaching the ultimate performance of the pure fiber component of the composite within the limits of the normalized fiber volume reinforcement fractions.

This report describes the development of an improved silicone resin impregnated, multidirectional, quartz composite which is capable of meeting the aforementioned performance requirements, while exhibiting a lesser degree of brittleness compared to monolithic ceramic antenna window material. The process utilized for the preparation of the silica-silicone composite (ADL-10) can also be used to produce a silica-silica composite (Markite) in accordance with the following schematic representation:



2.2 MATERIALS SELECTION

2.2.1 Omniweave

Omniweave is a GE-developed multidirectional weaving technology which is capable of producing composites having tailored fiber geometries. The standard Omniweave construction involves the weaving of fibers in a three-dimensional fashion, so that the reinforcing fibers (in this case, quartz roving) follow paths which are parallel to intersecting diagonals - that is, the fibers travel from surface to surface at a constant radial angle, while forming a nominal 45-degree angle in the lengthwise and crosswise directions. An isometric representation of this type of 45-degree, body-centered cubic construction is illustrated in Fig. 1. Because of the projection of the fibers in four principal spatial directions, Omniweave composites are termed "Four Directional". It should be emphasized, however, that Omniweave is a three dimensional construction. In order to avoid confusion with the standard orthogonal 3D construction, directional designations are used in lieu of the general 3D classification. Recent studies at

[4 - DIRECTIONAL FIBROUS REINFORCEMENT]

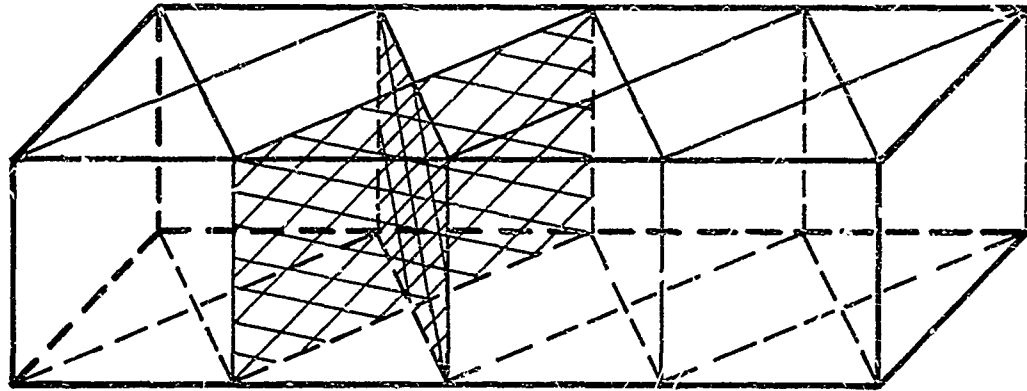
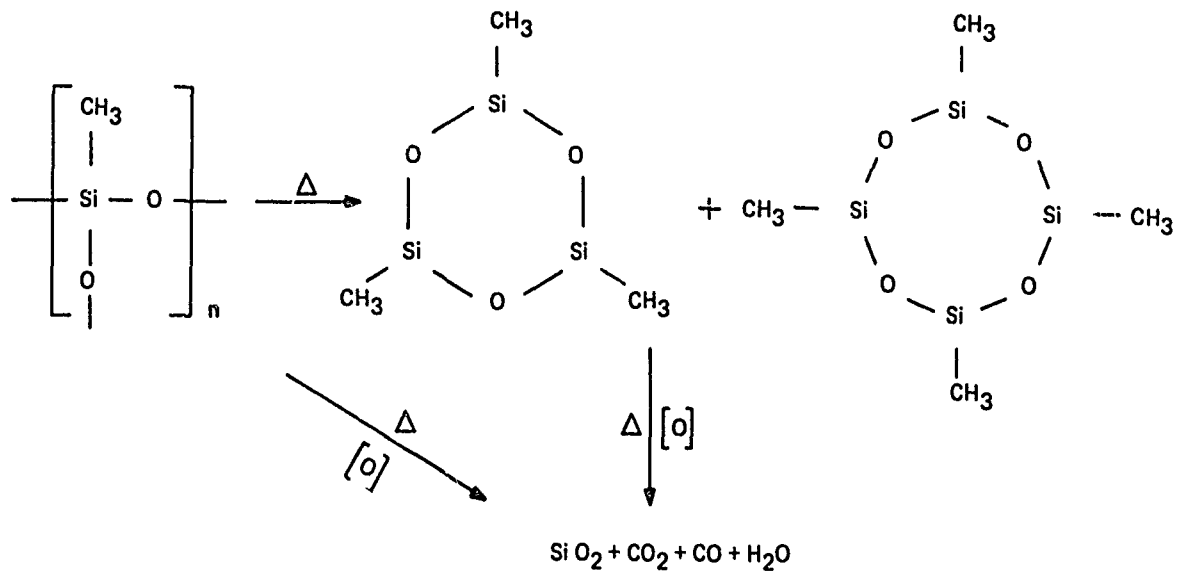


Fig. 1 Multidimensional Reinforcement in Which The Fibers Follow Paths Parallel to the Diagonals of Intersecting Planes

GE-RESF have resulted in 7 directional constructions for carbon/carbon composites. This 7 directional construction is an interwoven combination of 3 and 4-directional constructions. A photograph of a 7-D model is shown in Fig. 57 of Section 4 of this report.

2.2.2 Impregnating Resin

SR-350, a GE-developed methyl silicone polymer, was used as the resin for the impregnation of the quartz Omniweave. TGA data, shown in Fig. 2, indicates that approximately 85 weight percent of the resin is converted to SiO_2 upon pyrolysis in air. The theoretical thermal degradation mechanism can be represented by the following equation:



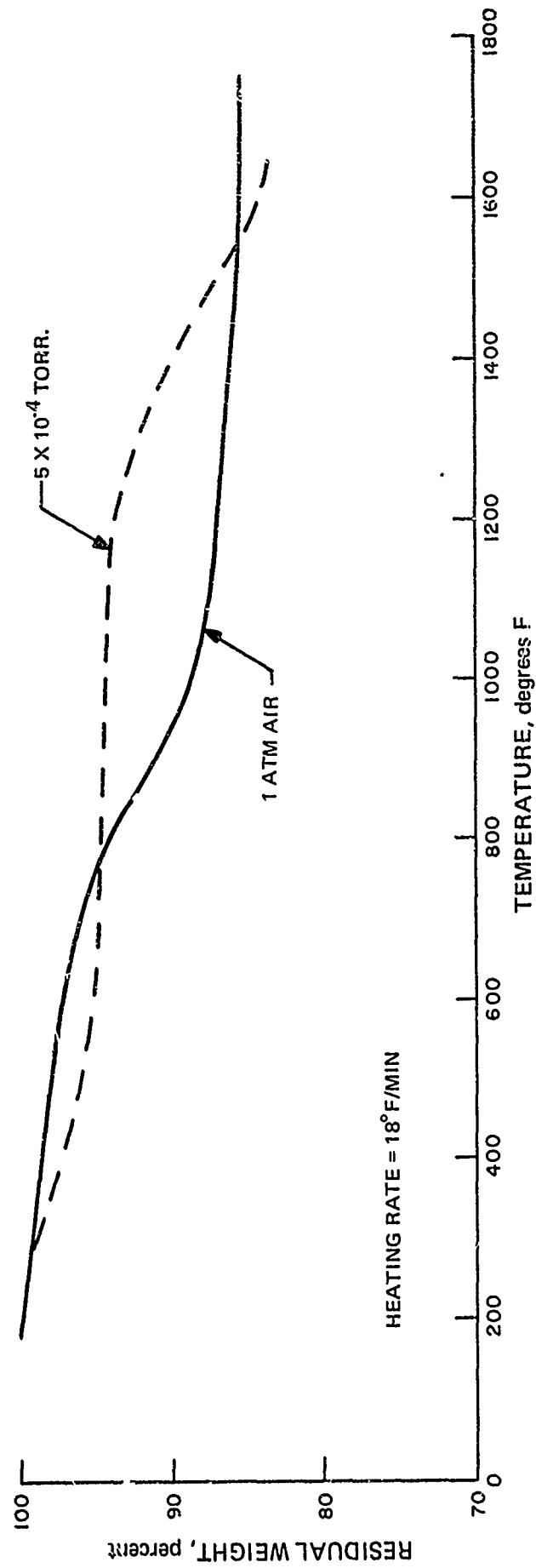


Fig. 2. Thermogravimetric Analysis of SR-350 Resin

2.3 PROCESSING CONSIDERATIONS (PHASE 1)

2.3.1 Control of Fiber Notching (Pyrolysis of Woven Construction)

One of the factors which could be considered responsible for the premature failure of the composite involves the generation of numerous notches on the surfaces of the quartz fibers. While notches on the fibers may be produced during weaving of the multidirectional quartz reinforcement, it is believed that fiber notching is primarily induced during pyrolysis of the woven construction. The differential coefficient of expansion of the quartz and the polyurethane coating (used to facilitate Omniweave processing) may be a major notch contributor during pyrolysis of the coating. This situation is compounded by handling of the pyrolyzed quartz construction prior to impregnation with SR-350 resin.

One technique which has been considered as a remedial measure to decrease the deleterious effect of the fiber notching is the treatment of the quartz fibers, after pyrolysis, with dilute hydrofluoric acid. This etching treatment would tend to convert sharp notches to more rounded notches, thus reducing the effect of high stress concentration sites of the static and dynamic mechanical performance of the composite.

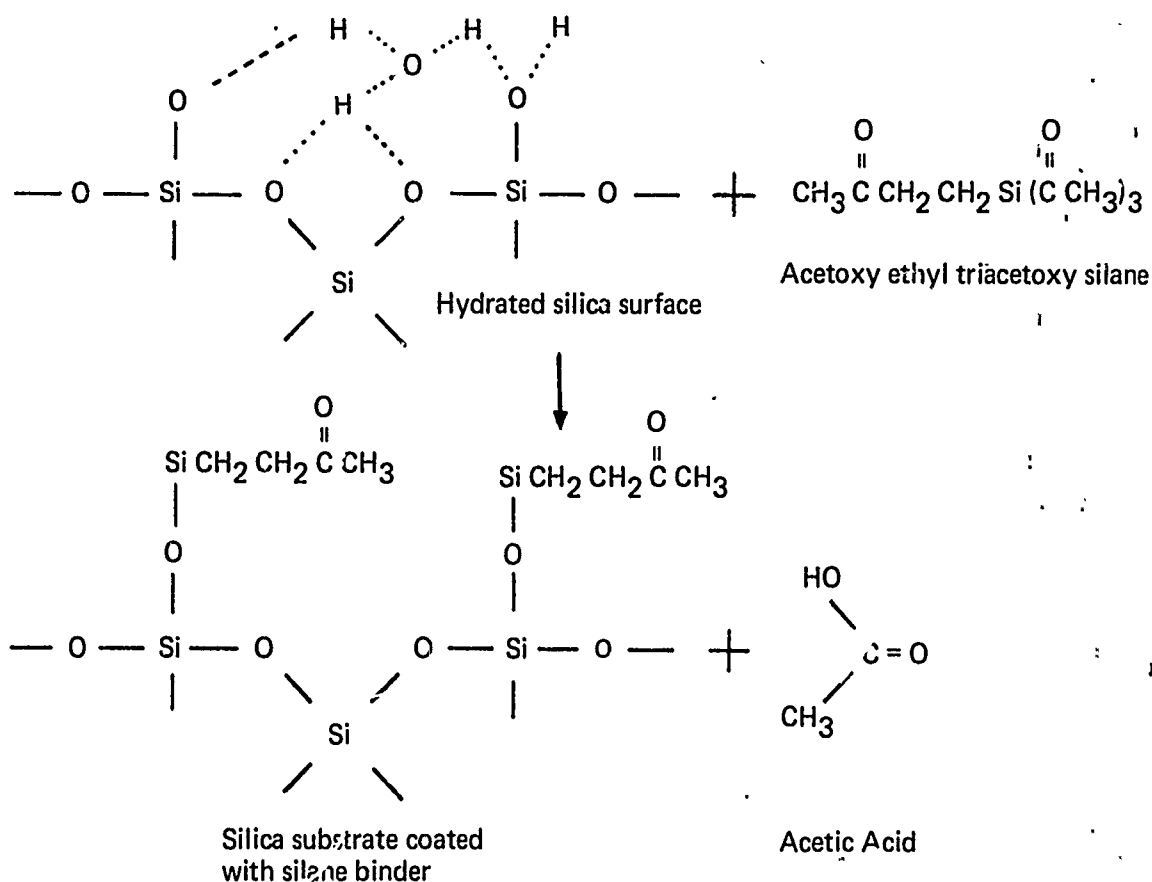
A more positive method which can be used to inhibit the deleterious effect of fiber notching involves the use of Teflon coated quartz fibers. The quartz fibers are coated with Teflon as they are drawn during the production of the roving. This precludes the necessity for the application of either a binder coating (A-1100) during drawing of the fibers or the use of a polyurethane coating to facilitate the weaving of the quartz construction.

An additional advantage is gained from the use of Teflon coated quartz fibers in the preparation of the Omniweave construction. The excellent lubricity characteristics of the coating permitted much tighter fiber packing during weaving and hence a higher woven bulk density (e.g., >1.0 g/cc) is attained.

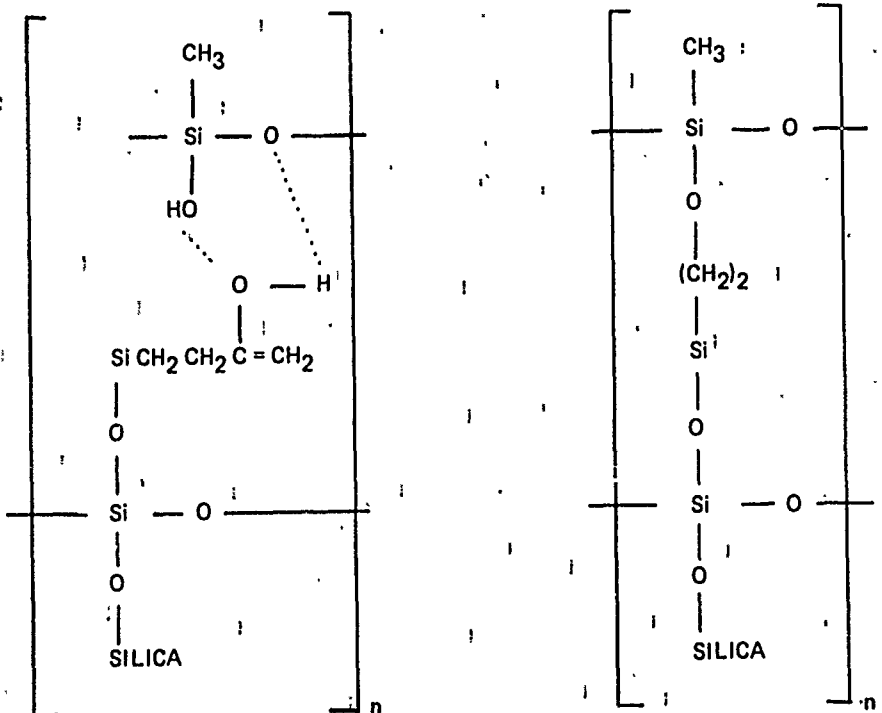
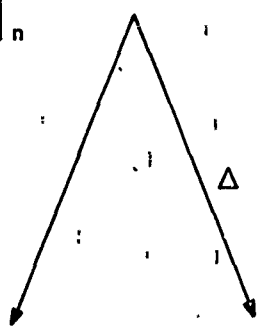
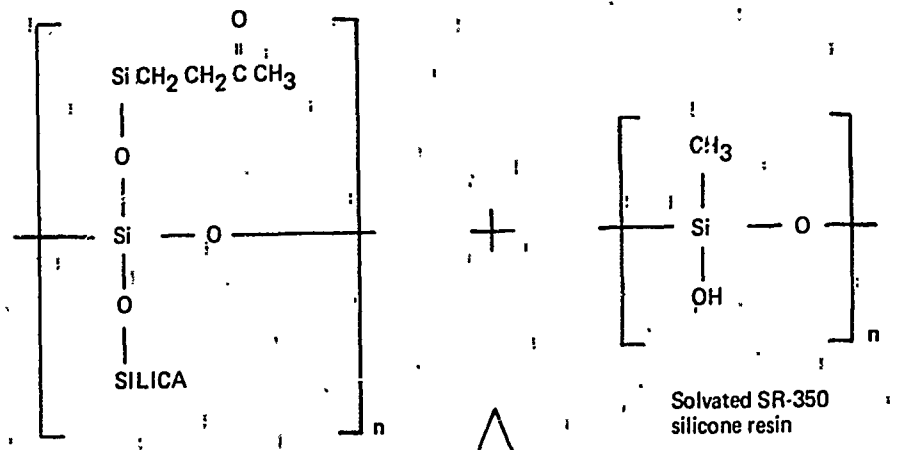
2.3.2 Silane Coupling Agent

Maximum mechanical performance of a conventional composite material is attained by effecting a tenacious bond between the reinforcing construction and the resin matrix. This results in efficient stress distribution among the relatively high modulus fibers through the resin. In the case of quartz, silica and glass, tenacious bonding is facilitated by the use of a coupling agent which is applied to the fiber prior to impregnation with resin. In general, coupling agents act as a bridge between the fiber, substrate and the resin. These reagents possess functional groups which are capable of forming chemical bonds with reactive groups on both the substrate and the resin more efficiently than if the resin were directly applied to the substrate. Most coupling agents for quartz fibers have the general formula $R-CH_2-CH_2-Si(OCH_3)_3$ ⁴. The silicon portion of the molecule has a unique affinity for glass silica, quartz and other silicious inorganic substrates, while the organic portion of the molecule is tailored to combine with the particular resin. After treatment of the quartz fibers with the silane coupling agent, it is necessary to effect hydrolysis of the coating. This is achieved

from exposure to atmospheric moisture and from molecular water attached to the silica surface by hydrogen bonding. These mechanisms are represented by the following reactions.



Reaction between silane coupling agent and SR-350 resin



2.3.3 Pyrolyzation Effects

Another processing step in which damage to the structural integrity of quartz fibers can occur is in the processing of the composite when the material is subjected to pyrolysis. Initial pyrolysis of the Omniweave construction is carried out at 1100° F to volatilize the A-1100 binder, the polyurethane coating or the Teflon coating which may have been applied to facilitate weaving. Removal of one or a combination of the fiber coatings is necessary prior to the application of silane coupler and/or impregnation with SR-350 resin in order to achieve tenacious bonding between the resin and the quartz substrate. This is the only pyrolysis step used in the processing of the ADL-10 resin impregnated composites.

In the case of the Markite silica-silica composite, the ADL-10 material is subjected to multiple pyrolyzation at 1100° F and reimpregnations with SR-350 resin to produce silica bridges between the quartz fibers. A final Markite pyrolyzation usually involves sintering the material at 2250° F. The objective of the final sintering is to achieve incipient sintering of the quartz fibers with the silica matrix without causing significant devitrification of the silica.

A number of contaminants and environmental conditions synergize the devitrification of silica at 2250° F and even at lower temperatures. Alkali metal contamination at concentrations as low as 550 ppm have markedly decreased the mechanical performance of silica-silica composites after exposure of 1100° F.⁵

The aforementioned considerations have been included in the Test Plan which was used to guide the effort described in this report⁶. It should be emphasized however, that there is an alternative school of thought with respect to the attainment of maximum mechanical performance from this type of composite material. This opinion states that, while maximum mechanical properties are produced by conventional composites which exhibit tenacious bonding between matrix and reinforcement, such is not the case with composites with brittle, low strain-to-failure matrices. Beneficial reinforcement from the relatively high modulus fibers is not realized because brittle failure of the matrix resin does not permit efficient stress transfer to and among the fiber reinforcements. Thus, this approach emphasizes that the supporting fiber should be insulated from the resin matrix to preclude premature failure of the reinforcement via the resin.

2.4 PROCESSING OF TEST SPECIMENS (PHASE I)

2.4.1 Quartz Omniweave Reinforcement (Scarf 290-Q3BA-1)

An Omniweave scarf illustrated in Fig. 3, was woven as a pseudo-continuous "A" (45-degree cubic) construction. Except for a three-inch wide continuous woven band

across the top, the scarf was separated into six 21 x 1 inch sections with woven edges. The characteristics of the Omniweave scarf are described in Table 1, while the properties of the quartz roving and filaments used in all woven constructions are included in Table 2.

The strip segments of the scarf were processed as separate groups to determine the effect of a number of variables on mechanical performance. These variables included: 1) concentration of hydrofluoric acid used to etch the quartz fibers, 2) a silane coupler for application to the quartz fibers, and 3) molding pressure.

The ends and two sites at the midsection of each segmented strip were bound with 20-end quartz roving to preclude unravelling of the Omniweave after cutting. Each segmented strip was then cut from the scarf and between the two bands of roving at each midsection. This resulted in 12 woven test specimens, 10 x 1 x 0.4 inch (nominal dimensions), from the scarf. A typical specimen is illustrated in Fig. 4, while Fig. 5 illustrates a magnified section of a typical woven strip. The dimensions, weight and density of the samples are included in Table 3.

The succeeding processing steps are divided into those which are applicable to the sectioned, segmented strips cut from Omniweave scarf 290-1 and those from scarf 290-2. These series of specimens are designated Series 1 and Series 2, respectively.

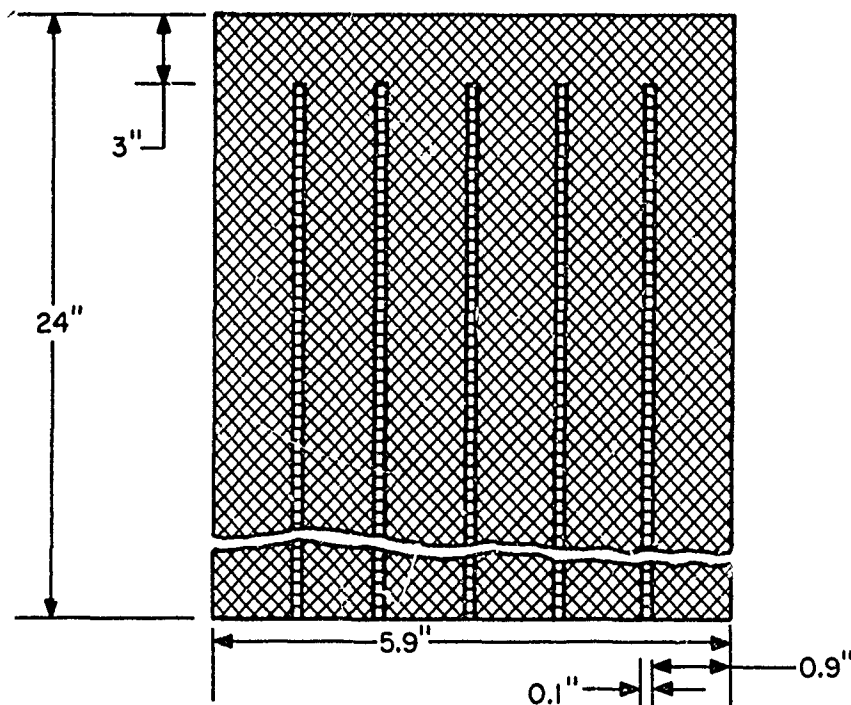


Fig. 3. Segmented Omniweave Scarf 290-Q3BA

TABLE 1. CHARACTERISTICS OF SEGMENTED OMNIWEAVE SCARF - 290-Q3BA
(Phase 1, Series 1 and 2)

| | |
|-----------------------------------|---|
| Thickness x Width | 7 x 13 |
| Weave Pattern | "A" (Cubic) |
| Type of Fiber | No. 552 (20-End) Astroquartz Roving (Lot 173-2759) |
| Fiber Binder Coating | A-1100 (9073) |
| Fiber Treatment | Scotchcast 221, Polyurethane (4 pbw in acetone) |
| Woven Dimensions, in. | 24.4 x 5.5 x 0.40 |
| Woven Bulk Density, g/cc | 0.81 |
| Axial Angle, deg. | 45 |
| Through-the-Thickness Angle, deg. | 43 |

TABLE 2. CHARACTERISTICS OF QUARTZ FILAMENTS AND ROVING

| | |
|--|---------------------------------|
| <u>Filament Properties</u> | |
| Designation | Astroquartz* (Brazilian Quartz) |
| Filament Diameter, in. | 3.55×10^{-4} (nominal) |
| Filaments/20-end | 5000 (nominal) |
| Filament Density, g/cc | 2.2 |
| Young's Modulus, psi | 1×10^7 |
| Poisson Coefficient | 0.17 |
| Chemical Analysis SiO ₂ , % | 99.95 |
| alkali metals, ppm | 15 |
| alkaline metals, ppm | 26 |
| boron, ppm | 10 |
| aluminum, ppm | 100 |
| others, ppm | 21 |
| <u>Roving Properties</u> | |
| Designation | 552 Astroquartz* |
| End Count | 20 |
| Yards/lb. | 750 |
| Breaking Strength, lb. | 50 |

*Designation of J. P. Stevens & Co., Inc.

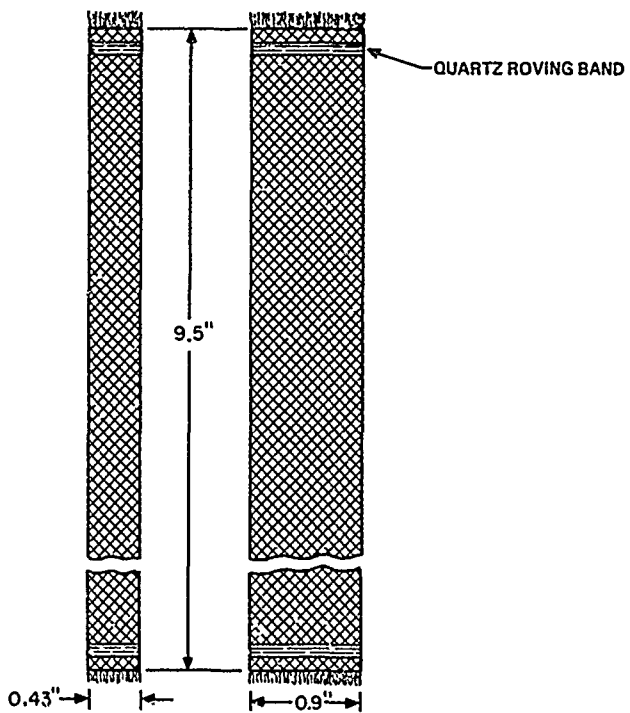


Fig. 4. Woven Omniweave Segment

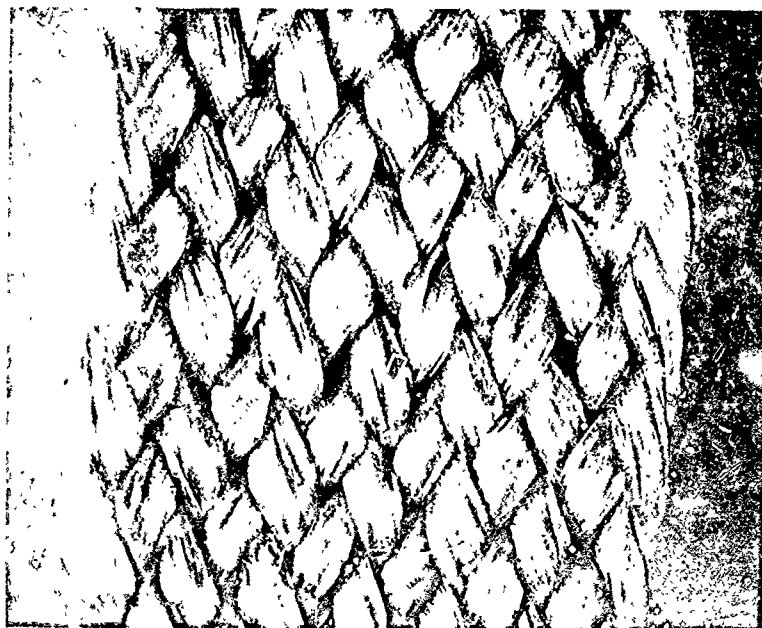


Fig. 5. Woven Omniweave Segment (4.5x)

TABLE 3. CHARACTERISTICS OF SERIES NO. 1 TEST SPECIMENS

| Sample Number | Approx. Woven Dimensions (in x in x in) | Woven Density (gm/cc) | Density ¹ Post Pyrol. (gm/cc) | Conc. HF (Wt %) | Density Post HF (gm/cc) | Density ² Post Silane (gm. cc) | Molding Pressure (psi) | Molded Density (gm/cc) | Fiber Wt. (%) | Resin Wt. (%) | Fiber Vol. (%) | Resin Vol. (%) | Porosity Vol. (%) |
|---------------|---|-----------------------|--|-----------------|-------------------------|---|------------------------|------------------------|---------------|---------------|----------------|----------------|-------------------|
| A1 | 8.50 x 0.960 x 0.426 | 0.70 | 0.68 | -- | ---- | 0.68 | 300 | 1.71 | 92.2 | 7.8 | 71.7 | 10.4 | 17.9 |
| A2 | | | | | | 0.69 | | 1.67 | 86.8 | 13.2 | 65.9 | 17.2 | 16.9 |
| G1 | 10.12 x 0.870 x 0.390 | 0.83 | 0.80 | 5 | 0.79 | 0.80 | 1000 | 1.69 | 91.9 | 8.1 | 70.6 | 10.7 | 18.7 |
| G2 | | | | | | 0.81 | | 1.67 | 86.6 | 13.7 | 65.7 | 17.9 | 16.4 |
| J1 | 9.90 x 0.880 x 0.390 | 0.80 | 0.77 | 10 | 0.74 | 0.75 | 125 | 1.68 | 90.6 | 9.4 | 69.2 | 12.3 | 18.5 |
| J2 | | | | | | 0.76 | | 1.61 | 85.4 | 14.6 | 62.5 | 18.4 | 19.1 |
| B1 | 9.75 x 0.920 x 0.415 | 0.74 | 0.71 | -- | ---- | 0.72 | 1000 | 1.66 | 88.3 | 11.7 | 66.7 | 15.2 | 18.1 |
| B2 | | | | | | 0.73 | | 1.69 | 91.2 | 8.8 | 70.1 | 11.6 | 18.3 |
| H1 | 9.88 x 0.890 x 0.400 | 0.79 | 0.76 | 5 | 0.75 | 0.76 | 1000 | 1.76 | 95.9 | 1.1 | 76.7 | 5.7 | 17.6 |
| H2 | | | | | | 0.76 | | 1.68 | 95.0 | 5.0 | 72.5 | 6.6 | 20.9 |
| K1 | 9.38 x 0.850 x 0.390 | 0.81 | 0.78 | 10 | 0.75 | 0.76 | 125 | 1.71 | 95.7 | 4.3 | 74.4 | 5.7 | 19.9 |
| K2 | | | | | | 0.76 | | 1.75 | 99.0 | 1.0 | 78.7 | 1.4 | 19.0 |
| C1 | 9.50 x 0.910 x 0.395 | 0.79 | 0.76 | -- | ---- | 0.76 | 1000 | 1.66 | 91.5 | 8.5 | 69.9 | 11.1 | 19.0 |
| C2 | | | | | | 0.77 | | 1.64 | 87.9 | 17.1 | 61.8 | 21.9 | 16.3 |
| I1 | 9.75 x 0.820 x 0.390 | 0.87 | 0.84 | 5 | 0.83 | 0.83 | 125 | 1.59 | 81.6 | 18.4 | 59.9 | 22.8 | 18.2 |
| I2 | | | | | | 0.84 | | 1.68 | 91.2 | 8.8 | 68.6 | 11.6 | 18.8 |
| L1 | 9.25 x 0.810 x 0.370 | 0.94 | 0.90 | 10 | 0.87 | 0.88 | 1000 | 1.55 | 82.0 | 18.0 | 59.8 | 21.8 | 20.4 |
| L2 | | | | | | 0.89 | | 1.68 | 91.0 | 9.0 | 69.5 | 11.8 | 18.7 |
| D | 9.50 x 0.870 x 0.395 | 0.83 | 0.80 | 1 | 0.80 | ---- | 1000 | 1.66 | 85.2 | 14.8 | 64.3 | 19.2 | 16.6 |
| E | 9.80 x 0.860 x 0.395 | 0.83 | 0.80 | 1 | 0.80 | ---- | 1000 | 1.68 | 85.2 | 14.8 | 65.1 | 19.4 | 16.6 |
| F | 9.00 x 0.860 x 0.400 | 0.80 | 0.80 | 1 | 0.78 | ---- | 1000 | 1.69 | 85.0 | 15.0 | 65.1 | 19.7 | 15.2 |

1-Pyrolysis carried out at 800° F for 16 hours.

2-Upper value resulted from impregnation with 1% silane coupler solution, while lower value was the cumulative result after impregnation with 9% silane coupler.

2.4.1.1 Pyrolyzation of Omniweave Specimens (Series No. 1)

The 12 woven sections were placed in clean, stainless steel trays and heated in an oven at 800° F for 16 hours. After cooling, each specimen was weighed and the change in density is shown in Table 3.

2.4.1.2 Hydrofluoric Acid Etching

Three stainless steel trays were lined with polyethylene film. One percent aqueous HF solution was added to the first tray, while 5 and 10 percent aqueous HF solutions were added to the second and third trays respectively. One group of 3 specimens was retained as a control and not subjected to HF treatment. Sets of three 10-inch long pyrolyzed Omniweave segments, described in Section 2.4.1.1, were added to the solution in each tray for 1 minute. The aqueous HF solutions were then poured from the trays and the woven specimens were flooded with cold tap water until a pH indication of >6.5 was attained. The specimens were then washed with distilled water and then dried at 250° F for 4 hours. The density of each specimen is tabulated in Table 3.

2.4.1.3 Application of Coupler

Three groups of 3 specimens each were placed in 3 stainless steel trays lined with polyethylene film. One group of 3 specimens was retained as a control group and not treated with silane coupler solution.

A one percent solution of acetoxy ethyl triacetoxy silane* in acetone (reagent grade) was added to the specimens contained in the stainless steel trays. After a 15 minute immersion, the specimens were removed from the silane coupler solution and allowed to stand 4 days. During this time interval, the acetone evaporated from the coated quartz fiber facilitating hydrolysis of the coupler by reaction with atmospheric moisture. The specimens were then placed into an oven at 225° F for 4 hours and allowed to cool over phosphorus pentoxide desiccant. The density change produced by the silane treatment is included in the data described in Table 3.

A second treatment with a 9.1 percent solution of silane coupler solution was carried out. The density increase caused by this second silane treatment is in Table 3.

2.4.1.4 Impregnation with SR-350 Resin

SR-350 methyl silicone resin was dissolved in an equal weight of acetone. The solution was then filtered through a Buchner funnel to remove solid contaminants. All 12 ten-inch long test specimens (Sample A through J) were immersed in the filtered silicone resin solution and subjected to vacuum to facilitate impregnation of the quartz construction

*Hereafter referred to as silane coupler.

by the resin. The impregnated specimens were then removed from the resin solution and allowed to stand for 16 hours. The impregnated samples were then B-staged at 180° F for 4 hours.

2.4.1.5 Molding Procedure

An aluminum mold was fabricated to accommodate three processed Omaiweave strips 9.5 inches long x 0.9 inch wide. The mold consisted of a removable bottom plate, a center section containing three 10.5 x 0.80 inch channels and a top plate having aluminum bars designed to fit into the aforementioned channels. An aluminum plug, inserted at the end of each of the three channels, was fitted with an external adjustment screw to conform to the slightly varying lengths of the test specimens. The mold is shown in Fig. 6.

A very thin coating of silicone grease was applied to the internal surfaces of the mold. The mold was then preheated to 180° F at which time the three B-staged test specimens (described in Section 2.4.1.4) which were also at 180° F, were inserted into the channels of the preheated mold. The male lid was then fitted into the mold. The entire assembly was then placed between the platens of a press, which had been preheated to 180° F.

Groups of three processed specimens were subjected to a pressure of 125 psi, 300 psi or 1000 psi. After the maximum indicated pressure was attained, the temperature of the platens was increased to 400° F over a period of 30 minutes. The specimens were allowed to remain in the press at maximum pressure and temperature for 4 hours. The mold assembly was then transferred to an oven preheated to 400° F and the molded specimens were post-cured at that temperature for 16 hours. After cooling to room temperature, the mold was disassembled and the specimens removed.

2.4.1.6 Preparation of Specimens for Test

With the exception of test specimens D, E, and F, each 9.5-inch long molded test specimen was cut into two specimens approximately 4.5 inches long using a cut-off wheel. The ends of the specimens still containing the quartz roving ties were removed in this process. Flashing was then removed from the test specimens by wet sanding, first with 325 grit silicone carbide paper and then with 400 grit paper. After removal of loose abrasion particles by rinsing in cold tap water, the specimens were dried at 250° F for 4 hours. The characteristics of the molded specimens are summarized in Table 3.

In order to prepare the specimens for tensile testing, it was necessary to bond doublers to the ends of the test specimens to protect them from the gripping fixture on the tensile tester. A one-inch square area on each surface and at the end of each specimen was abraded with 325 grit silicone carbide paper and then wiped with a clean cotton cloth moistened with acetone. Doublers, 1 x 1 x 0.125 inch, were cut on a bias from a G-10 epoxy-fiberglass panel. The bonding surfaces of the doublers were also abraded and solvent wiped as in the case of the composite test specimen.

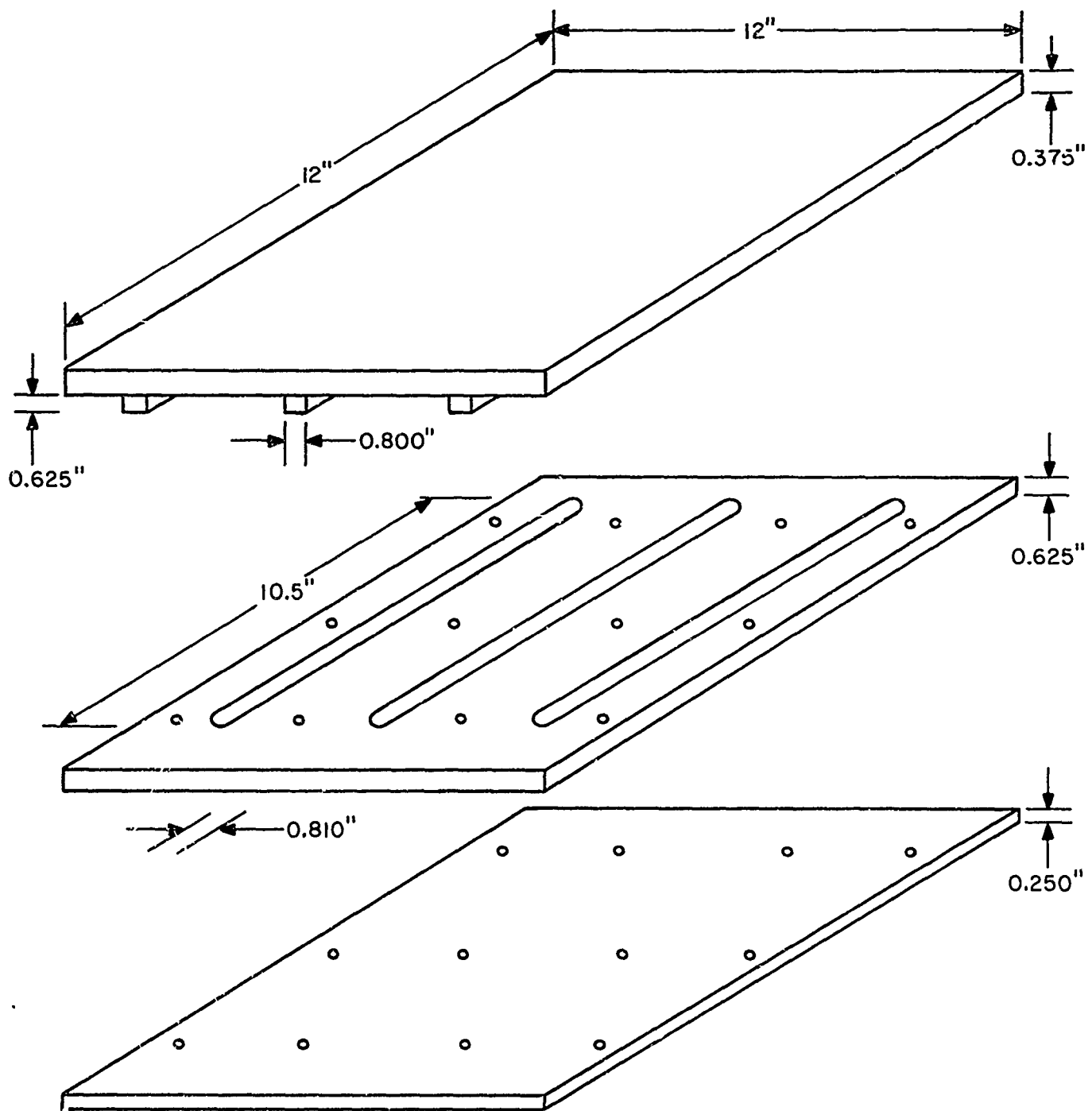


Fig. 6. Omniweave Strip Mold

The doublers were bonded to the test specimens using a filled epoxy-polyamide adhesive having the following formulation:

| | |
|--------------|---------|
| Epon 828 | 25 pbw |
| T-61 Alumina | 40 pbw |
| Versamid 115 | 27 pbw |
| DETA | 1.8 pbw |

The adhesive coated doublers were fixed to the coated specimens using C-clamps. The bonded assemblies were cured overnight at 140° F. A typical tensile specimen is illustrated in Fig. 7.

2.4.1.7 Fiber Angle Measurements

The samples were then submitted to the Materials Performance Laboratory for optical measurement of fiber angle in the axial and through-the-thickness directions. The results of these measurements are shown in Table 4.

2.4.2 Quartz Omniweave Reinforcement (Scarf 290-Q3BA -2, Series 2)

An Omniweave scarf, almost identical to the one described in Section 2.4.1, was used as a source of test specimens for a second series of tests. Based on preliminary results of tensile tests on series 1 specimens, all processed segments were subjected to a 10 percent HF etch and a molding pressure of 125 psi. The evaluation of the mechanical performance of the series 2 test specimens involved determination of variables including: 1) silane coupler concentration, 2) the effect of machined edges (destruction of continuity of fiber reinforcement), and 3) the incorporation of finely divided silica into the impregnating resin.

In order to determine the tensile performance of unprocessed Omniweave, one of the six 20-inch long strips was banded at each end with quartz roving and cut from Scarf No. 2. The ends of this control strip were suspended between two pulleys with a 10 pound load suspended from each end. Two 4-inch long segments of the strip were banded, through-the-thickness, with RTV-511 silicone rubber to prevent wicking by the epoxy resin which was then applied to the estimated grip areas on the tensile specimen. After curing of the epoxy resin, the unprocessed Omniweave specimen was cut into two 4-inch long specimens containing RTV-511 collars and epoxy resin impregnated ends.*

The remaining five 20-inch long strips were bound with quartz roving and cut in half as described in Section 2.4.1.

In addition, a small bundle of Omniweave quartz fibers were carried along with all processing steps of series 2 test specimens. After each processing step, a number of fibers were retained for inspection by a scanning electron microscope at the GE Research and Development Center, Schenectady, N. Y.

*Both of these specimens failed prematurely at the epoxy doubler edges so that no strength data on the silica omniweave fabric itself was obtained.

Reproduced from
best available copy. 

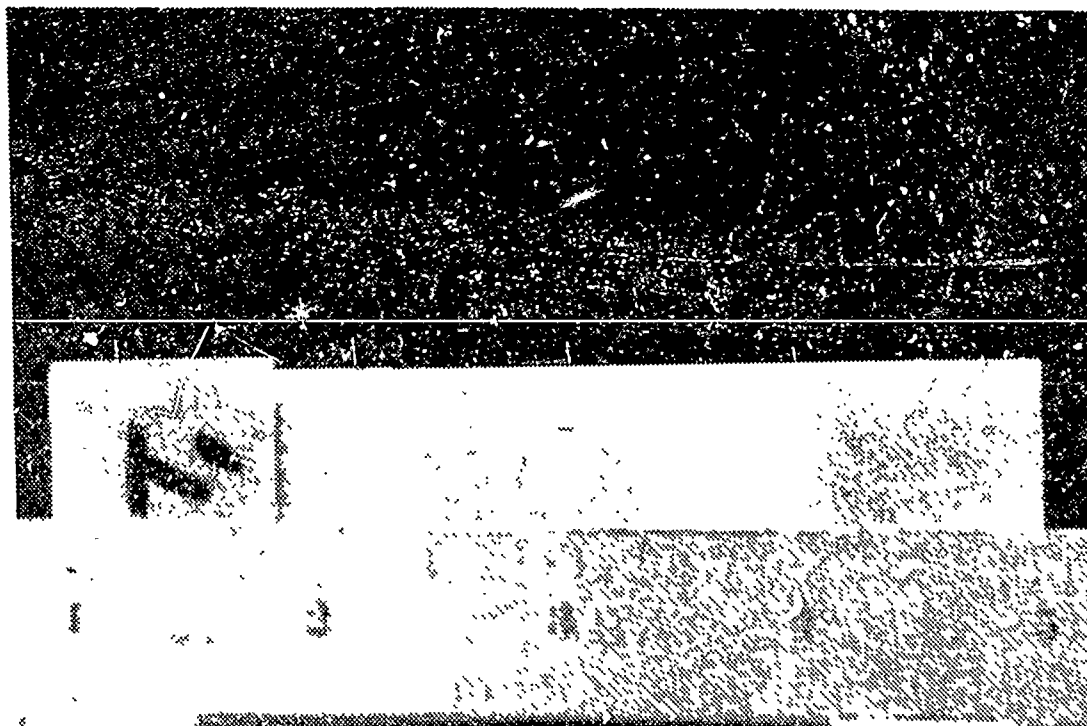


Fig. 7. Tensile Specimen

In Fig. 8, four views are shown of the fibers with A1100 and Scotchcast coatings applied to prevent fiber damage during weaving. Note that the individual filaments, visible beginning with the 170X photo, have a diameter of 10 microns. The fiber bundles are generally clean, but flecks of dust and broken fiber ends are visible at times. In the 1700X and 4250X views, clumps of the polyurethane coating are visible, adhering to the filaments.

2.4.2.1 Pyrolyzation of Omniweave Specimen (Series No. 2)

Ten woven sections were placed in clean, stainless steel trays and heated in an oven at 800°F for 16 hours. After cooling, each specimen was weighed and the change in density is shown in Table 5.

In Fig. 9, the fibers are seen after pyrolysis at 800° F to remove the Scotchcast polyurethane and A-1100 coatings. The 1000X view shows increased presence of dust or broken filament particles. Ragged filament undersides are also apparent in this view. The presence of these ragged edges was carefully studied by varying view angles in the SEM and is accurately represented by this photo micrograph. The fractured ends of an individual pyrolyzed fiber are shown in 1700X and 4250X magnification. However, the ragged edges do not appear under these higher magnifications.

2.4.2.2 Hydrofluoric Acid Etching

A large stainless steel tray was lined with polyethylene film. Ten percent aqueous HF solution was added to the tray which contained all of the Series 2 test specimens. Etching was carried out for one minute. The aqueous HF solution was then poured from the tray and the woven specimens were flooded with cold water until a pH indication of >6.5 was attained. The specimens were then washed with distilled water and then dried at 250°F for 4 hours. The density of each specimen is tabulated in Table 5.

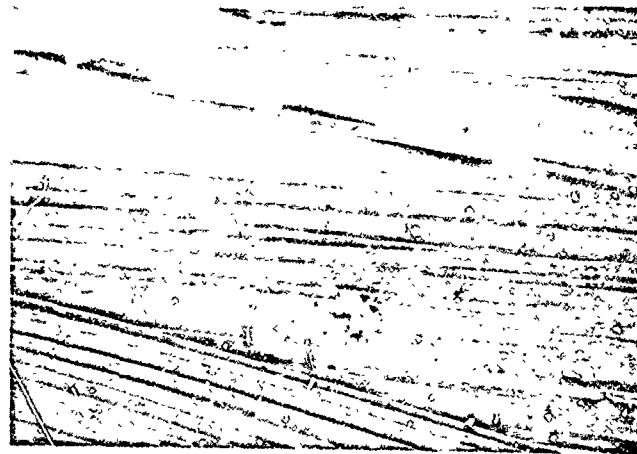
2.4.2.3 Application of Coupler

The ten etched specimens were placed in a stainless steel tray lined with polyethylene film. A one percent solution of silane coupler in acetone was added to the tray. After the specimens were immersed for 15 minutes, they were removed from the silane coupler solution and allowed to stand overnight allowing volatilization of the acetone and hydrolysis of the silane resin by atmospheric moisture. The specimens were then placed into an oven at 225°F for 4 hours and allowed to cool over phosphorus pentoxide desiccant. Five of the ten silane coated specimens were subjected to an additional impregnation with a 10 percent solution of silane in acetone. These specimens were impregnated and cured using the procedures already described. The density change produced by the silane treatments is included in the data described in Table 5.

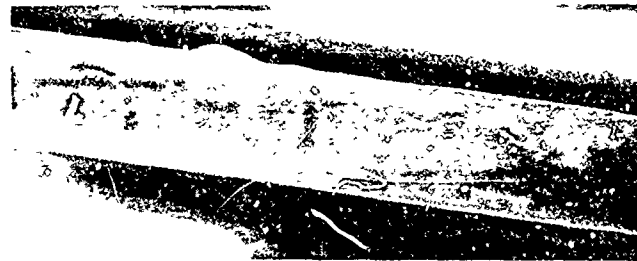
In Fig. 10 the progression of the fiber system from hydrofluoric etching through silane treatments is depicted in 2000X magnification. The first view shows a filament



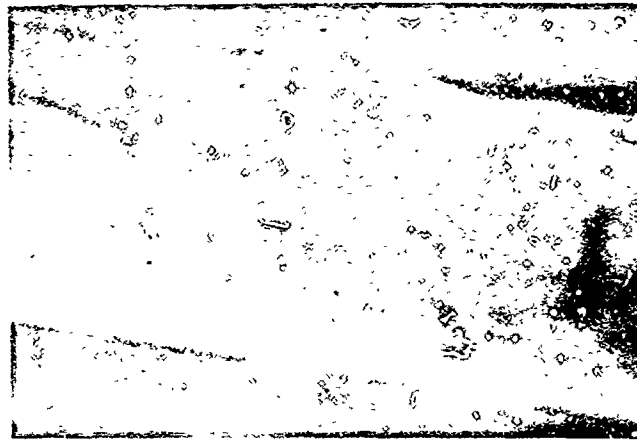
17X



170X



1700X



4250X

Note: Nominal fiber diameter is 10 microns.

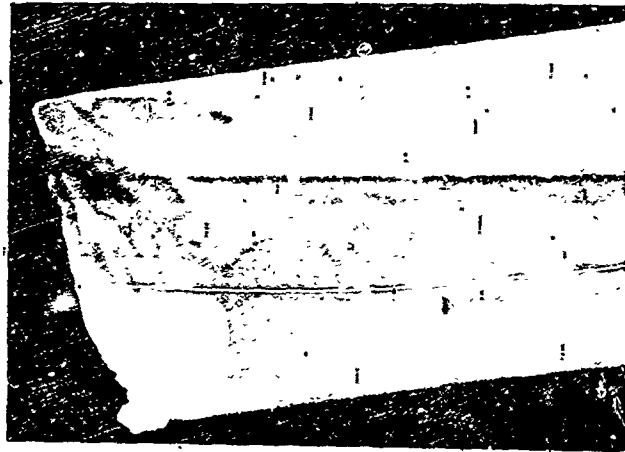
Fig. 8. Scanning Electron Microscope Views of Astroquartz Fibers with A-1100 Scotchcast Coating

TABLE 4. MEASUREMENTS OF FIBER ANGLE
(Series 1 Test Specimens)

| Sample Number | Molding Pressure (psi) | Axial Direction ¹ | | Thickness Direction ² |
|----------------|------------------------|------------------------------|----------------------------|----------------------------------|
| | | Average Angle (deg) | Standard Dev. (\pm deg) | Range of Angle (deg.) |
| A1 | | 33.0 | 2.22 | 20 - 22 |
| A2 | | 34.8 | 5.08 | 28 - 33 |
| B1 | 1000 | 37.9 | 5.90 | 22 - 28 |
| B2 | | 36.3 | 3.93 | 23 - 31 |
| C1 | 125 | 30.4 | 2.54 | 23 - 26 |
| C2 | | 31.5 | 3.03 | 20 - 22 |
| D ^b | 1000 | 25 - 27 | | 19 - 27 |
| E ^b | | 25 - 28 | | 16 - 21 |
| F ^b | | 22 - 26 | | 15 - 18 |
| G1 | 300 | 30.6 | 4.81 | 16 - 20 |
| G2 | | 33.3 | 5.09 | 24 - 26 |
| H1 | 1000 | 31.8 | 2.80 | 18 - 23 |
| H2 | | 28.7 | 2.93 | 16 - 21 |
| I1 | 125 | 35.2 | 5.20 | 20 - 28 |
| I2 | | 32.2 | 5.08 | 20 - 23 |
| J1 | 300 | 31.5 | 5.21 | 20 - 23 |
| J2 | | 30.6 | 5.00 | 20 - 25 |
| K1 | 1000 | 30.0 | 3.52 | 22 - 24 |
| K2 | | 30.0 | 4.75 | 18 - 22 |
| L1 | 125 | 35.2 | 5.20 | 22 - 26 |
| L2 | | 29.9 | 5.00 | 21 - 23 |

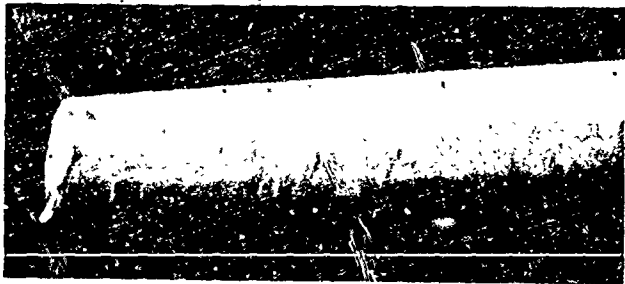
1-Data involve 12 measurements.

2- Fiber angles of specimens D, E and F measured by protractor, while fiber angle measurements on all other specimens were made optically.



4250X

Reproduced from
best available copy.



1700X



1000X



170X

Note: Nominal fiber diameter is 10 microns.

Fig. 9. SEM Views of Astroquartz Fibers After Pyrolysis at 800°F.

TABLE 5. CHARACTERISTICS OF SERIES NO. 2 TEST SPECIMENS
(All Molded At 125 psi)

| Sample Number | Approx. Woven Dimensions (in. x in. x in) | Woven Density (gm/cc) | Density ¹ Post Pyrol. (gm/cc) | Density Post HF (gm/cc) | Density ² Post 1st Silane (gm/cc) | Density ³ Post 2nd Silane (gm/cc) | Impregnation Condition | Molded Density (gm/cc) | Fiber Wt. (%) | Resin Wt. (%) | Fiber Vol. (%) | Resin Vol. (%) | Porosity Vol. (%) |
|---------------|---|-----------------------|--|-------------------------|--|--|------------------------|------------------------|-------------------|---------------|-------------------|----------------|-------------------|
| M1 | 10.13 x 0.9 x 0.410 | 0.74 | 0.71 | 0.69 | 0.70 | 0.70 | | 1.64 | 81.8 | 18.2 | 61.0 | 23.3 | 15.7 |
| M2 | | | | | | | | 1.71 | 88.7 | 11.3 | 68.9 | 15.1 | 16.0 |
| N1 | 10.50 x 0.9 x 0.410 | 0.74 | 0.71 | 0.68 | 0.69 | 0.70 | 3 Impreg. | 1.63 | 80.2 | 19.8 | 59.4 | 25.2 | 15.4 |
| N2 | | | | | | | | 1.67 | 87.0 | 13.0 | 66.0 | 17.0 | 17.0 |
| O1 | 10.13 x 0.9 x 0.410 | 0.77 | 0.70 | 0.72 | 0.72 | 0.73 | | 1.60 | 83.4 | 16.6 | 60.7 | 20.8 | 18.5 |
| O2 | | | | | | | | 1.69 | 89.8 | 10.2 | 69.0 | 13.5 | 17.5 |
| P1 | 10.13 x 0.9 x 0.425 | 0.73 | 0.70 | 0.68 | 0.68 | --- | Single Impreg. | 1.72 | 91.3 | 8.7 | 71.4 | 11.7 | 16.9 |
| P2 | | | | | | | | 1.75 | 95.9 | 4.1 | 76.3 | 8.6 | 18.1 |
| Q1 | 10.25 x 0.9 x 0.420 | 0.73 | 0.70 | 0.68 | 0.68 | --- | | 1.72 | 92.1 | 7.9 | 72.0 | 10.6 | 17.4 |
| Q2 | | | | | | | | 1.74 | 96.3 | 3.7 | 76.2 | 5.0 | 18.8 |
| R1 | 10.13 x 0.9 x 0.425 | 0.74 | 0.71 | 0.69 | 0.69 | --- | | 1.80 | 99.9 | 0.1 | 81.7 | 0.14 | 18.1 |
| R2 | | | | | | | | 1.76 | 93.6 | 3.4 | 74.3 | 4.7 | 20.4 |
| S1 | 10.13 x 0.9 x 0.425 | 0.74 | 0.71 | 0.68 | 0.69 | 0.69 | Cab-O-Sil Added | 1.61 | 75.2 ⁴ | 24.8 | 55.0 ⁵ | 31.3 | 10.6 |
| S2 | | | | | | | | 1.68 | 74.4 ⁴ | 25.6 | 56.8 ⁵ | 33.6 | 6.3 |
| T1 | 10.0 x 0.9 x 0.440 | 0.74 | 0.69 | 0.67 | 0.67 | 0.68 | | 1.52 | 78.1 ⁴ | 21.9 | 54.0 ⁵ | 26.0 | 17.0 |
| T2 | | | | | | | | 1.60 | 78.2 ⁴ | 21.8 | 56.9 ⁵ | 27.3 | 12.8 |
| U1 | 10.13 x 0.9 x 0.425 | 0.72 | 0.69 | 0.67 | 0.67 | --- | Single Impreg. | 1.80 | 86.1 | 13.9 | 70.4 | 19.6 | 10.0 |
| U2 | | | | | | | | 1.83 | 92.8 | 7.2 | 77.2 | 10.3 | 12.5 |
| V1 | 10.0 x 0.9 x 0.435 | 0.72 | 0.69 | 0.67 | 0.67 | --- | | 1.79 | 87.2 | 12.8 | 70.9 | 17.9 | 11.2 |
| V2 | | | | | | | | 1.81 | 95.6 | 4.4 | 78.7 | 6.2 | 15.1 |
| X1 | 10.0 x 0.9 x 0.425 | 0.72 | | | | | | | | | | | |
| X2 | | | | | | | | | | | | | |

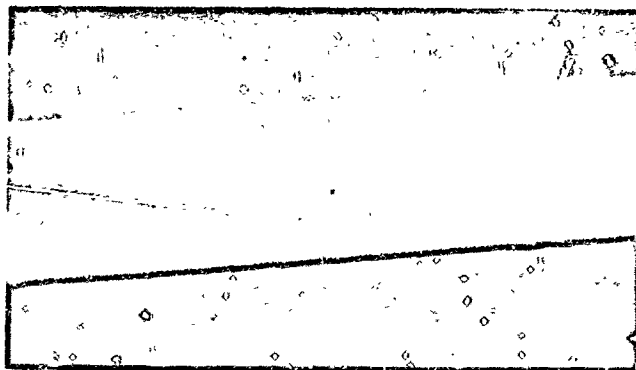
1- Pyrolysis carried out at 800°F for 16 hours

2- First silane treatment involved a 1% solution of silane in acetone.

3- Second silane treatment: involved a 10% solution of silane acetone.

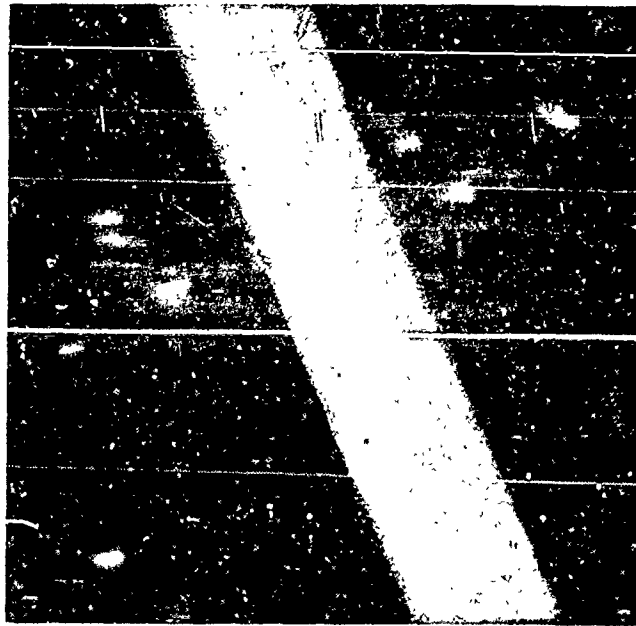
4- Value includes 4.3 weight percent of Cab-O-Sil.

5- Value includes 3.0 volume percent of Cab-O-Sil.



2000X

Etched with 10% HF
for 1 minute.



2000X

Etched fibers treated with
1% silane.



2000X

Etched fibers treated with
10% silane.

Note: Nominal filament diameter is 10 microns.

Fig. 10. SEM Views of Etched, One and Ten Percent Silane-Treated Astroquartz Fibers

after etching with 10 percent HF for one minute. No fiber notching or ragged edges are apparent in this view; as they are not visible in the previous 1700X view of the pyrolyzed fibers, although as discussed, the 1000X view shows apparent damage. The next two photos in Fig. 10 show the 1 percent and 10 percent silane treatments. No additional material adhering to the filaments is apparent for the 1 percent case, although some film may appear at the top of the center and leftmost fiber treated at 10 percent. It is observed in the discussion of the phase 1 mechanical testing that the 1 percent silane treated fibers gave about 25 percent superior mechanical strength.

2.4.2.4 Impregnation with SR-350 Resin

SR-350 methyl silicone resin was dissolved in an equal weight of acetone. The solution was then filtered through a Buchner funnel to remove solid contaminants. Three 10-inch long specimens (samples M, N, and O) were immersed in the filtered silicone resin solution and subjected to vacuum to facilitate impregnation of the quartz construction by the resin. The impregnated samples were then removed from the resin solution and allowed to stand for 4 hours. This impregnation process was repeated. A third impregnation of these specimens was carried out using a filtered 65/35 SR-350/acetone solution and then allowed to stand for 16 hours. Single impregnations, using the 65/35 solution, were carried out with specimens P, Q, R, U, and V.

A single impregnation was made using a 50/50 resin/solvent solution to which 4.3 weight percent of Cab-O-Sil (previously dried at 250°F) had been added. Samples S and T were impregnated with this solution.

2.4.2.5 Molding Procedure

The same molding procedure described in Section 2.4.1.5 was employed with the molding of series 2 test specimens, M through V, except all samples were molded at 125 psi.

2.4.2.6 Preparation of Specimens for Test

All series 2 test specimens were sectioned and prepared in accordance with the description in Section 2.4.1.6. In order to determine the effect of a non-continuously woven edge, approximately 0.035 inch was machined from the edges of the specimens specified in Table 6 which also summarizes the processing variables to which the test specimens were subjected.

An optical comparator was again used to determine fiber angle. The results of angular measurements are summarized in Table 7 for comparison with the series 1 data of Table 4.

TABLE 6. PROCESSING VARIABLES
(Series 2 Test Specimens)

| Sample Number | Group No. | High Silane ¹ Conc. | Low Silane ² Conc. | Non-Machined Edges | Machined ³ Edges | Cab-O-Sil ⁴ Addition | Platco-Slap Tested |
|----------------------------------|-----------|--------------------------------|-------------------------------|--------------------|-----------------------------|---------------------------------|--------------------|
| M1 M2 N1 O1 | A | X | | X | | | X |
| N2 O2 | B | X | | | X | | |
| P1 P2 U1 Q1 U2 V2 | C | | X | X | | | X X X |
| Q2 R1 R2 V1 | D | | X | | X | | |
| S1 S2 | E | X | | X | | X | |
| T1 T2 | F | X | | | X | X | |

1- High silane concentration--10 weight percent in acetone.

2- Low silane concentration--1 weight percent in acetone.

3- Edges of tensile specimen machined from 0.81 in. wide to 0.74 inch wide.

4- 4.3 weight percent Cab-O-Sil (silica) added.

TABLE 7. MEASUREMENTS OF FIBER ANGLE
(Series 2 Test Specimens)

| Sample Number | Pre-Test Characterization ¹ Optical Comparator | | Post-Test Fiber Bundle Tracing | Thickness Direction |
|---------------|--|------------------------------------|-----------------------------------|-------------------------|
| | Average Angle (deg) | Standard Deviation (\pm deg) | Average Angle (deg) | Range of Angle (deg) |
| M1 | 28.0 | 4.40 | 34.0 | - |
| M2 | 31.0 | 4.82 | 33.7 | 24 - 36 |
| N1 | 30.0 | 4.90 | 31.5 | 15 - 20 |
| N2 | 27.8 | 3.91 | 31.5 | 14 - 21 |
| O1 | 23.8 ³ | 5.09 | 30.0 | 19 - 21 |
| O2 | 25.8 | 3.32 | 31.0 | 18 - 20 |
| P1 | 23.5 ² | 3.51 | 33.0 | 17 - 22 |
| P2 | 23.6 ² | 3.64 | 28.5 | 16 - 20 |
| Q1 | 24.6 | 3.63 | 33.0 | 10 - 20 |
| Q2 | 24.5 | 2.20 | 32.0 | 16 |
| R1 | 23.8 | 2.25 | 32.0 | 15 - 25 |
| R2 | 26.5 | 2.61 | 34.0 | 21 - 23 |
| S1 | 19.6 ² | 3.33 | 27.0 | - |
| S2 | 19.9 ⁴ | 4.46 | 26.0 | - |
| T1 | 17.9 | 3.80 | 28.0 | 17 - 21 |
| T2 | 21.8 | 4.88 | 29.0 | 20 - 25 |
| U1 | 23.3 ² | 5.26 | 34.0 | 14 - 18 |
| U2 | 24.0 | 2.04 | 31.0 | - |
| V1 | 27.2 | 4.28 | 34.0 | 20 - 24 |
| V2 | 25.4 | 2.35 | 30.0 | - |

1- data involves 12 measurements for most specimens unless otherwise indicated

2- data involves 24 measurements

3- data involves 8 measurements

4- data involves 10 measurements

NOTE: Two different axial direction measurement techniques discussed in Section 2.4.2.6.

However, using the same technique as for series 1, the series 2 specimens were found to yield a confusing range of angles, especially for the specimens loaded with Cab-O-Sil. The narrow geometry of the specimen in general, and the woven edges in particular, resulted in fiber distortions during compression molding which would not be as much a factor with the normally larger dimension specimen. At the time of post-test evaluation, the angles were remeasured by tracing out fiber bundles in a specimen area representative of the fracture zone. These angles are generally larger than those initially measured in Table 7, but are comparable to those found for the series 1 specimens. It will be seen in the analysis of the mechanical test results below that the angular parameter is of paramount importance for interpretation of the results.

2.5 PROCESSING OF TEST SPECIMENS (PHASE 2)

2.5.1 Quartz Omniweave Construction (Scarf 331-Q3BA)

Omniweave scarf 331-Q3BA was woven in the standard "A" (45-degree cubic) construction. The properties of the quartz scarf are described in Table 8.

2.5.1.1 Pyrolyzation of Omniweave Construction

The woven construction was pyrolyzed in an air circulating oven at 930° F for 16 hours. After cooling, the construction was weighed and the change in density is shown in Table 9.

2.5.1.2 Hydrofluoric Acid Etching

The pyrolyzed construction was immersed into a polyethylene lined, stainless steel tray containing 10 percent weight aqueous hydrofluoric acid. The quartz construction was etched for 60 seconds. The aqueous HF solution was then poured from the tray and the woven structure was flooded with cold tap water until a pH indication of > 6.5 was attained. The scarf was then washed with distilled water and dried at 250° F for 4 hours. The density of the etched construction is tabulated in Table 9.

The etched construction was then cut into three sections approximately 8 x 6 inches each. The sections were designated as 331-1, 331-2 and 331-3.

2.5.1.3 Application of Coupler

Scarf segment 331-1 was immersed in a 1 percent weight solution of silane coupler for 15 minutes. The specimen was allowed to air-dry 16 hours and then cured at 225° for 4 hours. The density change produced by the silane treatment was negligible.

2.5.1.4 Impregnation with SR-350 Resin

SR-350 methyl silicone resin was dissolved in an equal weight of acetone. The solution was then filtered through a Buchner funnel to remove solid contaminants. All three sectioned quartz constructions (331-1, 331-2 and 331-3) were immersed in the silicone resin solution and subjected to vacuum to efficiently impregnate the scarf segments with the resin solution. After allowing the impregnated segments to air-dry for 16 hours, they were B-staged at 180° F for 3 hours.

2.5.1.5 Molding Procedure

A mold was fabricated to accommodate each of the three impregnated Omniweave segments. The mold consisted of aluminum bars bonded in the form of a frame onto a 3/8-inch thick aluminum base plate. The aluminum bars, 1-inch wide x 1/4-inch

TABLE 8. CHARACTERISTICS OF OMNIWEAVE CONSTRUCTIONS, PHASE 2

| Parameter | 331-Q3BA | 318-Q3JA | 319-Q3JA | 320-Q3JA |
|-----------------------------------|---|-------------------|----------------------------------|------------------|
| Weave No. | | | | |
| Thickness x Width, layers | 10 x 84 | 8 x 84 | 16 x 84 | 32 x 84 |
| Weave Pattern | | | | "A" (Cubic) |
| Type of Fiber | | | #552 (20-End) Astroquartz Roving | |
| Fiber Binder Coating | 9089 Silicone | | Teflon (2.7%) | |
| Fiber Treatment | Scotchcast 221, Polyurethane (4 pbw in acetone) | | | None |
| Woven Dimensions, in. | 25.2 x 6.0 x 0.56 | 26.8 x 5.4 x 0.35 | 23.0 x 5.0 x 0.75 | 23 x 4.75 x 1.63 |
| Woven Bulk Density, g/cc | 0.79 | 1.01 | 1.10 | 1.02 - 1.07 |
| Axial Angle, deg.* | 40 | 37 - 45 | 45 | 30 - 35 |
| Through-the-Thickness Angle, deg. | 45 | 45 | 45 | 45 |

*Designated "fiber pitch angle", as in Reference 1.

TABLE 9. CHARACTERISTICS OF ADL-10 COMPOSITE PANELS 331

| Sample No. | Density Woven (gm/cc) | Density Post Pyrol (gm/cc) | Density Post HF (gm/cc) | Density Post Silane (gm/cc) | Molding Pressure (psi) | Final Process* Density (gm/cc) | Fiber Wt. (%) | SiO ₂ Wt. (%) | Resin Wt. (%) | Fiber Vol. (%) | SiO ₂ Vol. (%) | Resin Vol. (%) | Porosity Vol. (%) |
|------------|-----------------------|----------------------------|-------------------------|-----------------------------|------------------------|--------------------------------|---------------|--------------------------|---------------|----------------|---------------------------|----------------|-------------------|
| 331 -1 | | | | 0.72 | 150 | 1.59 | 82.5 | -- | 17.5 | 59.6 | -- | 21.8 | 18.6 |
| 331 -2 | 0.79 | 0.76 | 0.72 | ---- | 1000 | 1.68 | 87.7 | -- | 12.3 | 67.0 | -- | 16.1 | 16.9 |
| 331 -3 | | | | ---- | 150 | 1.47 | 78.3 | -- | 21.7 | 52.3 | -- | 24.9 | 22.8 |

* After second resin impregnation.

high, were situated to conform to the approximate length and width of each impregnated Omniweave segment. It was assumed that the applied pressure would compress the woven segment to the 1/4-inch height of the aluminum bars.

A thin film of silicone grease was applied to the surface of the mold to facilitate release after molding of the ADL-10 panels. The mold was then preheated to 180° F. One of the hot B-staged, woven segments (described in Section 2.5.1.4) was then placed in the pre-heated mold. A 3/8-inch thick, mold released, aluminum plate was also pre-heated to 180° F and used as a top plate on the mold assembly. The entire assembly was placed between the platens of a press, preheated to 180° F.

After subjecting impregnated specimen 331-1 to 150 psi, the temperature of the platens was adjusted to 250° F for 1 hour, 325° for 1 hour and, finally 400° F for 16 hours. Specimens 331-2 and 331-3 were also subjected to the same curing temperature, except specimen 331-2 was subjected to 1000 psi instead of 150 psi.

In all three instances, the 1/4-inch high aluminum bars restricted dimensional change in the length and width directions. This dimensional restriction inhibited shouldering of the top mold plate on the 1/4-inch aluminum bars which served as mold stops, both at 150 psi and 1000 psi. This resistance to compression resulted in the attainment of panels having relatively low densities. Panels 331-1, 331-2 and 331-3 had densities of 1.52 to 1.64 and 1.40 gm/cc respectively. Therefore, the panels were reimpregnated with solvated SR-350 resin. The panels were immersed in the resin solution and subjected to alternating 30 minute cycles of vacuum and pressure (70 lb) over a period of 4 hours. The panels were then removed from the impregnation chamber and allowed to air dry 16 hours. The panels were then cured in an air circulating oven for 2 hours at 150° F and 16 hours at 400° F. The densities of the 331-1, 331-2 and 331-3 panels increased to 1.59, 1.68 and 1.47 gm/cc respectively. It should be emphasized that the densities are still relatively low, compared to the 1.7 gm/cc density that it should be possible to attain with a starting Omniweave density of 0.9-1.0 gm/cc and successful molding.

2.5.1.6 Preparation of Specimens for Test

Various configurations of test specimens were machined from the panels. The specimens were subsequently subjected to the following tests:

- | | |
|-------------------------|----------------|
| a. Tensile | e. Ultrasonic |
| b. Flexure | f. Dielectric |
| c. Thermal Conductivity | g. RF/Ablation |
| d. Thermal Expansion | h. Plate-Slap |

The dimensions of these specimens are included in the applicable test description in Section 3.1, "Sampling Plan".

Specimens were prepared for tensile testing in accordance with the method given in Section 2.4.1.6.

2.5.2 Quartz Omniweave Construction (Scarf 318-Q3JA)

Omniweave scarf 318-Q3JA was woven in the standard "A" (45 degree cubic) construction. Unlike previous Omniweave constructions, the quartz fibers comprising the 20-end roving were coated with Teflon in lieu of a silane or silicone binder coating. This lubricative coating precluded the necessity for the application of a polyurethane coating to facilitate weaving. In addition, the Teflon coating was responsible for the attainment of closer fiber packing during the weaving process which resulted in the attainment of woven densities greater than 1.0 gm/cc compared to 0.8 gm/cc using the polyurethane coating. The properties of the woven construction are summarized in Table 8. The woven scarf was cut in half prior to further processing.

2.5.2.1 Pyrolyzation of Omniweave Construction

Both Omniweave segments were pyrolyzed in an air circulating oven at 930° F for 16 hours, followed by 3 hours at 1000° F and 1 hour at 1100° F. After cooling, each pyrolyzed section was weighed and the change in density is shown in Table 10.

2.5.2.2 Hydrofluoric Acid Etching

The pyrolyzed constructions were etched in hydrofluoric acid in accordance with the description in Section 2.5.1.2. The density change caused by the etching process is included in Table 10.

2.5.2.3 Application of Coupling Agent

The quartz fibers in both etched constructions were coated with silane coupler in accordance with the description in Section 2.5.1.3. The density change produced by the silane treatment was negligible.

Each of the two treated constructions were again cut in half resulting in 4 segments designated as 318-1, 318-2, 318-3 and 318-4.

2.5.2.4 Impregnation with SR-350 Resin

All 4 segments were immersed in a filtered, 65 weight percent SR-350 in acetone and subjected to vacuum to efficiently impregnate the scarf segments with the resin solution. The segments were allowed to air-dry at least 16 hours.

TABLE 10. CHARACTERISTICS OF MARKITE SILICA/SILICA 318 COMPOSITE PANELS

| Sample No. | Density Woven (gm/cc) | Density Post Pyrol (gm/cc) | Density Post HF (gm/cc) | Density Post Silane (gm/cc) | Molding Pressure (psi) | Final(1) Density (gm/cc) | TTT(2) Angle (deg) | Fiber Wt. (%) | SiO ₂ Wt. (%) | Resin Wt. (%) | Fiber Vol. (%) | SiO ₂ Vol. (%) | Resin Vol. (%) | Porosity Vol. (%) |
|------------|-----------------------|----------------------------|-------------------------|-----------------------------|------------------------|--------------------------|--------------------|---------------|--------------------------|---------------|----------------|---------------------------|----------------|-------------------|
| 318-1R2 | | | | | Cast | 1.74 | 18 | 61.1 | 6.5 | 32.4 | 48.3 | 5.1 | 44.1 | 2.5 |
| 318-1P3 | | | | 1.67 | | 18 | 63.6 | 28.5 | 7.9 | 10.3 | 19.8 | | | |
| 318-2P2 | | | | 1.70 | | 25 | 59.2 | 13.8 | 27.0 | 35.8 | 7.7 | | | |
| 318-2P3 | 1.01 | 0.98 | 0.94 | 0.94 | | 1.64 | 25 | 61.4 | 30.6 | 8.0 | 45.8 | 22.8 | 10.2 | 21.2 |
| 318-3R2 | | | | | 15 | 1.86 | 28 | 79.7 | 2.6 | 17.7 | 67.4 | 2.2 | 25.7 | 4.7 |
| 318-3P3 | | | | | | 28 | | | | | | | | |
| 318-4R1 | | | | | | 1.92 | 12 | 80.1 | 5.8 | 14.1 | 69.9 | 5.1 | 21.1 | 3.9 |
| 318-4P3 | | | | | 1000 | 1.89 | 12 | 81.4 | 14.1 | 4.5 | 69.9 | 12.1 | 6.7 | 11.3 |
| 318-4S3 | | | | | | 12 | | | | | | | | |

(1) Sec Section 2. 5. 2. 6 for process labelling.

(2) TTT - through-the-thickness

2.5.2.5 Casting and Molding Procedures

A. Casting of Scarf 318-2

A filtered solution of 65 weight percent SR-350 in acetone was degassed in a vacuum desiccator until viscous bubbles were evident. The solution was then decanted into a casting mold containing the pre-impregnated 318-2 scarf. The casting mold with its contents was then placed in a vacuum desiccator and the solution was again subjected to vacuum until the bubbles were too viscous to break.

The mold containing the scarf and resin solution was then placed into an air circulating oven and subjected to the following cure cycle:

| <u>TEMP.</u> (° F) | <u>TIME</u> (hr.) |
|-----------------------|----------------------|
| 135 | 16 |
| 200 | 2 |
| 225 | 2 |
| 250 | 5 |
| 325 | 1 |
| 400 | 16 |

B. Casting of Scarf 318-1

The techniques employed in casting the 318-2 scarf were also used in casting the 318-1 scarf, except for the cure cycle which was carried out in accordance with the following time-temperature history:

| <u>TEMP.</u> (° F) | <u>TIME</u> (hr.) |
|-----------------------|----------------------|
| 135 | 16 |
| 200 | 2 |
| 225 | 2 |
| 250 | 16 |
| 325 | 2 |
| 400 | 168 |

C. Molding of Scarf 318-3

Impregnated scarf 318-3 was B-staged 4 hours at 200° F. The B-staged scarf was then placed in a press with platens preheated to 200° F.

After subjecting the woven specimen to 15 psi, the temperature of the platens was adjusted to and maintained at 250° F for 2 hours, 325° F for 2 hours, and finally 400° F for 16 hours. The molded panel was allowed to cool to room temperature under 15 psi and then removed from the press.

D. Molding of Scarf 318-4

The same procedure employed in the molding of the 318-3 scarf was also used to mold the 318-4 woven construction, except a pressure of 1000 psi was applied in lieu of 15 psi.

2.5.2.6 Pyrolyzation and Reimpregnation Cycles

The two cast and two molded ADL-10 panels were subjected to pyrolysis at 950° F for 16 hours followed by 2 hours at 1100° F. After cooling, the properties of the panels were recorded. The panels were then immersed in a filtered solution of 65 weight percent SR-350 in acetone contained in a pressure chamber. The panels and the solvated resin were subjected to 30 minutes cycles of vacuum (25 inches of mercury) and pressure (75 lb.) over a period of 8 hours. The panels were then permitted to remain in the evacuated chamber for 16 hours. The translucent panels were then removed from the pressure chamber and allowed to air-dry for at least 16 hours. The panels were cured in an air circulating oven for 2 hours at 135° F, followed by 16 hours at 400° F.

This pyrolyzation-reimpregnation cycle was repeated a second time prior to the machining of test specimens. This material would then be designated by the panel number (e.g., 318-4) with a suffix for the processing which indicates the number of pyrolyses and reimpregnations. After the above initial pyrolysis, reimpregnation, second pyrolysis and second reimpregnation, the material would be designated 318-4R2. The characteristics of the four panels are included in Table 10.

2.5.2.7 Preparation of Specimens for Test

Various configurations of test specimens were machined from the panels. The specimens were subsequently subjected to the tests tabulated in Section 2.5.1.6.

It should be emphasized, however, that after machining, some of the specimens were subjected to final pyrolysis at either 1600° F or 2250° F. Those specimens subjected to a final pyrolyzation at 1600° F were assigned a suffix "P" and those sintered at 2250° F for 1 hour, a suffix "S". These specimens would then have a final suffix of either P3 or S3 (see Table 10).

2.5.3 Quartz Omniweave Construction (Scarf 319-Q35A)

The quartz Omniweave construction 319-Q3JA was very similar to that described in Section 2.5.2 except for thickness. The 319 scarf was 0.75 inch thick, while the 318 construction had a woven thickness of 0.35 inch. The properties of the 319 scarf are included in Table 8.

The woven scarf was cut in half. One segment, designated 319-2, was set aside for direct impregnation with SR-350 resin, while segment 319-1 was processed in accordance with the description in the following sections.

2.5.3.1 Pyrolyzation of Omniweave Construction 319-1 to Remove Teflon Coating

Omniweave segment 319-1 was pyrolyzed in an air circulating oven at 930° F for 24 hours, followed by 16 hours at 1000° F, and 2 hours at 1100° F. After cooling, the pyrolyzed section was weighed and the change in density is shown in Table 11. The Teflon coating was not removed from 319-2 before impregnation.

2.5.3.2 Hydrofluoric Acid Etching

The pyrolyzed construction was etched in hydrofluoric acid in accordance with the description in Section 2.5.1.3. The density change caused by the etching process is included in Table 11.

2.5.3.3 Application of Coupling Agent

The quartz fibers in the etched construction was coated with silane coupler in accordance with the description in Section 2.5.1.3. The density change produced by the silane treatment was negligible.

2.5.3.4 Impregnation with SR-350 Resin

Teflon coated segment 319-2 and processed segment 319-1 were immersed in a filtered solution of 65 weight percent SR-350 in acetone and subjected to vacuum to efficiently impregnate the scarf segments with the resin solution. The impregnated segments were allowed to air-dry at least 16 hours.

2.5.3.5 Molding Procedure

The impregnated constructions were B-staged 4.5 hours at 200° F. Each B-staged segment was then transferred to a press with platens preheated to 200° F.

After subjecting each impregnated specimen to 125 psi, the temperature of the platens was adjusted to and maintained at 250° F for 1 hour, 325° F for 1 hour and finally 400° F for 16 hours. Each molded panel was allowed to cool to room temperature under 125 psi and then removed from the press.

TABLE 11. CHARACTERISTICS OF 319 PYROLYZED COMPOSITE PANELS
(WOVEN WITH TEFLON COATED FIBERS)

| Sample No. | Density Woven (gm/cc) | Density Post Pyrol (gm/cc) | Density Post HF (gm/cc) | Density Post Silane (gm/cc) | Molding Pressure (psi) | Final Density (gm/cc) | TTT ⁽¹⁾ Angle (deg) | Fiber Wt. (%) | SiO ₂ Wt. (%) | Resin Wt. (%) | Fiber Vol. (%) | SiO ₂ Vol. (%) | Resin Vol. (%) | Porosity Vol. (%) |
|------------|-----------------------|----------------------------|-------------------------|-----------------------------|------------------------|-----------------------|--------------------------------|---------------|--------------------------|---------------|----------------|---------------------------|----------------|-------------------|
| 319-1R1 | | 1.13 | 1.09 | 1.09 | | 1.93 | 18 | 82.5 | 5.9 | 11.5 | 72.4 | 5.2 | 17.4 | 5.0 |
| 319-1P2 | | | | | | 1.90 | 18 | 83.8 | 15.7 | 0.4 | 72.4 | 13.6 | 0.6 | 13.4 |
| 319-2R2 | 1.16 | | | | 125 | 2.00 | 24 | 78.4 | 8.4 | 13.2 | 71.3 | 7.6 | 20.7 | 0.4 |
| 319-2P3 | | | | | | 1.98 | 24 | 79.2 | 18.6 | 2.2 | 71.3 | 16.8 | 3.3 | 8.6 |

(1) TTT = through the thickness

2.5.3.6 Pyrolyzation and Reimpregnation Cycles

The techniques described in Section 2.5.2.6, which were used to pyrolyze and reimpregnate the 318 panels were also used to process the 319 panels. It should be noted, however, that while scarf 319-2 was subjected to two pyrolyzation-reimpregnation cycles, scarf 319-1 was subjected to one cycle. The characteristics of the two panels are included in Table 11.

2.5.3.7 Preparation of Specimens for Test

The preparation of the 318 specimens as well as the sample nomenclature described in Section 2.5.2.7 are also applicable for the 319 test specimens.

2.5.4 Quartz Omniweave Construction (Scarf 320-Q3JA)

Quartz Omniweave construction 320-Q3JA was very similar to that described in Section 2.5.2 except for thickness. The 320 scarf was 1.6 inch thick, while the 318 construction had a woven thickness of 0.35 inch. The properties of the 320 scarf are included in Table 8.

The woven scarf was cut in half. One segment was temporarily designated 320-1, 2 and set aside for direct impregnation with SR-350 resin, while the other segment was designated 320-3, 4.

2.5.4.1 Pyrolyzation of Omniweave Construction 320-3, 4

Omniweave segment 320-3, 4 was pyrolyzed in an air circulating oven at 950° F for 16 hours followed by 2 hours at 1100° F. After cooling, the pyrolyzed segment was weighed and the change in density is shown in Table 12.

2.5.4.2 Impregnation with SR-350 Resin

Teflon coated segment 320-1, 2 and pyrolyzed segment 320-3, 4 were immersed in filtered, 65 weight percent SR-350 in acetone and subjected to vacuum to efficiently impregnate the scarf segments with the resin solution. The segments were allowed to air-dry at least 16 hours.

2.5.4.3 Molding Procedure

The impregnated constructions were B-staged 4 hours at 200° F. The B-staged segments were fitted with a vacuum bag assembly and subjected to 12.7 psi (vacuum) at 400° F for 8 hours. The segments were then removed from the vacuum bag and post-cured at 400° F for 16 hours. After cooling, each segment was cut in half using a cut-off wheel. Segment 320-1, 2 was divided into segments 320-1 and 320-2, while segment 320-3, 4 was divided into segments 320-3 and 320-4.

TABLE 12. CHARACTERISTICS OF MARKITE SILICA/SILICA 320 COMPOSITE PANELS

| Sample No. | Density Woven (gm/cc) | Density Post Pyrol (gm/cc) | Density Post HF (gm/cc) | Density Post Silane (gm/cc) | Molding Pressure (psi) | Process* Density (gm/cc) | Fiber Wt. (%) | SiO ₂ Wt. (%) | Resin Wt. (%) | Fiber Vol. (%) | SiO ₂ Vol. (%) | Resin Vol. (%) | Porosity (%) |
|------------|-----------------------|----------------------------|-------------------------|-----------------------------|------------------------|--------------------------|---------------|--------------------------|---------------|----------------|---------------------------|----------------|--------------|
| 320-1R2 | | | | | | 1.66 | 80.8 | 10.5 | 8.7 | 61.0 | 7.9 | 11.2 | 19.9 |
| 320-1P3 | | | | | | | | | | | | | |
| 320-2R2 | 1.02 | -- | -- | -- | | 1.63 | 77.5 | 13.5 | 9.0 | 57.4 | 10.0 | 11.5 | 21.1 |
| 320-2P3 | | | | | 12.7 | | | | | | | | |
| 320-3R2 | | | | | | 1.55 | 74.3 | 15.3 | 10.4 | 52.3 | 10.8 | 12.6 | 24.3 |
| 320-3P3 | | | | | | | | | | | | | |
| 320-4R2 | 1.07 | 0.98 | -- | -- | | 1.56 | 75.7 | 13.7 | 10.6 | 53.7 | 9.7 | 12.9 | 23.7 |
| 320-4P3 | | | | | | | | | | | | | |

* Processing not completed.

2.5.4.4 Pyrolyzation and Reimpregnation Cycles

The techniques described in Section 2.5.2.6, which were used to pyrolyze and reimpregnate the 318 panels, were also used to process the 320 panels. The panels were subjected to the 1100° F pyrolyzation portion of a third cycle, when work on this phase of the development effort was concluded. The characteristics of the partially processed 320 panels are included in Table 12.

2.5.5 Unidirectional Quartz Construction

An effort was made to determine the maximum tensile capabilities of a unidirectionally oriented-composite comprised of the same constituents used to prepare the ADL-10 Omniweave constructions. This was carried out to compare the performance of the two types of constructions as well as to determine whether tenacious adhesion between fiber and matrix resin was achieved. Since the tensile strength and modulus of the unidirectional quartz fibers are known, the evaluation of the tensile performance of the unidirectional composite could serve as a useful indicator with respect to resin-fiber adhesion.

2.5.5.1 Impregnation of Quartz Roving

Approximately 1000 feet of 20-end Astroquartz roving coated with A-1100 coupler coating were also coated with a 1 weight percent acetone solution of the silane coupling agent used to coat the Omniweave constructions prior to impregnation with SR-350 resin.

The coated roving was allowed to air-dry 16 hours. The roving was then filament wound, in a circumferential fashion, around an 11-inch diameter aluminum drum, covered with Mylar film to facilitate release after impregnation. As the filaments were wound onto the drum, a 65 weight percent solution of SR-350 in acetone was brushed onto the roving. After a 12 inch long circumferential layer of impregnated roving had been applied to the drum, filament winding was terminated. The impregnated sheet on the drum was slit along its length yielding a unidirectionally oriented composite sheet 36 x 12 x 0.025 inch. A second sheet of Mylar film was used to cover the impregnated sheet of roving.

2.5.5.2 Molding Procedure

While still sandwiched between the Mylar parting film, strips, 9.5 x 0.8 inch, were cut along the axis of the unidirectional fibers. After removal of the film, stacks of 7 strips were placed into each of the three channels of the mold illustrated in Fig. 6. After the lid of the mold was set in place, the entire assembly was placed into an air circulating oven at 180° F for 2½ hours. The mold was then transferred to a press with platens pre-heated to 180° F. After adjusting the pressure on the specimens to 1000

psi the temperature was adjusted and maintained at 250° F for 1 hour, at 325° F for 1 hour and finally at 400° F for 16 hours. The mold was allowed to cool to room temperature while still under the aforementioned pressure. The specimens were then removed from the mold. The characteristics of the specimens are described in Table 13.

TABLE 13. CHARACTERISTICS OF UNIDIRECTIONAL COMPOSITE

| | 1 | 2 | 3 |
|------------------|------|------|------|
| Density, gm/cc | 1.41 | 1.44 | 1.39 |
| Fiber, Wt, % | 46.6 | 45.8 | 44.5 |
| Resin, Wt., % | 53.4 | 54.2 | 55.5 |
| Fiber Vol., % | 29.9 | 30.0 | 28.1 |
| Resin Vol., % | 58.8 | 61.0 | 60.3 |
| Porosity Vol., % | 11.3 | 9.0 | 11.6 |

2.5.5.3 Preparation of Tensile Test Specimens

Tensile specimens were prepared in accordance with the description in Section 2.4.1.6. Radiographs of these specimens are shown in Fig. 21.

2.5.6 SR-350 Disc Molding Procedure

The SR-350 silicone resin was aged at 180° F for 24 hours, then loaded into a 4-3/4 inch diameter compression mold and given the following cure cycle:

3000 psi - 180° F - 4 hrs.
 " " - 250° F - 16 hrs.
 " " - 300° F - 4 hrs.
 " " - 400° F - 4 hrs.
 " " - cool to R. T.

The cured disc was approximately one-half inch thick, translucent and appeared well molded except at the outer edge where small cracks were evident. The density was 1.28 with zero percent porosity.

2.6 PRELIMINARY STUDY OF SILICA CHEMICAL VAPOR DEPOSITION FOR DENSIFYING MARKITE

2.6.1 Introduction

Under certain circumstances, chemical vapor deposition techniques can be used to improve the mechanical properties of an existing porous or fibrous body. A case in point is the infiltration, or deposition in depth, of a thin layer of carbon or graphite within the pores of hot pressed polycrystalline carbon and graphite. Strength improvements of up to 100-200 percent can be achieved, depending on the initial strength of the body. The improvement is probably the result of filling in surface voids and defects which serve as stress concentrators and lead to premature failure. High strength composite materials can also be prepared from fibrous woven constructions by the introduction of part or all of the matrix through chemical vapor deposition methods as has been demonstrated in the currently developing carbon-carbon composites, in which the carbon matrix is incorporated within the structure by pyrolysis of methane under controlled conditions.

The first of the above approaches to improving the strength of an existing structure was tried with prefabricated silica/silica 4D (Omniweave) composites prepared for eventual use as antenna window materials (Markite plate 309-3). These materials, although satisfactory with respect to dielectric properties, would be vastly improved by increases in mechanical strength. The brittle nature of the silica matrix and fibers and the presence of surface voids and defects make it likely that premature failure is brought about by such imperfections. Therefore, several specimens of the preformed silica/silica composite were coated with a thin layer of pyrolytic silica, through decomposition of ethyl orthosilicate vapor, in order to evaluate the effectiveness of this approach.

2.6.2 Experimental

Pyrolytic silica can be deposited on a heated surface by the thermal decomposition of ethyl orthosilicate ($\text{Si}(\text{OC}_2\text{H}_5)_4$) at temperatures above $800 - 900^\circ\text{C}$. The structure of the deposit is determined generally by the conditions of deposition: gas concentration, temperature, pressure and gas residence time. Infiltration, because of the depth of deposition desired, requires the use of either low temperatures or very dilute gas mixtures, i.e., conditions which typify very low deposition rates. These conditions are required to prevent the formation of a surface skin which blocks passage of the infiltration gas mixture to interior voids.

The apparatus used for infiltration of the Markite silica/silica 4D (Omniweave) specimens is sketched in Fig. 11. It consisted primarily of a one inch I.D. resistance heated deposition furnace, capable of operation to 1800°C , a heated reservoir containing the active pyrolysis specie, in this case ethyl orthosilicate, and a pumping system capable of producing the desired low pressure. In operation, a carrier gas of dry

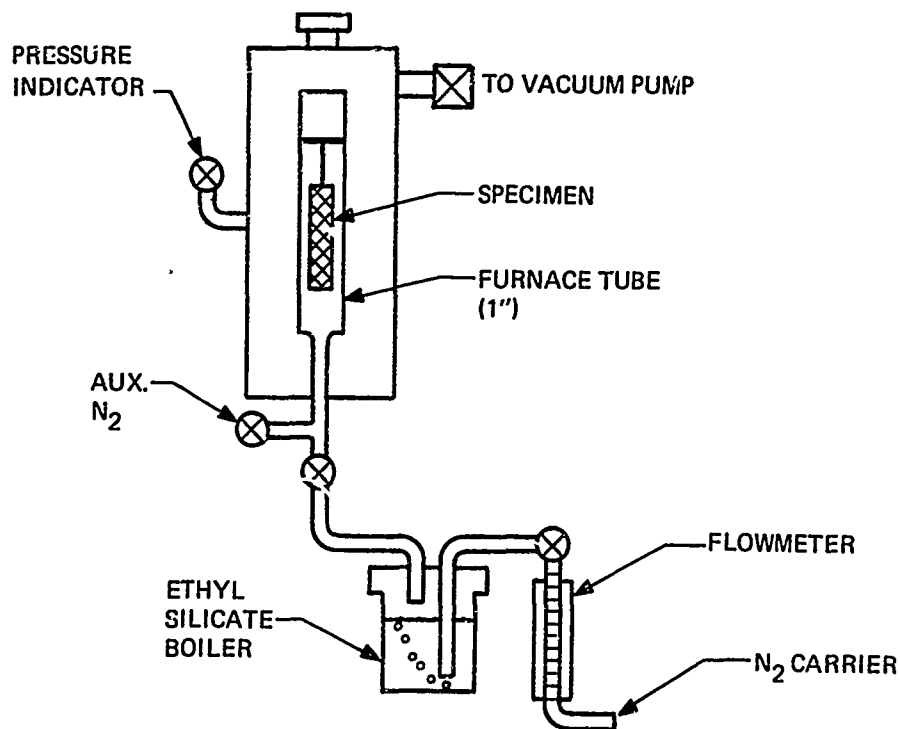


Fig. 11. Schematic of Apparatus Used for Chemical Vapor Deposition Studies

nitrogen was passed through the reservoir at a known rate and at atmospheric pressure, and then into the furnace after passing through a flowmeter beyond which the pressure was reduced to that desired by means of a control valve.

Four specimens from plate 309-3 were selected for infiltration. These were: AV-1, ACVD, BCVD, and TCVD.

Control specimens were also selected from the same block for comparison of their mechanical strength and elastic properties and the density improvement upon CVD.

The specimens consisted of strips, 2 - 3 inches long by 0.5 - 0.6 inches wide by 0.25-inch thick. These were mounted within the deposition tube by means of tungsten wire hooks. Infiltration of each specimen was carried out under the conditions listed in Table 14.

The deposited silica was glassy, yellowish and translucent in appearance, and quite adherent to the substrate silica. Each specimen was subjected to a flexure test to determine if a measurable increase in strength had occurred. These results are presented in Table 25, in the mechanical test section of this report, from which it is clear that both strong and weak specimens remained unchanged. This is not particularly surprising however, in view of the glassy nature of the deposit produced under the conditions used. Although the modulus of the deposit is not known, it is likely to

TABLE 14. DEPOSITION CONDITIONS

| Specimen | Temperature (°C) | P (torr) | Flow (cc/min) | Time (hours) | Weight Increase (%) |
|----------|---------------------|-------------|------------------|-----------------|---------------------|
| AV-1 | 1000 | 5 | 280 | 24 | 4.60 |
| ACVD | 1000 | 5 | 280 | 24 | 3.82 |
| BCVD | 1000 | 5 | 280 | 6 | 0.95 |
| TCVD | 900 | 5 | 280 | 6 | 1.37 |

be higher than that of the base composite because of the ability of the fibers in the composite to deform under stress in the latter. Therefore, failure of the coating could be expected to occur before loading of the composite, with the result that no reinforcement by the surface layer would be observed.

2.6.3 Prognosis

Although no improvement in mechanical strength was observed in these experiments, several options remain to be explored. These include: 1) variation of the structure of the deposit through alterations in the deposition conditions, 2) the use of a less densely structured composite as the substrate, and 3) development of an optimum resin/CVD silica combination matrix in which either the resin or the CVD silica would appear at the fiber/matrix interface. Variations in CVD silica structure would be factored into the second and third options.

TABLE OF CONTENTS: SECTION 3

| | Page |
|---|-------------|
| 3.0 Characterization | 3-1 |
| 3.1 The Sampling and Characterization Plan | 3-1 |
| 3.1.1 Introduction and Program Background | 3-1 |
| 3.1.2 The Sampling Plan | 3-1 |
| 3.1.3 Detailed Sampling Plan and Radiographic NDT | 3-5 |
| 3.2 Mechanical Characterization | 3-31 |
| 3.2.1 Phase 1 | 3-31 |
| 3.2.1.1 SEM Studies of Fractured ADL-10 Specimens | 3-39 |
| 3.2.2 Phase 2: Quartz-Silicone Systems | 3-39 |
| 3.2.2.1 Test Data | 3-39 |
| 3.2.2.2 Basic Resin Behavior | 3-44 |
| 3.2.3 Silica/Pyrolyzed Silicone Resin System | 3-49 |
| 3.2.3.1 Introduction | 3-49 |
| 3.2.3.2 Discussion of Mechanical Test Data | 3-49 |
| 3.3 Ultrasonic Measurements | 3-58 |
| 3.4 Shock Testing | 3-65 |
| 3.4.1 Introduction | 3-65 |
| 3.4.2 Results of Flyer Plate Testing | 3-66 |
| 3.4.2.1 Phase 1 | 3-66 |
| 3.4.2.2 Phase 2 | 3-67 |
| 3.5 Electromagnetic Characterization | 3-71 |
| 3.5.1 Introduction | 3-71 |
| 3.5.2 Definition of Terms | 3-71 |
| 3.5.3 Measurement Techniques | 3-72 |
| 3.5.4 Results of Electromagnetic Characterization Program | 3-75 |
| 3.5.4.1 Laboratory Waveguide Measurements, Room Temperature | 3-75 |
| 3.5.4.2 RF/Ablation Tests on 4½ x 5 Inch Plates | 3-75 |
| 3.5.4.3 RF Ablation Tests on C-Band Waveguide Samples | 3-75 |
| 3.5.4.4 RF Coefficient Measurement Before and After Ablation Test | 3-76 |
| 3.6 Thermal Characterization | 3-83 |

3.0 CHARACTERIZATION

3.1 THE SAMPLING AND CHARACTERIZATION PLAN

3.1.1 Introduction and Program Background

The characterization plan for the "Advanced Hardened Antenna Window" program has placed major emphasis on mechanical properties. This was obviously motivated by the first "Hardened Antenna Window Program" in which the electromagnetic and thermal performance and the shock resistance of ADL-10 were at high levels. However, the mechanical strength of the composite had to be improved above the 2000 - 4000 psi ultimate tensile strength levels in the weakest orientation of the composite material.

The characterization plan described in this section therefore reflects the accent on improvement of structural properties in this program. The two material types, ADL-10 and Markite, have been variously characterized as emphasis on particular properties merited. The structural performance was assessed via tensile and flexural strength, modulus and thermal expansion measurements; the dynamic structural performance via ultrasonic and magnetic flyer shock testing; the electromagnetic and thermal performance by extensive combined RF/ablation systems tests and separate electromagnetic property and thermal conductivity measurements.

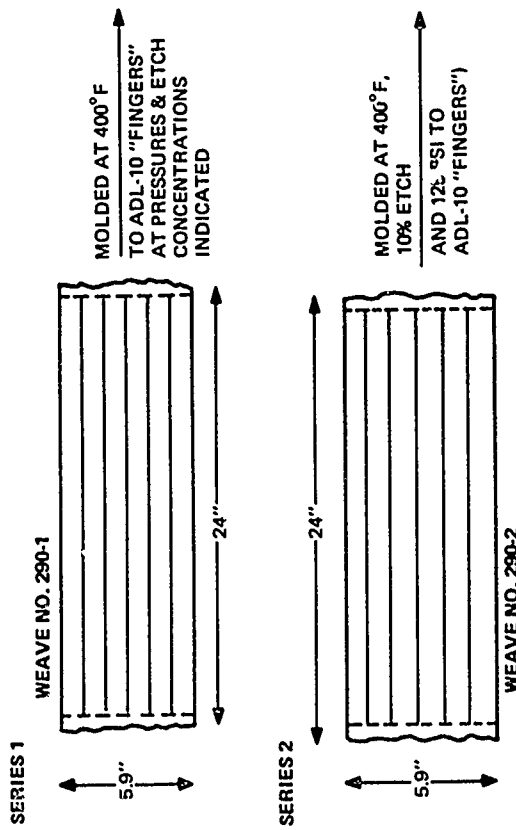
In addition, the basic properties of the composite constituents have been determined to permit an analysis of the ultimate capabilities of the silicone resin/quartz Omniweave. The properties include direct measurements of flexural and shear strength and modulus on the cured SR-350 resin matrix and tensile testing of unidirectionally reinforced silica/SR-350 composite strips.

The Sampling Plan is first given below as Section 3.1.2. This section serves to catalogue and trace both the fabricated materials and the test sampling from them. The detailed plate layouts and individual radiographs are then given in Section 3.1.3 with the rationale for the detailed testing selection.

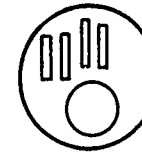
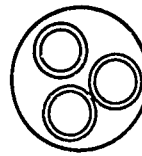
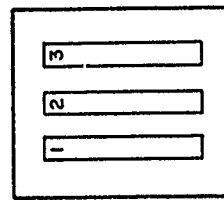
3.1.2 The Sampling Plan

In Phase I of the study, two "segmented" Omniweave scarfs were woven in a configuration which yielded closed cell tensile or flexure specimens. The processing and sampling of these "ADL-10 Omniweave fingers" is represented schematically in Figure 12 which keys the more detailed radiographs to follow. In series 1 testing of the first woven scarf (No. 290-Q3BA -1), testing was limited to determine the flexure and unidirectional tensile strength of the samples molded at 1000, 300 and 125 psi with the HF etching and silane coupling parameters noted in Table 3.

PHASE 1, SEGMENTED WEAVE, ADL-10 SILICA/SR-350 SILICONE COMPOSITES



BASIC CONSTITUENT PROPERTIES



FLEXURAL AND TORSIONAL SHEAR
STRENGTH AND MODULUS MEASUREMENTS
ON CURED SR-350 RESIN

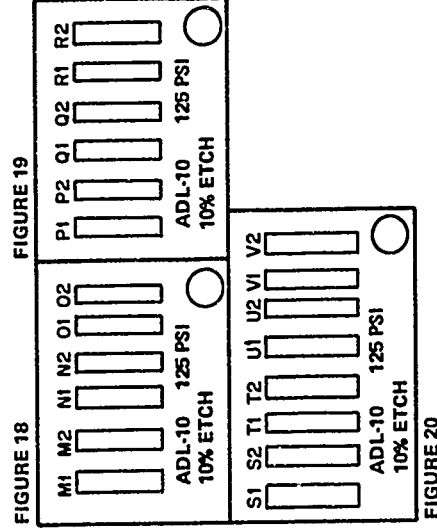
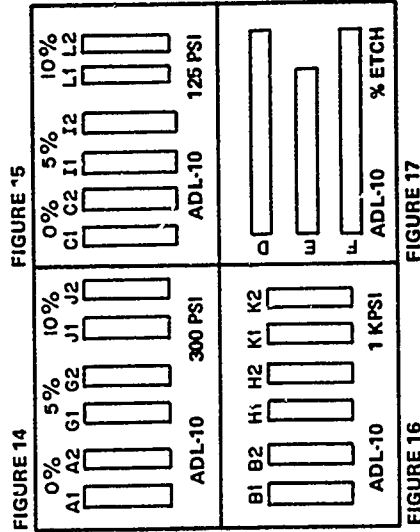


Fig. 12. Phase 1 Processing and Sampling Plan

In the series 2 testing of the second segmented Omniweave (No. 290-Q3BA-2), a single molding pressure of 125 psi was used, with variations in the silane concentration. The single most important cross-characterization parameter for rationalizing the ultimate tensile strength results of both the series 1 and 2 tests was found to be the fiber orientation angle as measured at the surface of each individual specimen. These are given in detail and correlated to strength in the discussion of the "Mechanical Testing" results below, Section 3.2. The effects of the closed-cell design of the woven finger sample on apparent strength were also studied by machining the edges off identically processed tensile bars.

Additional characterization was introduced in series 2 consisting of magnetic flyer-plate shock tests on tensile bars which were then pulled for direct assessment of the effects of shock impingement on the structural performance. Ultrasonic characterization of all Phase 1 woven finger specimens was performed including post test measurements on the flyer-plate specimens.

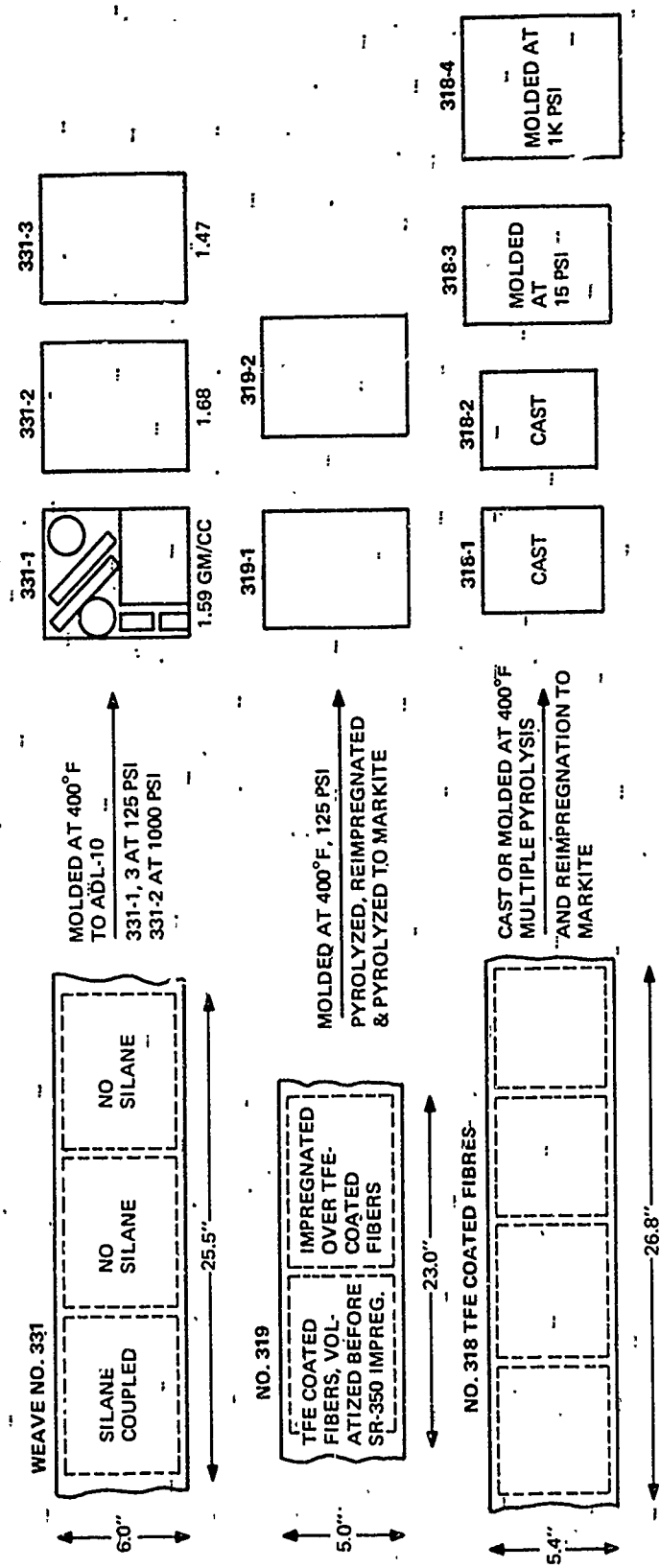
All segmented scarf specimens were radiographed before test to detect structural flaws or density gradients, as were the plates of Phase 2, as discussed below in Section 3.2.3.

The testing of two 4-inch discs of cured SR-350 resin is also represented schematically in Fig. 12. Four flexure bars, an ultrasonic specimen and three torsional shear rings were produced as indicated. TGA studies in air on the cured resin were also made for the first time.

In Phase 2 of this program, covering work performed after the mid-program "Progress Report" (Reference 7), ADL-10 was further studied in the flat plate construction used in the previous "Hardened Antenna Window Program". The purpose of this characterization was to establish the same high tensile properties for specimens cut from flat panels as was found for the segmented scarf closed cell specimens, while using the processing parameters developed in Phase 1, i.e., 125 psi molding pressure, etched fibers and silane coupling. Two series of Markite flat panels were also produced and sampled, as shown in the schematic of Figure 13, "Phase 2 Processing and Sampling Plan" and panels cut from each scarf are shown at the right of the diagram with pertinent identifying process variations.

The Phase 2 ADL-10 plates 331-1 and 331-2 were sampled similarly to those in the earlier program, as described in Reference 1. Plate 331-3 was not tensilely tested due to its low density and the intention to retain it for further demonstration or other less critical characterization tests. The six Markite panels 318-1 through 4 and 319-1 and 319-2 were similarly sampled, but with selected testing also done at stages in the reimpregnation and pyrolysis processes, and variations in pyrolysis temperatures. These are discussed in detail in the individual test sections and are noted in the individual plate layout plans of this section.

PHASE 2, STANDARD 45° EPA WEAVES, HF ETCHED SILICA FIBERS



STUDIES ON SILICA CHEMICAL VAPOR DEPOSITION

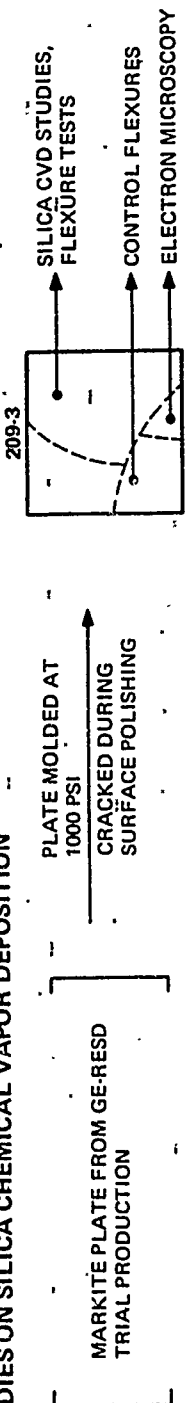


Fig. 13. Phase 2 Processing and Sampling Plan

Again referring to Fig. 13, an additional plate of Markite, acquired from another program's trial production lot* was sampled and tested for some preliminary studies of silica chemical vapor deposition (CVD), a method of densifying silica composites.

As a further material characterization technique, selected electron microscopy and scanning electron microscopy studies have been performed on the basic materials, on the finished composite and on surfaces of tested samples. These results are interspersed throughout the report text where their content affects the composite process studies or test results.

3.1.3 Detailed Sampling Plan and Radiographic NDT

The segmented Omniweave scarf specimens of Phase 1 of this program, having been molded to size for flexure and tensile testing, were not cut out of any parent plate. This obviates any requirement for detailed tracing of specimen origins, such as location near edges of weaves or near density gradients or weave flaws. The molded "fingers" were therefore radiographed in groups corresponding to their processing, and expediency for full scale reproduction of the radiographs. Thus, in Fig. 14 through 17, radiographs of the 21 series 1 specimens are grouped by the three molding pressures of 300, 125 and 1000 psi, with the indicated etchant and silane concentrations, as keyed in Fig 12. Figures 18 through 20 present radiographs of the three series 2 groupings.

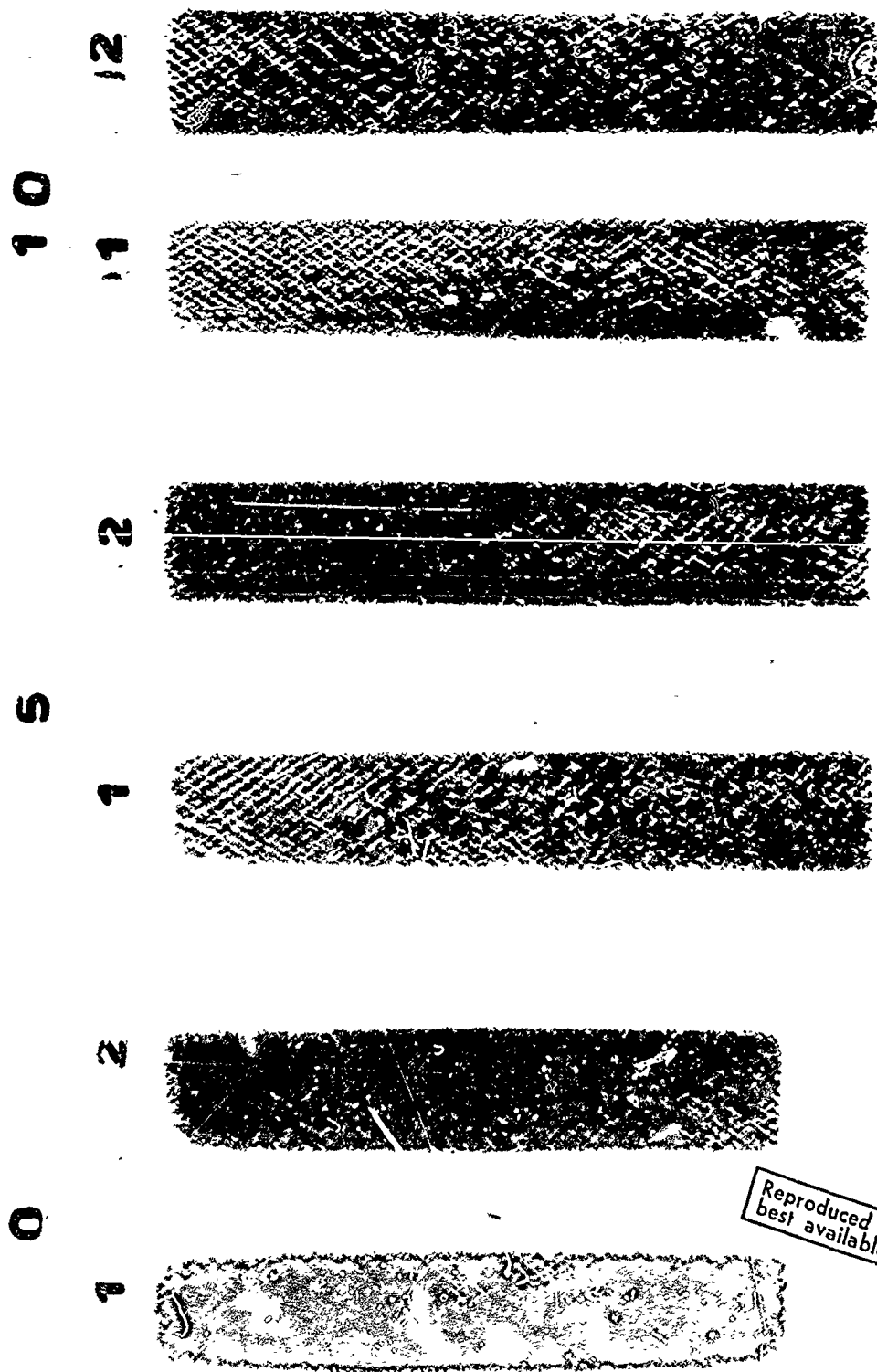
In most of the radiograph groups, a 1.5-inch diameter disc of Engelhard Amersil fused optical silica, 1/8-inch thick, has been inserted as a radiographic density and quality standard.

The only apparent defects detected by radiography are the cracks in samples S1 and S2, Fig. 20, to both of which had been added "Cab-o-Sil". These cracks were however also evident on the surface by visual examination. These two tensile specimens broke prematurely near the doublers where they are gripped and gave the anomalous strength versus reinforcement angle dependence shown below in Section 3.2.

Figure 21 shows the radiograph of the three filament wound unidirectional long tensile strips. The silica filament alignment is apparent.

The Phase 2 plates are then shown in the format used in Reference 1, a detailed plate sampling layout followed by accompanying radiograph. ADL-10 plates 331-1 and 331-2 are shown in the pairs of Figs. 22 through 25, while Fig. 26 is the radiograph of plate 331-3 which was not tested.

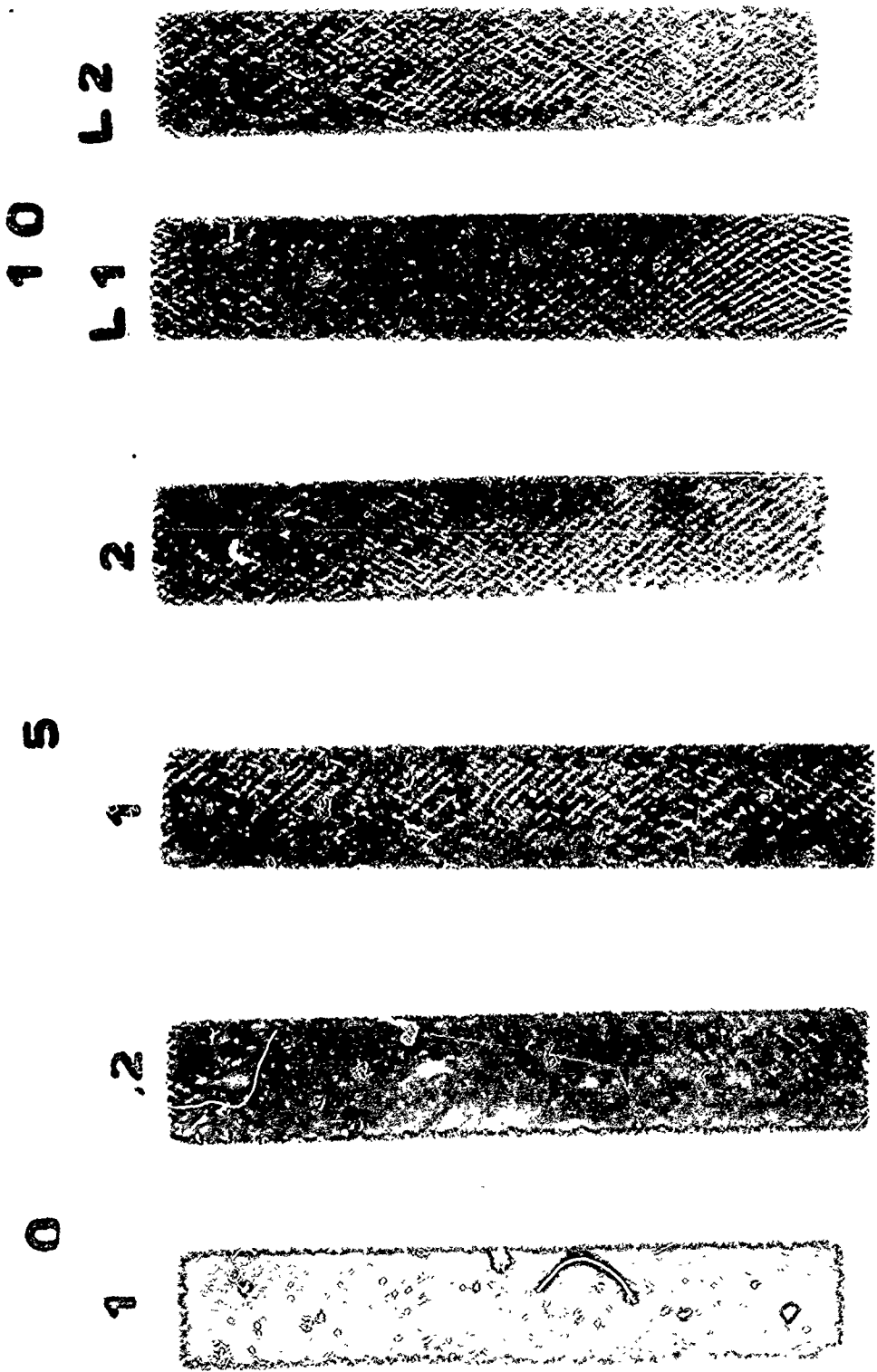
*Under NASA/Langley Contract NAS1-10769, "Antenna Window Materials" 2/4/71-7/19/71



10 300

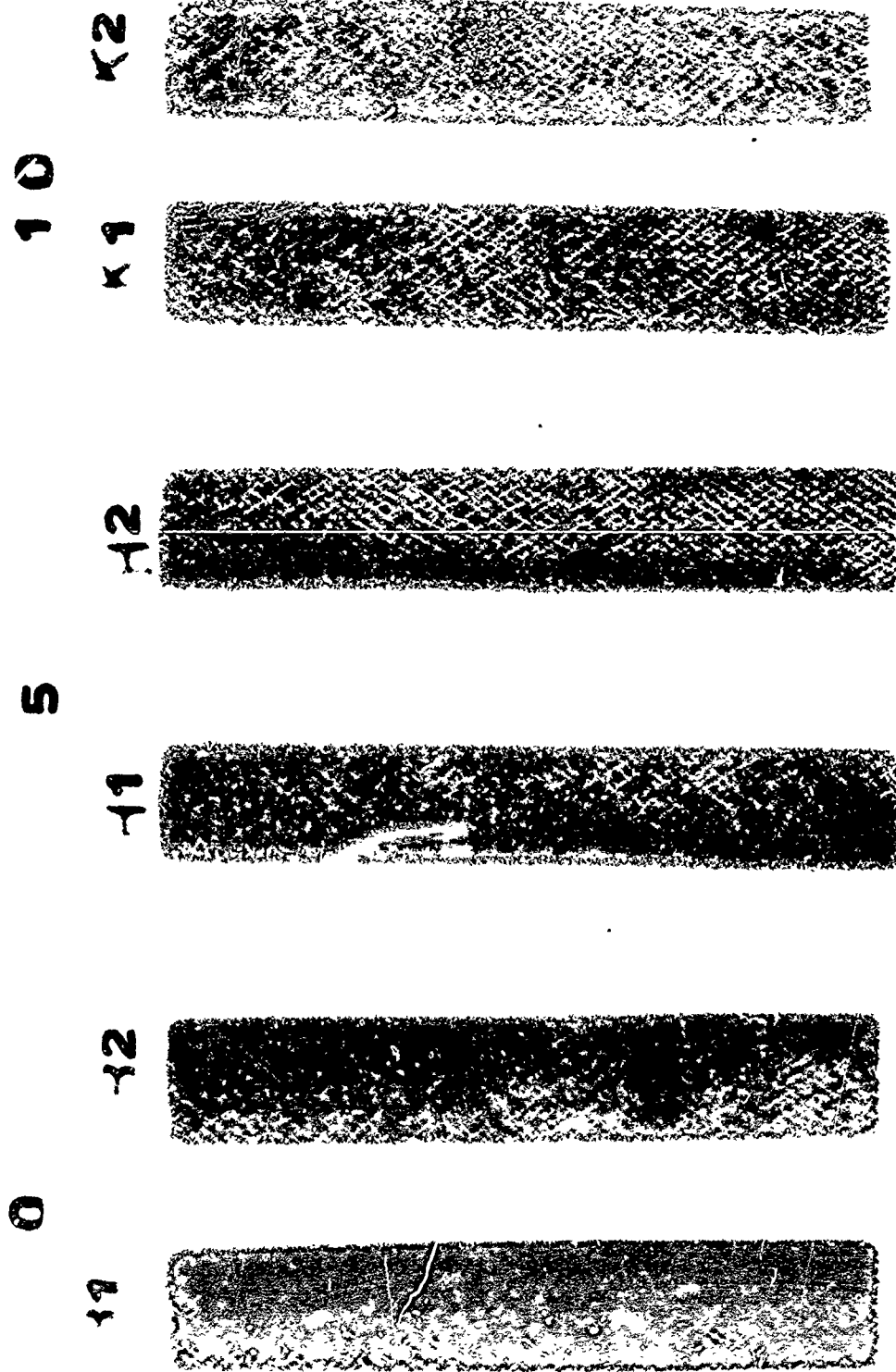
Reproduced from
best available copy.

Fig. 14. Radiograph of Series 1 ADL-10 "Finger" (Specimens Molded at 300 PSI)



AD 10 '2 5 P -

Fig. 15. Radiograph of Series 1 ADL-10 "Finger" (Specimens Molded at 125 PSI)



AD 10 M P S

3-8

Fig. 16. Radiograph of Series 1 ADL-10 "Finger" (Specimens Molded at 1000 PSI,

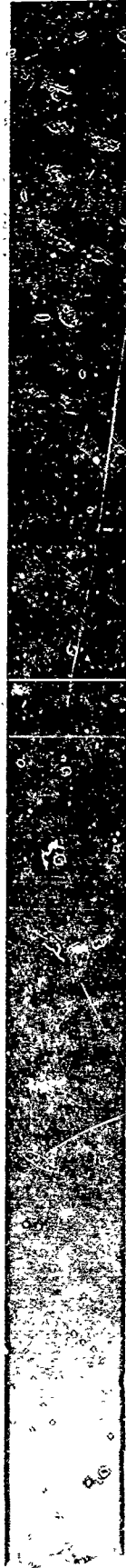
MP01048
22471



D



E

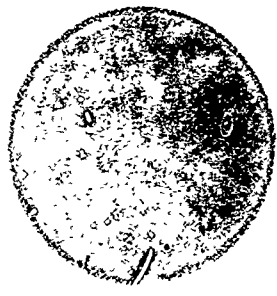
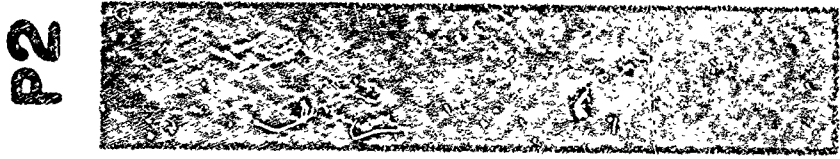
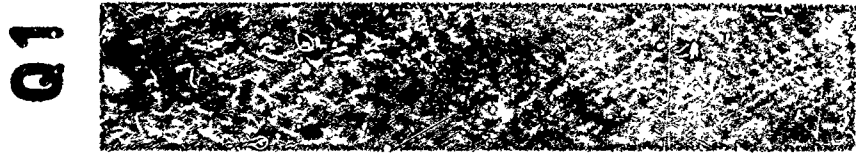
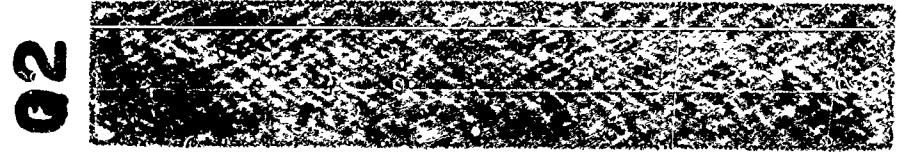
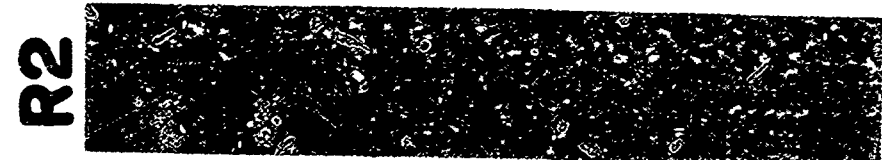


F

19% ETCH

ADL-10

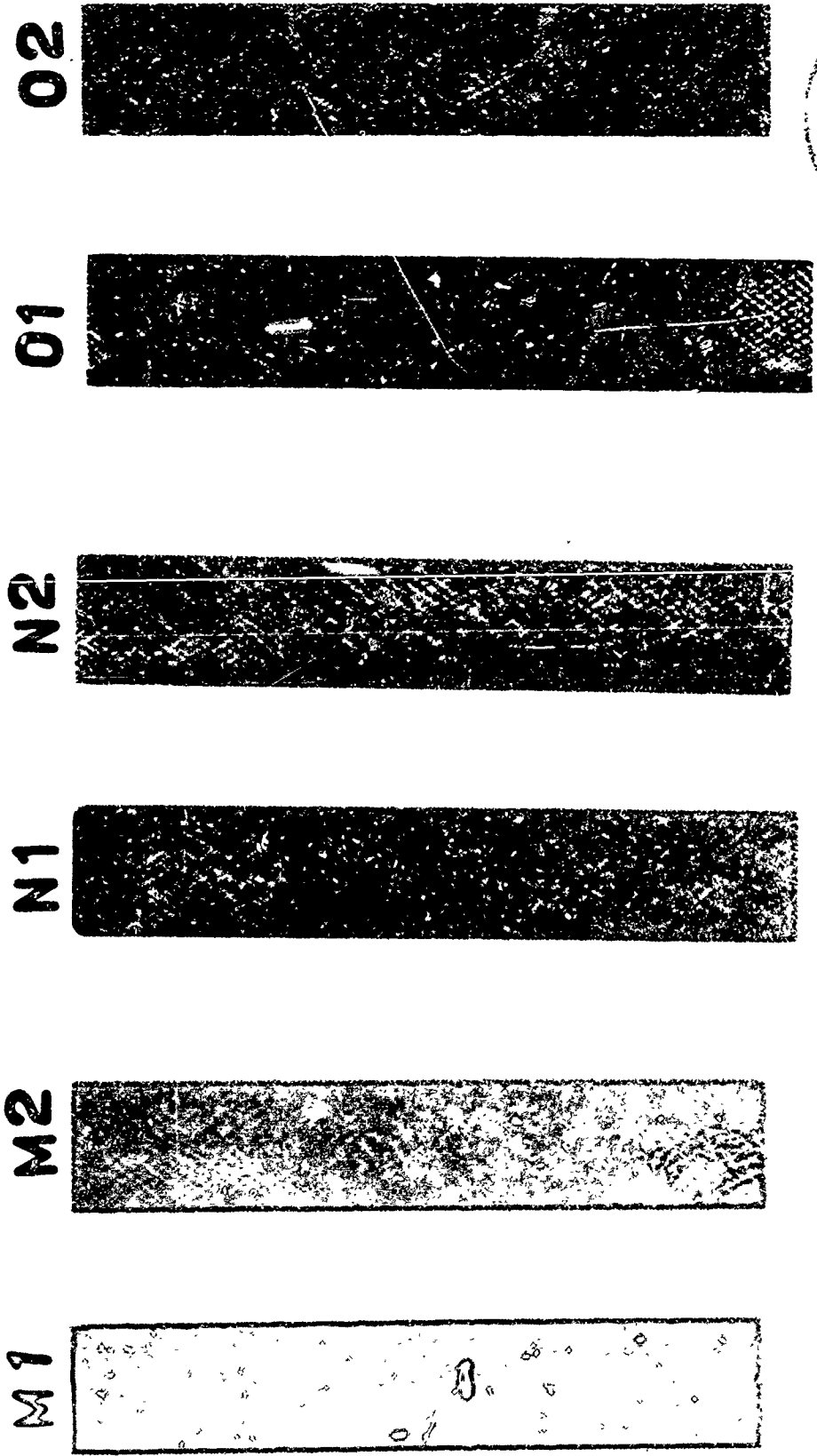
Fig. 17. Radiograph of Series 1 ADL-10 "Long Finger" (Flexure Specimens Molded at 1000 PSI)



**ADL 10 125 PSI
10 % ETCH**

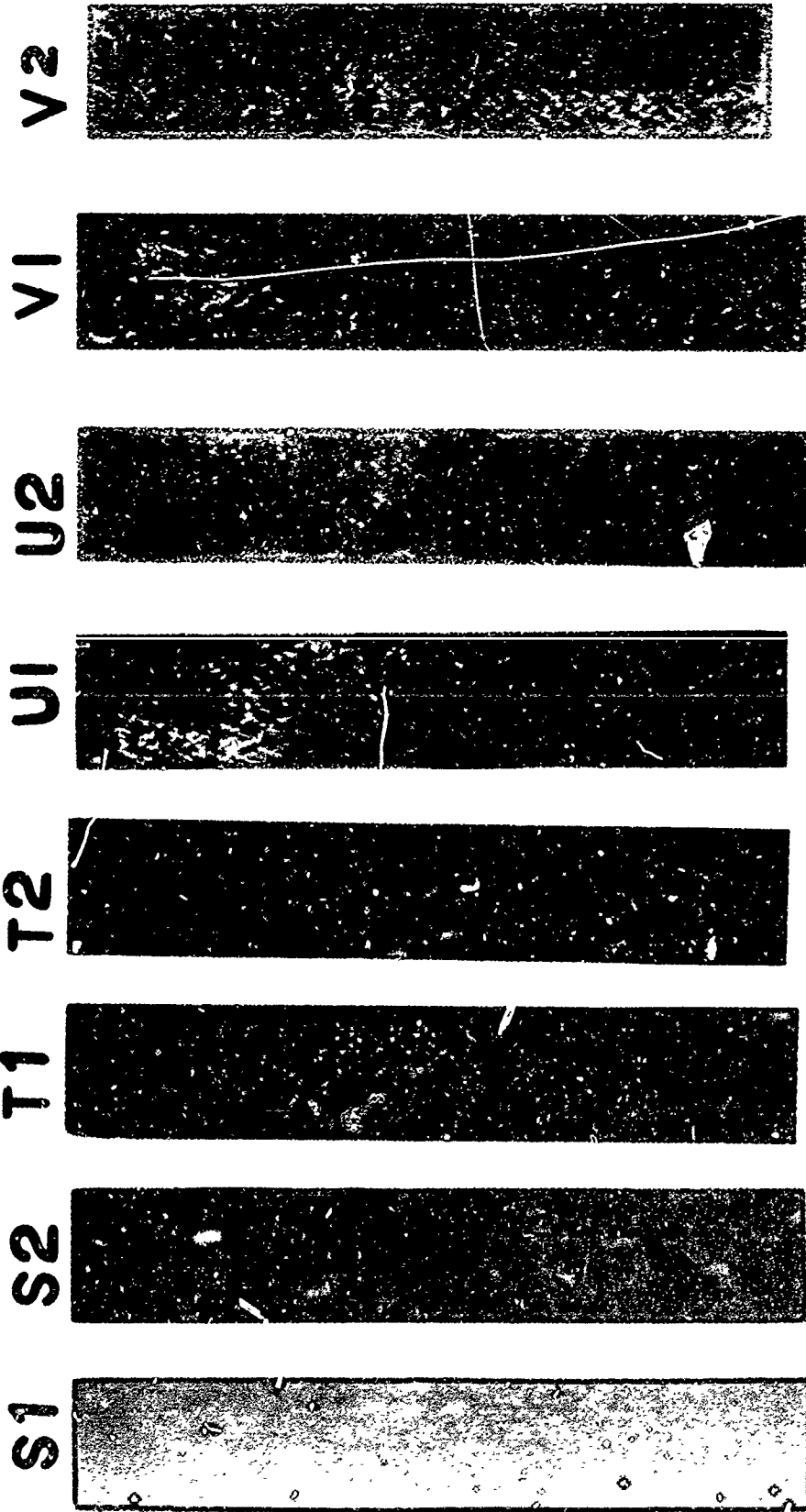
Reproduced from
best available copy

Fig. 18. Radiograph of Series 2 ADL-10 "Finger" Specimens, 125 PSI Molding Pressure, 10% HF Etch and High Silane Coupler Concentration



ADL 10 125 PSI
10 % ETCH

Fig. 19. Radiograph of Series 2 ADL-10 "Finger" Specimens, 125 PSI Molding Pressure, 10% HF Etch and Low Silane Coupler Concentration



**ADL 10 125 PSI
10 % ETCH**

Fig. 20. Radiograph of Series 2 ADL-10 "Finger" Specimens, 125 PSI Molding Pressure, 10% HF Etch; S1, S2, T1, T2 containing "Cab-O-Sil" Colloidal Silica; U1, U2, V1, V2 with Low Silane Concentration

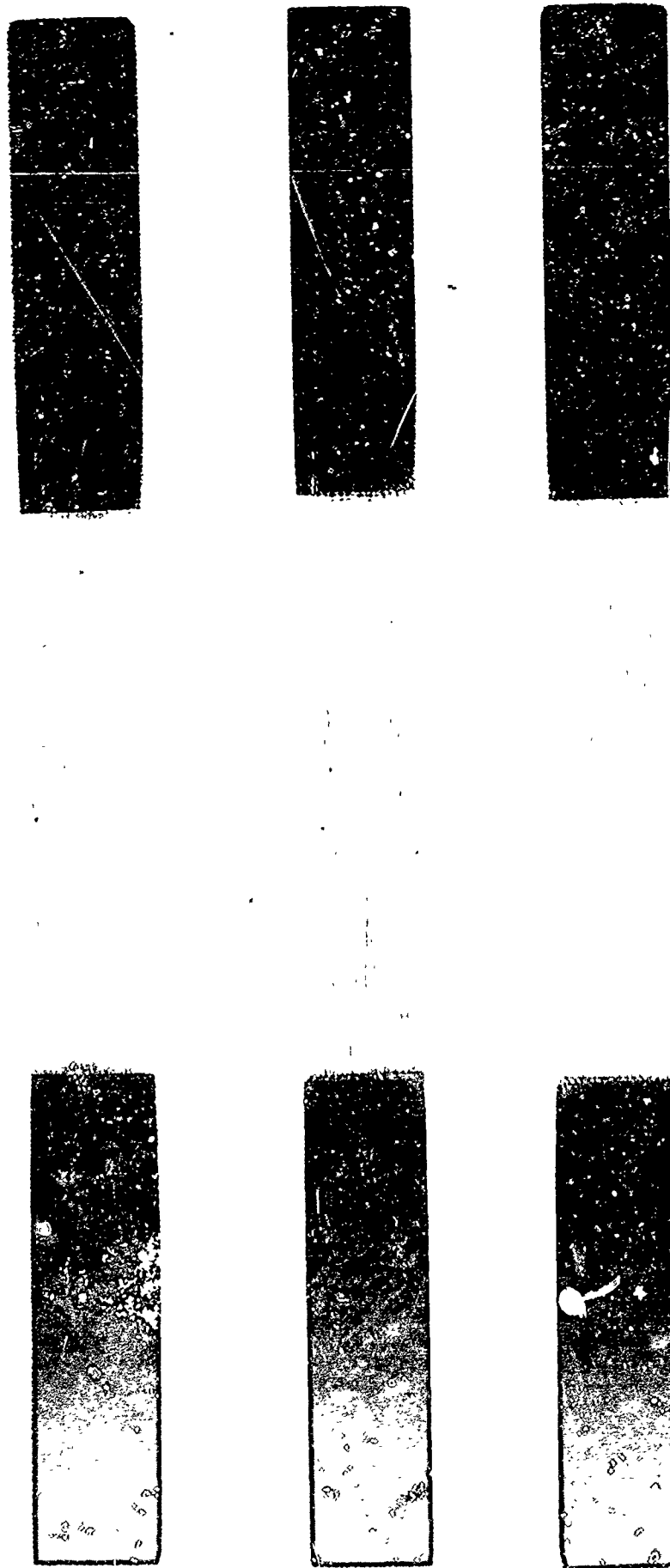


Fig. 21. Radiograph of Filament-Wound Unidirectional ADL-10 Composites, Etched and Silane-Coupled

The symbols used in these layouts are identified below:

- σ - tensile or flexure specimen
- α - thermal expansion
- US - ultrasonic and slap plate hockey puck specimens
- EMC - C band electromagnetic test specimens
- K&L - combined thermal conductivity and L band RF specimen

The sample orientations in the plate layouts are also indicated by the suffix letter designations:

- B - "bias," at an angle on the plate, along the fiber reinforcement
- A - "axial," along the Omniweave weaving direction, along the length of the plate
- T - "transverse" to the weaving direction, across the plate width
- C - through the thickness (used principally to designate thermal expansion specimens)

The large 4.25 x 5 inch RF/ablation test specimens required for arc tunnel testing are seen in these layouts for the first time. The smaller C-band specimens for the Gerdien Arc tests, described below in Sections 3.4 and 3.5, are far more economical in test material (and test performance). The same design 2-inch diameter flyer plate and ultrasonic test specimens are shown as is the approximately 4 to 5.5-inches long by 0.75 to 1-inch wide tensile bar and the standard GE-RESD 2.00 inches length thermal expansion specimen. The two-inch diameter disc US2, 331-1 was submitted to AMMRC for particulate erosion testing. Two specimens in the configuration required by Harry Diamond Laboratories for RF/heating tests were prepared and are designated 331-2 HD in Fig. 2. These will be tested by HDL at some time in the near future and the results conveyed to GE-RESD and AMMRC.

All of these ADL-10 specimens were taken without modifying the plate thickness and with the as-molded faces, with the exception of the C-directional thermal expansion specimens, α_c , which were machined to 0.250-inch thickness.

Flexure bars in the standard 1-1/2 long by 1/2-inch wide dimensions were also selected to compare both with the tensile bar results and also with the extensive flexure bar testing conducted in the earlier program on plates 113-1 and 113-2 (Fig. 74,

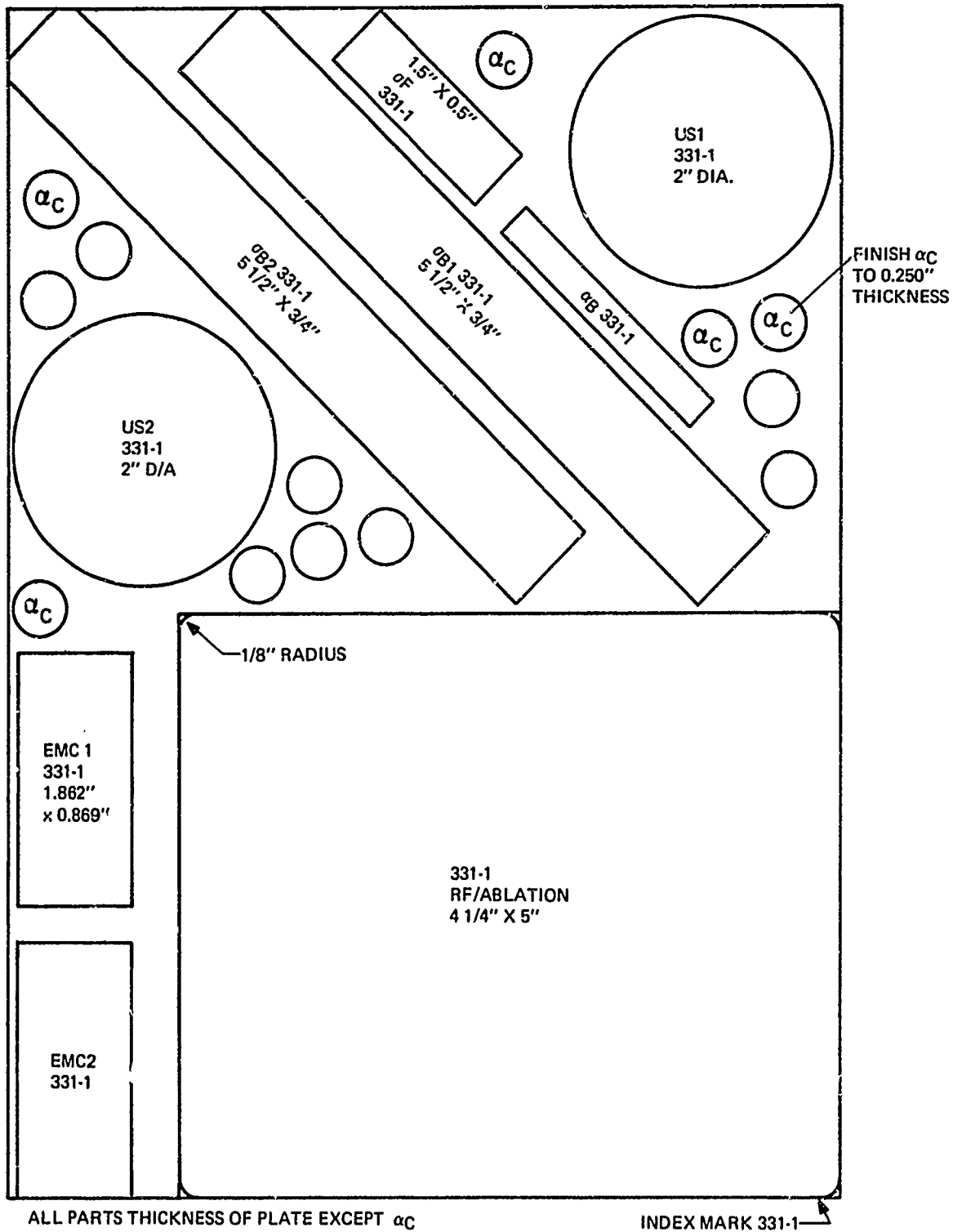
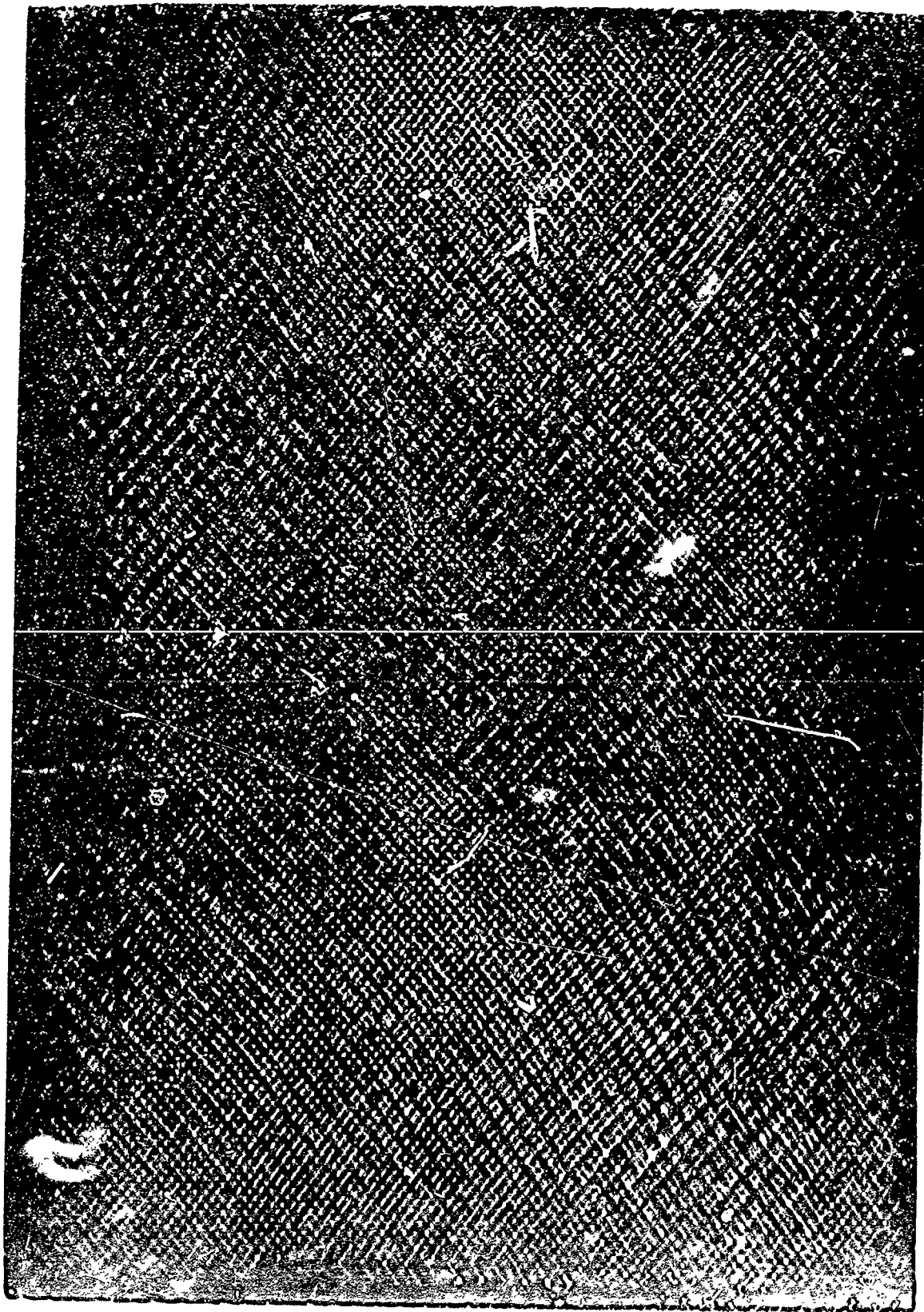


Fig. 22. Sample Layout: ADL-10 Plate 331-1



ADL 10 331 1

Reproduced from
best available copy. 

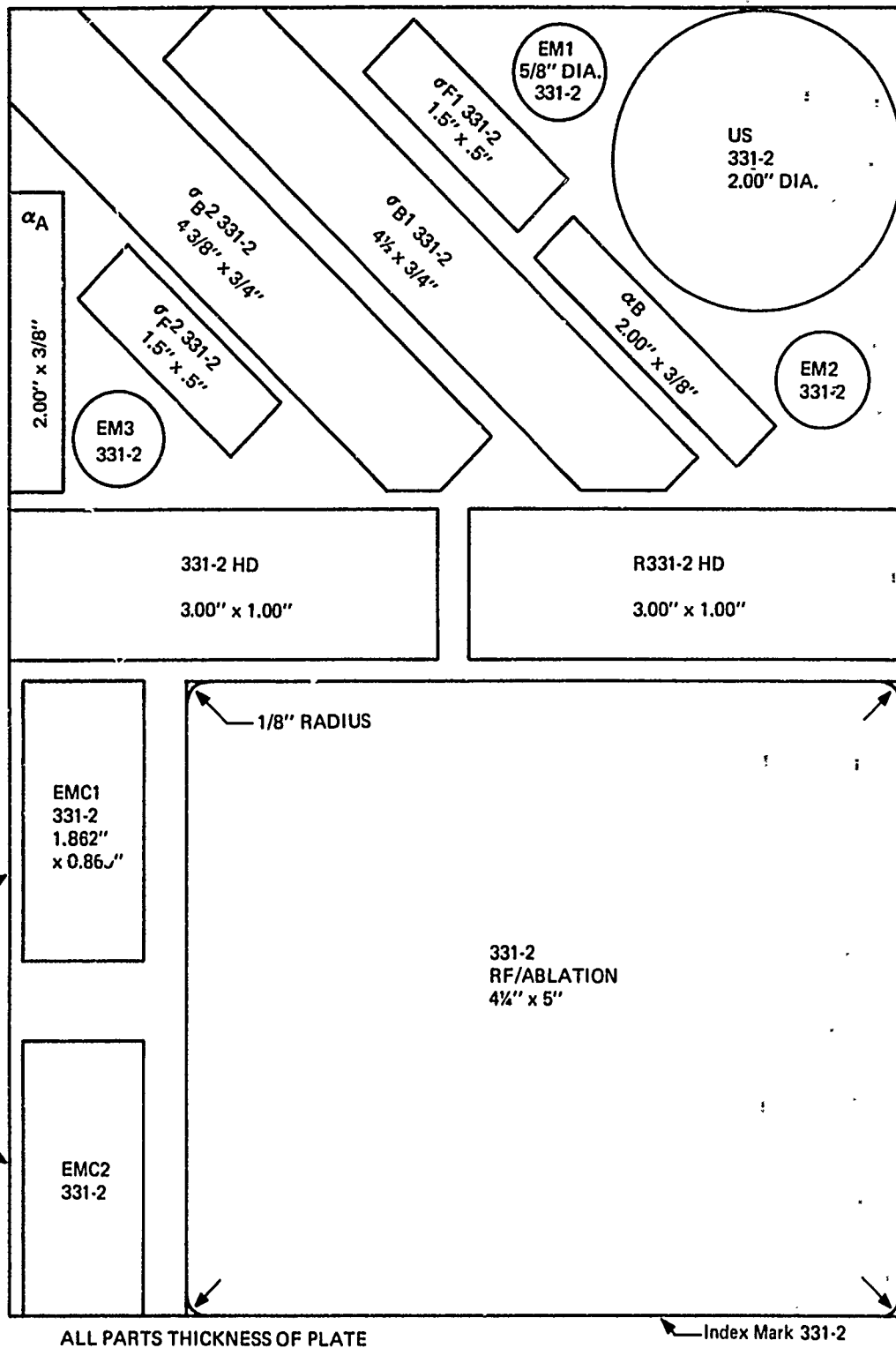
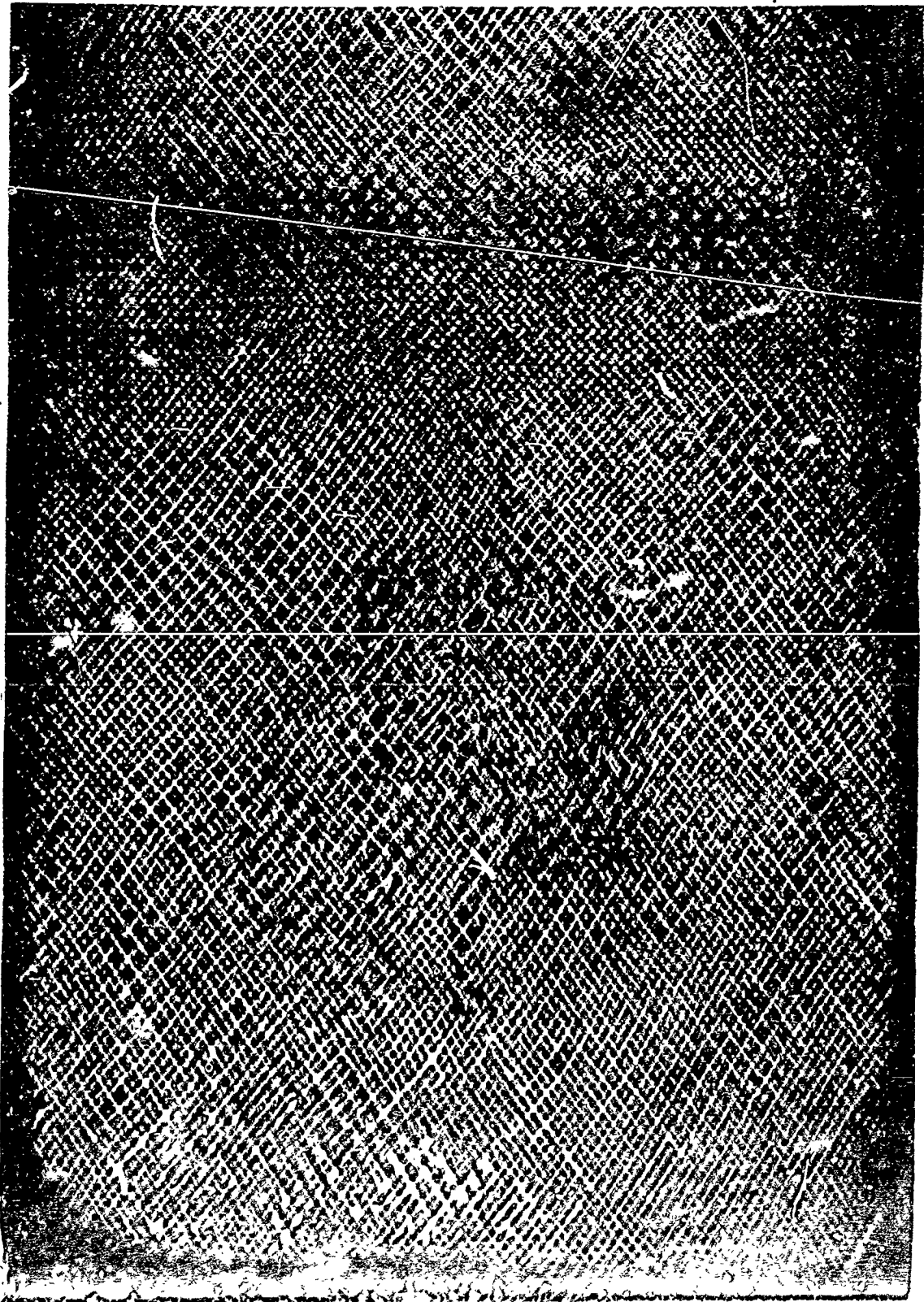

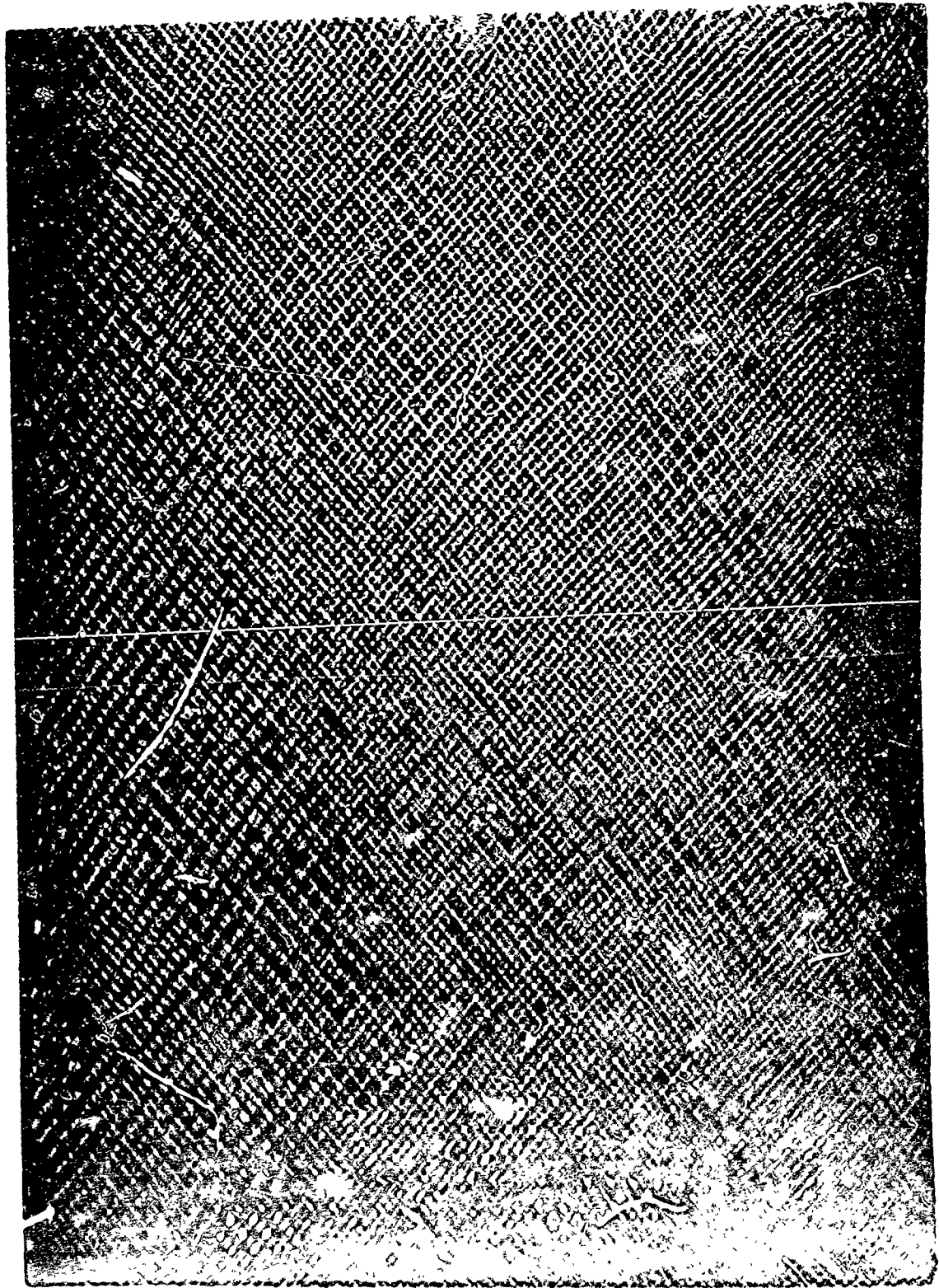


Fig. 24. Sample Layout: ADL-10 Plate 331-2



ADL 10 331 2

Reproduced from
best available copy. 



ADL 10 331 3

Fig. 26. Radiograph of ADL-10 Plate 331-3

Reference 1). Comparable results seem to have been found for both specimen sizes, certainly so for the more brittle ceramicized versions of the material. This not only represents an important economy and simplification in sampling for the ultimate strength behavior of these materials but it also allows more detailed study of process modifications as seen in the referenced Figure 74* and the variations carried out below on Markite.

Figure 27 is the radiograph of Markite plate 318-1, from which only one sample, EMC-1, 318-1 has been taken, from the upper left edge.

The sampling layouts for Markite panels 318-1 through 4 are shown, each followed by its radiograph in Fig. 28 through 33. Thermal conductivity specimens labelled "K&L" were taken from these panels, the L indicating possible later double use as L-band waveguide specimens.

Figures 34 and 35 illustrate the sampling layouts for Markite plates 319-1 and 319-2.

In both of these plates, tensile bars σ AX2 and σ AX1, were taken before the second pyrolysis step. After tensile fracture, they were then each recut to six 1.5 long x 0.5-inch wide flexure bars which were then pyrolyzed as discussed in Sections 2 and 3.2.

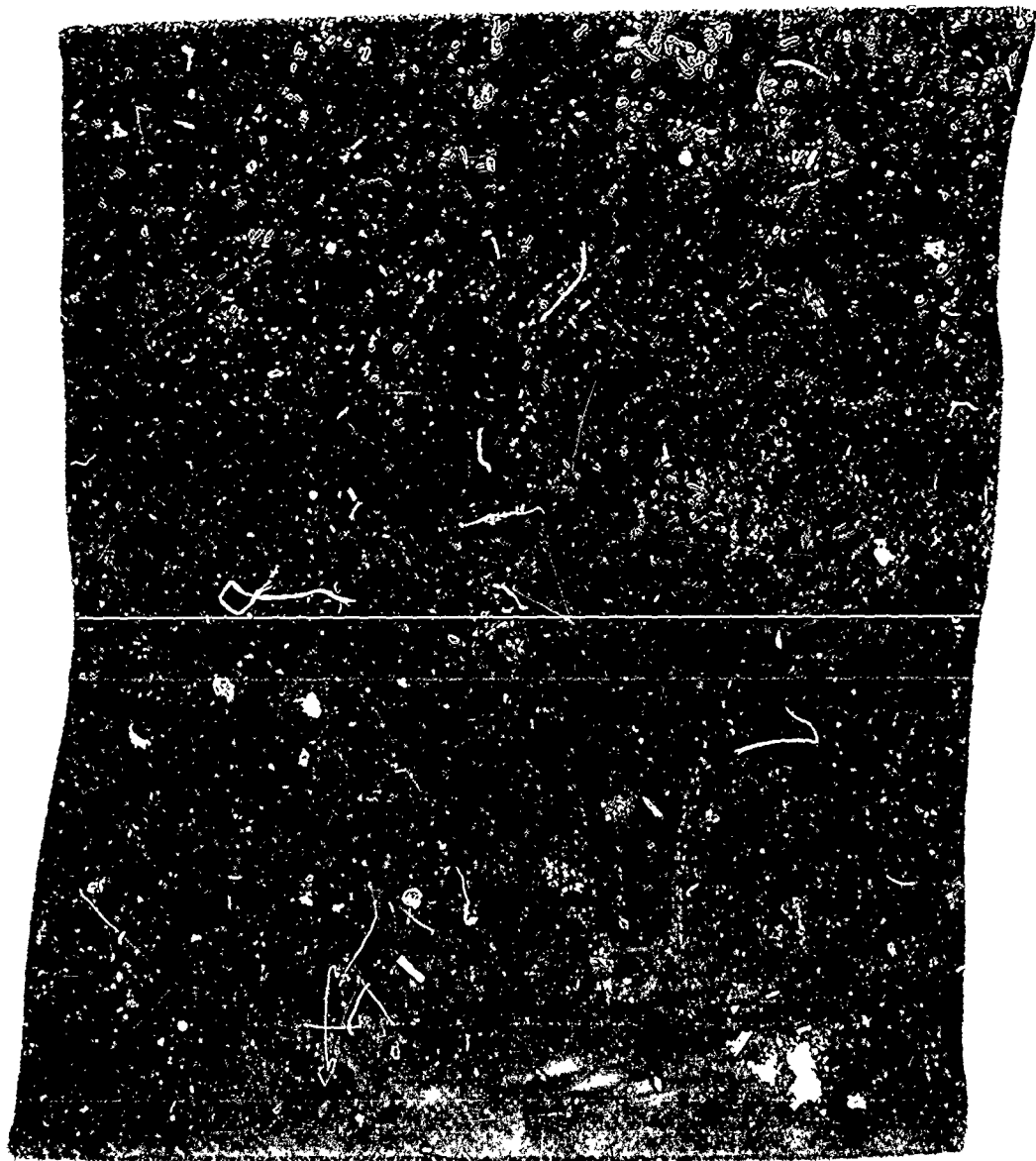
A labelling convention has been adopted for identifying the stage of sampling of Markite specimens. A suffix is appended according to the following scheme:

| <u>Sample State as Tested</u> | <u>Suffix</u> | <u>Example</u> | |
|-------------------------------|---------------|----------------|---------|
| Reimpregnated | R | σ AX2 | 319-1R1 |
| Pyrolysis to 1600° F | P | σ A5 | 319-1P3 |
| Sintering at 2250° F | S | σ A2 | 318-4S3 |

A second suffix number is also added to indicate the repetition of the pyrolysis or reimpregnation. "P2" for example indicates "pyrolyzed twice" (after one reimpregnation).

The sample layout for Markite plate 209-3 is shown in Fig. 36. Dashed lines indicate the fracture that resulted during polishing of the faces of this specimen which was then made available to the Advanced Hardened Antenna Window program for preliminary fiber-matrix studies and experiments in CVD of silica.

*See Fig. 44 of this report for a reproduction of this figure and superposed data from the Markite studies in this program.



MARKITE PLATE

Reproduced from
best available copy.

318

CAST

Fig. 27. Radiograph of Markite Plate 318-1 (Cast)

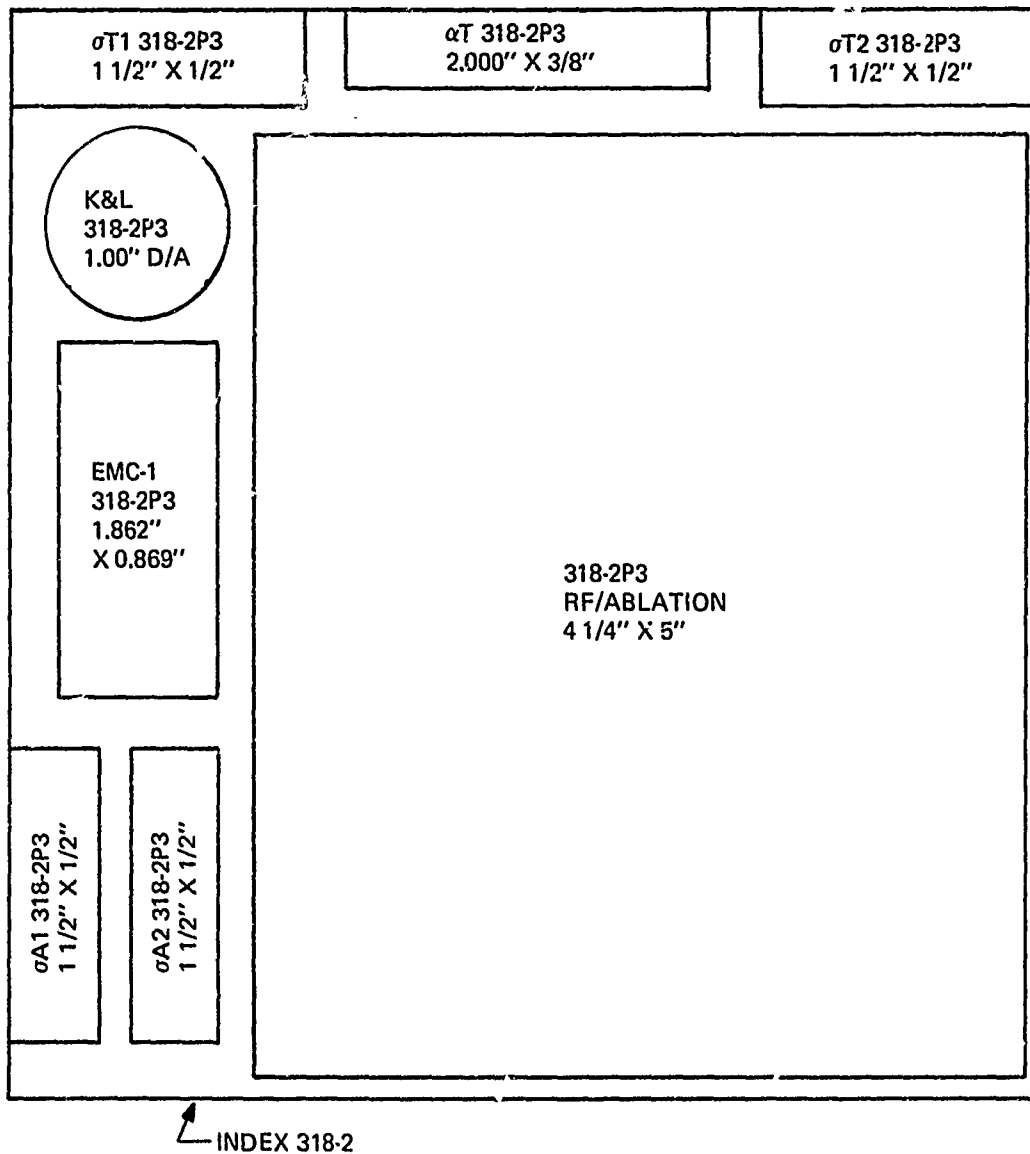
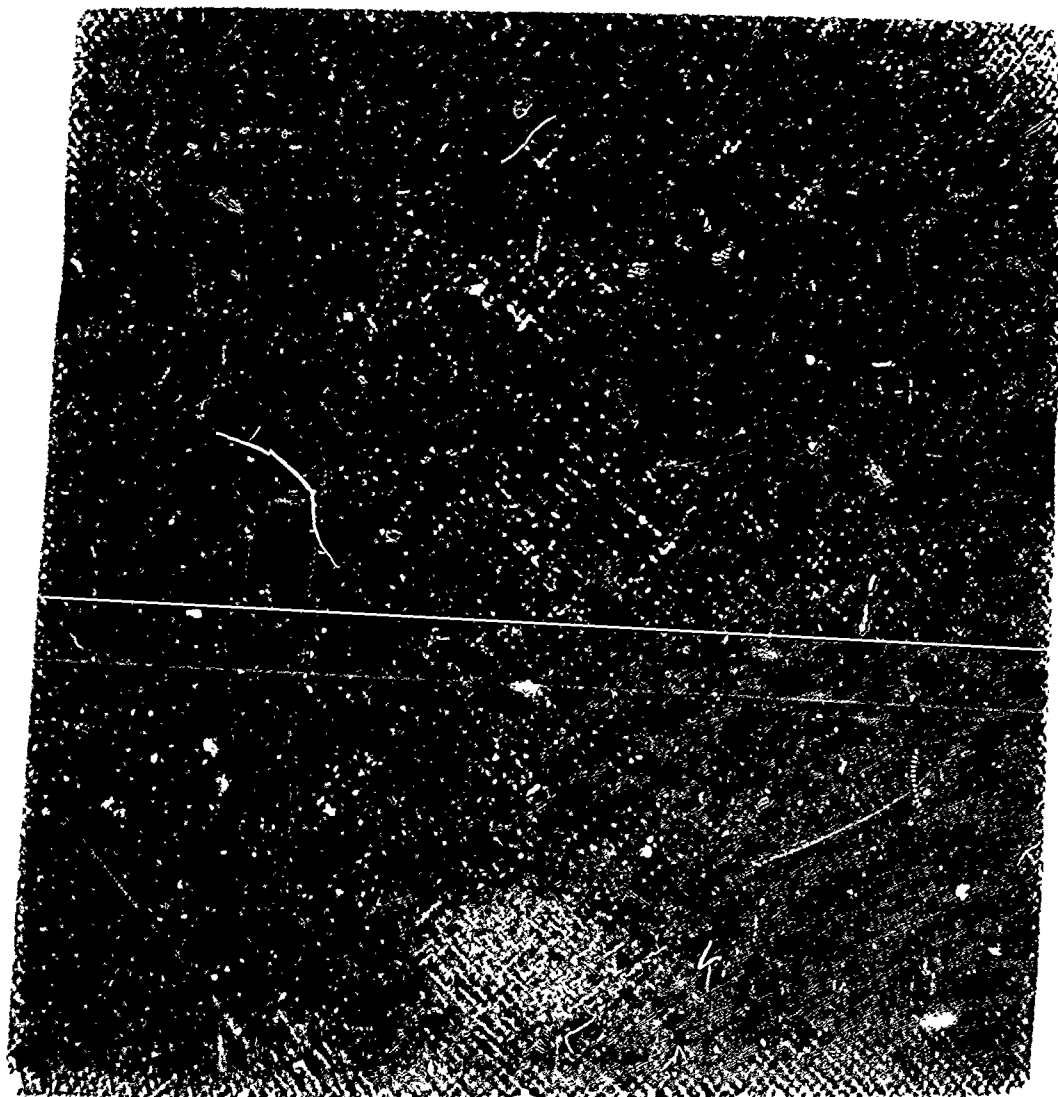


Fig. 28. Sample Layout: Markite Plate 318-2 (Cast)



MARKITE PLATE

318

CAST

Fig. 29. Radiograph of Markite Plate 318-2 (Cast)

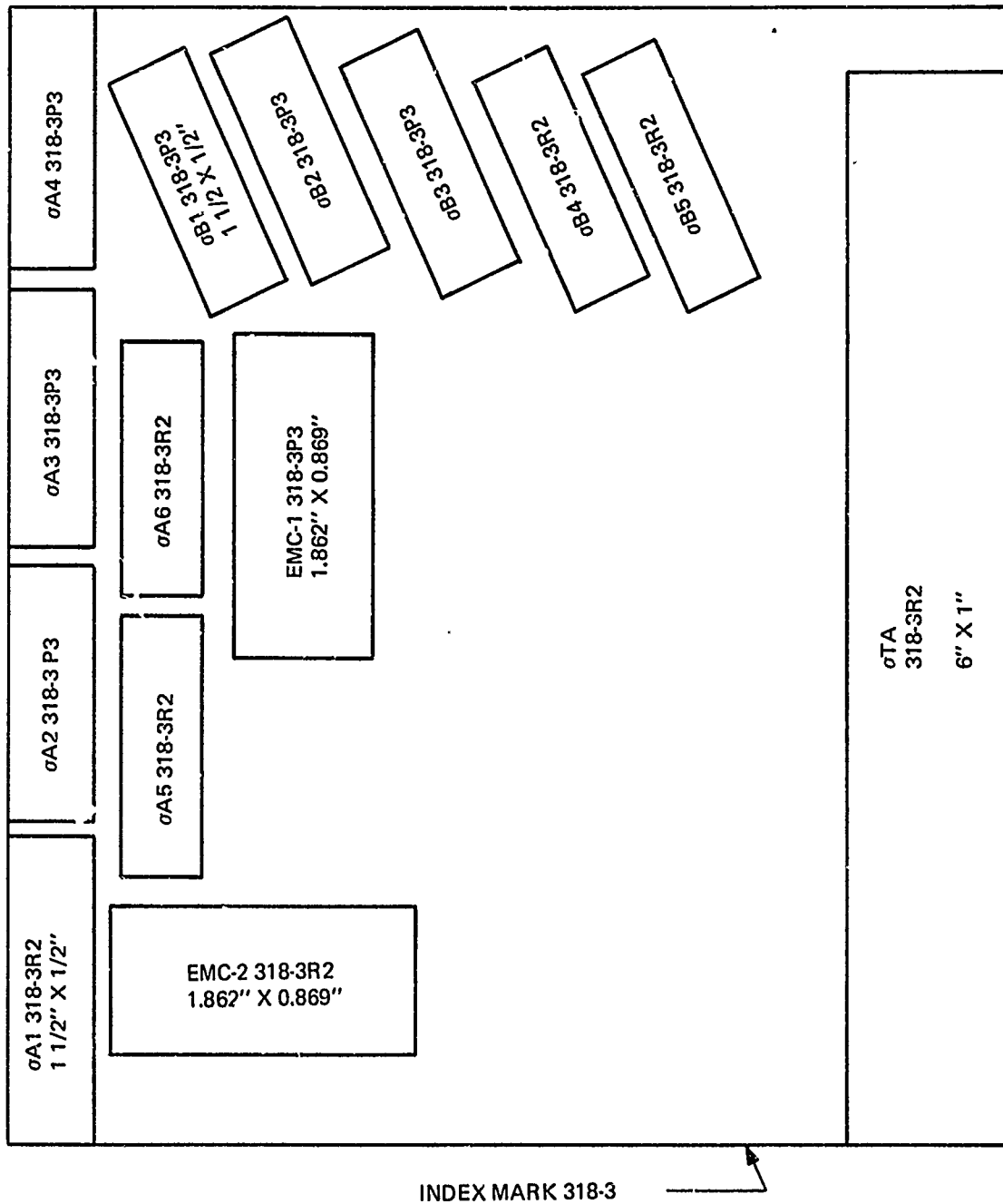
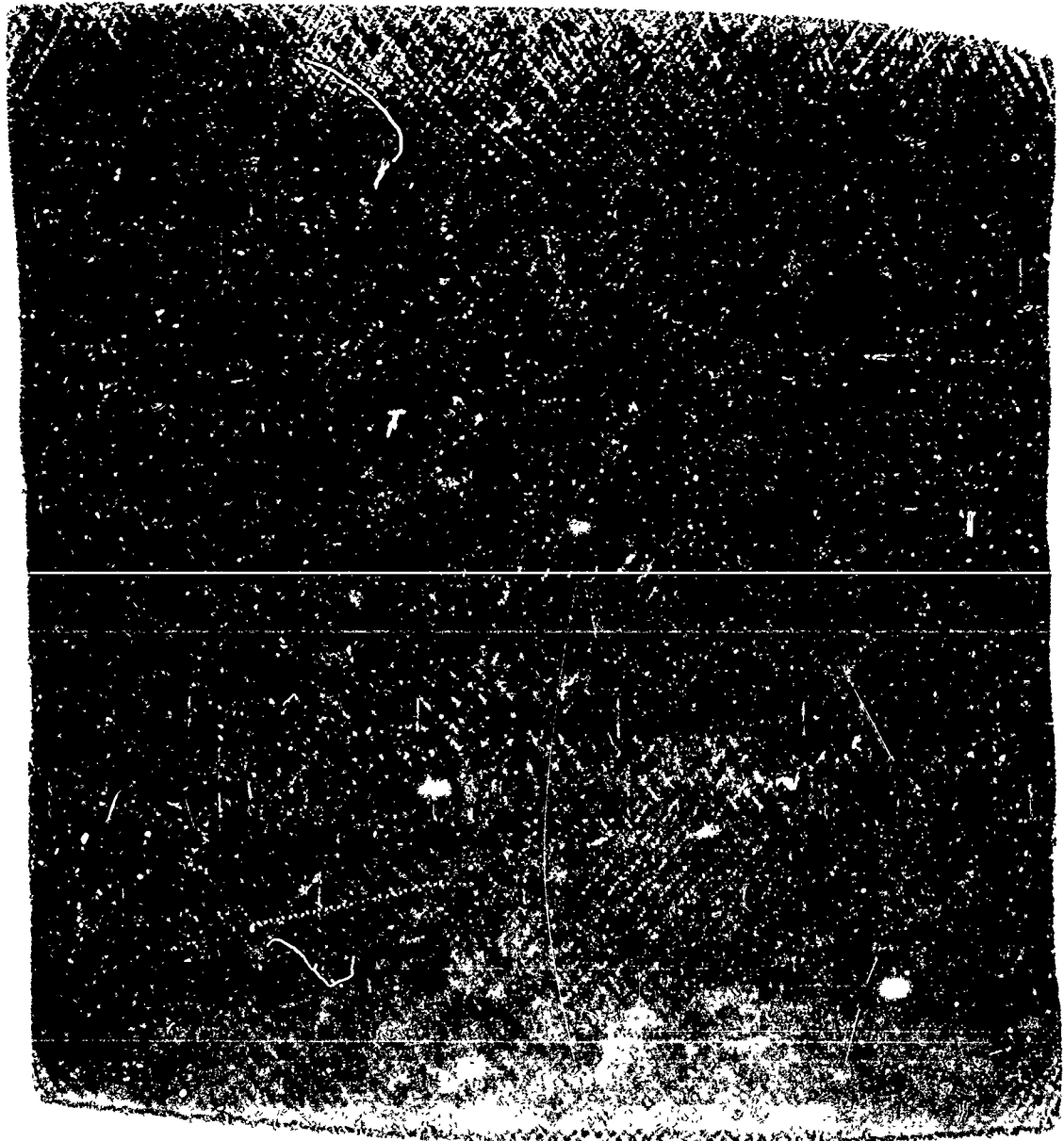


Fig. 30. Sample Layout: Markite Plate 318-3 (15PSI Molding Pressure)



MARKITE PLATE

318 3

15 PSI

Fig. 31. Radiograph of Markite Plate 318-3 (Molded at 15 PSI)

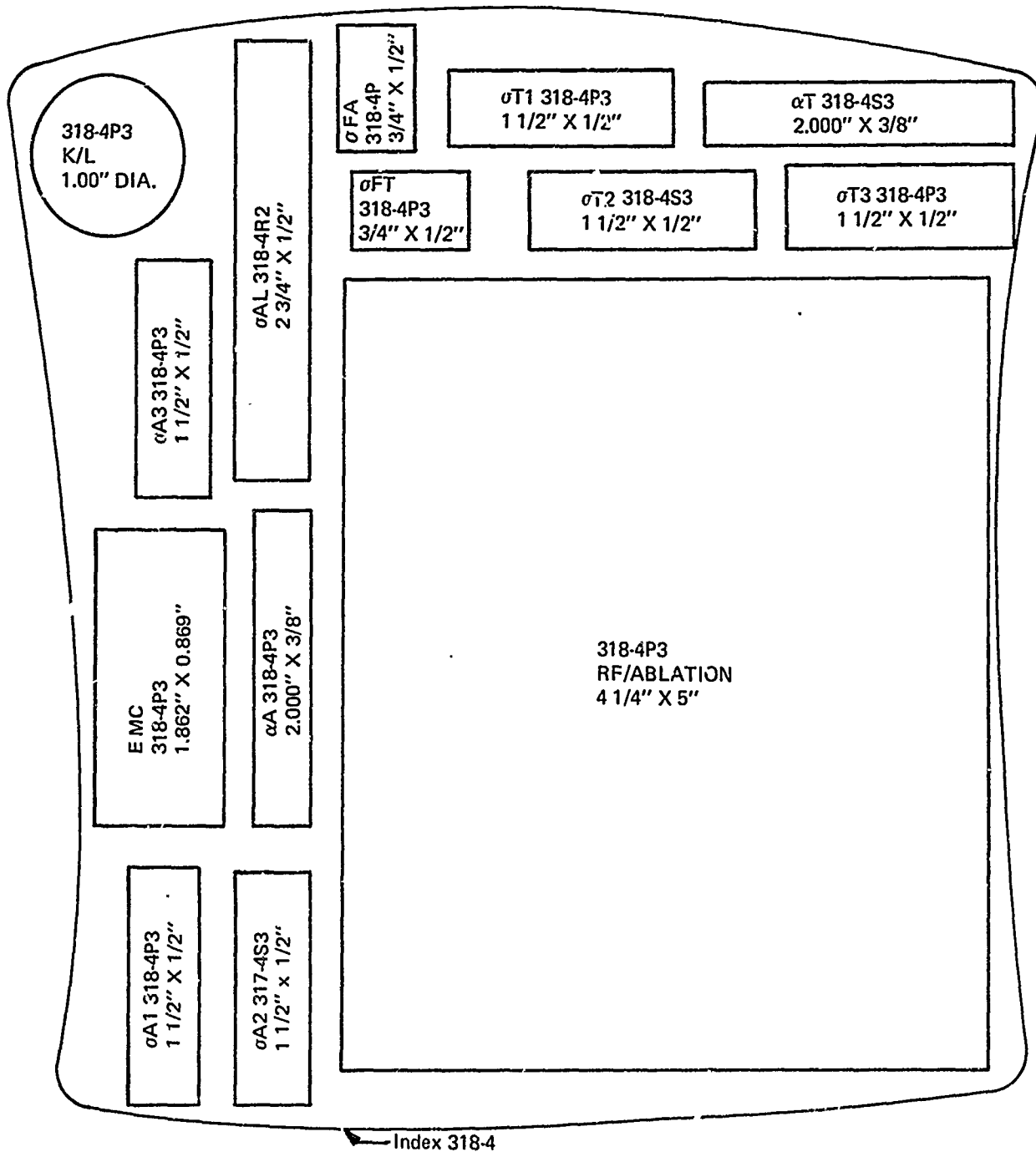
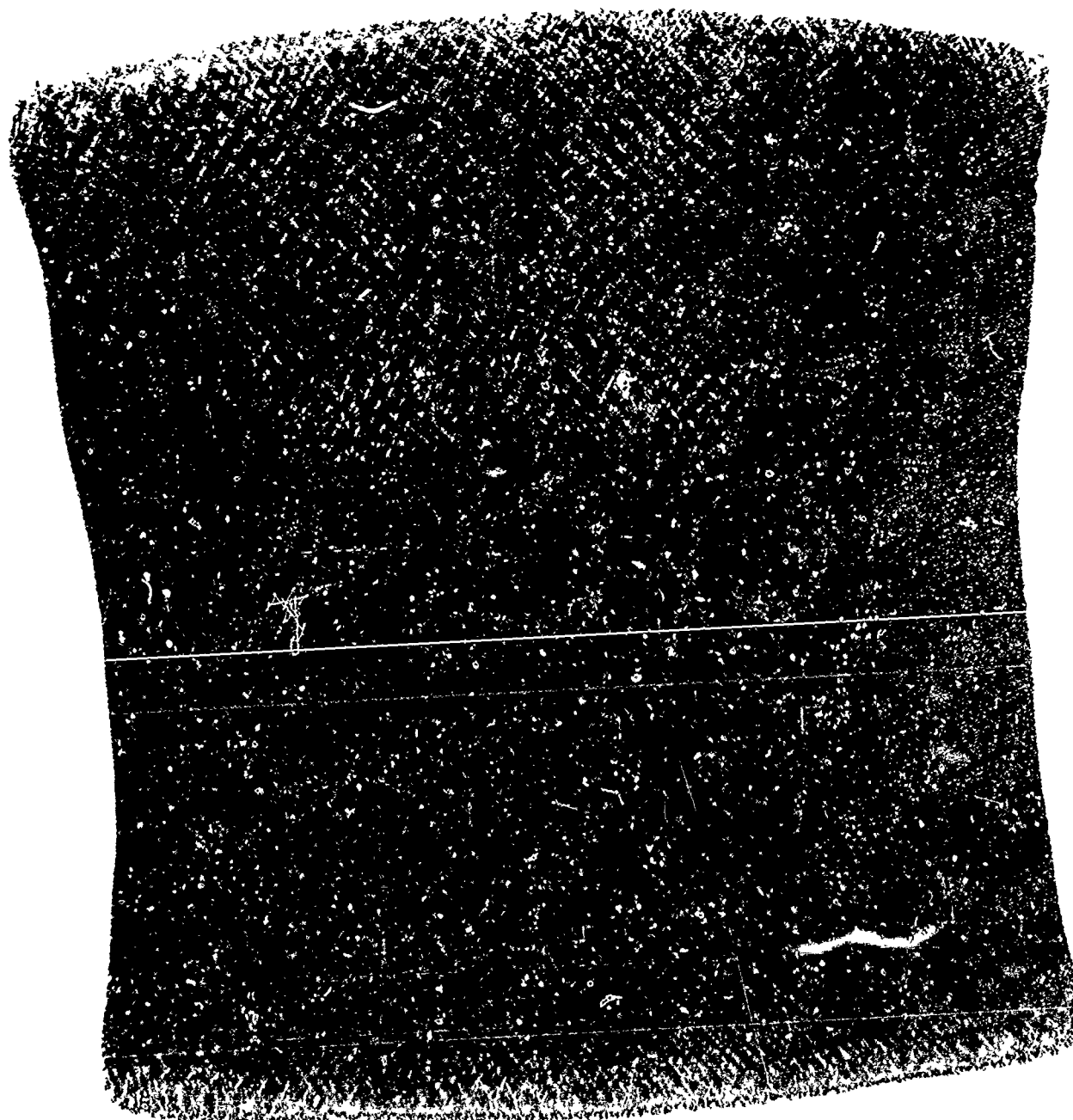


Fig. 32. Sample Layout: Markite Plate 318-4 (1000 PSI Molding Pressure)



MARKITE PLATE

318

4

Reproduced from
best available copy. 

1000 PSI

Fig. 33. Radiograph of Markite Plate 318-4 (Molded at 1000 PSI)

3-27

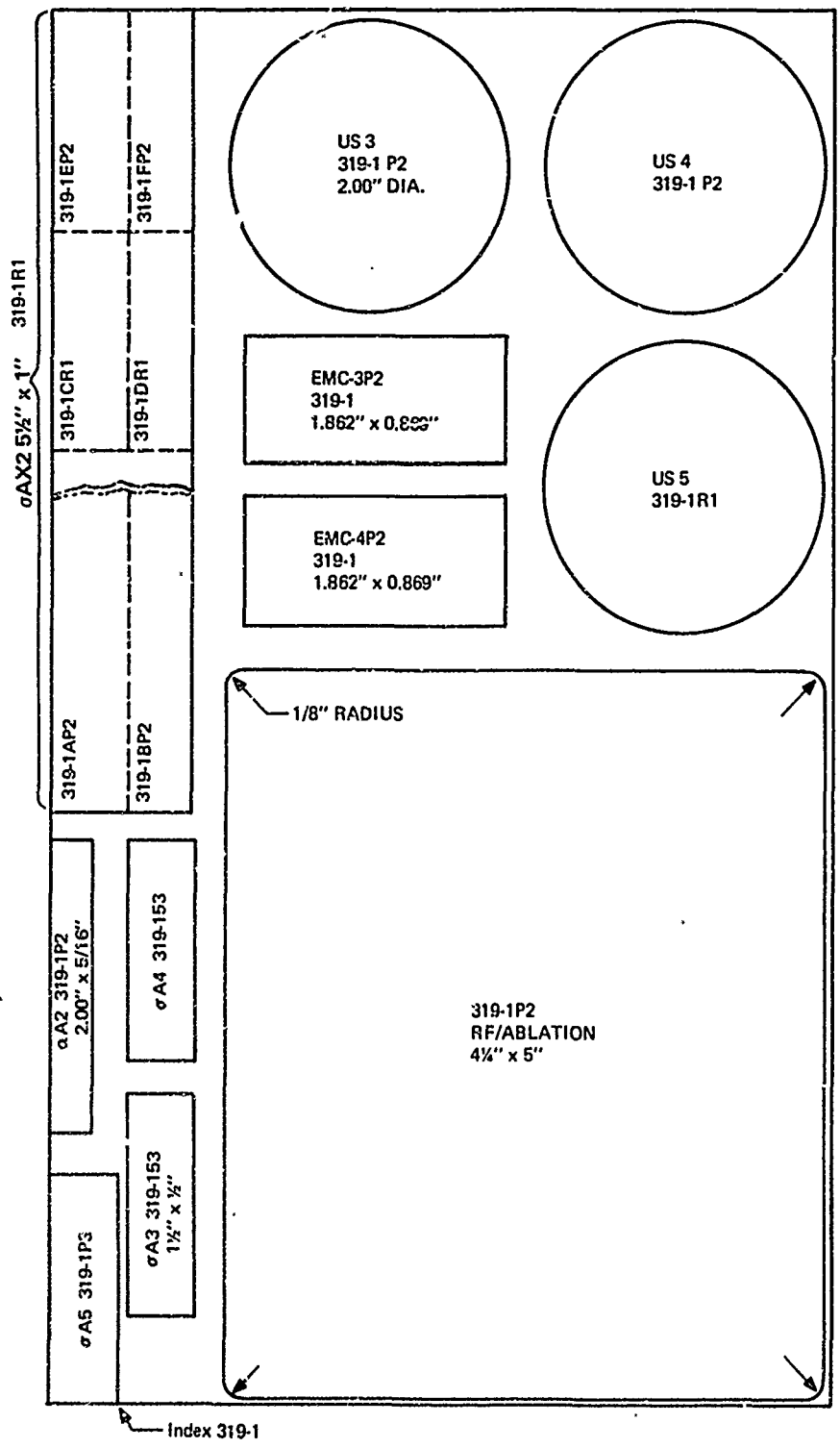


Fig. 34. Sample Layout: Markite Plate 319-1

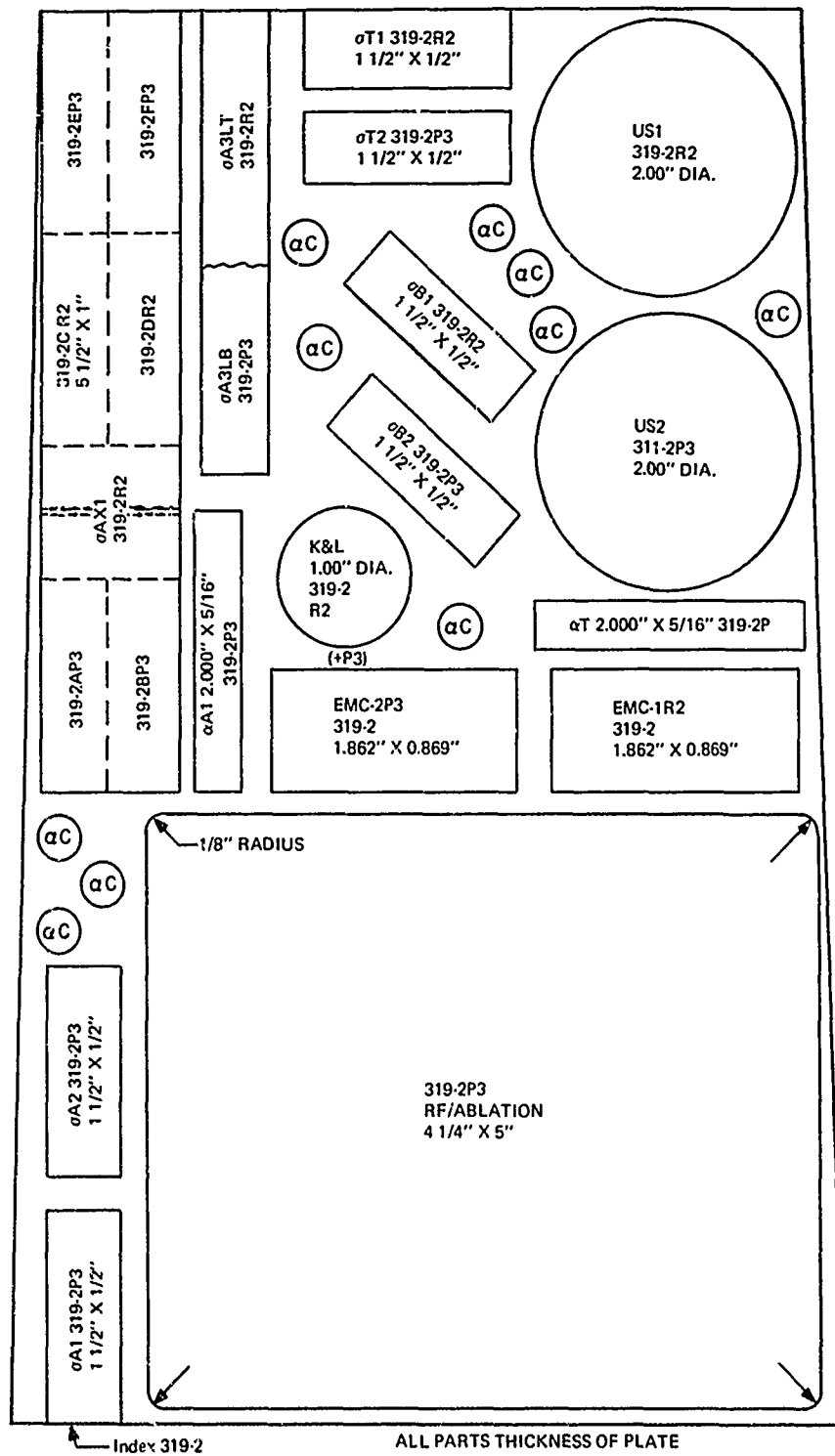


Fig. 35. Sample Layout: Markite Plate 319-2

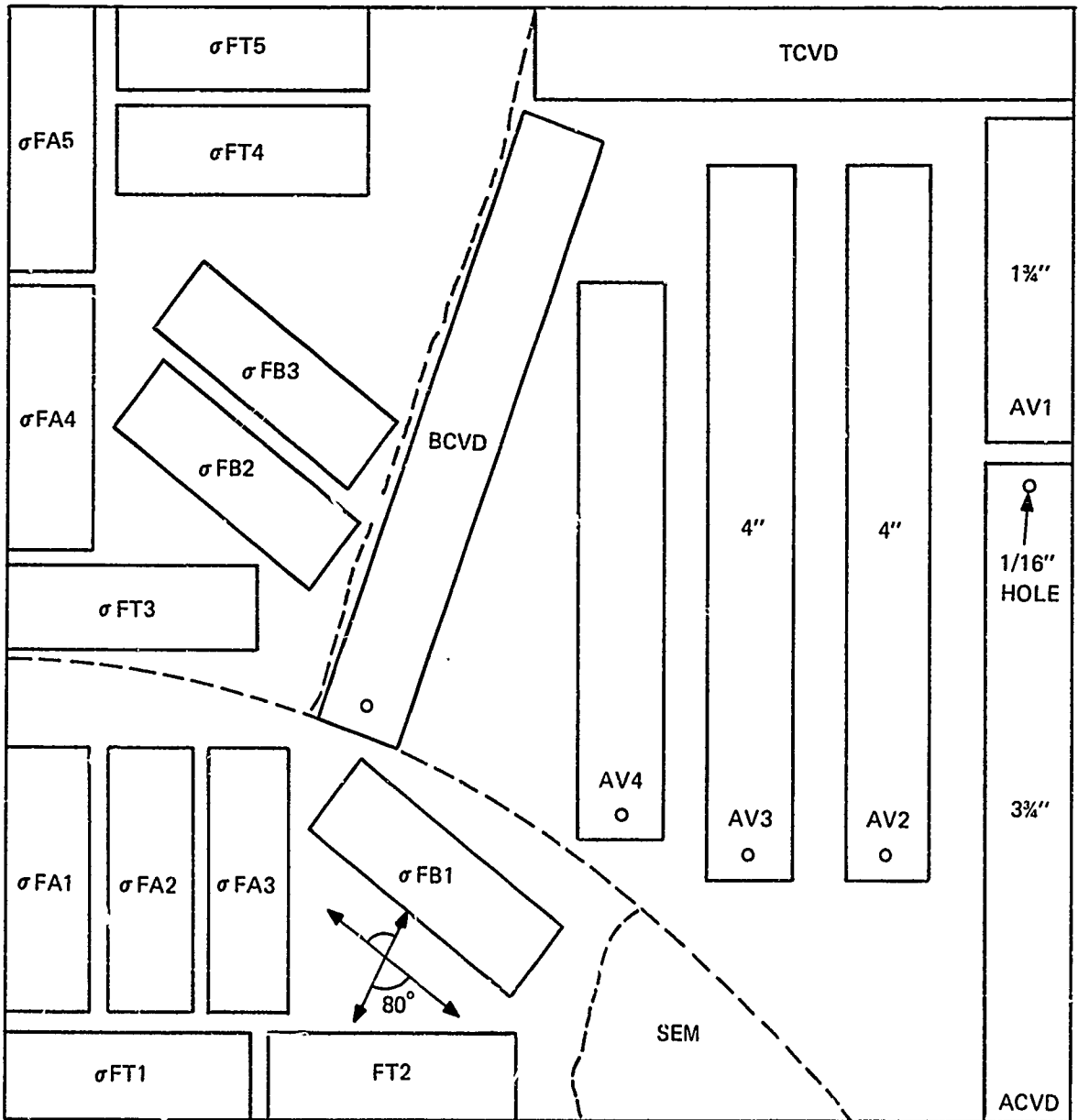


Fig. 36. Sample Layout: Markite Plate 209-3

3.2 MECHANICAL CHARACTERIZATION

3.2.1 Phase 1

In the first Hardened Antenna Window Program, reported in Reference 1, the orientation of specimens was designated as "axial" -- meaning parallel to the length of the 8 x 10-inch plates which had been molded from the approximately three-foot long omnivave scarves; or "bias" -- meaning approximately along the direct fiber reinforcement angle, about 35 to 45 degrees off the axial direction of the plate; or "transverse" -- meaning across the width of the plate and the original woven Omniweave scarf. Several other measurements, e. g. , slapplate testing, thermal conductivity and expansion were made in the "C" or through-the-thickness direction.

It was generally observed in this earlier work that, as expected, the highest strengths were obtained from "bias" specimens; and because of the tendency of the weaves to have surface -- measured fiber reinforcement angles in the range of 35 to 45 degrees rather than the nominal 45 degrees, the axial tensile strengths were generally higher than the transverse. Examination of the overlay sampling layouts and plate radiographs of the final report (Reference 1) shows this angular distribution to have actually ranged from 38 to 55 degrees for plates 87-1 and 87-2.

The three different weaving geometries of the work with these 8 x 10 plates focussed attention on the variations between the weave fiber reinforcement designs themselves rather than on detailed geometry or specific sample considerations. Since the strength levels in the axial direction ranged to a maximum of 2,000 - 4,000 psi and to 12,000 in the bias direction (plates 87-1 and 87-2), the first category for improving the materials' overall antenna window systems performance was the mechanical strength. The process variables identified as sensitive for this study were discussed above in Section 2. However, when the collected test results were initially examined for the effects of the process variables such as HF etchant, silane coupler, molding pressure, density and fiber volume fraction, the only obvious discriminant was found to be the molding pressure, apparently optimal at 125 psi, the lowest pressure. Table 15 gives the flexural results on long bars, i. e. , of a loading geometry intended to produce tensile failure rather than shear failure, and Table 16 gives the uniaxial tension tests on bars similar to that shown in Fig. 7.

As the detailed treatment of the characterization data proceeded, the series 1 test results were plotted. Ultimate tensile strengths versus the fiber reinforcement angle, as measured at the sample surface (Fig. 37), clearly show the sharp dependence of the mechanicals on surface FPA. Also, the effect of such processing variables as molding pressure is clearly observed. Note that specimens L_1 , L_2 , I_1 , I_2 , and C_1 (but not the maverick C_2) clearly form the highest family of curves in Fig. 37, despite their fiber volume fractions being on the order of 60 percent as compared to about 70 for the 300 psi moldings and 73 - 74 for the 1000 psi case. The effects of etching and

TABLE 15. RESULTS OF FLEXURAL TESTS (SERIES 1 TEST SPECIMENS) (1)

| Sample Number | Specimen Dimensions (in) | Density (gm/cc) | Axial Fiber Angle (\pm deg) | Molding Pressure (psi) | Span Upper/Lower (in) | Apparent(2) Flexural Strength (psi) | Flexural Modulus ($\times 10^6$ psi) | Remarks |
|---------------|--------------------------|-----------------|--------------------------------|------------------------|-----------------------|-------------------------------------|---------------------------------------|-----------------|
| F | 10.3 x 0.736 x 0.226 | 1.69 | 22 - 26 | 1000 | 9 | 8640 | 3.12 | 3-Point Loading |
| D | 10.6 x 0.740 x 0.235 | 1.66 | 25 - 27 | 1000 | 0.75 / 3.5 | 9074 | 2.66 | 4-Point Loading |
| E | 10.8 x 0.740 x 0.233 | 1.68 | 25 - 28 | 1000 | 0.75 / 3.5 | 6030 | 2.00 | 4-Point Loading |
| A1 | 4.01 x 0.810 x 0.214 | 1.71 | 33 | 300 | 0.75 / 3.5 | 6672 | | 4-Point Loading |
| A2 | 3.90 x 0.810 x 0.232 | 1.67 | 35 | 300 | 3.5 | 6872 | | 3-Point Loading |
| H2 | 4.53 x 0.810 x 0.208 | 1.68 | 29 | 1000 | 0.75 / 3.5 | 7956 | | 4-Point Loading |
| K2 | 4.38 x 0.819 x 0.181 | 1.75 | 30 | 1000 | 0.75 / 3.5 | 8454 | | 4-Point Loading |
| L1 | 4.40 x 0.809 x 0.254 | 1.55 | 35 | 125 | 0.75 / 3.5 | 10274 | | 4-Point Loading |

(1) See Table 3 for processing details.

(2) Specimen not completely failed.

TABLE 16. RESULTS OF TENSILE TESTS (SERIES 1 TEST SPECIMENS) (1)

| Sample Number | Molding Pressure (psi) | Density (g/cc) | Axial Fiber Angle (\pm deg) | Ult. Tensile Strength (psi) | Strain (%) | Elastic Modulus (10^6 psi) | Remarks |
|---------------|------------------------|----------------|--------------------------------|-----------------------------|------------|-------------------------------|------------------------------------|
| A1 (2) | | 1.71 | 33 | 8950 | 0.5 | 0.90 | Failure close to doubler |
| A2 (2) | | 1.67 | 35 | 5758 | --- | ---- | Visual crack after flexure test |
| G1 | 300 | 1.69 | 31 | 11161 | 1.8 | 1.44 | Center failure |
| G2 | | 1.67 | 33 | 8468 | 2.3 | 1.42 | Failure close to and under doubler |
| J1 | | 1.68 | 32 | 13651 | 1.45 | 1.48 | Center failure |
| J2 | | 1.61 | 31 | 13179 | 2.35 | 1.90 | Center failure |
| B1 | | 1.66 | 38 | 6440 | ---- | ---- | Failure under and close to doubler |
| B2 | | 1.69 | 36 | 6472 | 1.6 | 1.22 | Center failure |
| H1 | | 1.76 | 32 | 7031 | 0.95 | 2.18 | Center failure |
| H2 (2) | 1000 | 1.68 | 29 | 15233 | ---- | ---- | Center failure |
| K1 | | 1.71 | 30 | 11977 | 1.9 | 1.84 | Failure close to and under doubler |
| K2 (2) | | 1.75 | 30 | 13611 | ---- | ---- | Center failure |
| C1 | | 1.68 | 30 | 17724 | 2.3 | 1.20 | |
| C2 | | 1.64 | 32 | 7490 | 1.5 | 1.08 | Center failure |
| I1 | | 1.59 | 35 | 10779 | ---- | 1.16 | Center failure |
| I2 | 125 | 1.68 | 32 | 17332 | 1.75 | 1.90 | Failure under doubler |
| L1 (2) | | 1.75 | 35 | 11193 | ---- | ---- | Center failure |
| L2 | | 1.68 | 30 | 13634 | 2.00 | 1.60 | Failure close to and under doubler |

(1) See Table 3 for processing details.

(2) Specimens previously flexure tested to near failure.

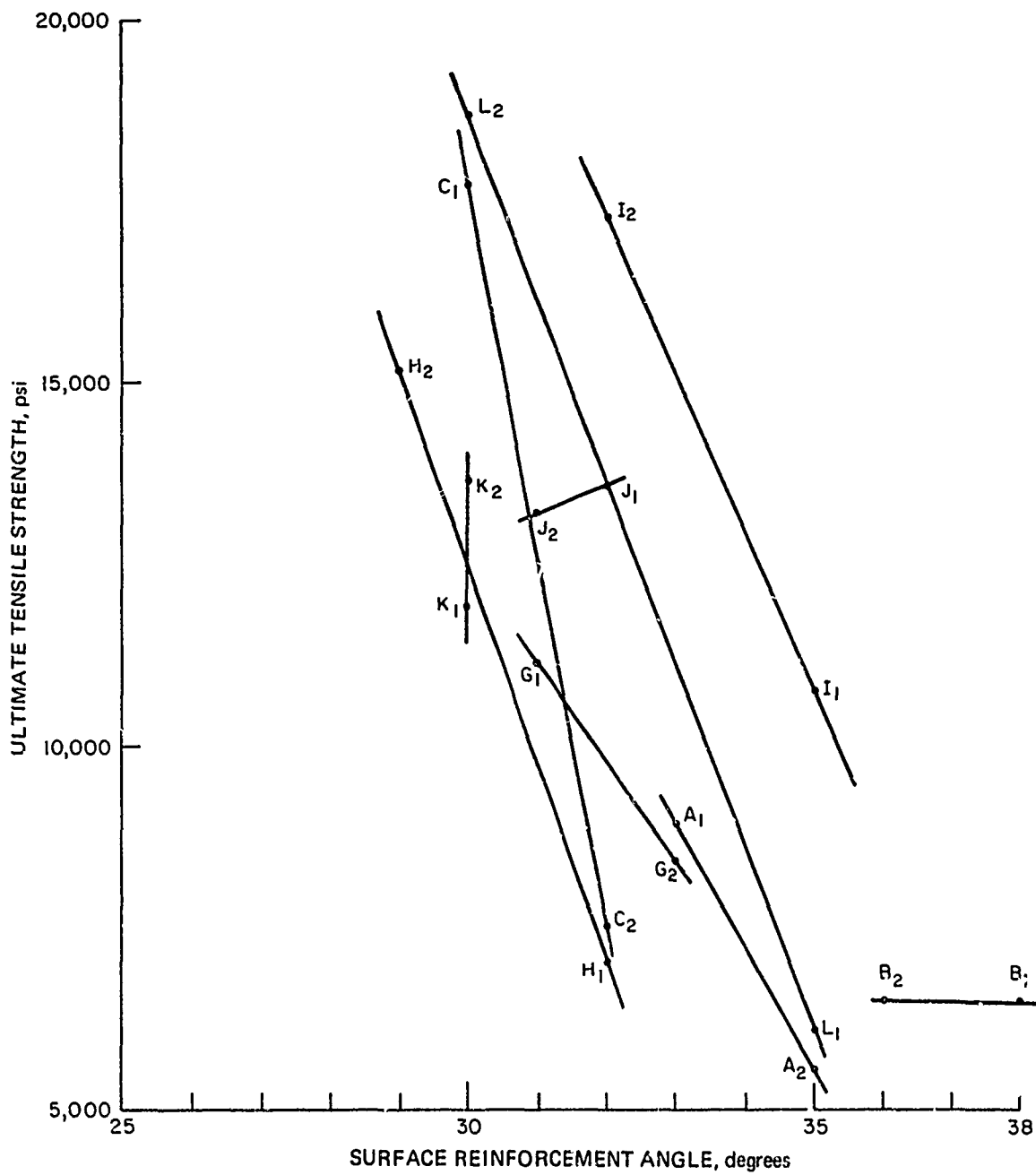


Fig. 37. Series 1 Tensile Tests: Ultimate Tensile Strength vs. Surface Reinforcement Angle

coupling were not apparent from these tests, so that series 2 was devoted to an examination of the effects of the coupler concentration at 1 and 10 percent, and possible detection of a characterization "fluke" in the closed-cell woven specimen design. The single 10 percent etching concentration was selected on the basis of the small mass losses observed on the series 1 tests and the desire to reduce the number of processing parameters.

The series two results of Table 17 are plotted in Fig. 38, again as a function of surface FPA, but in three separate subplots for 10 percent silane, 1 percent silane and Cab-O-Sil loaded specimens. In each subplot, the effects of machined sample edges are compared to as-woven closed cell results. The four specimens impacted in flyer plate testing are also indicated by addition of an X in the symbols. Note that the three 1 percent silane specimens were each impacted at 4000 taps after sample O₁ of the 10 percent silane group was observed to survive 2000 taps.

The difficulty of validly measuring the surface FPA for series 2 must again be emphasized, as is evident in our inclusion of both sets of measured data in Table 7. In plotting the trend lines of Fig. 38, the functional dependence so clear for the series 1 specimens was assumed intrinsic to the material. In fact, little conflict is evident with curve-fitting to this dependence, except for non-machined specimens with Cab-O-Sil which both failed under the doublers and are drawn in as a positive slope dashed line for easy identification. These two specimens were also noted above in Section 3.1.3 "Detailed Sampling Plan and Radiographic NDT" to have surface cracks.

Among the process categories, the material with one percent silane coupler and the closed cell (unmachined) specimens demonstrates the highest strength and lies along the upper boundary lines of the similarly processed series 1 specimens. The spread of the data is larger however, and again may reflect either the difficulty of meaningful surface reinforcement angle measurement or critical performance of the near-optimal specimens.

The machined material similar to the above, i.e., 1 percent silane clearly lies below the unmachined material; whereas this is not evident from the 10 percent silane treated specimen. The overall strength of the 10 percent silane lies below that of the 1 percent material and in line with these specimens treated with Cab-O-Sil (which had an apparent lower surface angle).

These latter specimens were molded to a lower density and homogeneity than the conventional materials because of the higher viscosity resulting from the colloidal silica addition. The surface finishes, which were in some cases resin-rich, made angular measurements very difficult. This lower density at the same 125 psi molding pressure and the cracks noted above by radiography may explain the lower overall strength.

TABLE 17. RESULTS OF TENSILE TESTS (SERIES 2 TEST SPECIMENS)

| Specimen Number | Density (g/cc) | Axial Fiber Angle (\pm deg.) | Thru-The Thickness Fiber Angle (deg.) | Processing ^{1,2} Parameter | Cross-Section Area (in ²) | Ultimate Tensile Strength (psi) | Elastic Modulus ($\times 10^6$ psi) | Remarks |
|-----------------|----------------|---------------------------------|---------------------------------------|-------------------------------------|---------------------------------------|---------------------------------|--------------------------------------|--|
| M1 | 1.64 | 34.0 | ----- | 10% silane | 0.190 | 14,200 | 0.91 | Center Failure |
| M2 | 1.71 | 33.7 | 24-36 | unmachined | 0.168 | 8,910 | 1.05 | Center Failure |
| N1 | 1.63 | 31.5 | 15-20 | edges | 0.194 | 11,600 | 1.05 | Center Failure |
| O1 | 1.60 | 30.0 | 19-21 | | 0.198 | 10,858 | 0.23 | Plate-Slap Tested ³ , 2000 taps |
| N2 | 1.67 | 21.5 | 14-21 | 10% silane | 0.160 | 11,715 | 0.71 | Center Failure |
| O2 | 1.69 | 31.0 | 18-20 | machined edges | 0.160 | 12,462 | 1.04 | Center Failure |
| P1 | 1.72 | 33.0 | 17-22 | 1% silane | 0.165 | 21,000 | 0.99 | Center Failure |
| P2 | 1.75 | 28.5 | 16-20 | unmachined edges | 0.155 | 20,450 | 1.72 | Center Failure |
| Q1 | 1.72 | 33.0 | 10-20 | edges | 0.162 | 9,876 | 0.18 | Plate-Slap Tested ³ , 4000 taps |
| U1 | 1.80 | 34.0 | 14-18 | | 0.165 | 17,400 | 1.24 | Center Failure |
| U2 | 1.83 | 31.0 | ----- | | 0.151 | 21,060 | 0.23 | Plate-Slap Tested ³ , 4000 taps |
| V2 | 1.81 | 30.0 | ----- | | 0.151 | 16,556 | 0.31 | Plate-Slap Tested ³ , 4000 taps |
| Q2 | 1.74 | 32.0 | 16 | 1% silane | 0.141 | 18,200 | 0.87 | Center Failure |
| R1 | 1.80 | 32.0 | 15-25 | machined | 0.136 | 14,197 | 1.63 | Center Failure |
| R2 | 1.76 | 34.0 | 21-23 | edges | 0.147 | 10,207 | 0.91 | Center Failure |
| V1 | 1.79 | 34.0 | 20-24 | | 0.154 | 10,254 | 0.77 | Center Failure |
| S1 | 1.61 | 27.0 | ----- | Cab-O-Sil added | 0.216 | 21,600 | 1.95 | Failure close to doubler |
| S2 | 1.68 | 26.0 | ----- | unmachined | 0.210 | 13,900 | 2.11 | Failure close to doubler |
| T1 | 1.52 | 28.0 | 17-21 | Cab-O-Sil added | 0.204 | 18,026 | 1.09 | Center Failure |
| T2 | 1.60 | 29.0 | 20-25 | machined | 0.193 | 14,246 | 1.30 | Center Failure |

1 - See Tables 5 and 6.

2 - All specimens treated with 10% HF and molded at 125 psi.

3 - Indicated specimens subjected to plate slap testing prior to tensile testing. Tensile failure occurred in area of flyer plate impression.

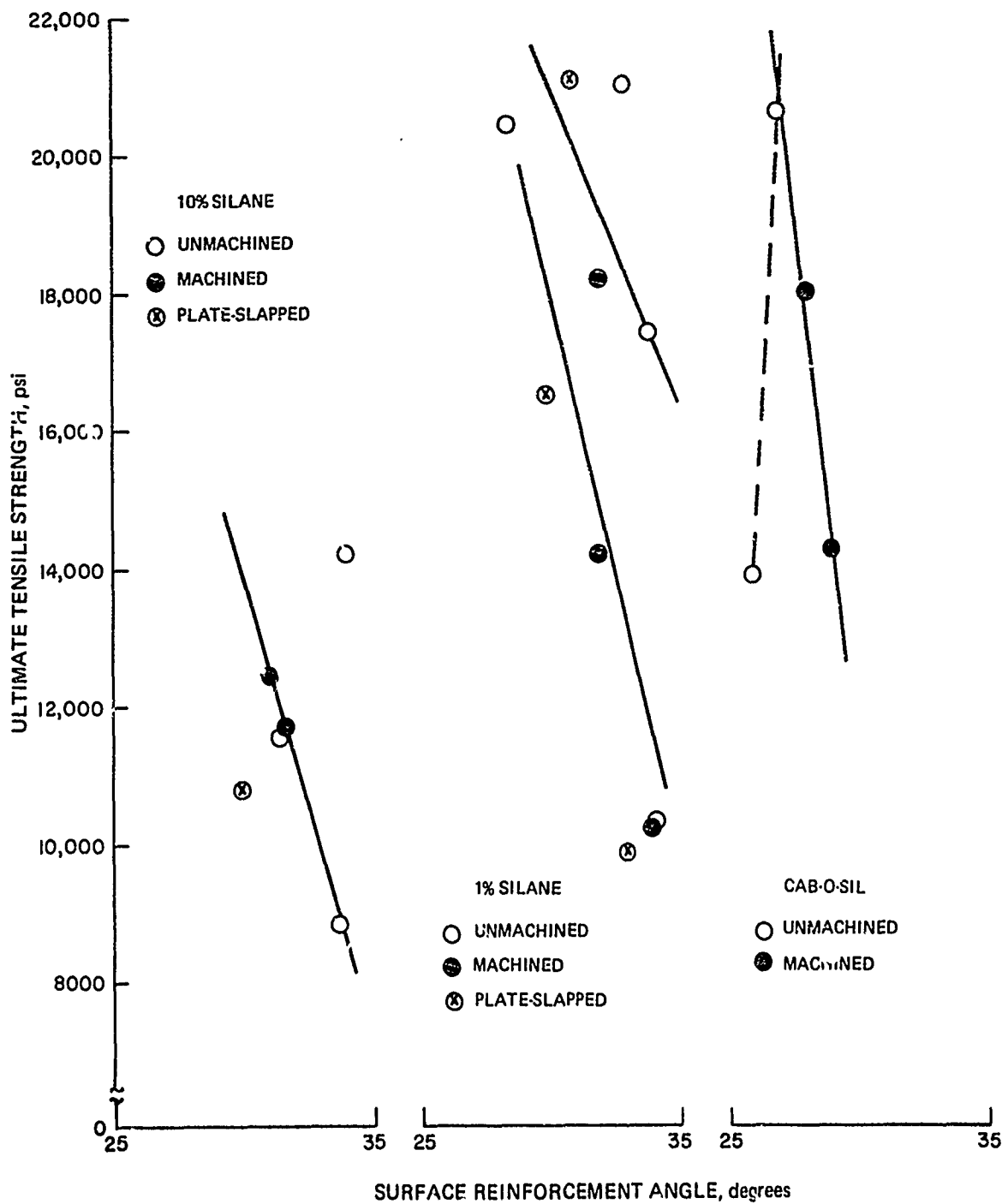


Fig. 38. Ultimate Tensile Strength vs. Surface Reinforcement Angle
Series 2 Specimens

Machining the edges — taking 1/32-inch off each side of the 0.81-inch wide specimens (equivalent to two molded fiber bundle diameters) — has the effect of reducing the ultimate tensile strength by about 25 to 35 percent for the 1 percent silane material. It also gives the result for the two conventional ADL-10 compositions of yielding far less scatter in the observed data points. This suggests a different failure mechanism for closed-cell woven fibers versus machined-edge specimens, with the closed-cell specimens perhaps more dependent on the fiber quality, achieving higher than the average strengths for statistically "lucky" specimens.

Although machining of closed-cell or segregated weave "finger" samples yields about 25 percent lower strengths, the overwhelming technical fact remains that axial tensile strengths on the order of 10,000 to 20,000 psi have been observed, for fiber geometries where strengths of only 2,000 to 4,000 were previously achieved. Examination of Table 47 of Reference 2 shows this result contrasted to the maximum of 12,000 psi for the 0° reinforcement angle of the bias specimens.

The results of both series 1 and 2 show the elastic modulus of the material to lie in the range from 0.7 to 2.2 ($\times 10^6$ psi), with strains to failure of from 1.5 to 2.35 percent. Although these modulus values are comparable to those obtained on the conventional 45 degree fiber pitch angle (FPA) material of the earlier program previous values, the strains to failure are much higher. They were only 0.04 to 0.48 percent for axial and transverse specimens and 0.32 to 0.55 for bias specimens. This is a particularly encouraging result for use of the material as a non or low load bearing member along with other very high strength structural heat shield materials.

The spread of the moduli and strain to failure can also be normalized somewhat by accounting for the angular dependence.

Flyer plate impact at the extraordinarily high levels of 2000 and 4000 taps seems only to have lowered the modulus, while having no drastic effect on strength. In fact, specimen U2 at 21,060 psi ultimate tensile strength actually was the highest strength ADL-10 specimen tested, this after 4000 taps impact testing. Within the already emphasized constraints of accurately measuring a representative value of surface FPA, and the limited number of normalized parameter samples, the maximum reduction in tensile strength due to impact would be approximately 20 to 30 percent, the same as the effect of machining edges.

The moduli of impacted specimens range from 0.18 to 0.31. The shock testing seems to have "mashed" the matrix while causing little damage to the fibers which were subsequently permitted to travel 4 to 10 times farther through or with the matrix (lower modulus) before ultimate tensile failure.

3.2.1.1 SEM Studies of Fractured ADL-10 Specimens

Figure 39 shows a fractured surface of ADL-10 tensile specimen A2. The 50X view shows a fractured fiber bundle end, its individual filaments and the impregnated and cured SR350 resin matrix. The 200X view gives detail of the end of this same fiber bundle and the fiber-matrix bond. The 1000X view shows that the filaments have been sheared free of the matrix along much of the exposed length of the fracture surface. Specimen A2 (no etching or silane coupling) had the lowest observed tensile strength of all the Phase I material, 5758 psi. The fracture is nevertheless seen to have been in the composite shear mode rather than brittle as for many of the ADL-10 specimens described in Reference 1.

Figure 40 shows two stereo SEM views of the fracture surface of specimen S1 which was a Cab-O-Sil filled ADL-10. In the 37.5X view the sample's resin matrix face is seen at the top of the photo and the individual sheared filaments of the fracture surface are seen in fiber bundles.

The 375X view shows a close-up of the sheared 10 micron filaments emerging from the matrix. The filleting and bonding of the matrix around the filaments is apparent.

In Figure 41, additional SEM's are shown of the fracture surface of S1. At 20X the specimen's face and the intertwining fiber bundles are seen, while at 100X the fiber-matrix bond and matrix fracture surface show an apparently more resin and Cab-O-Sil rich character than the micrographs of A2. Reference to Tables 2 and 5 shows this to be definitely the case, 31.3 percent resin and Cab-O-Sil volume percent for S1, 17.2 percent for A2. S2 also failed anomalously low in its processing group (Fig. 38).

3.2.2 Phase 2: Quartz Silicone Systems

3.2.2.1 Test Data

The data accumulated in the Phase 1 study on specimens obtained from the finger weaving and the demonstrated improved processing led to the application of these techniques to actual plate processing. Tensile data was obtained therefore on plate material subjected to the improved processing techniques. The tensile data from these plates 331-1 and 331-2 is shown in Table 18, together with some flexure data in Table 19. These measurements were all made in the 0° fiber reinforcement orientation, along the "bias" of the plate.

It can be seen that there is a marked difference in the tensile capability of each panel. Plate 331-2 has an average strength of 18,000 psi, versus 7,300 for plate 331-1. Reference to Table 9 shows that plate 331-1 was molded at 150 psi, to 1.59 gm/cc, plate 331-2 at 1000 psi to 1.68 gm/cc. In the series 1 molding studies on woven fingers, 125 psi molding yielded higher strength than 1000 psi. Note that the 125 psi finger



Reproduced from
best available copy.

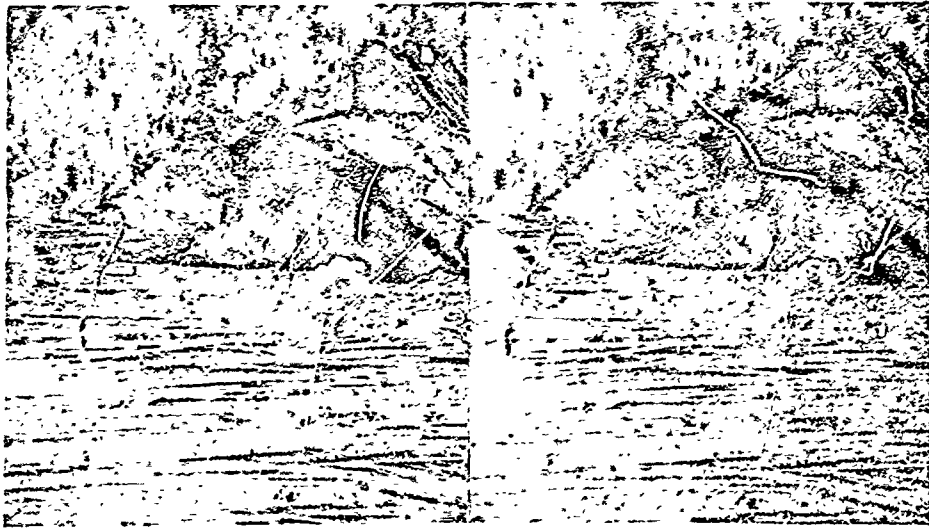
1000X

200X

50X

Tensile Specimen A2 (no etch, silane coupled) had the lowest observed strength at 5758 psi of the closed-cell woven ADL-10 specimens.

Fig. 39. SEM's of Fracture Surface of Tensile Specimen A2



37.5X

Reproduced from
best available copy.



375X

Fig. 40. Stereo SEM's of Fracture Surface of S1 (Cab-O-Sil Filled) Tensile Specimen



100X

Resin Face of Specimen

Figure 41: SEM's of Fracture Surface of Cab-O-Sil Loaded Tensile Specimen S1.

Reproduced from best available copy.



20X



1000X



TABLE 18. TENSILE TEST DATA - PLATES 331-1 AND 331-2
(IMPROVED PROCESSING)⁽⁴⁾

| Plate Number | Specimen Number | Density ⁽¹⁾ (gm/cm ³) | Ultimate ⁽³⁾ Tensile Strength (psi) | Elastic Modulus (10 ⁶ psi) | Failure ⁽²⁾ Strain (%) |
|--------------|-----------------|---|---|---|---|
| 331-1 | B1 | 1.59 | 7560 | 1.85 | >0.10 (.41) |
| | B2 | 1.59 | 6910 | 1.90 | >0.29 (.36) |
| 331-2 | B1 | 1.68 | 18,450 | 2.71 | >0.51 (.85) |
| | B2 | 1.68 | 17,720 | 2.70 | >0.37 (.77) |

(1) Density represents measurements on the plate.

(2) Failure strain in parentheses represents the projection of elastic behavior to the failure load. Strain gauge failure occurred at strain levels indicated.

(3) All specimens were cut along a principal weave direction, i.e. bias.

(4) Processing details are given in Table 9 and Fig. 13.

TABLE 19. FLEXURE TEST DATA - PLATES 331-1 AND 331-2⁽³⁾
(IMPROVED PROCESSING)

| Plate Number | Specimen Number | Density ⁽¹⁾ (gm/cm ³) | Specimen Thickness (in) | Ratio: Span Thickness | Flexural ⁽²⁾ Stress (psi) |
|--------------|-----------------|---|-------------------------------|--------------------------|--|
| 331-1 | F | 1.59 | 0.278 | 3.59 | 13,839 |
| 331-2 | F1 | 1.68 | 0.251 | 3.98 | 15,121 |
| | F2 | 1.68 | 0.251 | 3.98 | 16,667 |

(1) Density represents plate measurements.

(2) All specimens cut along a principal weave direction.

(3) Processing details are given in Table 9 and Fig. 13.

specimens had fiber volume fractions in the range of 60 - 70 percent, while the denser 1000 psi specimens were in the range 66 - 79 percent. It has been shown analytically (Section 4) that the maximum useful fiber volume fraction for four directional Omni-weave is 68 percent. Above this percent, the fibers cannot be straightly aligned to bear loads in the true composite mode. In the case of the 331 series molded plates, the ur-impregnated silica Omniweave fabric had a higher original density of 1.1 gm/cc, compared to a nominal 0.9 for the Omniweave fibers. Thus molding this particular weave at 1000 psi produced an ADL-10 composite with fiber volume fraction of 67 percent, compared to 59.6 percent for the 125 psi molding. The fiber volume fraction of plate 331-2 was nearly optimal; density was coincidentally higher. The implication is that a higher molding pressure and fiber volume fraction would have produced a strength lower than that of plate 331-2.

Since there is only a single flexural test point on 331-1 there is the possibility that this is "statistically" high and may be a rare upper bound data point. It is always possible to obtain good flexural data in comparison to tension data since the flexural stress represents the outer fiber tensile stress at the maximum applied load. This specimen may have had good bonding of the outer surface fibers, for instance, and does not represent the overall tensile capability of the panel through the total thickness. A tensile test on a specimen with similar capability would apply the maximum stress essentially over the total crosssectional area so that the total thickness capability is evaluated.

Thermal expansion data for plates 331-1 and 331-2 is shown in Fig. 42. As can be seen, the expansion in the through the thickness direction is much greater than the in-plane data and is actually similar to data reported in Reference 1 for plates 87-1, 87-2, 88-1 and 88-2 (See Fig. 62, Reference 1). The in plane expansion is however slightly negative and consistently so, on the three specimens tested. This is in disagreement with earlier data in which very slight positive expansions were seen (numerically similar). The reason for this is not obvious but may be associated with an internal stress state within the plates produced during the processing. In any case the thermal expansion of the material is quite small.

3.2.2.2 Basic Resin Behavior

The improved mechanical behavior demonstrated by the quartz silicone fabricated in this program, compared to the earlier work, led to the question of the maximum level strength which this material could theoretically reach. This computation requires a knowledge of the behavior of the actual resin in order to compute approximate ultimate load capabilities by simple "laws of mixtures" type equations, i.e.,

$$UTS_{\text{composite}} = UTS_{\text{fiber}} \times \nu_{\text{fiber}} + UTS_{\text{resin}} \times \nu_{\text{resin}}$$

ν = volume %

UTS = ultimate tensile strength

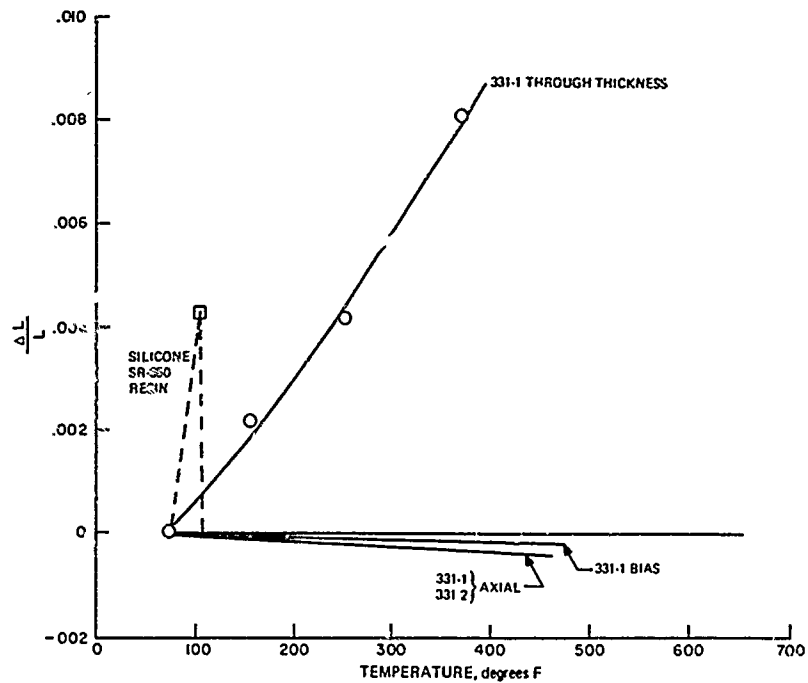


Fig. 42. Thermal Expansion, Plates 331-1 and 331-2

The above equation holds reasonably well for the unidirectionally oriented composites, however more sophisticated models are required for multidimensional weaves, etc. Flexural properties were determined on the silicone resin since it was not feasible to fabricate tensile specimens of the resin due to their fragility. This flexure data is shown in Table 20.

TABLE 20. FLEXURE DATA ON SILICONE RESIN (FOUR POINT)

| Specimen | Width (in) | Thickness (in) | Span | | Flexural Strength (psi) | Flexural Modulus ($\times 10^6$ psi) |
|----------|---------------|-------------------|---------------|---------------|-------------------------------|---|
| | | | Lower (in) | Upper (in) | | |
| 1 | 0.500 | 0.250 | 2.0 | 0.75 | 854 | 0.22 |
| 2 | 0.500 | 0.250 | 2.0 | 0.75 | 1185 | 0.25 |
| 3 | 0.500 | 0.250 | 2.0 | 0.75 | 915 | 0.24 |
| 4 | 0.500 | 0.250 | 1.25 | 0.75 | 876 | ---- |

Note: Flexural deflection measurements obtained from machine crosshead travel calibrated for machine deflection with a heavy steel bar.

The more complex mathematical models of elasticity used for the results of Section 4 also require some evaluation of the shear modulus of the resin. The shear modulus measurements were made directly using a standard torsion test for adhesives. The test specimen geometry consists of an annulus of SR-350 resin having:

outside diameter = 1.75 in.

inside diameter = 1.50 in.

thickness = 0.25 - 0.30 in.

bonded between two concentric, 1.75-inch diameter aluminum loading blocks. Three such specimens were prepared and subjected to torque at a constant rate of angular twist until a fracture occurred. Shear deformation was sensed and recorded as a continuous function of applied torque using a strain gage twistometer. Shear modulus and shear stress at failure were computed from the resulting torque - twist curve and the measured specimen geometry using the well known relationships;

$$T = \frac{MR}{J}$$

$$E = \frac{R\phi}{L}$$

$$G = \frac{T}{E}$$

T = torsional shear stress

M = applied moment

R = radius

J = moment of inertia

ϕ = twist angle

L = cylinder length

E = shear strain

G = shear modulus

The data generated by these tests is shown in Table 21.

TABLE 21. TORSIONAL SHEAR DATA FOR CURED AND MOLDED SR-350 SILICONE RESIN

| Specimen | Shear Strength (psi) | Shear Modulus (psi) | Ultimate Strain (percent) |
|----------|----------------------|---------------------|---------------------------|
| 1 | 620 | 77,600 | 0.81 |
| 2 | 554 | 64,800 | 0.91 |
| 3 | 775 | 69,700 | 1.22 |

Since it was a principal intent of this program to optimize the strength of these multi-dimensional composites, a target value of ultimate tensile capability was required. This target value can only be an analytical value based upon the capabilities of both resin and fiber as indicated earlier. Some data is required therefore, on the tensile

strength of the impregnated quartz fiber bundles. A method of measuring this is to tensile test unidirectional quartz-resin samples and, using the law of mixtures, to evaluate that component of strength associated with the quartz volume fraction. Since the strength of the resin has been shown to be less than 1000 psi (flexure data), it can be assumed that this will be a negligible strength component in an actual composite. Uniaxial quartz silicone tensile specimens were therefore fabricated. Three specimens were tested in an Instron test machine at crosshead speed of 0.02-inch/min. The specimens took the form of strips 3/4 wide x 0.15-inch thick having bonded doublers at each end. These were similar to the tensile specimen design used throughout this program. Strain was measured from strain gage outputs and the data in Table 22 was obtained. Some basic characterization data on the tested material is shown in Table 13.

TABLE 22. UNIDIRECTIONAL QUARTZ-SILICONE TENSILE TEST DATA

| Specimen Number | Ultimate Tensile Strength (psi) | Elastic Modulus (psi x 10 ⁶) | Poisson's Ratio |
|-----------------|---------------------------------|--|-----------------|
| 1 | 40,050 | 2.58 | 0.40 |
| 2 | 54,725 | 2.90 | 0.39 |
| 3 | 39,100 | 2.86 | ---- |

Applying the previously mentioned law of mixtures to the strength data:

$$\begin{aligned} \text{UTS (composite)} &= \text{UTS}_{\text{fiber}} \times \nu_{\text{fiber}} + \text{UTS}_{\text{resin}} \times \nu_{\text{resin}} \\ 40,000 &= (X) \times 0.30 + 1,000 \times 0.60 \end{aligned}$$

The strength of the quartz fiber bundle is of the order of 130,000 psi.

Applying the same rule to the elastic modulus and substituting the established modulus of quartz = 10.0×10^6 psi

$$\begin{aligned} E_{\text{composite}} &= E_{\text{fiber}} \times \nu_{\text{fiber}} + E_{\text{resin}} \times \nu_{\text{resin}} \\ &= 10.0 \times 10^6 \times 0.30 + 0.2 \times 10^6 \times 0.60 \end{aligned}$$

The computed elastic modulus of the composite is approximately 3.0×10^6 psi, which compares well with the measured values of $2.5 - 2.9 \times 10^6$ psi.

A full discussion of the theoretical strengths of the Omniweave composites is presented in Section 4.

A thermal expansion measurement was made on the SR350 resin without reinforcement. It was the intent to use it in the explanation of the negative expansion experienced by plates 331-1 and 2. This particular specimen consisted of two one-inch long, $1/4 \times 1/4$ -inch cross-section bars butted together to make the required two-inch long specimen. The material expanded rapidly up to 103°F from 70°F ($\Delta L/L = 0.0043$) and then showed immediate contraction. Examination of the specimen after test showed the two pieces to be welded together. This curve is also plotted as a dashed line in Figure 42 along with the ADL-10 data.

3.2.3 Silica/Pyrolyzed Silicone Resin System

3.2.3.1 Introduction

The second phase of this program was aimed at further development of a silica matrix in place of the silicone matrix. The intent was to improve the load bearing capability of the resulting silica fiber - silica matrix composite. Since this program was a processing study, rather than a design data study, there was a need for quick, reliable and cheap strength tests. This has been satisfactorily met by the determination of flexural behavior of the composite. It was shown in Reference 1 that this test is quite adequate for following process changes, e.g., impregnation - pyrolysis-reimpregnation sequences.

By comparison, tension testing is a relatively sophisticated and higher risk procedure for non-ductile materials such as ceramics. Precautions are necessary to insure accurate alignment of specimen/grip arrangements, etc. The available techniques and associated experimental problems are summarized in Reference 8. Although three tensile tests were made in instances where some plastic behavior was anticipated, it was not thought necessary at this stage in the materials development to place a major emphasis on this mode of testing.

The tensile and flexural test data is presented in Tables 23, 24, and 25. This data has been separated with respect to processing condition. Thermal expansion data is shown in Fig. 43. As with tensile testing, thermal expansion was not considered to be a significant measurement to be made in great detail at this time. It would be expected that the thermal expansion behavior of the quartz-silica composite would be similar to that for fused silica and quartz and it is sufficient at this time to demonstrate this fact.

The techniques for tensile, flexural and thermal expansion measurements have been adequately covered in the earlier report (Reference 1) and only the data and its significance is considered here.

3.2.3.2 Discussion of Mechanical Test Data

A. Panels 319-1 and 319-2

The principal difference between panels 319-1 and 319-2 is the timing of the Teflon removal from the silica fibers. In 319-1, the Teflon was removed by pyrolysis of the fibers prior to impregnation with SR-350. Panel 319-2, however, was impregnated with the coated fibers prior to pyrolysis. It is clear from an examination of the tensile and flexure data that the 319-1 is a stronger panel suggesting that better adherence of the matrix to the fiber is caused by pyrolysis of the fiber prior to impregnation. The inference is that the Teflon prevented effective matrix-fiber shear load transfer even after a second impregnation with SR350. It is interesting to see, however, that the

TABLE 23. TENSILE TEST DATA ON MARKITE PANELS*

| Plate, Processing | Specimen | Density (gm/cc) | Gage Area (in x in) | Ultimate Tensile Strength (psi) | Elastic Modulus (10 ⁶ psi) | Failure Strain (%) |
|-------------------|--------------|-----------------|---------------------|---------------------------------|---------------------------------------|--------------------|
| 319-1R1 | σ AX2 | 1.93 | 1.00x0.438 | 3596 | 2.96 | 0.28 |
| 319-2R2 | σ AX1 | 2.00 | 1.00x0.446 | 2595 | 4.76 | 0.07 |
| 318-3R2 | σ TA | 1.86 | 0.947x0.215 | 1360 | 4.26 | 0.03 |

*All tensile bars in reimpregnated condition, see Section 3.1.3 for suffix labelling convention, e.g., 319-2R2 indicates second reimpregnation after two pyrolyses. All specimens taken in "axial" direction of plate, with reinforcement fibers running at angle, along "bias" direction.

highest flexural strength recorded was with a specimen from panel 319-2 following a second reimpregnation, i.e., specimen σ A3LT 319-2R2 at 5908 psi.

Flexure specimens taken from beneath the doubler region of the tensile specimen effectively confirm the strength difference. It is interesting to note also from panel 319-2, that a small difference in flexural capability exists between specimens cut along a principal weaving direction (bias) and an axial/transverse plate direction. When a final version of this material is produced, this will be an aspect of characterization which will be evaluated. It would not be too surprising if this result were confirmed, since the effect appears in other ceramic composites, e.g., carbon-carbon composites. Data from panel 319-2 also shows that localized areas may have significantly lower capability, i.e., flexure data for σ T1 319-2R2 as compared with σ A3LT 319-2R2 and σ A3LB 319-2P3 as compared with any of the remaining third pyrolysis specimens in that group.

The average data from panel 319-1 is shown in Figure 44, which allows a comparison of the more recent material with that established in Reference 1. It can be seen that the absolute values are marginally improved and within the limited data available follow the same processing trends. The single data point from panel 319-2 corresponding to the second impregnation (i.e., σ A3LT 319-2R2) demonstrates an improved capability. This may be due to the higher woven density of these composites (1.1 gm/cm³) as compared to the earlier materials 0.52 gm/cc woven density.

B. Panels 318-2, 318-3 and 318-4

The flexural data generated on panel 318-2 demonstrate the extremely low strength, associated with producing a cast panel and subjecting it to pyrolysis. The purpose of this experiment was to take a dense weave (1.1 gm/cm³) and not to distort it by molding. It is obvious from this strength data and the low density that this technique is unacceptable.

TABLE 24. SHORT BEAM FLEXURE TESTS, MARKITE PYROLYSIS AND REIMPREGNATION STUDY**
(THREE POINT LOADING, 1" SPAN)

| Specimen | Specimen Thickness | Span : Thickness Ratio | Flexure Stress (psi) | Comment |
|---|--------------------|------------------------|----------------------|---|
| PLATE NO. 319-1 WOVEN FROM TEFLON COATED SILICA FIBERS, TEFLON REMOVED BY PYROLYSIS BEFORE SR-350 IMPREGNATION (SEE FIGURE 34) | | | | |
| After 2 pyrolysis cycles (1.90 gm/cc) | | | | |
| 319-1AP2 | 0.445 | 2.24 | 2434 | Flexure specimens cut from under grip area of tensile specimen AX2-319-1 |
| 319-1BP2 | 0.435 | 2.29 | 2637 | |
| 319-1EP2 | 0.425 | 2.35 | 2735 | |
| 319-1FP2 | 0.427 | 2.34 | 3017 | |
| Mean = 2700 | | | | |
| After 3 pyrolysis cycles | | | | |
| σ A5, 319-1P3 | 0.417 | 2.39 | 3053 | |
| Sintered at 3rd pyrolysis: | | | | |
| σ A4, 319-1S3 | 0.425 | 2.35 | 3039 | |
| σ A4, 319-1S4 | 0.420 | 2.38 | 3010 | |
| Mean = 3025 | | | | |
| PLATE NO. 319-2 WOVEN FROM TEFLON COATED SILICA FIBERS, FIRST SR-350 IMPREGNATION CARRIED OUT BEFORE REMOVAL OF TEFLON BY PYROLYSIS (SEE FIGURE 35) | | | | |
| After 2nd reimpregnation (2.0 gm/cc) | | | | |
| σ B1, 319-2R2 | .445 | ----- | ----- | Broken accidentally while loading |
| σ T1, 319-2R2 | .449 | 2.23 | 319 | Top half of 3" long flexure bar broken during machining. |
| σ A3LT, 319-2R2 | .445 | 2.25 | 5908 | |
| Mean = | | | | |
| After 3rd pyrolysis (1.98 gm/cc) | | | | |
| σ A3LB, 319-2P3 | .438 | 2.29 | 532 | Bottom half of 3" long flexure bar broken during machining |
| σ A1, 319-2P3 | .410 | 2.44 | 1838 | Bias specimen, apparently shows higher strength along fiber reinforcement direction |
| σ A2, 319-2P3 | .419 | 2.38 | 1828 | |
| σ B2, 319-2P3 | .428 | 2.34 | 2321 | |
| 319-2AP3 | .419 | 2.38 | 1876 | Density 1.64gm/cc, four short flexure |
| 319-2BP3 | .413 | 2.42 | 1762 | |

along fiber reinforcement direction

Density 1.64 gm/cc, four short flexure bar samples machined from area under grips of tensile specimen AXI 319-2R.

| | | | |
|----------|------|------|------|
| 319-2AP3 | .419 | 2.38 | 1876 |
| 319-2BP3 | .413 | 2.42 | 1762 |
| 319-2EP3 | .424 | 2.30 | 2045 |
| 319-2FP3 | .433 | 2.30 | 1933 |
| Mean = | | | 1767 |

PLATE NO. 318-2 CAST MARKITE (SEE FIGURE 29)

After 3rd pyrolysis (1.64 gm/cc)

| | | | |
|---------------------|------|------|------|
| σ T1 318-2P3 | .310 | 3.22 | 421 |
| σ T2 318-2P3 | ---- | ---- | ---- |
| σ A1 318-2P3 | .312 | 3.21 | 678 |
| σ A2 318-2P3 | .313 | 3.19 | 276 |
| Mean = | | | 444 |

Broken in machining

PLATE NO. 318-3 MARKITE MOLDED AT 15 PSI (SEE FIGURE 30)

After 2nd Reimpregnation (1.86 gm/cc)

| | | | |
|---------------------|------|------|------|
| σ A1 318-3R2 | .219 | 4.57 | 3751 |
| σ D4 318-3R2 | .220 | 4.55 | 3892 |
| σ B5 318-3R2 | .220 | 4.55 | 586 |
| Mean = | | | 2743 |

(3822 without 586 value)

After 3rd Pyrolysis

| | | | |
|---------------------|------|------|------|
| σ A2 318-3P3 | .195 | 5.13 | 2534 |
| σ A3 318-3P3 | .199 | 5.03 | 1987 |
| σ A4 318-3P3 | .202 | 4.95 | 2426 |
| σ B1 318-3P3 | .208 | 4.81 | 1996 |
| σ B2 318-3P3 | .209 | 4.78 | 425 |
| σ B3 318-3P3 | .209 | 4.78 | 735 |
| Mean = | | | 1684 |

(2315 without 425 & 735 values)

PLATE 318-4 MARKITE MOLDED AT 1000 PSI (SEE FIGURE 32)

After 2nd Reimpregnation (1.92 gm/cc)

| | | | |
|---------------------|------|------|------|
| σ A1 318-4R2 | .180 | 5.55 | 5902 |
|---------------------|------|------|------|

Long span flexure to detect composite rather than brittle failure

After 3rd Pyrolysis (1.80 gm/cc)

| | | | |
|---------------------|------|------|------|
| σ A1 318-4P3 | .190 | 5.26 | 1032 |
| σ A3 318-4P3 | .183 | 5.46 | 1159 |
| σ T1 318-4P3 | .203 | 4.93 | 1036 |
| Mean = | | | 1076 |

Sintered at 3rd Pyrolysis at temperature 2250 °F

| | | | |
|---------------------|------|------|------|
| σ A2 318-4S3 | .190 | 5.20 | 2767 |
| σ T 318-4S3 | .182 | 5.49 | 2000 |
| Mean = | | | 2384 |

Chipped thermal expansion specimen, tested as flexure bar

1. All specimens unless noted were nominally 1.5 long by 0.5-inch wide
2. Failure of all pyrolyzed specimens was in a brittle manner suggesting that the flexural strength is comparable to the tensile strength.

** See Section 3.1 for explanation of labelling convention for process identification.

TABLE 25. SHORT BEAM FLEXURE TESTS, CHEMICAL VAPOR DEPOSITION STUDIES ON PLATE 209-3 MARKITE MOLDED AT 1000 PSI (SEE FIGURE 36)*

| Specimen | Specimen Thickness | Span: Thickness Ratio | Flexure Stress (psi) | Comment |
|------------------|--------------------|-----------------------|----------------------|---------|
| <u>As Molded</u> | | | | |
| FA1 | .275 | 3.67 | 1745 | |
| FA2 | .275 | 3.67 | 1597 | |
| FA3 | .270 | 3.70 | 1646 | |
| FA4 | .265 | 3.77 | 1753 | |
| FT1 | .275 | 3.67 | <u>2783</u> | |
| | | | Mean = | 1905 |
| <u>After CVD</u> | | | | |
| BCVD | .275 | 3.64 | 1700 | |
| TCVD | .274 | 3.65 | 1784 | |
| AV1 | .28 | 3.57 | 1530 | |
| ACVD | .275 | 3.64 | <u>1730</u> | |
| | | | Mean = | 1686 |

Notes:

1. All specimens unless noted were nominally 1.5 long by 0.5-inch wide
2. Failure of all pyrolyzed specimens was in a brittle manner suggesting that the flexural strength is comparable to the tensile strength.

* The chemical vapor deposition (CVD) process for silica is described in Section 2.6.

Equally, the data generated on panel 318-3 which was molded at a low pressure (15 psi), demonstrated inferior capability as compared to 319-1 and 319-2 in the second impregnation and in the third pyrolysis state.

Panel 318-4 again demonstrates a high strength value associated with reimpregnating a pyrolyzed material, i. e., specimen AL 318-4R2 having a flexural strength of 5902 psi. This data together with the data point from 319-2 suggest that impregnating, if found acceptable for other reasons (such as transmittance) would be a good technique for improving the strength of the composite. The data from the third pyrolysis and sintering of this material at 2250°F demonstrates no improvement.

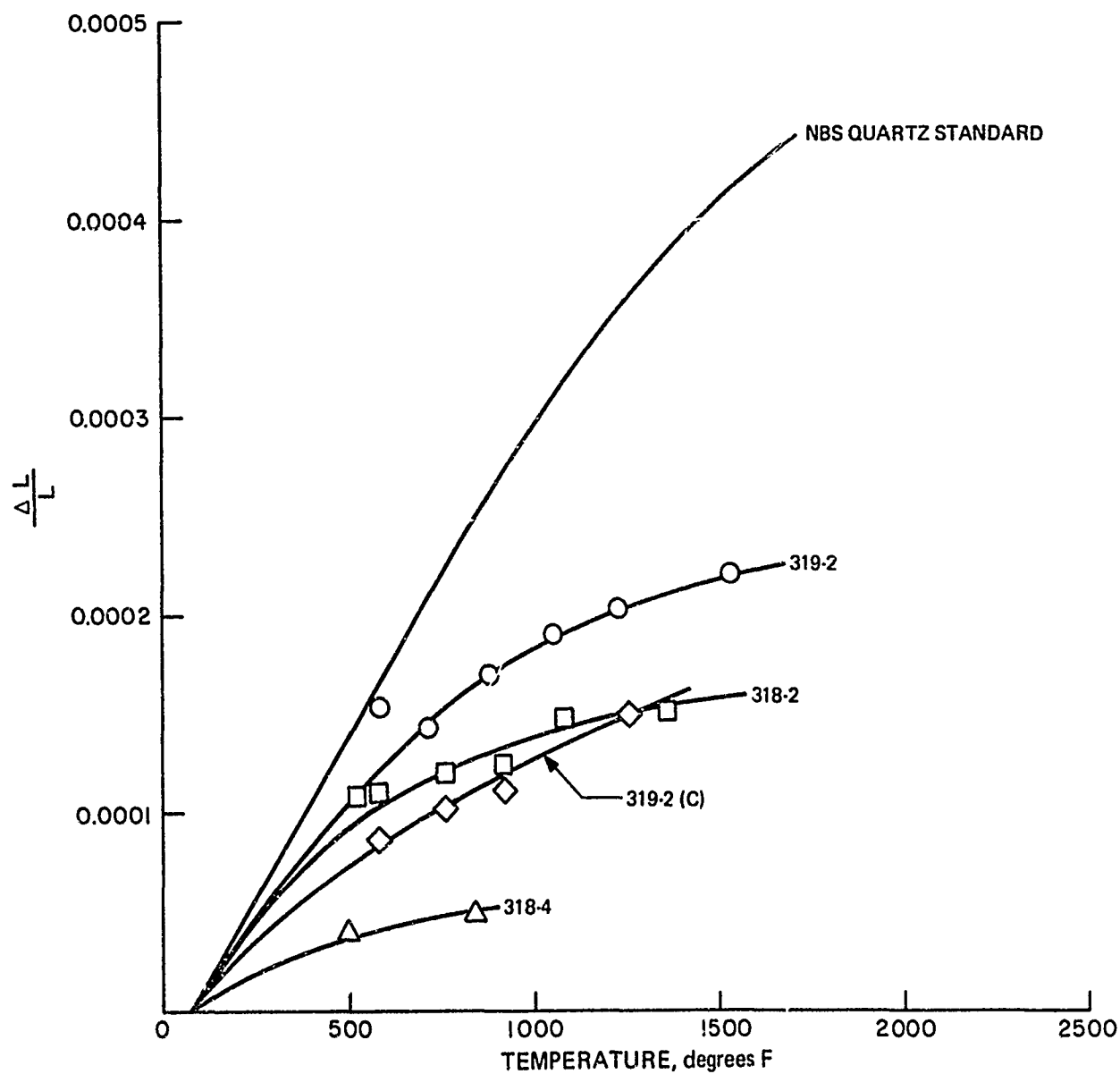


Fig. 43. Thermal Expansion of Markite Silica/Pyrolyzed Silicone

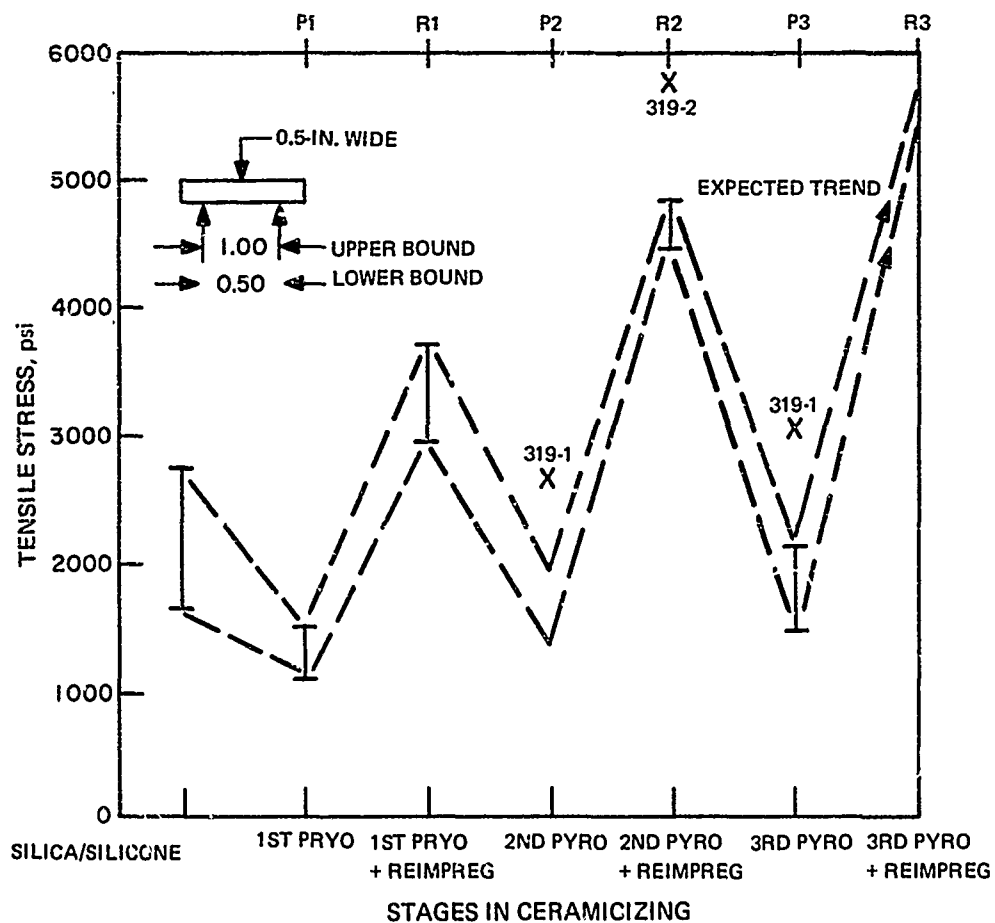


Figure 44. Silica/Silicone Transformation, Short Beam Flexure; Tensile Stress at Failure as a Function of Processing Operations, Latest Values Superimposed on Data from Reference 1

C. CVD Studies

There was no measurable improvement in flexural capabilities by the application of this technique to matrix production. See Section 2.6 for characterization data on these materials and Table 25 for the results of short beam flexure measurements.

D. SEM Studies on Markite

Figure 45 shows three SEM's of a fracture surface from the trial Markite plate 209-3. The 180X view includes portions of the sample face adjacent to the fracture and the embedded filaments. In the 530X view, the brittle nature of the fracture is obvious. The silica matrix is intimately adhering to the filaments. The 2100X view is a detail of interfilament fracture.

At the bottom of Figure 45, a scanning specimen current electron micrograph of the fracture surface, taken at the GE Space Sciences Laboratory in Valley Forge, is shown. The cylindrical void left by removal of a fiber bundle is at left center. Again, the multiply fractured individual filaments are seen at the silica fillets around the filaments.



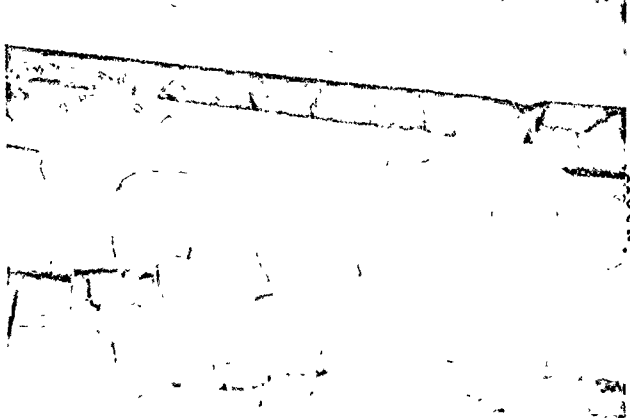
2100X



530X



180X



300X

Reproduced from
best available copy.

Figure 45. Top: Scanning Electron Micrographs of Fracture Surface from Markite Plate 209-3; Left: Electron Micrograph on Sample from Same Plate. Taken at GE Space Sciences Laboratory

Note: Nominal filament diameter is 10 microns.



3.2 ULTRASONIC MEASUREMENTS

The technique utilized in these studies for ultrasonic velocity and attenuation measurement is described in Section 3.4 of Reference 1. Some of the tests described in the following differ from the earlier tests in that woven strips in a tensile pull specimen configuration were used which were approximately 0.20-inch thick by 0.80-inch wide. All of the earlier tests were on 2.0-inch diameter "hockey-puck" type specimens.

The first group of tests conducted during the current phase of the program were made on these woven strips and were aimed at the study of process variables such as pressure and silane level. The results of the ultrasonic measurements on these strips are given in Table 3-11. With the exception of specimen "E", which was flex tested before being measured, all of the specimens are in the "as manufactured" state. In general, the observed velocities are low and the attenuations high as a result of scattering, indicative of extensive microcracking (probably both in the resin and at the resin-fiber interfaces) due to a failure of the cured resin to completely wet the quartz fibers. These two different locations of microcracking, in the resin and at the resin-fiber bend area are of course indistinguishable by ultrasonic techniques. However, the thoroughness of impregnation of SR-350 into the Omniweave before curing was indicated by the high degree of translucence of the wet composition.

Considering Series 1 (Table 26), the first group of specimens tested (Specimen "A" through "L"), a number of factors were varied. These included silane level concentration of the HF acid used to etch, and molding pressure. In general, the acid concentration was at three levels (0, 5 and 10 percent), the silane at two levels (approx. 0.3 and 1.6 percent) and the pressure at three levels (125, 300 and 1000 psi) if one neglects specimens D, E, and F. If these specimens are included, we add another level for the acid (1 percent) and for the silane (0 percent) but no longer have a complete factorial experiment. In an attempt to correlate the ultrasonic velocity with variations in these factors, the experiment was subdivided into several 3 factor, 2 level experiments in order to apply Yates method (Reference 9) of analysis. This analysis however indicated very little effect except possibly a pressure-acid interaction. The major difficulty was a lack of extensive replication which made it impossible to conclusively determine which effects were significant and which were not. Consequently, the data are probably best examined graphically as in Fig. 46, where the series 1 specimen data are plotted.

In Fig. 46, the open symbols represent low silane level and the closed symbols represent high silane. The type of symbol (circle, square or triangle) indicates the HF acid etch concentration as noted on the figure. Examining this figure, it appears that the ultrasonic velocity decreases with increase in molding pressure (at least at pressures above 300 psi) and that the silane level has no effect. The acid-pressure interaction noted in the Yates analysis is also noted in that the high acid concentration seems to give higher velocities at low pressure and lower velocities at high pressure. However, it is very doubtful that this is significant.

TABLE 26. ULTRASONIC VELOCITY AND ATTENUATION DATA - WOVEN ADL-10 STRIPS

| (Frequency = 0.73 ± 0.02 MHz) | | | | | |
|-------------------------------|----------------------|---------------------|--------------------|----------------------|---------------------|
| Series 1 Specimens | | | Series 2 Specimens | | |
| Specimen | Velocity (mm/μ-sec.) | Attenuation (dB/cm) | Specimen | Velocity (mm/μ-sec.) | Attenuation (dB/cm) |
| A1 | 2.27 | 84 | M1 | 1.92 | 101 |
| A2 | 2.26 | 107 | M2 | 1.90 | 84 |
| B1 | 1.78 | 94 | N1 | 2.12 | 112 |
| B2 | 2.19 | 94 | N2 | 1.81 | 92 |
| C1 | 1.92 | 104 | O1 | 2.09 | 84 |
| C2 | 2.09 | 85 | O2 | 1.93 | 113 |
| D | ---- | --- | P1 | 1.81 | 124 |
| E | (1.31)* | (103)* | P2 | 1.93 | 114 |
| F | 2.16 | 83 | | | |
| G1 | 2.07 | 91 | Q1 | 2.08 | 118 |
| G2 | 2.11 | 98 | Q2 | 2.01 | 128 |
| H1 | 1.94 | 91 | R1 | (2.14) [‡] | >140 |
| H2 | 1.84 | 108 | R2 | (1.63) [‡] | >130 |
| I1 | 2.02 | 88 | S1 | 1.92 | 72 |
| I2 | 2.10 | 121 | S2 | 2.14 | 51 |
| J1 | 1.90 | 92 | T1 | 1.92 | 78 |
| J2 | 1.98 | 98 | T2 | (1.54) [‡] | >101 |
| K1 | 1.89 | 111 | U1 | 2.08 | 87 |
| K2 | 1.72 | 127 | U2 | 2.58 | 76 |
| L1 | 2.13 | 95 | V1 | (1.35) [‡] | ≈ 129 |
| L2 | 2.07 | 78 | V2 | 1.98 | 108 |

* Tested after flex test. Specimen is damaged.

‡ Questionable velocity data due to high attenuation.

Strips approximately 0.2 inch thick, 0.8 inch wide.

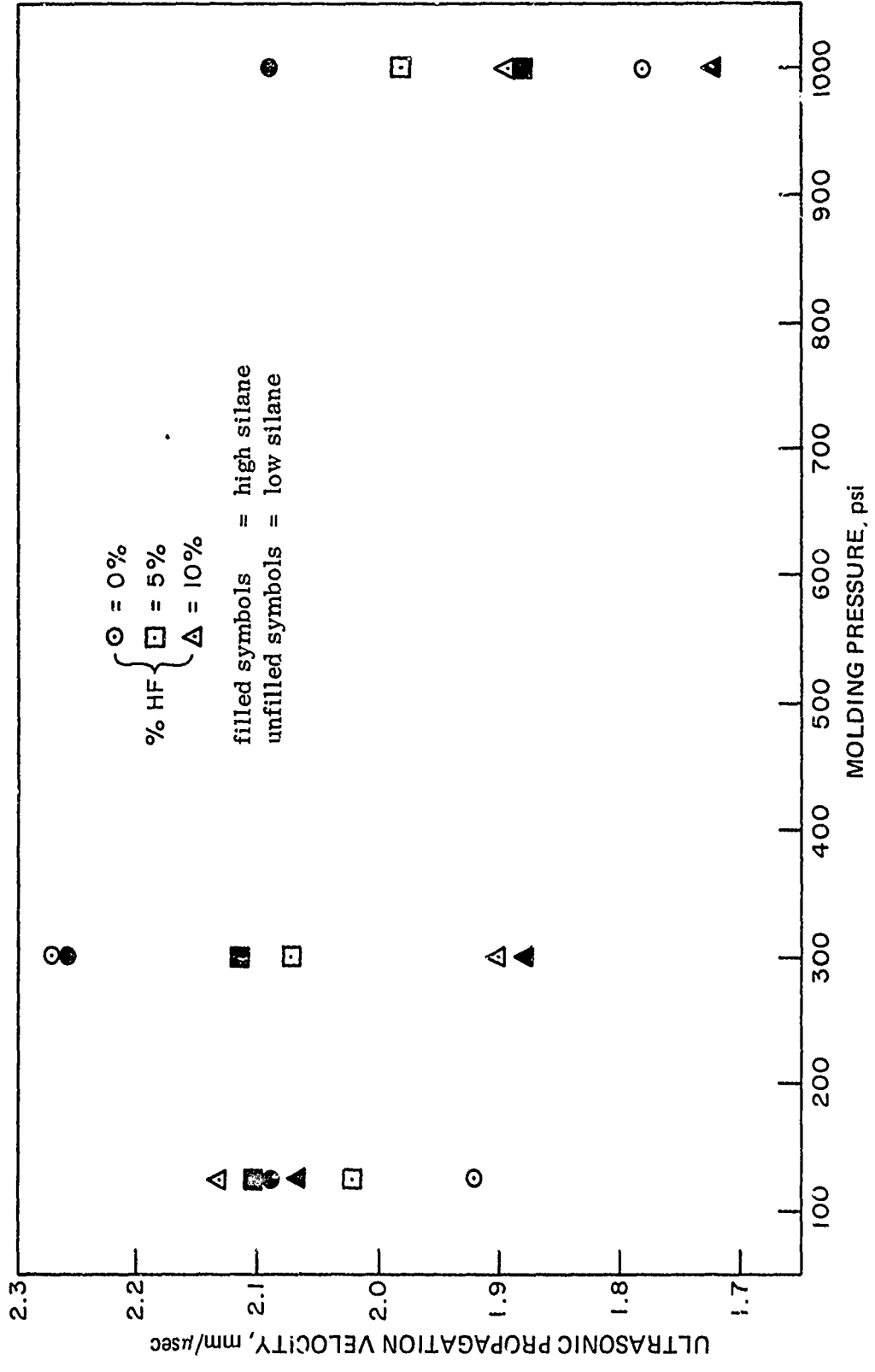


Fig. 46. Effect of Process Parameters on Ultrasonic Velocity: Series 1 ADL-10 Specimen

Considering the second group of specimens (Specimens "M" through "V") listed in Table 26, all were molded at 125 psi pressure and all were etched at the high HF concentration. Neglecting specimens "S" and "T", which contain "Cab-O-Sil," the remaining specimens again demonstrate a lack of any effect of silane concentration on the velocity. They also demonstrate that the velocity can vary from about 1.8 to 2.1 for specimens which were presumably made in the same way. This observed scatter supports the contention that the apparent acid-pressure interaction noted with the first group is not significant.

It may be noted that specimen U2 had the highest density and the highest ultrasonic wave velocity of all the specimens tested. However, a plot of velocity against density (Fig. 47) is essentially a shot-gun pattern so that density does not appear to be a dominant factor. Similarly, there does not appear to be a correlation of the velocity with fiber angle. This again raises the question, "What does the velocity depend on?" As noted earlier, it is suspected that the answer is microcracking.

Measurements of velocity and attenuation have been made on the resin alone with the results given in Table 23. The velocity in the SR-350 is considerably less than that measured in a phenolic resin* but the attenuation is about the same. Note that the velocity in the SR-350 is only slightly less than that in many of the specimens. This means that the uniaxial strain modulus of many of the specimens is comparable to that of the resin alone in spite of the fact that these contain a high percentage of quartz (velocity in quartz is 5.90 mm/ μ sec). This unexpectedly low velocity in the composite specimens is what originally led to the hypothesis of microcracking at the fiber-resin interface.

Following the exploratory work on the narrow, woven strips, several larger panels were fabricated. The results of ultrasonic measurements on specimens cut from these panels are given in Table 27. The first three specimens listed in this table (panels 331-1 and 331-2) are ADL-10 quartz-silicone and, although the densities are low, the ultrasonic velocity and attenuation are fairly representative for this class of material. For example, the conventional weave material (unground) reported in Reference 1 showed velocities from 1.99 to 2.10 mm/ μ sec and attenuations from 35 to 55 dB/cm. The material from panel 331-1 shows somewhat higher attenuation than the earlier material and this may be associated with the lower density. That the velocity remains at 2.0 + mm/ μ sec in spite of the lower density may be indicative of better continuity (less microcracking) in the current material.

*Measurements on a phenolic at 0.73 MHz gave a velocity of 2.80 mm/ μ sec and an attenuation of 4.4 \pm 1.3 dB/cm.

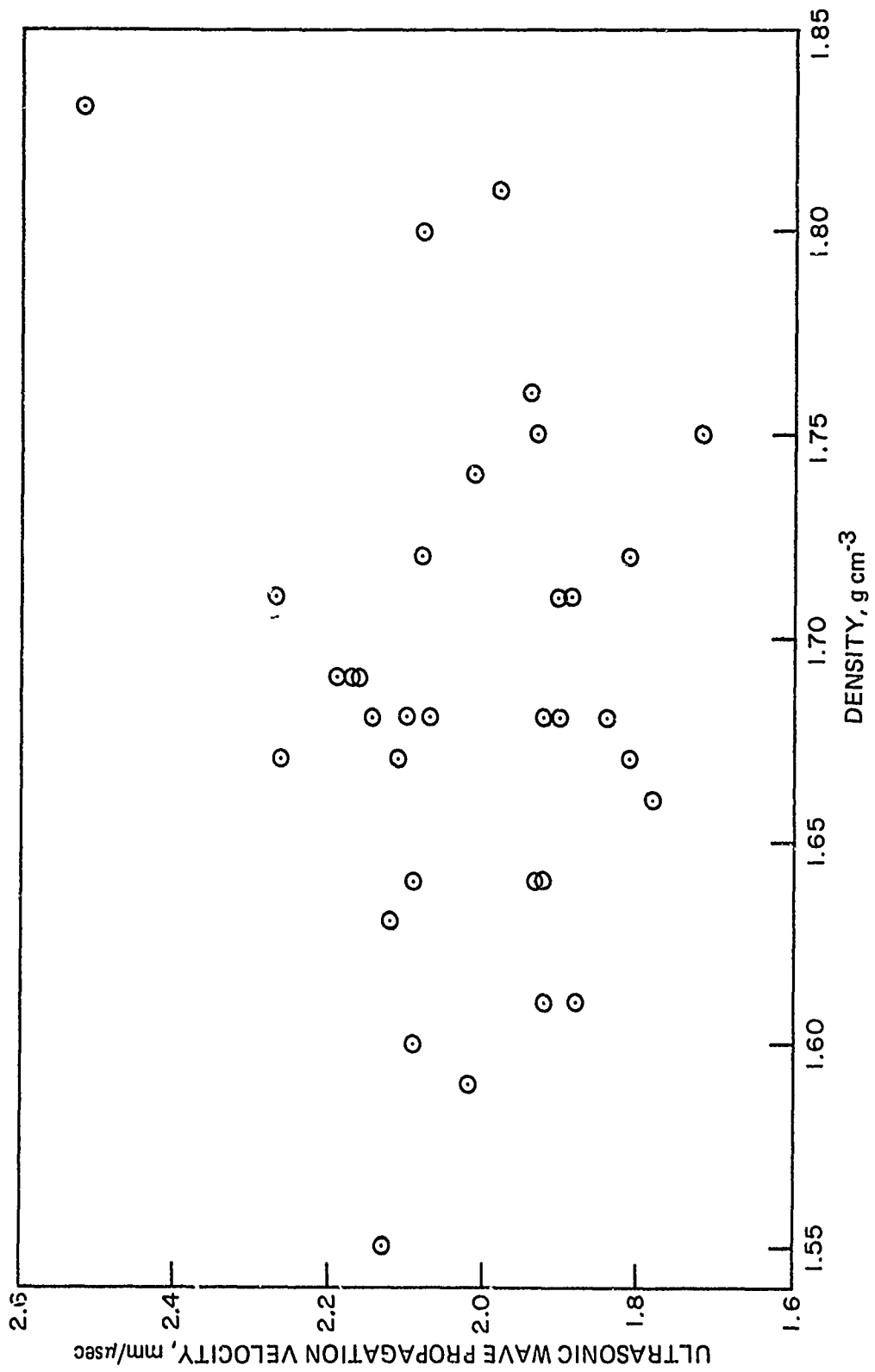


Fig. 47. Variation of Ultrasonic Wave Propagation Velocity with Density (Series 1 and 2 Woven Finger Specimens)

TABLE 27. ULTRASONIC VELOCITY AND ATTENUATION DATA - SPECIMENS FROM PLATES

| (Frequency = 0.73 ± 0.02 MHz) | | | | | |
|-------------------------------|---------------------------------|-------------------|------------------------|------------------------|--|
| Specimen | Density (g/cm ³) | Thickness (cm) | Velocity (mm/μ-sec) | Attenuation (dB/cm) | Remarks |
| 331-1/US1 | 1.64 | 0.70 | 2.02 | 62 | ADL-10 Quartz silicone |
| 331-1/US2* | 1.60 | 0.73 | 2.00 | 66 | |
| 331-2/US | 1.73 | 0.66 | 2.06 | 46 | |
| 319-1/US | 1.93 | 1.14 | 3.35 | 4.4 | Markite, pyrolyzed once at 1100° F and reimpregnated |
| 319-1/US4 | 1.93 | 1.16 | 3.38 | 6.0 | |
| 319-1/US5 | 1.94 | 1.14 | 3.41 | 6.3 | |
| 319-2/US1 | 2.00 | 1.10 | 3.39 | 26 | |
| 319-2/US2 | 2.02 | 1.07 | 3.62 | 19 | |
| 319-1/US3 | 1.89 | 1.15 | (1.60)** | 60 | Markite, further pyrolyzed at 1600° F |
| 319-1/US4 | 1.88 | 1.17 | 1.76 | 52 | |
| 319-2/US1 | 1.96 | 1.09 | (-)+ | 63 | |
| 1 | 1.41 | 0.37 | 1.43 | 23 | Uniaxial ADL-10 tensile specimens. Measured perpendicular to fibers. |
| 2 | 1.44 | 0.38 | 1.43 | 78 | |
| 3 | 1.39 | 0.39 | 1.42 | 25 | |
| Cured, molded | 1.315 | 0.63 | 1.60 | 4.4 ± 2 | (at 0.93 MHz) |
| SR-350 resin | 1.315 | 0.63 | 1.59 | 7.5 ± 2 | |

* Submitted to AMMRC for particulate erosion testing.

** Some uncertainty because of high attenuation (scattering).

+ Received signal gradually increased after about 11.4 μsec. Apparent velocity about 0.96 mm/μsec.

Considering the second and third groups of specimens, it is interesting to note the high velocities and low attenuations achieved after pyrolysis and re-impregnation. Apparently the resin attaches readily to the pyrolyzed material to give very good continuity through the plates. However, this continuity is destroyed by the second pyrolysis, resulting in a sharp decrease in wave velocity and a very sharp rise in attenuation.

In addition to the measurements on the "hockey puck" specimens, Table 23 also gives the results of some measurements made on uniaxial tensile specimens. Specimen No. 2, which shows the highest density and highest attenuation was significantly stronger than the other two although it had about the same volume percent of quartz as No. 1 and was intermediate to No. 1 and No. 3 on a weight percent basis (see Section 2.5.5). Specimen No. 2 also showed the lowest porosity. Its radiograph (Figure 21) also shows a clearer definition of the fibers than specimens 1 and 3. It has not been demonstrated for these composite materials that there is any correlation of the ultrasonic data with the material strength. However the measurements still serve the purpose of recording the internal bonding and microstructure and are definitely indispensable for evaluation of the lower damage levels currently being experienced by the ADL-10 specimens exposed to flyer plate testing.

3.4 SHOCK TESTING

3.4.1 Introduction

Shock testing was conducted at GE-RESA by means of a magnetic flyer facility. In this test, a thin sheet (flyer) of aluminum is accelerated to a high velocity and impacts the test specimen. This impact generates a short duration compressive stress pulse in the test specimen. Upon reflection at the back face of the specimen, this becomes a tensile stress pulse which can rupture (spall) the specimen. The amplitude of the stress wave at the front face is a function of impact velocity, the material densities and the material shock velocities. By way of illustration, if an aluminum plate impacted an aluminum specimen at a velocity of 0.09 millimeters per microsecond, the initial stress amplitude would be about 100,000 psi. Where the flyer and specimen are different materials, the stress can differ considerably from this value even at the same impact velocity.

The flyer impulse density is usually reported as some number of taps. The tap is a unit of momentum per unit area and one tap is equal to one dyne-sec/cm². The GE-RESA facility has been improved since the last reporting period to a routine capability of 4000 taps maximum.

When a sufficient number of tests can be conducted to define a failure threshold, this threshold value provides a convenient means of comparison. However, not everyone defines threshold damage in the same way and hence a comparison of data emanating from different laboratories necessitates a careful and common definition. It should also be noted that, depending again on the definition, threshold damage may not mean catastrophic failure of the material in service. Depending on the specific requirements for a given application, it is possible that extensive damage could be tolerated.

Again, as in the previous "Hardened Antenna Window Material" program, all the materials studied were based on an Omniweave fabric of silica fibers, variously impregnated with silicone, molded, and further processed for use as antenna windows or radomes. The comparative rating scale set up in Reference 1 is again used for evaluation of damage due to flyer plate testing. This scale, reproduced as Table 28, runs from 0 to 10 and includes levels ranging from no detectable effect — visual, ultrasonic or dimensional, through a series of measurably discrete damage levels, as detected by the applicable characterization tools, and ends with visually obvious levels of damage and catastrophic failure. The two bracketing categories of estimated tolerable ranges of damage for antenna window or radome use are also indicated. This estimate is necessarily arbitrary as the tolerable damage will depend on the specific design and environment. For example, if it is expected that about one-half of the thickness of a window would be lost due to ablation, then a damage level of 9 would be intolerable as burn-through would occur. However, if a thicker window could be tolerated, then even a level 9 damage could be acceptable. From an electromagnetic

TABLE 28. DEFINITION OF DEGREE OF DAMAGE

| Degree of Damage | Description | | |
|------------------|---|---|--|
| 0 | No damage detected. | | |
| 1 | No visible damage but increased ultrasonic attenuation. | | |
| 2 | Delams visible at 10X magnification. | | |
| 3 | Delams visible with unaided eye. | | |
| 4 | Delams visible at edges, some pieces raised at rear surface. | | |
| 5 | Scattered few pieces off back face. | | |
| A* { | B* { | 6 | Numerous small pieces off back face. |
| | | 7 | Small pieces off rear face, additional pieces loose. |
| 8 | Extensive damage in back half of specimen but generally holding together. | | |
| 9 | Back 1/4 to 1/2 blown off or exfoliated. | | |
| 10 | Complete shattering of specimen. | | |

*Estimated tolerable damage levels for:

- A. Antenna window
- B. Frustum or Radome

standpoint, a window used for sighting or homing purposes, when radar optical considerations such as beam refraction and divergence become important, could not tolerate any shape change or spall, especially for a high dielectric permittivity where tuned thicknesses are used. But a window used for guidance communications or fusing, especially at longer wavelengths, would be insensitive to large spalls and dimensional changes, as it would also be to transmission losses of several decibels due to a rise in the intrinsic material loss tangent.

3.4.2 Results of Flyer Plate Testing

3.4.2.1 Phase 1

In Phase 1 of this program only tensile test geometry bars were produced, rather than "hockey pucks" cut from plate material as in the previous program. This

was used, however, to make direct measurements of the effects of impact on the strength and elastic properties of four series 2 specimens. One uncertainty, caused by impact in only the center portion of the test bars, is the flexing of the specimen by the impulse. It is possible that this flexing includes additional damage beyond that caused by the stress wave.

Four test bars were impacted. The first of these was specimen "O1" which was hit with a 2000 tap impulse. The specimen showed no visible signs of damage but the ultrasonic velocity decreased from 2.09 to 1.64 mm/ μ -second and the attenuation increased from 84 to 102 dB/cm (Tables 26 and 29), suggesting that the impulse caused cracking of the resin and debonding from the fibers.

Specimens Q1, U2 and V2 were all impacted at 4000 taps and all were bent by the impact.

The damage suffered by these three specimens is very similar but was not quite like that previously observed. As a result there was initially some question as to what damage level they should be assigned. In handling the specimens, it was readily seen that they were bent and one could also note that the flexural modulus was much reduced. Thus, one could readily infer delamination had occurred although cracking was not visible in the same way that it was in the machined "hockey pucks." However, there were a few raised pieces visible on the backface of one specimen (U2) and it was concluded that the damage was equivalent to about a level 4 for this specimen and 3 to 4 for the other two. This performance is at least as good, and perhaps a little better, as that previously obtained with the "balanced construction with radials" (Reference 1). That material, it may be recalled, experienced a damage level of 3 to 4 at an impulse of 3500 taps (also tested with a 12 mil aluminum flyer). However the balanced weave samples had a thickness of about 1/2 inch, about 2-1/2 times the present specimen thickness. It seems probable that much of the excellent performance of the present specimens can be attributed to the continuity of the fibers at the specimen face. This is probably not a restriction since machined faces and edges could be avoided in manufacturing an antenna window or a frustum. The advantage of providing closed-cell woven and molded antenna window shapes should be further investigated as it could be an important consideration in the future as development progresses.

The mechanical testing described in Section 3.2 shows that no drastic loss in ultimate tensile strength was observed, although the modulus was decreased by a factor of 10 and the strain to failure increased by a factor of 10 due to "mashing" of the matrix — while the fiber system retained its integrity.

3.4.2.2 Phase 2

In Phase 2 the conventional ultrasonic and flyer plate specimens were 2 inch discs, machined from plate material. Note that only the disc edges were machined, not the

TABLE 29. MAGNETIC FLYER PLATE TEST RESULTS

| Specimen | Flyer Velocity (mm/ μ -sec) | Impulse (taps) | Degree of Damage | Post Test Ultrasonic Attenuation (dB) | Remarks |
|-------------------------------------|------------------------------------|---|---------------------|---|---|
| Phase 1 - ADL-10 Tensile Specimens | | | | | |
| O1 | 1.64 | 2000* | 1 | 102 | No detectable loss in ultimate tensile strength, elastic modulus down by a factor of 10, strain to failure increased by a factor of 10. (See Section 3.2) |
| Q2 | 1.38 | 4000** | 3-4 | 121 | |
| U2 | 1.24 | 4000 | 4 | 125 | |
| V2 | 1.31 | 4000 | 3-4 | 135 | |
| Phase 2 - 2 inch Diameter Specimens | | | | | |
| ADL-10 | | | | | |
| 331-US1 | | 4000 | 3 | >90 | Specimen thickness increased by about 50 mils. Specimen thickness increased by about 50 mils. |
| 331-US2 | | Not tested, submitted to AMMRC for particulate erosion testing. | | | |
| 331-US | | 4000 | 3 | >90 | |
| Pyrolyzed Materials | | | | | |
| 319-1P2, US3 | | 1000 | 9 | | Flyer may not have impacted uniformly, spall over half of backface. |
| 319-1P2, US4 | | 1000 | 9 | | Flat impact, uniform spall over backface. |
| 319-1R1, US5 | | 2000 | 9 | | Flat impact, uniform spall over backface. |
| 319-2R2, US1 | | 2000 | 9 | | Flat impact, uniform spall over backface. |
| 319-2P3, US2 | | 2000 | 9 | | Flat impact, uniform spall over backface. |

*5 mil aluminum flyer

**12 mil aluminum flyer

faces. The first tested specimens were ADL-10 material from plates 331-1 and 331-2, impacted at the maximum facility capacity of 4000 taps (Table 28). The resulting assessed damage level of 3 — "delams visible with unaided eye" is conservative for the 331-2 specimen as the effect was noticed only at one location on the circumference of each machined 2-inch disc. The ultrasonic attenuations increased to near the immeasurable level, as did the woven closed edge tensile bars of Phase 1. This material would almost certainly be suitable for a hardened antenna window in an application where all but the most stringent of optical sighting requirements were imposed. This is especially so in light of the comparatively small molded thickness of material that was used, nominally 1/4 to 3/8 inch.

The failure threshold of ADL-10 in realistic use thicknesses of from 1/4 to 1/2 and even 1-inch thicknesses for extreme hardening must be assessed at well above this 4000 tap level and further testing will be recommended to determine this threshold, with realistic edge effects and evaluation of the electromagnetic optics implications.

The partially pyrolyzed and Markite silica-silica systems were also impacted as indicated in Table 26. In all cases, the unacceptable damage level of 9 was observed — "back 1/3 to 1/2 blown off or exfoliated." This was lesser in degree within the discrete range of level 9 for specimens 319-2/US1 and 319-1/US5 which were tested in the re-impregnated state. Table 28 of Reference 1 shows that this is the same performance previously observed for Markites.

A family of variously pyrolyzed versions of ADL-10 have been studied in this program in an attempt to derive a simultaneously hardened, high strength (>4000 psi) silica-silica composite not limited by heat flux considerations in its electromagnetic transmittance. It has been observed that multiple reimpregnation of high density Markites does improve the in-plane strength to the 2000 - 4000 psi level, and that the resin wetting on reimpregnation is especially effective in lowering the ultrasonic attenuation. These reimpregnated forms also show some improvement in hardening levels over monolithic fused silica, which would experience level 9 damage at about 500 taps for a 1/2-inch thickness.

However, the conclusion must be drawn that no really significant improvement of both strength and hardening has been achieved for the various forms of completely pyrolyzed ADL-10 (Markite) formulated thus far.

In Section 2.3.3 "Pyrolyzation Effects," two differing concepts of silica-silica composite action were discussed. All of the reimpregnated and pyrolyzed materials subjected to ultrasonic and shock testing were processed for tenacious bonding of matrix to reinforcement. The implication is that the alternative model for high strength brittle matrix composites, which requires that the fiber system be maximally free to move within a low friction matrix is the model which offers the best promise of a hardened, inorganic silica-silica composite. This conclusion is reinforced by the excellent mechanical strength upon tensile testing of the four impacted specimens of Phase 1.

Other considerations present in competitive hardened antenna window concepts also pertain. For example, a larger thickness specimen could be utilized, resulting in the nonlinear effect of much smaller backface stresses in these high attenuation materials. Also, the effects of selecting fiber orientations specifically for shock resistance, i.e., sizing and orientation normal to the surface, with lesser emphasis on in-plane properties, remain to be investigated for these materials.

The basic and overriding consideration however is the fiber-matrix bonding mechanism as manifested in improved tensile in-plane strength and through-the-thickness hardening. Study and solution of this problem is the first objective for further work.

3.5 ELECTROMAGNETIC CHARACTERIZATION

3.5.1 Introduction

The desirable characteristics for an antenna window material are low loss tangent and low dielectric permittivity. It is generally agreed that the loss tangent should be less than .010. No such upper limit can be set for the dielectric permittivity, since in most cases the antenna window can be made an optimum thickness, thus minimizing the effect of the higher permittivity. During the rapid heating of re-entry, the antenna window will change in three generally unfavorable ways. The loss tangent of the heated material will usually rise. This may either be a simple function of the temperature as in the case of quartz or it may be primarily due to a chemical change, as in some organic materials. The dielectric constant may change during heating, destroying the effect of the tuned thickness and causing distortion of off-axis viewing. Also during heating, ablative erosion changes the thickness of the window.

At present, the frequency range of interest for antenna windows has been between 200 MHz and 12 GHz. Unlike radar absorbers, the properties of the transparent materials are not a strong function of frequency. So, in a development program it is not necessary to characterize the material over the entire spectrum of interest. Of course, before a new material is used at a particular frequency, it would be advisable to check the properties at that frequency in case any anomalies occur.

3.5.2 Definition of Terms

1. The loss tangent or $\tan \delta$ of a material is defined as the ratio of the imaginary part of the complex permittivity to the real part or $\tan \delta = e''/e'$ where the complex permittivity is given by $e' - je''$.
2. The terms, power transmission coefficient, power reflection coefficient and transmission attenuation need further discussion. When a plane wave is incident on a flat sheet of uniform dielectric material, the result is rather complicated in that multiple reflections are set up in the material and the resultant transmitted and reflected beams are composed of an infinite series of components. When the sheet of dielectric material is not uniform, as in the case of the exposed specimens, the situation is even more complicated. To simplify this, we treat the sample as a black box and only measure its overt properties before, during and after exposure to the heat fluxes. When the measurements are made, three parameters are monitored: the power in the incident beam, and power in the transmitted and reflected beams. The power transmission coefficient is then simply the ratio of the total power in the transmitted beam to the power in the incident beam and when expressed as a percentage, it is referred to as percent power transmitted. Similarly, the power reflection coefficient is the ratio of the power in the reflected beam to the power in the incident beam.

3. Decibels is a common means of expressing power ratios. Transmission attenuation or "insertion loss" as it is often called is defined as $10 \log P_i/P_t$, where P_i is the power in the incident beam and P_t is the power in the transmitted beam. It is also common to use this notation when referring to a change in level of one particular wave. For example, when the transmitted power level is changed from P_{t1} to P_{t2} , the change would then be $10 \log P_{t1}/P_{t2}$ dB.

3.5.3 Measurement Techniques

Four different techniques were used to electromagnetically characterize the material on this program. These are briefly described below.

A. Permittivity Measurement (Room Temperature, C-Band, 5460 MHz)

The technique used here is a two position slotted wave guide method. This is a standard measurement technique (and is completely described in GE Document No. TIS 64SD252, Reference 10). Briefly, the rectangular shaped specimen is placed in a shorted waveguide specimen holder which is connected to a slotted line. Measurement of the standing wave is made in the slotted line with the specimen located at the open and short circuit positions in the waveguide. From these standing wave measurements, the properties of the sample material are calculated. The schematic is shown in Fig. 48. This technique is similar to the L-band permittivity measurement used on this program last year as described in Reference 1.

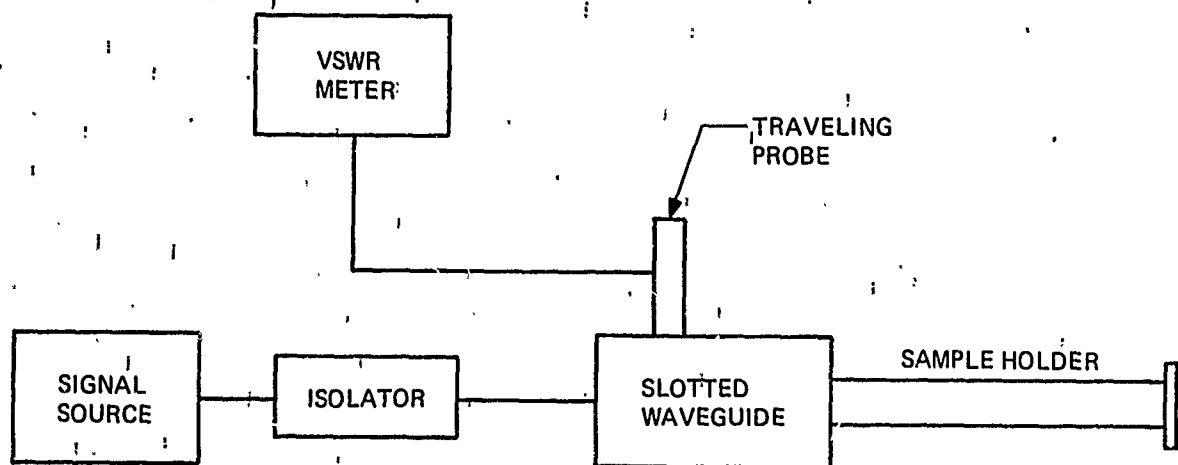


Fig. 48. Permittivity Measurement System Schematic

B. RF Measurement During Ablation in the Hyperthermal Arc Facility
(C-Band 5470 MHz)

The object of this measurement is to monitor the change in transmitted signal during ablation heating. A schematic of the apparatus used for this test is shown in Fig. 49. The specimen is mounted on a hydraulically moveable arm so it can be quickly removed from the flow of the hyperthermal arc and placed between the transmitting and receiving horns. The horns and specimen holder are all mounted on a moveable table which changes position with respect to the plasma orifice during heating in order to accurately duplicate a flux versus time curve of re-entry conditions. The specimen is removed from the flow for 0.75 second every 10 seconds during heating and the change in transmitted and reflected signals is recorded on a two-channel Brush recorder.

C. RF Measurement after Ablation in Tandem Gerdien Arc Facility (C-Band 5470 MHz)

The object here was to measure the change in the transmitted signal immediately after the sample was removed from flow of the Tandem Gerdien Arc Facility. This test was very similar to the test performed in the hyperthermal arc with the exception that the sample was mounted in the transmitting horn and the face of the horn was moved in and out of the heated flow of the arc. The transmitting horn used was simply a short piece of water cooled C-band waveguide with a waveguide to coax adapter mounted at the back. The circuitry used is the same as that used with the Hyperthermal Arc Facility (see Fig. 49).

This test, which was developed for this program's needs over the Hyperthermal Arc Test, has three advantages which are:

1. Fewer electromagnetic measurement errors are associated with the test since the specimen is mounted in the waveguide, thereby assuring a plane incident wave and reducing edge losses.
2. A smaller sample size is used, nominally 1 by 2-inch as opposed to $4\frac{1}{4}$ x 5-inches.
3. This arc facility is more economical to utilize than the Hyperthermal Thermal Arc Facility.

D. Coefficient Measurement, Room Temperature (C-Band 5470 MHz)

This technique was used to accurately compare the electromagnetic properties of small specimens before and after exposure to ablation environments, thereby providing a check on the aforementioned ablation tests. After exposure, the specimens would in general have a gradient of material properties through the specimen. So, the conventional techniques for measuring the dielectric properties of homogeneous specimens would give erroneous results. It was decided that the meaningful quantities that could

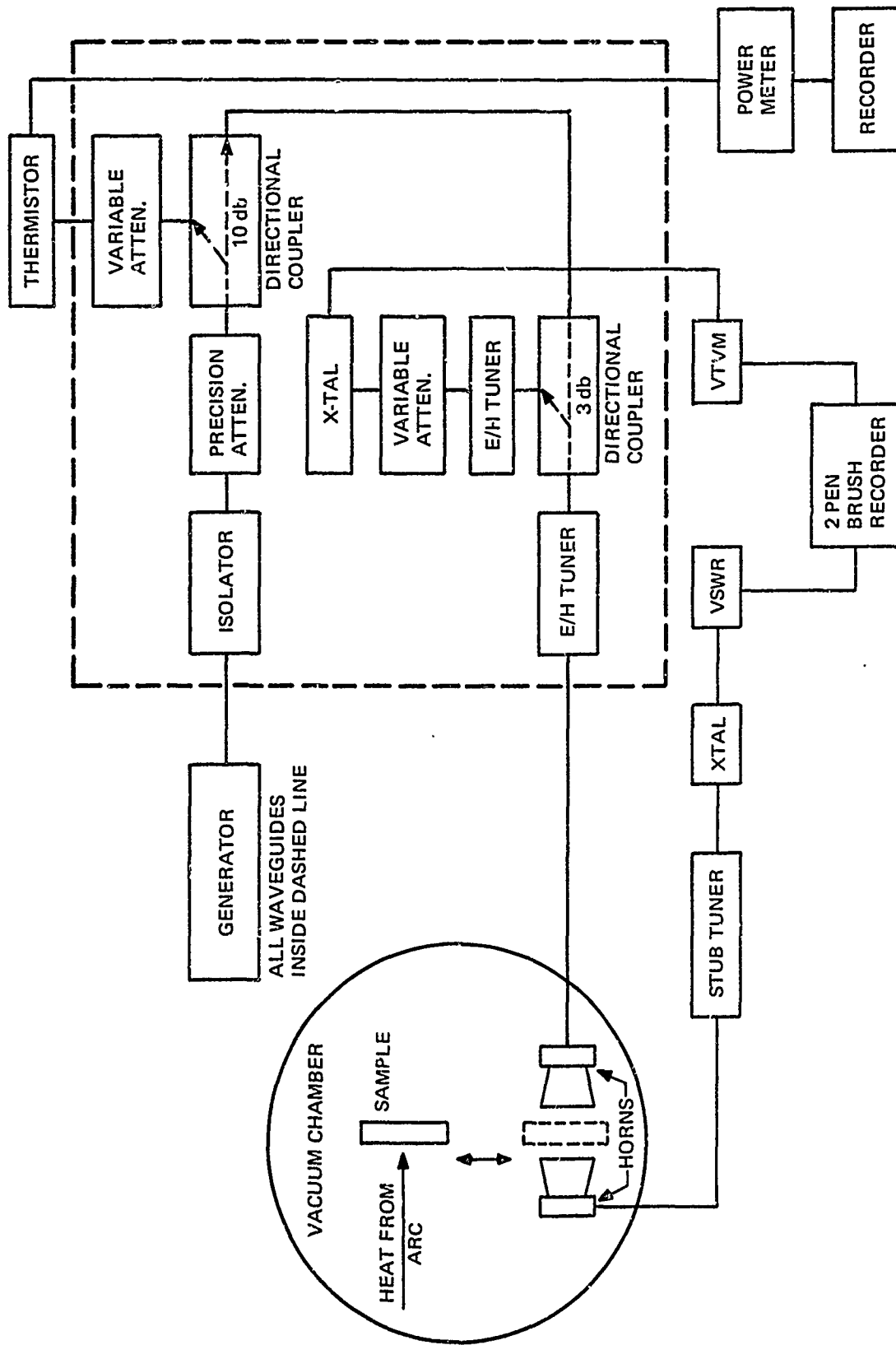


Fig. 49. Block Diagram of Microwave Ablation Test Facility

be measured would simply be the power transmission and reflection coefficient. The equipment used for this measurement is shown in Fig. 49 with the exception that the transmitting and receiving horns are replaced with a straight piece of waveguide. The procedure was to place the specimen in this waveguide before and after ablation and to measure the coefficients by a comparison technique.

3.5.4 Results of Electromagnetic Characterization Program

3.5.4.1 Laboratory Waveguide Measurements, Room Temperature

The dielectric properties of the various Omniweave material formulations were measured at C-band, 5470 MHz, and the results are shown in Table 30. The complex permittivity, $\epsilon' - j\epsilon''$, and the loss tangent, $\tan \delta$, are both tabulated for each specimen. The real part of the permittivities measured are between 2.9 and 3.8, depending on density and component fractions. The loss tangents of all the materials, with the exception of two, are less than .01 as desired for antenna window applications. The unusually high loss tangent of the unpyrolyzed Markite specimen and 318-4 molded Markite are apparently due to the two incomplete pyrolysis processes carried out to 1100°F in these specimens (see Section 2). Had they been pyrolyzed to 1600°F, the partially decomposed resin products would not have been present and the reimpregnated composite would have had a loss tangent intermediate to completely pyrolyzed Markite and virgin ADL-10.

3.5.4.2 RF/Ablation Tests on 4 $\frac{1}{4}$ x 5 Inch Plates

The RF performance of four specimens was measured at the Hyperthermal Arc Facility and the data is shown in Figs. 50 through 53. In these figures the maximum heat flux on the surface of the specimens is shown as a function of time. Also, the change in the transmitted RF signal is plotted for each point at which the specimen was removed from the arc flow and placed between the horns.

The ADL-10 specimen tested, Fig. 50, was comparable with samples of ADL-10 tested previously. The transmitted signal was not significantly attenuated until after the specimen had experienced a heat flux of greater than 100 Btu/ft² sec. After a heat flux of 130 Btu/ft² sec, the transmitted signal was attenuated 2.4 dB and after a heat flux of 160 Btu/ft² sec, the transmitted signal was attenuated by more than 10 dB.

The RF performance of the three Markite specimens (Figs. 51 through 53) tested is comparable to the RF performance of fused silica in that no significant attenuation was observed even after the samples experienced a heat flux of 425 Btu/ft² sec. This is expected since all the resin has been pyrolyzed out of the material leaving only silica.

3.5.4.3 RF Ablation Tests on C-Band Waveguide Samples

The data obtained in the tests performed in the Tandem Gradient Arc facility is given in Table 31. The change in transmitted signal reported was measured just after the sample was

TABLE 30. PRE ARC TEST DIELECTRIC PROPERTY DATA
(C-BAND - 5470 MHz)

| Specimen | Material | ϵ' | ϵ'' | $\tan \delta$ |
|------------------|-----------------------------------|-------------|--------------|---------------|
| 331-1 * | ADL-10 Silane coupled fiber | 2.89 | .011 | .004 |
| 331-2 * | ADL-10 No silane | 3.02 | .012 | .004 |
| 319-1P2 EMC-4 | Pyrolyzed Markite | 3.39 | .032 | .009 |
| 319-2P3 EMC-2 | Pyrolyzed Markite | 3.31 | .017 | .005 |
| 319-2R2 EMC-1 | Unpyrolyzed Markite | 3.78 | .125 | .033 |
| 318-4P3 EMC | Molded pyrolyzed Markite | 3.52 | .062 | .017 |
| 318-1P3 * | Cast, pyrolyzed | 2.91 | .013 | .005 |

* Average value of two specimens.

removed from the plasma flow, while the sample is still hot. The samples were heated with a flux of 460 Btu/(ft² sec) for a time of 30 seconds. The thickness of the samples tested was 0.25 inch with the exception of (318-3/EMC) which was 0.188 inch.

The usefulness of this simpler ablation test was demonstrated. The data agrees well with the more sophisticated and expensive hyperthermal arc tests. In general, the materials which contain resin attenuate the transmitted signal as a result of ablation at this level and the materials that don't contain resin only slightly affect the transmitted signal.

3.5.4.4 RF Coefficient Measurement Before and After Ablation Test

The transmission and reflection coefficients of the specimens used in the small arc test were measured before and after ablation and are recorded in Table 32. This data also shows the difference between the materials which contain resin, and the

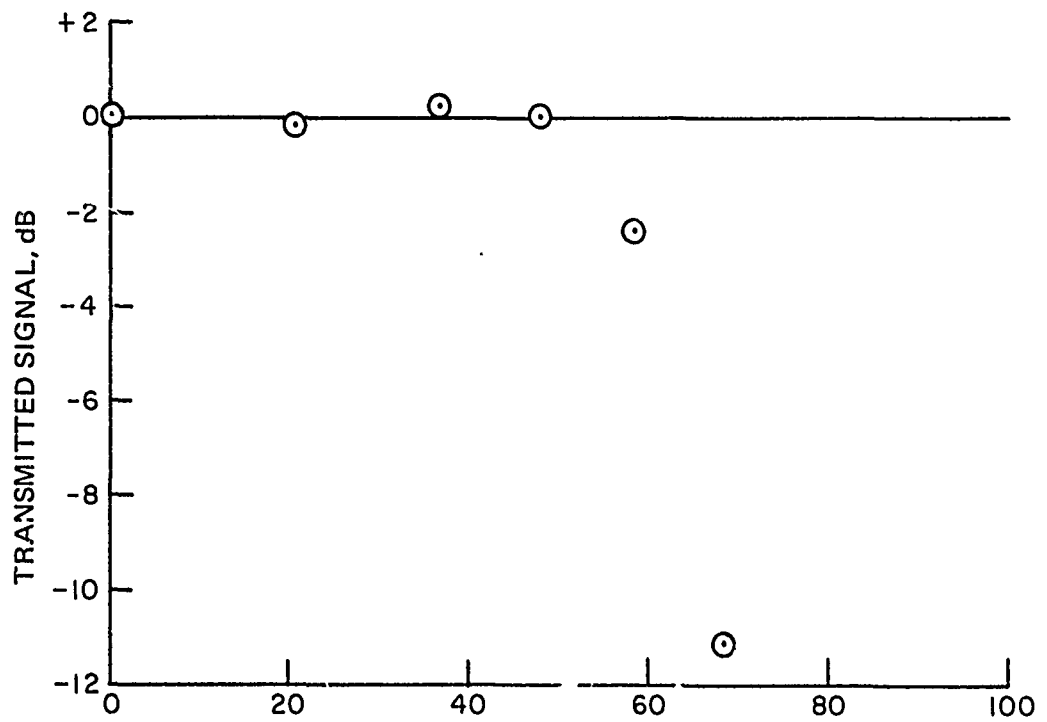
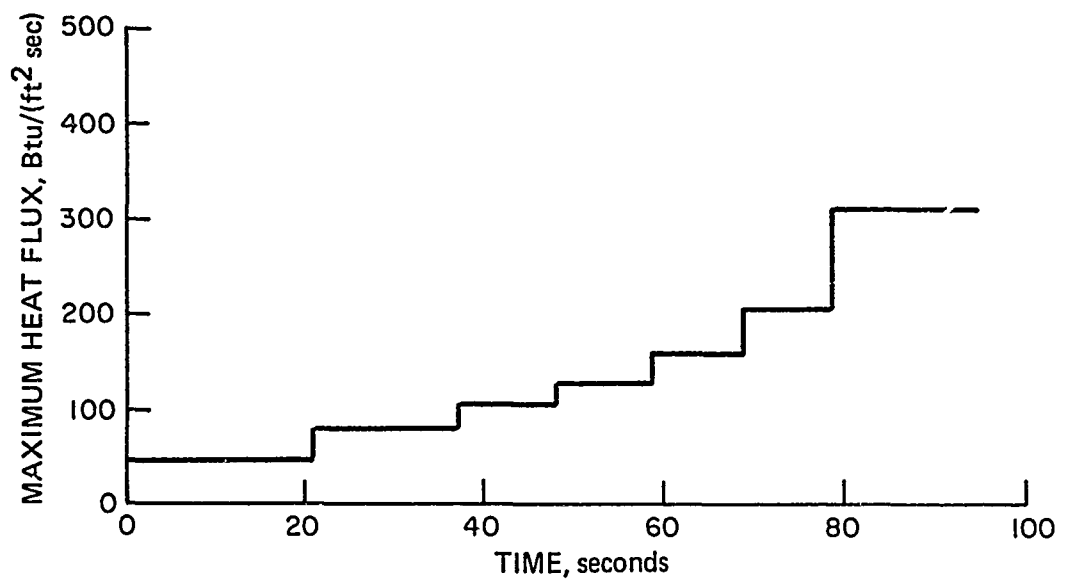


Fig. 50. Specimen 331-1 ADL-10

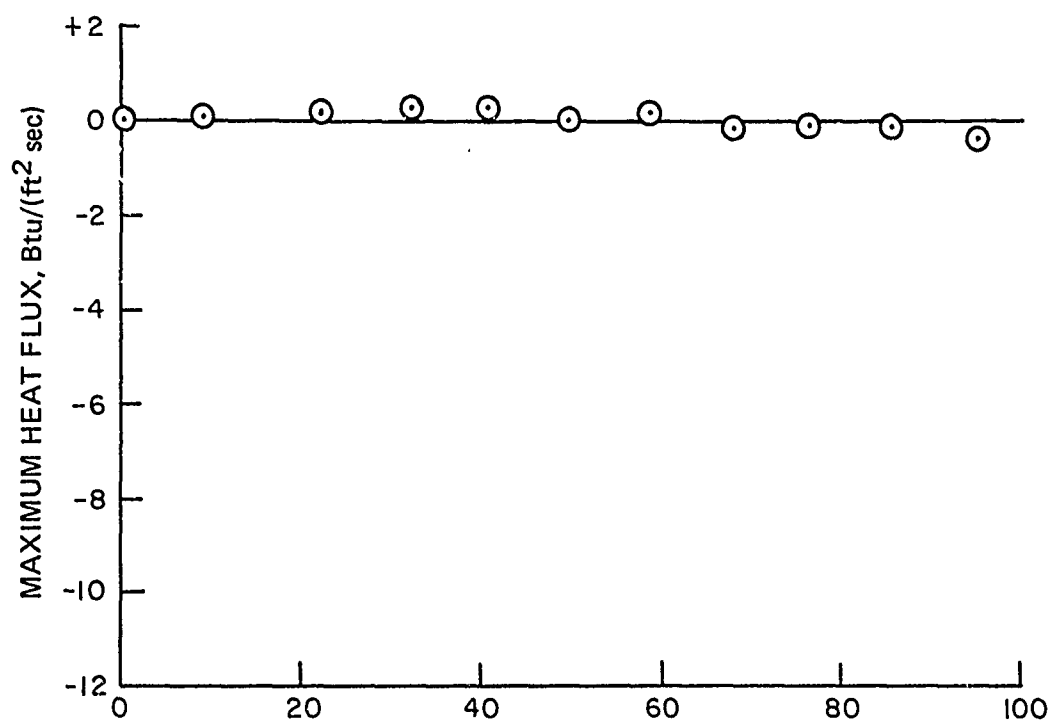
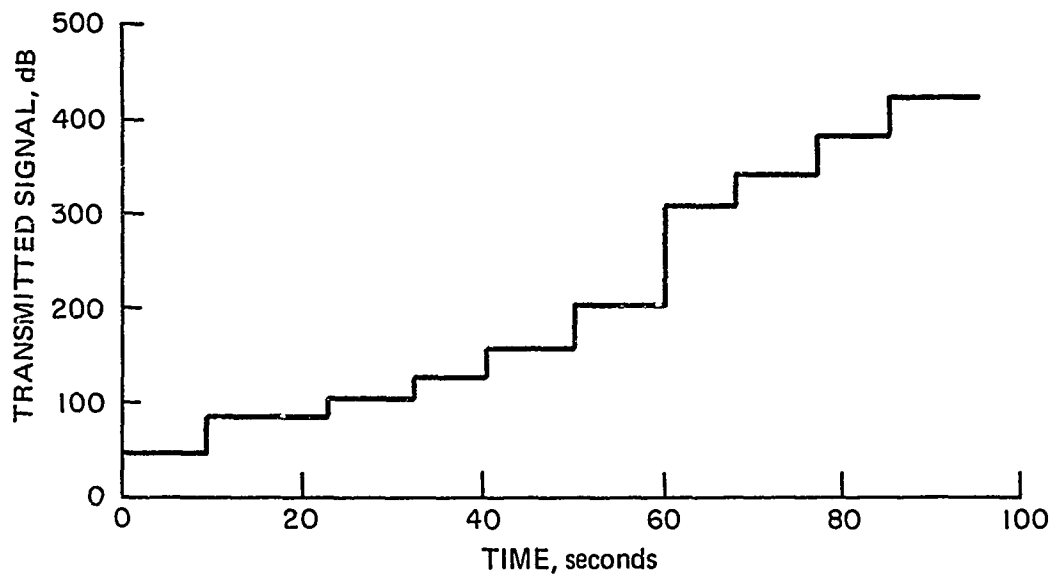


Fig. 51. Specimen 318-2 (Cast Markite)

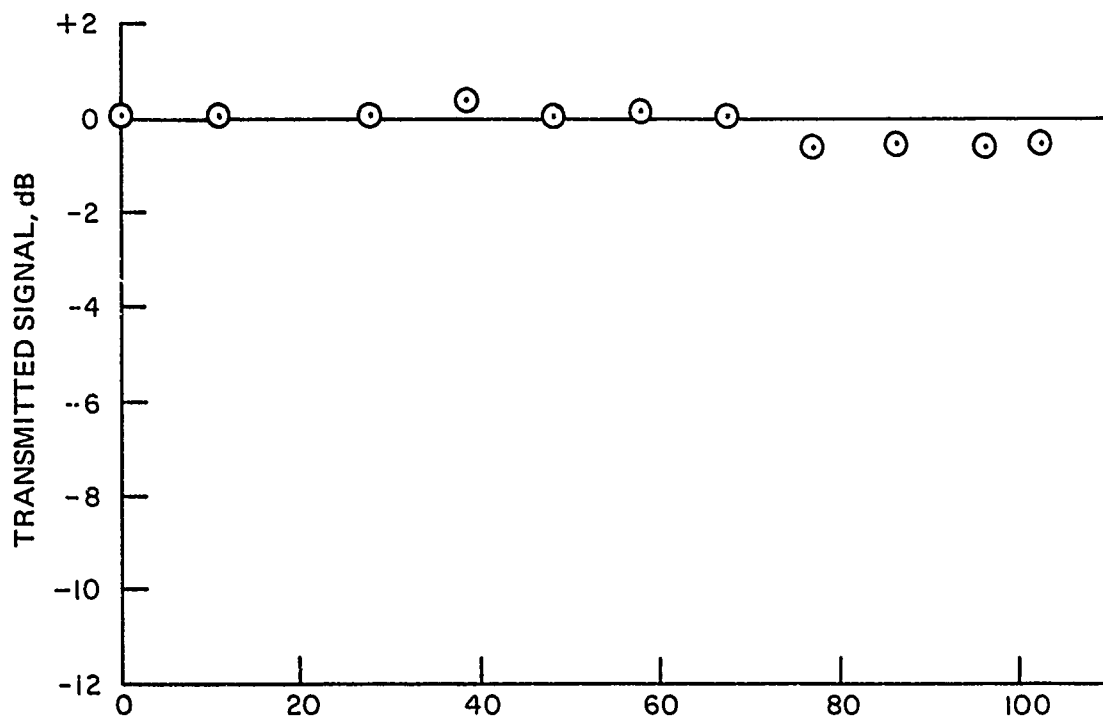
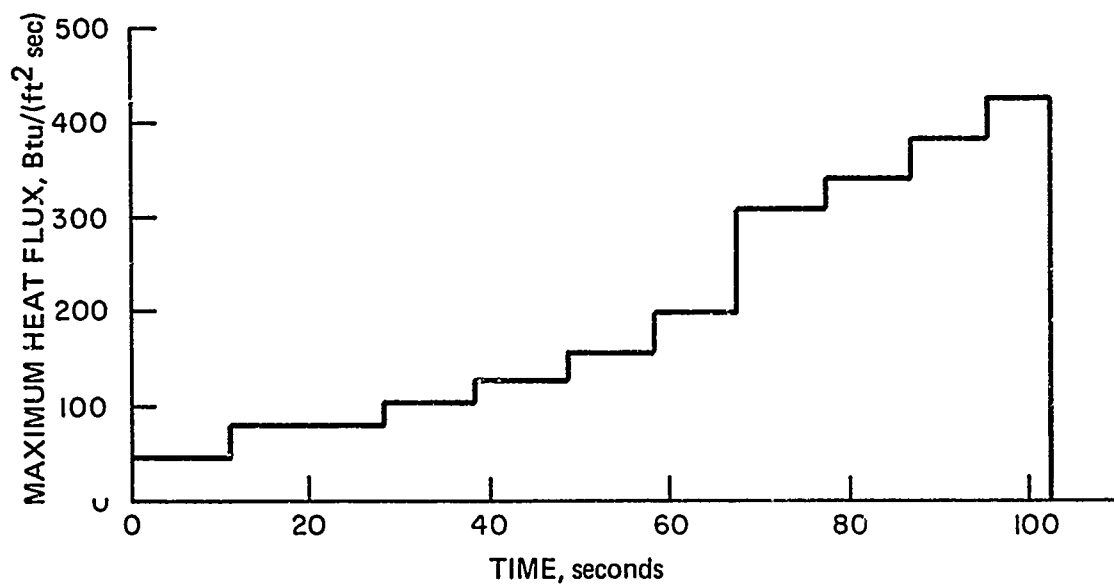


Fig. 52. Specimen 319-1 (Markite)

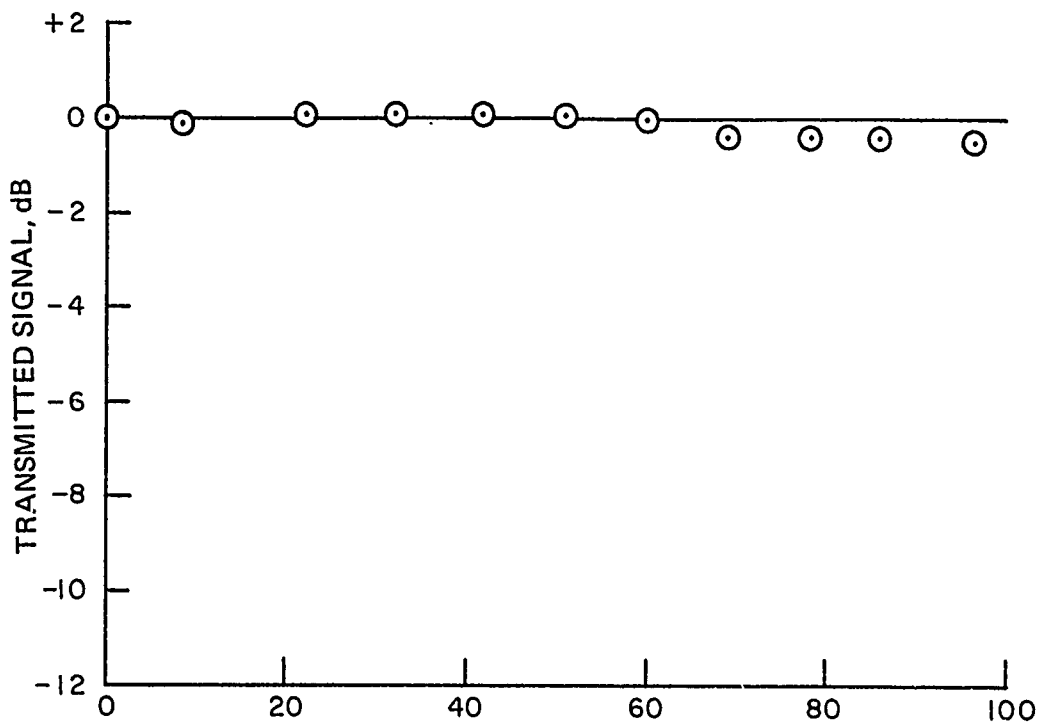
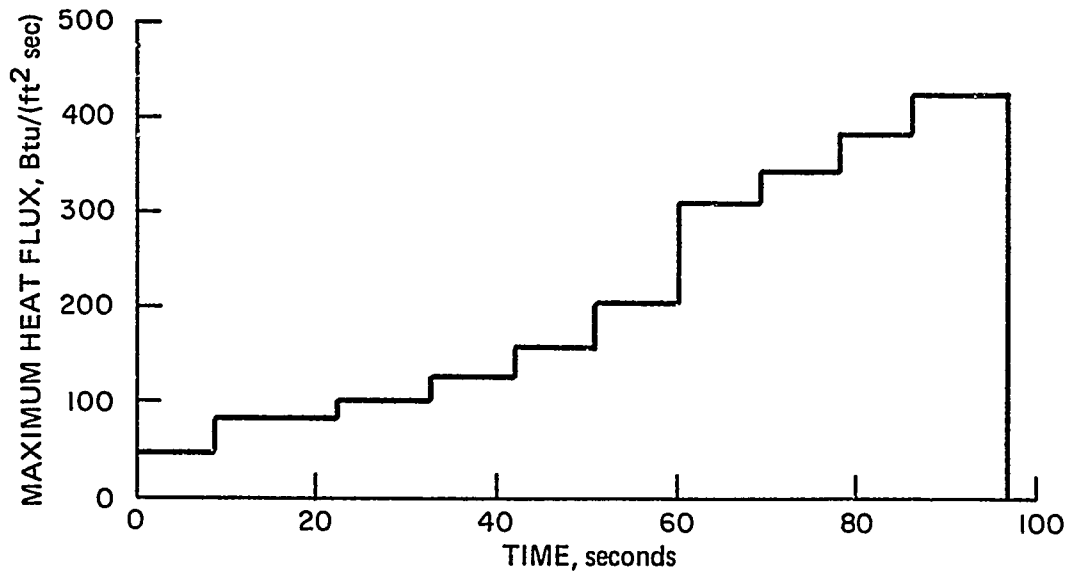


Fig. 53. Specimen 319-2 (Markite)

TABLE 31. CHANGE IN TRANSMITTED SIGNAL IN TANDEM GERDIEN ARC TEST
HEAT FLUX - 460 BTU/ft² sec (COLD WALL)

| Specimen | Description | Change in Transmission (dB) |
|------------------|--------------------------------|-----------------------------|
| 331-1 EMC-1 | ADL-10 Silane coupled fiber | -8.0 |
| *318-3R EMC-2 | Reimpregnated Markite | -2.5 |
| 319-2R EMC-1 | Unpyrolyzed Markite | -4.4 |
| 319-1P2 EMC-3 | Pyrolyzed Markite | +0.3 |
| 319-1P2 EMC-4 | Pyrolyzed Markite | 0.0 |
| 319-2P3 EMC-2 | Pyrolyzed Markite | +0.4 |
| 318-4P3 EMC | Molded Pyrolyzed Markite | -0.1 |
| 318-1P3 EMC-1 | Cast Pyrolyzed | +0.1 |
| 318-1P3 EMC-2 | Cast Pyrolyzed | +0.1 |

* The specimen fell out of holder after 20 sec. of ablation. It was then replaced in holder and measured after a 5 sec. reheat.

TABLE 32. A COMPARISON OF SAMPLE PROPERTIES BEFORE AND AFTER ABLATION TESTS,
HEAT FLUX = 460 Btu/(ft²sec)

| Specimen | Description | Transmission Attenuation (dB) | | Transmission Coefficient | | Reflection Coefficient | |
|-----------------|-----------------------------------|-------------------------------|-------|--------------------------|-------|------------------------|-------|
| | | Before | After | Before | After | Before | After |
| 331-1/EMC-1 | ADL-10 Silane coupled fiber | 1.3 | 6.5 | .74 | .22 | .26 | .48 |
| (1) 331-2/EMC-1 | ADL-10 No silane | 1.4 | 3.9 | .73 | .40 | .27 | .31 |
| 319-2R/EMC-1 | Unpyrolyzed Markite | 2.3 | 4.6 | .58 | .35 | .39 | .42 |
| 319-1P2-EMC-3 | Pyrolyzed Markite | 1.9 | 1.1 | .64 | .77 | .34 | .26 |
| 319-1P2/EMC-4 | Pyrolyzed Markite | 2.0 | 1.2 | .63 | .75 | .34 | .28 |
| 319-1P2/EMC-2 | Pyrolyzed Markite | 2.0 | 0.9 | .63 | .82 | .35 | .20 |
| 318-4P3/EMC | Molded Pyrolyzed Markite | 1.4 | 1.1 | .72 | .79 | .29 | .26 |
| 318-1P3/EMC-1 | Cast, Pyrolyzed | 1.3 | 1.1 | .74 | .77 | .29 | .26 |
| 318-1P3/EMC-2 | Cast, Pyrolyzed | 1.2 | 1.2 | .76 | .76 | .28 | .27 |

(1) Specimen turned in holder during ablation, so exact heat flux surface is not known.

materials that do not contain resin. The transmission coefficient of the materials which contain resin decrease considerably and the reflection coefficients tend to increase. This, of course, is due to the carbonized resin. The transmission coefficient of the materials containing no resin tends to increase slightly and the reflection coefficients tend to decrease slightly. This small change is due to the loss of material due to ablative erosion.

3.6 THERMAL CHARACTERIZATION

Additional TGA studies have been performed on cured and molded SR-350 resin to determine its actual mass loss characteristics when pyrolyzed in air at one atmosphere, as compared to the conventional available data which was determined in vacuum. The results are shown (earlier) in this report as Figure 2.

Thermal conductivity measurements were made on three Markite systems in the through the thickness direction, up to 1000°F. These results are shown in Figure 54. The conductivity is about twice that observed in Reference 1 for ADL-10 but is still lower than that for clear optically transparent fused silica, a commonly used antenna window material.

An infrared absorptance has also been run on the same specimen of cured and molded SR-350 resin used for basic resin mechanical and ultrasonic studies. This is shown in Figure 55. The measurement was made on a Model 21 Perkin Elmer Infrared Spectrometer, using a 0.012-inch thick specimen.

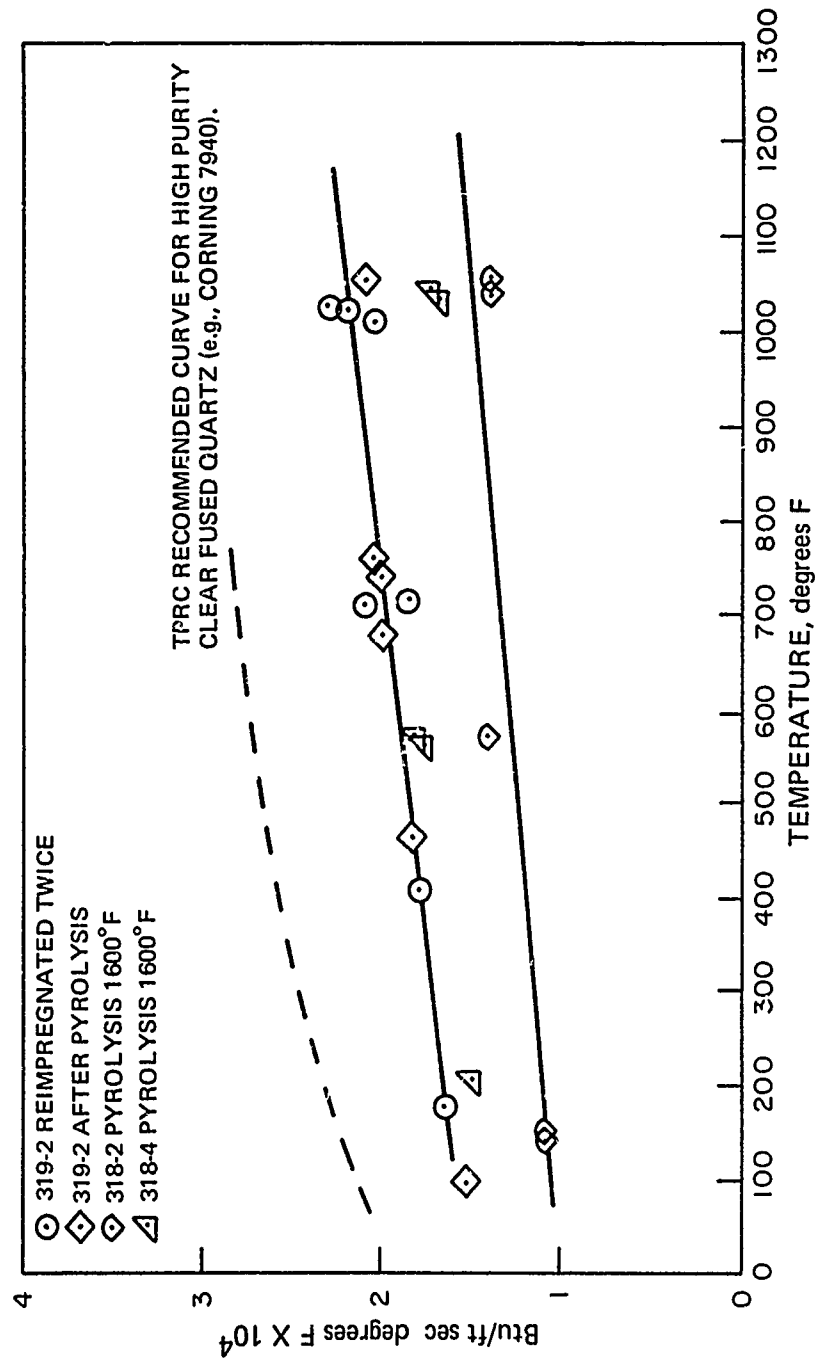


Fig. 54. Thermal Conductivity of Markite, C-Direction

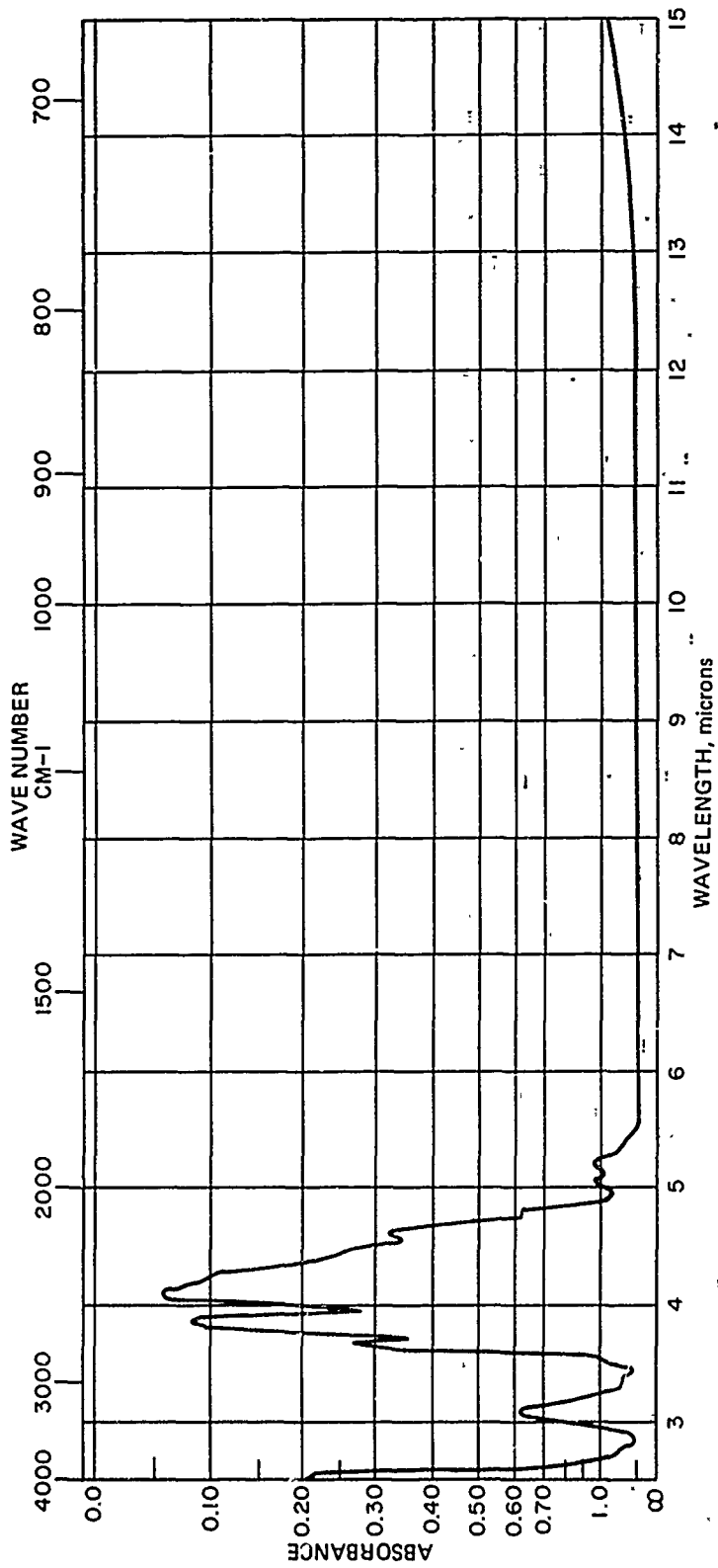


Fig. 55. Molded SR-350 Resin, Infrared Absorption (0.012" thickness)

TABLE OF CONTENTS: SECTION 4

| | Page |
|---|------|
| 4.0 Capability Analysis of ADL-10 and Markite | 4-1 |
| 4.1 Introduction | 4-1 |
| 4.2 Material Geometry | 4-2 |
| 4.3 Methods of Analysis | 4-10 |
| 4.4 Test Specimen Geometry | 4-11 |
| 4.5 Numerical Calculations | 4-14 |
| 4.5.1 ADL-10 Test Specimens | 4-15 |
| 4.6 Parametric Material Studies | 4-15 |
| 4.7 Analysis of "Markite" | 4-22 |
| 4.8 Modes of Failure | 4-25 |
| 4.9 Concluding Remarks | 4-26 |

4.0 CAPABILITY ANALYSIS OF ADL-10 AND MARKITE

4.1 INTRODUCTION

An understanding of the relative merits of Omniweave reinforced materials as a function of the material structure and the load orientation has been one of the major aims of the study described in this report. The Materials Sciences Corporation has performed this study for the General Electric Company to determine the theoretical structural performance levels of Omniweave silica reinforcement in a silicone matrix; to assess the degree to which actual ADL-10 composites achieve this potential and to provide recommendations for improving the properties of these types of materials, including a silica matrix version.

Fiber composite heat shield materials for aerospace applications are required to resist a combination of loads in different directions. Because of the resulting static and dynamic strength requirements in different directions, the laminate type of composite is no longer adequate for these applications. In contrast, composites utilizing an Omniweave reinforcement do offer substantial promise for such applications.

Fibrous composites, in general, have properties which vary significantly in different directions. Simple examples are provided by the characteristics of fiber composite laminates. These materials may be regarded as two dimensional composites in the sense that all reinforcing fibers are parallel to a given plane. A simple type of two dimensional composite is the cross-ply in which all fibers are oriented parallel to one of two orthogonal directions. Such a composite is relatively strong and stiff when loads are applied in the directions of either of the two fiber sets. On the other hand, such a composite is weak in shear and is weak when subjected to a load in a direction between the two fiber directions. As a result of this, practical two-dimensional fiber composites are generally fabricated with fibers in three or more directions within the plane. This strengthens and stiffens the composite for general loading conditions by eliminating weak shear directions.

A similar situation exists with three dimensional fiber composites. Thus, if a plastic is reinforced by fibers in three orthogonal directions, the resulting material will: 1) show high strength when loaded in those directions, 2) will show poor shear strength, and 3) will show low strength when loaded in directions between the three fiber directions. Again, the desirable solution, here, is the addition of fiber directions to eliminate planes of weakness. Such a solution is offered by the Omniweave fabrication process for the four directional (4-D) material.

The general 4-D reinforcement configuration may be defined by the body diagonals of a rectangular parallelepiped. The concepts which govern the behavior of such a material are illustrated most easily, by considering the special case in which the material orientation is defined by body diagonals of a cube (see Fig. 56). For this material,

the direction of highest strength is any one of the fiber directions, just as in the 3-D orthogonal material. Unlike the 3-D material however, the 4-D composite has high shear strength with respect to any one of the fiber axes. The next highest strength direction is parallel to any of the cube face diagonals. Finally, the weakest load directions (although directions of very high shear strength) are those parallel to the cube edges. In its most common application, Omniweave has been used in this latter orientation. Yet, even in this orientation, good potential for the material has been indicated.

The study required the formulation of a computer analysis which contained both realistic description of the internal material geometry, and a rational failure criterion. These analytical developments are discussed first in the body of this report. This is followed by an evaluation of the actual ADL-10 test specimen characteristics to define input data for the computer analysis. Numerical results are then obtained for both ADL-10 and "Markite" composites, and compared with experimental results. Numerical results are also obtained for certain suggested alternate material configurations.

The study shows that the ADL-10 composite is achieving the expected performance levels. An explanation of the low strength levels of Markite is presented along with recommendations for substantial improvements. The analytical methods developed appear to offer a reliable means of evaluating properties and performance of candidate materials.

4.2 MATERIAL GEOMETRY

The basic concept behind the 4-D material generated by the Omniweave process is that elimination of planes of shear weakness will provide a strong, reliable composite. (see Reference 11). Omniweave can be used to produce a material having four sets of fibers in directions parallel to the body diagonals of a rectangular parallelepiped (see Fig. 56). The geometry of this 4-D material is such that fibers can run from face to face of the material along a perfectly straight line, in a material having a fiber volume fraction up to 68 percent. This combination of high fiber volume fraction, straight fibers and multiple directions are the basis for the good properties of this 4-D material.

A model of the cubic material can be constructed readily from single rigid circular filaments in the maximum fiber volume packing array (see Fig. 57). If this material is sectioned parallel to one of the cube faces, the result is the pattern shown in Fig. 58, wherein each individual circular filament is represented by its elliptical cross-section. If, in place of single filaments, the material is formed from a bundle or roving containing a large number of filaments, the maximum fiber volume fraction is obtained when the individual rovings are distorted to form a hexagonal cylinder. In this case, the cross-section parallel to a cube face would appear as shown in Fig. 59, wherein each hexagon contains a large number of individual filaments. The fiber

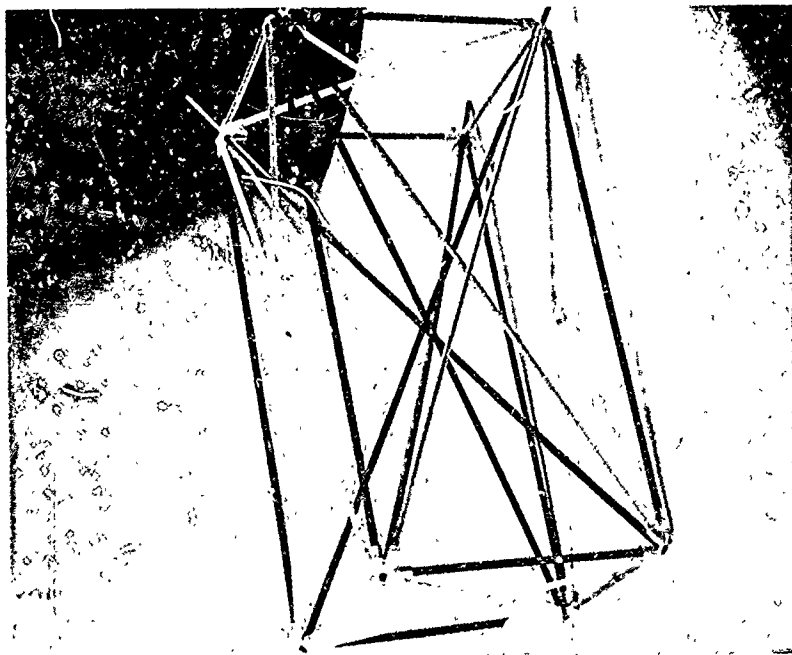


Fig. 56. Model of Omniweave Showing Relative Orientation of Fiber Axes

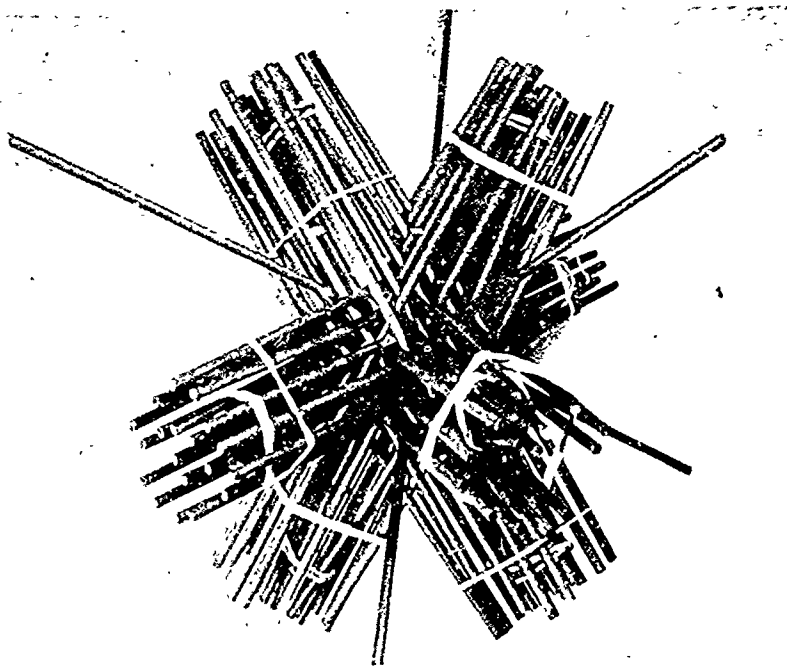
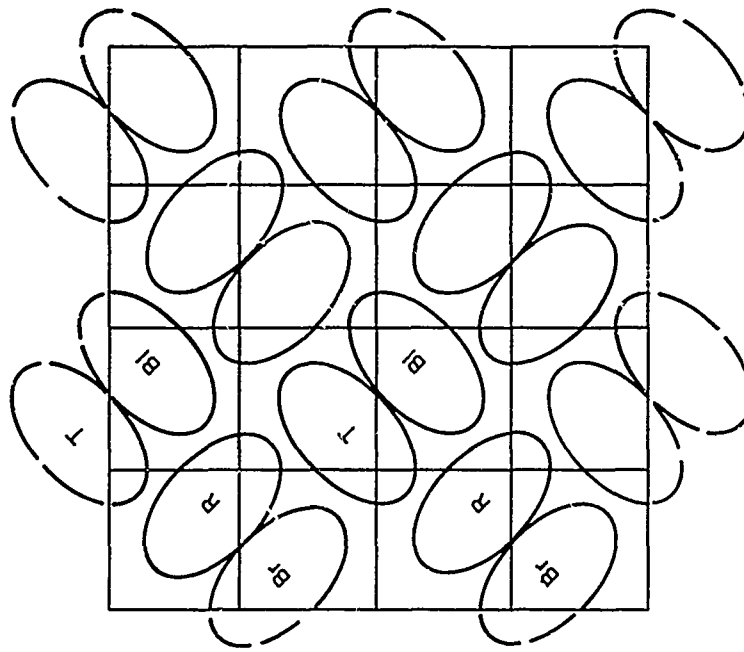
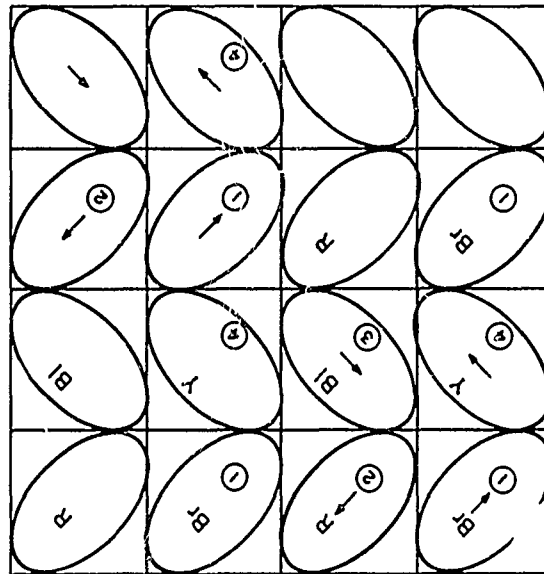


Fig. 57. Model of Rigid "Fibers" in Omniweave Pattern Showing High Volume Fraction for Straight Fibers



B. SECOND TYPICAL SECTION



A. FIRST TYPICAL SECTION

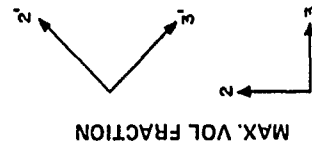


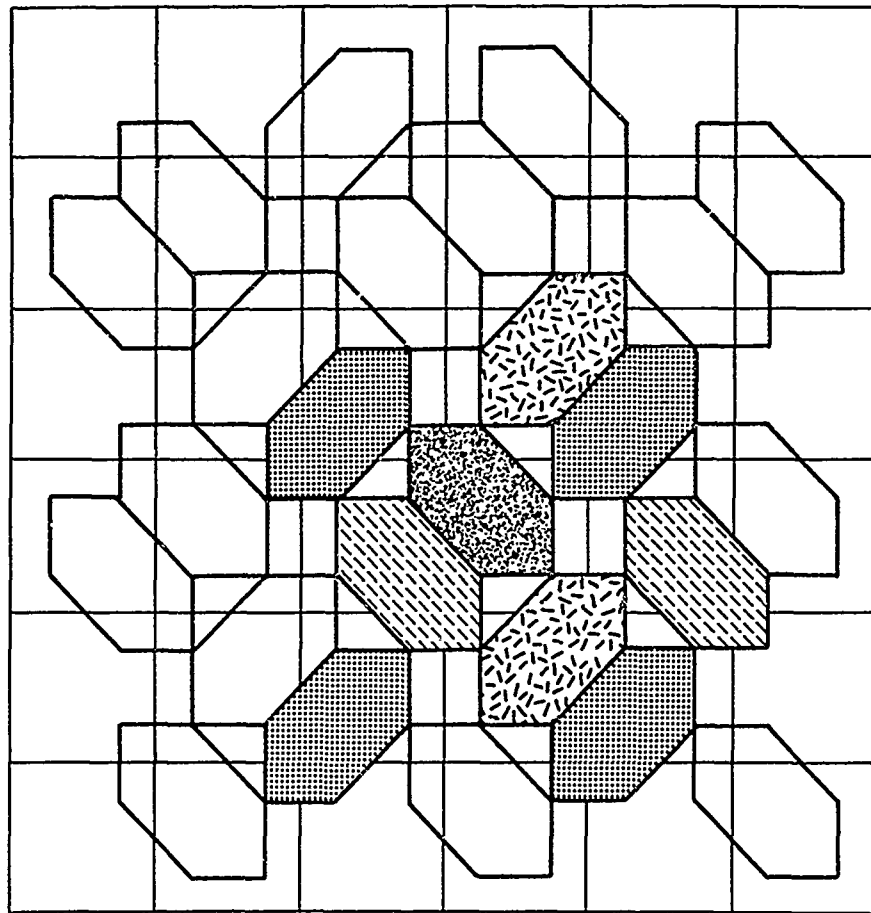
Fig. 58. Omniweave Cross Section Showing Solid Circular Fibers in Maximum Packing Array

volume fraction for this case is exactly the same as that for the single circular fiber case, when the filaments within a single roving are assumed to be in hexagonal close packing. Two characteristic patterns, representative of two different elevations within the material, are shown on Fig. 59. It is of interest to compare these results to actual cross sections of a carbon/carbon Omniweave composite as presented in Reference 12. Figure 60 is taken from that reference and shows carbon fiber rovings distorted into hexagonal arrays very similar to those predicted theoretically by Fig. 59 results.

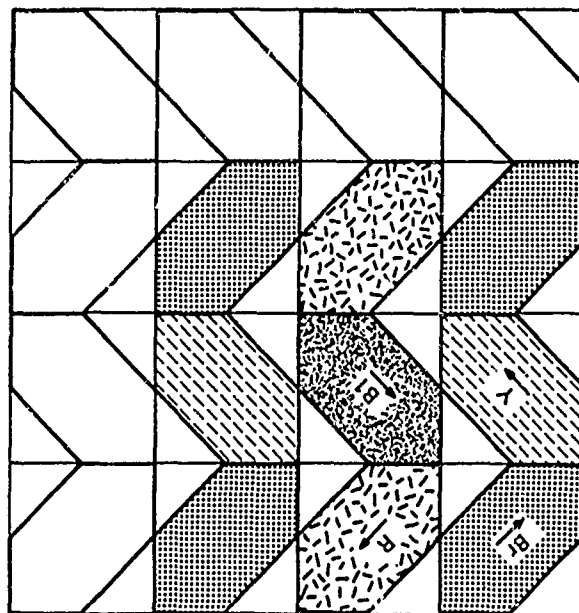
When the Omniweave is in a pattern which is not square symmetric - that is, when the two edges of the parallelepiped which are perpendicular to the weaving direction are unequal - the hexagons shown in Fig. 59 will become distorted and their aspect ratio will change. This has been studied and results are presented in Fig. 61. The weave pattern is measured by the angles projected onto the two material faces parallel to the weaving direction. The plan form angle* is denoted, θ_a , and the through-the-thickness angle is denoted, θ_t . The hexagon aspect ratio is plotted as a function of the through-the-thickness angle with $\theta_a = 45^\circ$. For example, in the case of $\theta_t = 15^\circ$ and $\theta_a = 15^\circ$, the aspect ratio is approximately 3. It was found in early impact tests of ADL-10, that the material separated into fiber strips having a flat ribbon like appearance not unlike that described in Figure 61.

With this understanding of the location of the fiber bundles, it is possible to examine the nature of the regions between the fibers. This is done in Fig. 62 for the material of Fig. 59. The model is sectioned at intervals along the weaving direction. These cross sections perpendicular to the weaving direction are shown in Fig. 62 and they define a matrix region between the fiber bundles. Thus, the Omniweave reinforced plastic consists of hexagonal cylinders composed of uniaxial fiber-plastic composites surrounded by irregularly shaped matrix regions. This type of inhomogeneity raises questions about the theoretical model proposed in Reference 11 (and executed for the computer in Reference 13). In the present program, an analytical model of the material which includes these different material regions has been utilized.

*Also designated fiber-pitch angle (FPA) previously and in Reference 1.



B. SECOND TYPICAL SECTION



A. FIRST TYPICAL SECTION

Fig. 59. Omniweave Cross section Showing Solid Hexagonal Fibers or Roving in Maximum Packing Array

Reproduced from
best available copy. 

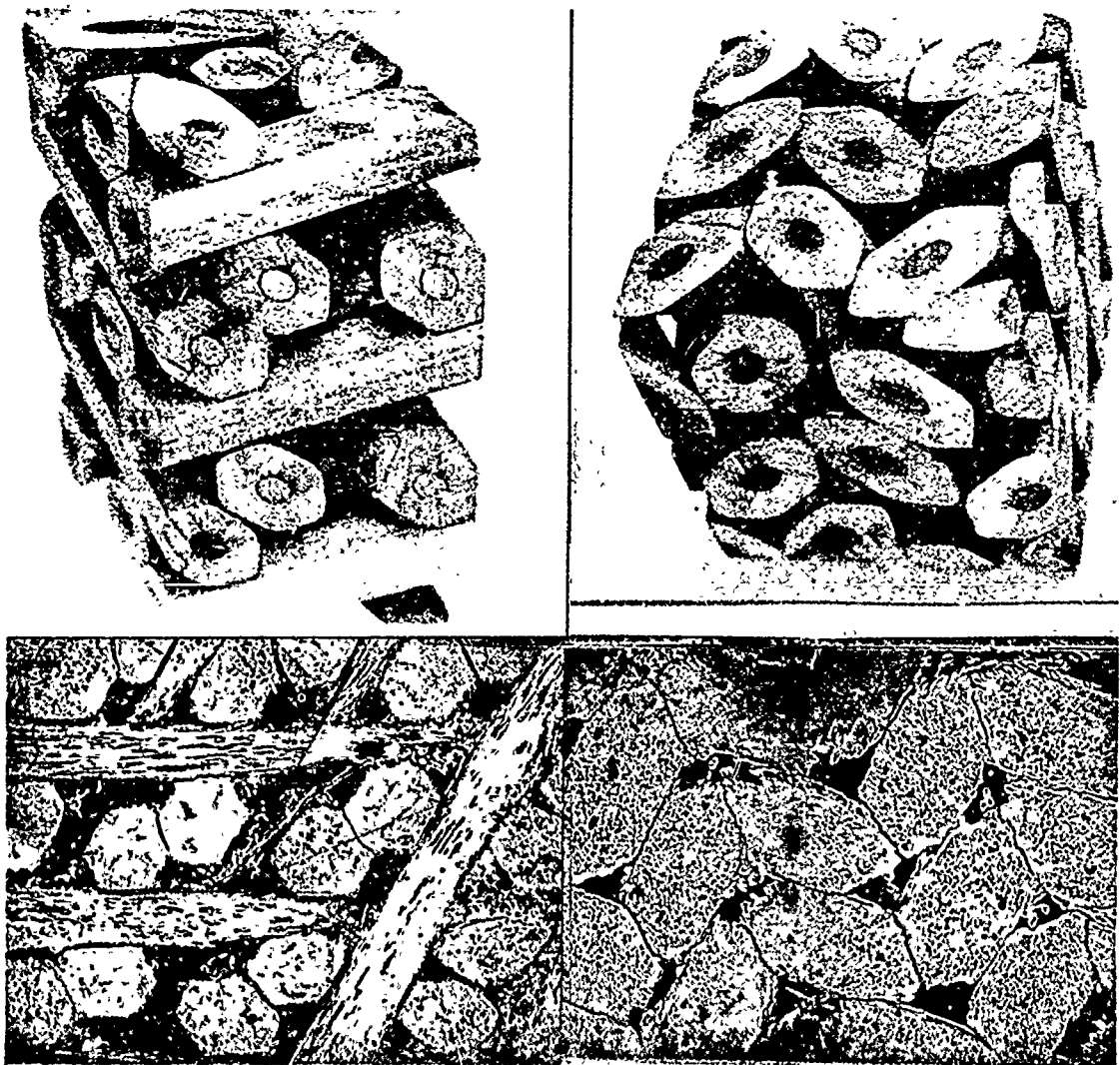


Fig. 60* Hexagonal rod packing models of cubic 4 directional packing and sections with similar orientations found in CVD infiltrated 4-D Omniweave made from Morganite II (left) and Thornel 50 yarns (10X). Surfaces at left are parallel to one pair of reinforcement directions; those at right are perpendicular to the weave direction.

* From Reference 12.

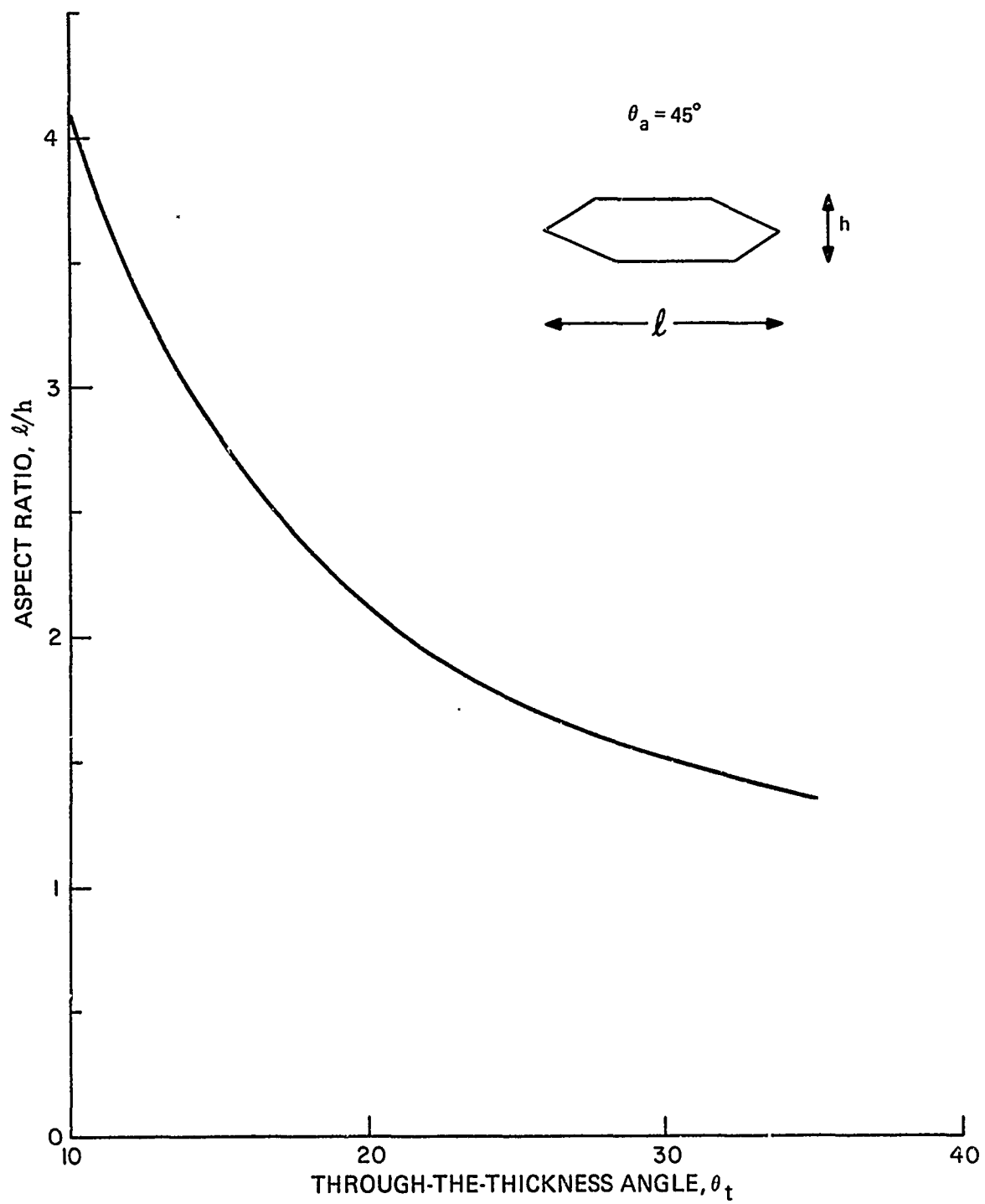


Fig. 61. Deformed Shape of Individual Rovings Due to Molding Pressures

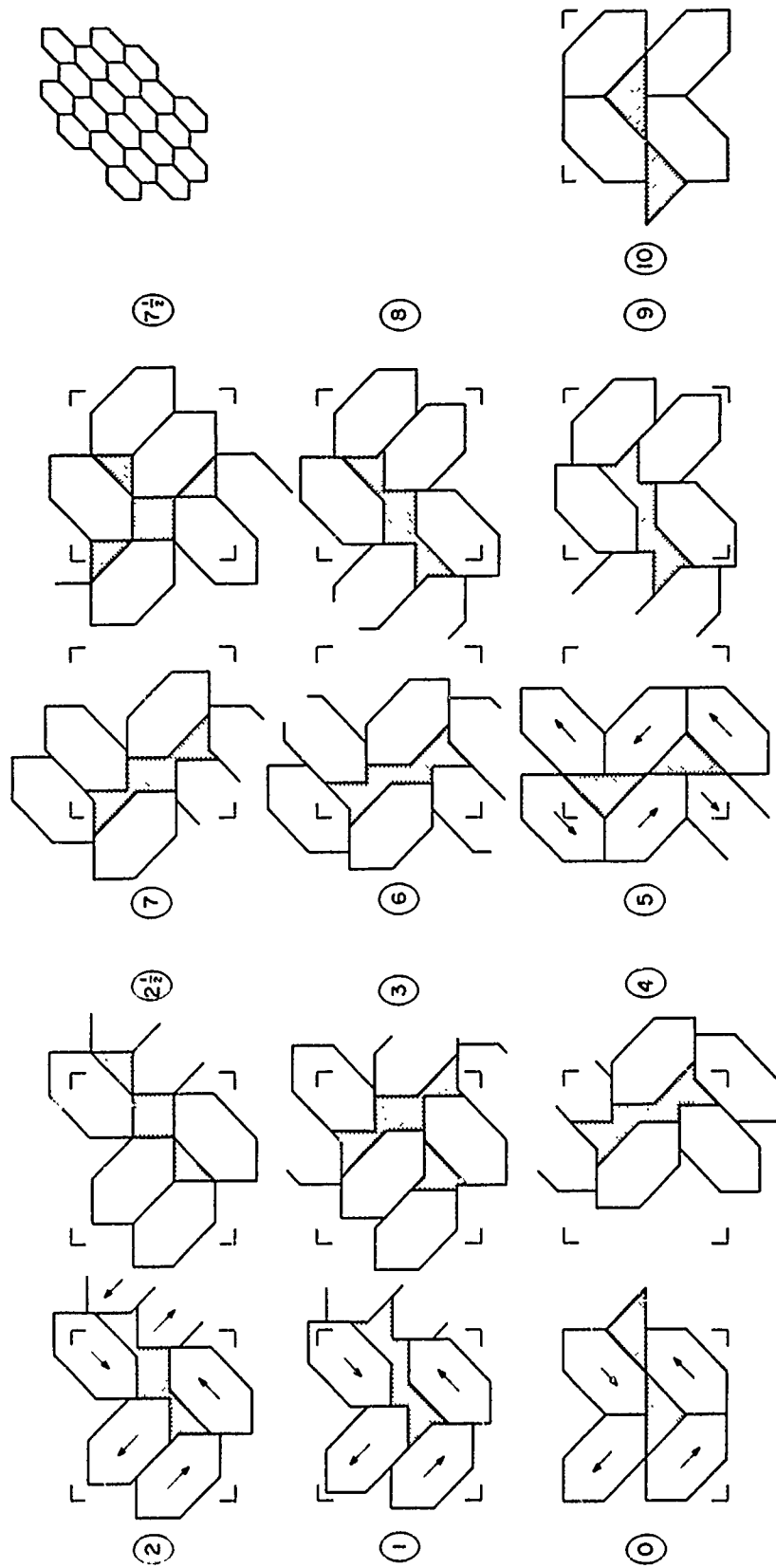


Fig. 62. Typical Sections Through Model of Fig. 59 Showing Shape of Matrix Region Between Hexagonal Rovings

4.3 METHODS OF ANALYSIS

The basic analytical tools used for analysis of these materials are based upon the methods of Reference 11. In this approach, the fiber bundle is treated as a homogeneous anisotropic material having known elastic constants and strengths.

The unidirectional bundle of fibers in a matrix forms a transversely isotropic material (i. e., isotropic axis). This is the building block in the construction of the 4-D material. The elastic constants are computed from fiber and matrix properties* using the methods of Reference 14. This yields a set of five independent elastic constants for the effective material, which is considered to be transversely isotropic. The strength values used are also based on fiber and matrix properties. These are discussed further subsequently.

In the original applications of this approach to assessing properties of 4-D composites, (i. e., References 11 and 13) it was assumed that the entire composite was composed of differently oriented regions each having the same principal elastic properties and strengths. In view of the internal geometry characteristics shown in Fig. 62, it is clear that the model should treat a separate matrix region between these cylinders of uniaxial fiber composites. The analysis of this geometry has now been incorporated into the MULTI computer program. This program is based upon the use of admissible displacement fields to define an approximation to the strain energy resulting from given boundary conditions.

In the present study, a revised failure criterion was introduced into the analysis to correct previous deficiencies (e. g., of References 11 and 13). The program can be briefly outlined for the case of composites which are orthotropic in terms of effective average stress to average strain relations, as follows:

- a. The material is considered to be composed of an assembly of basic composite volume elements, (all having the same constituent volume fractions), and of matrix regions. Displacement boundary conditions which would give rise to uniform strain states in homogeneous media are treated. Displacements on the boundary of each volume element are assumed to be those associated with these uniform strains. The average stresses in each basic volume element are computed from the effective stress-strain relations of a unidirectional fibrous composite having the same constituents and volume fractions as the element under consideration. The average stresses in the matrix region follow directly from the isotropic stress-strain relations for that material.
- b. The isothermal case is considered. The stress-strain relations for each set of basic volume elements, (where a set is defined by the fiber direction) with respect to local principal elastic axes, is given by the same set of transversely

*Some of which, e. g., the cured SR-350 resin properties, were specifically determined for this analysis.

isotropic constitutive equations. These equations as well as those for the matrix are transformed to the material principal axes. For the assumed displacement field, the average strains in each region are the same. Hence average stresses for the composite as a whole are found by summing the volume-weighted average of the stresses in each basic volume element and in the matrix region. The resulting overall average stress to average strain equations define the effective elastic moduli for the 4-D composite.

- c. With moduli known, it is then a straightforward matter to find the average stresses in each of the sets of fiber bundles. The failure criterion contained in the program is the maximum stress criterion. This is used here because it identifies the critical stress component, as well as the failure stress level, thus providing guidance for material improvement. A quadratic interaction type failure criterion was also used in certain cases, but it was found to yield almost identical results and to increase the complexity of solution.
- d. Since there is a general state of average stress introduced into each fiber composite set, even under the application of simple unidirectional stresses to the composite, the following stress components are considered in the failure criterion:
 - 1) Maximum extensional stress in the fiber direction within each fiber composite set.
 - 2) Maximum shear stress on a plane normal to the fiber directions.
 - 3) Maximum axial shear stress on a plane parallel to the fiber axis.

This failure criterion was introduced into the MULTI program and is now checked out and operational. It has been used for prediction of composite failure stress levels as described in the following sections.

4.4 TEST SPECIMEN GEOMETRY

The analytical methods described above were used to assess the expected performance of the test specimens of series 1 and 2 (defined in Section 2 of this report). The first problem was to define the degree of inter-dependence among the various geometric parameters. Earlier studies have emphasized the importance of the fiber orientation angles. Thus the axial projected angle, θ_a , was taken as the principal independent variable. The relationships between this angle and the through-the-thickness projected angle θ_t , and the fiber volume fraction ν_f , were studied.

The mean values of θ_a and θ_t for series 1 data are plotted in Fig. 63. A straight line fitted to these data indicate that for the test specimens in this group, the two angles are linearly related. Similar data for series 2 specimens are presented in Fig. 64.

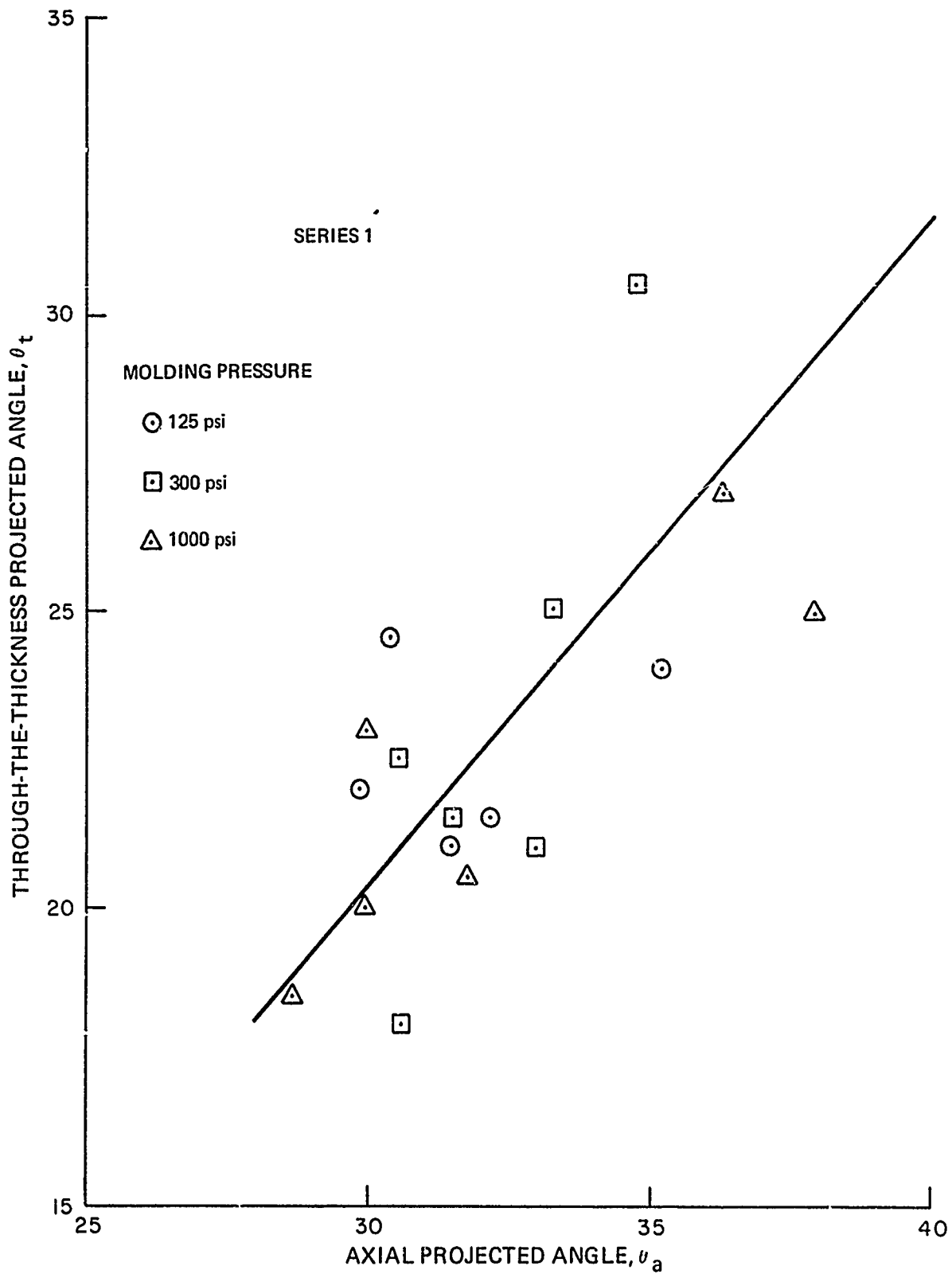


Fig. 63. Variation of Through-the-Thickness Projected Angle with Axial Projected Angle for Series 1 Specimens

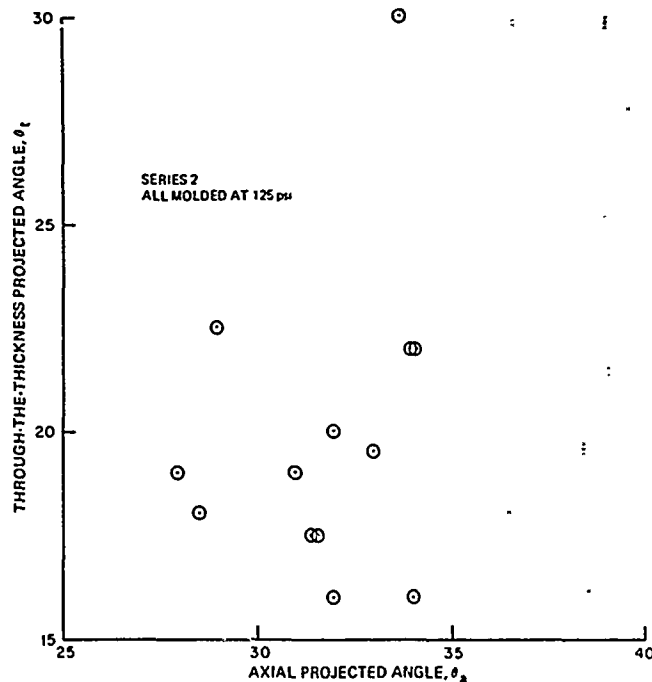


Fig. 64. Variations of Through-the-Thickness Projected Angle with Axial Projected Angle for Series 2 Specimens

Their relationship is insufficiently defined. On this basis, the straight line of Fig. 63 was used to define input for the numerical computations used for comparison with the test data.

The volume fraction data of Reference 7 are of uncertain accuracy because of changes in specimen length during fabrication. The very high fiber volume fractions do not appear to be consistent with the physical appearance of the test specimens. An attempt was made herein to revise these data based on an estimate of the deformations of Omni-weave during fabrication. Thus it was assumed that the original weave was a 1x1x1 configuration (i. e., cubic), that the basic hexagonal element length was unchanged during deformation, and that the finished (molded) axial projected angle, θ_a , was the same as the premolding angle. Composite density was assumed to be uniform along the entire length of the reinforcement. Based on these estimates, the data of Reference 7 were revised and the results are plotted in Fig. 65. There seems to be a consistent variation between the two parameters and the range of volume fractions is physically satisfying. However the nature of the calculation is of sufficient uncertainty, that the line $\nu_f = 0.5$ was considered to be equally applicable to the data. This fixed fiber volume fraction value was used in the computations for comparison with experimental data.

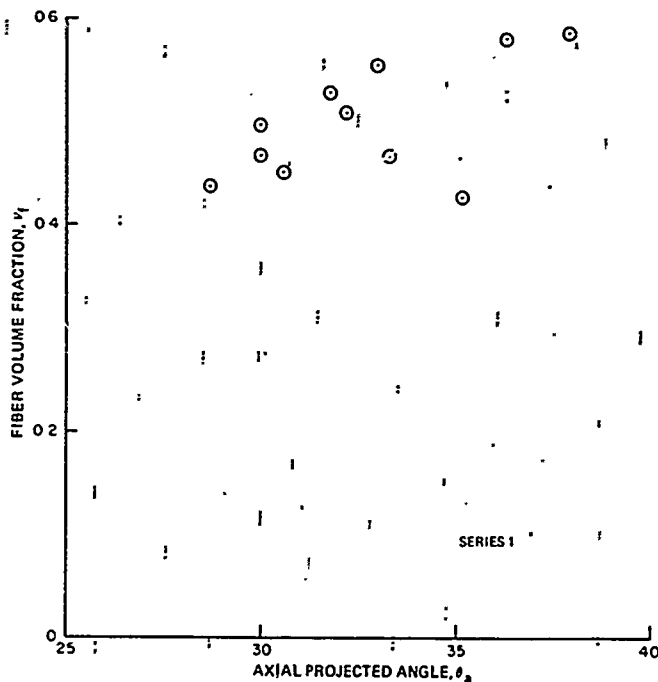


Fig. 65. Variation of Estimated Fiber Volume Fraction with Axial Projected Angle

The estimation of the weave distortions discussed above suggests the need to provide for controlled deformations during the fabrication process. It is recommended that any distortions of the Omniweave from woven to final configuration be performed in such a fashion that the ratios of specimen dimensions vary in the same way that the relative dimensions of a basic element vary, when the latter is constrained such that the distance between roving intersection points remains constant and equal to the woven value. This should greatly minimize both fiber distortions and damage.

4.5 NUMERICAL CALCULATIONS

The analytical methods described above have been used for evaluation of the test specimens to determine the degree to which the latter have achieved their potential performance. Satisfactory agreement between theory and experiment has motivated a parametric study to seek out potentially better performance material configurations. Included in this phase was an initial assessment of behavior under loads in directions other than the weaving axis. Finally, numerical evaluation of all-silica composites has been initiated. These studies are discussed in this section of the report.

4.5.1 ADL-10 Test Specimens

The MULTI computer program requires as input data the fiber and matrix elastic properties and volume fractions and the orientation parameters of the fibers. The first major section of the output defines the material elastic constants including Young's modulus in the weaving direction, which was also determined experimentally. The computations utilized θ_t vs. θ_a from Fig. 63 and $\nu_f = 0.5$. The matrix elastic modulus is computed from the SR-350 flex modulus data under the assumption that five percent of the composite or ten percent of the matrix is voids.

The predicted Young's modulus and the experimental data for series 1 and 2 are plotted in Fig. 66 as a function of the axial projected angle. The computed values are somewhat higher than the data but the variation with angle is not unreasonable. It should be noted that the use of admissible displacement fields to approximate modulus will give a result which will be off on the high side, if it is in error.

Computed internal average stresses are used to define failure. For the series 1 data, an interaction failure criterion was used. This was based on an axial strength for a unidirectional silica/silicone composite of 100 Ksi, an axial shear strength of 4.5 Ksi and a transverse shear strength of 4.5 Ksi. The computed result is compared with experimental data in Fig. 67. The scatter in the data is large, but the material may generally be regarded as achieving its strength.

As stated earlier, an understanding of the cause of failure is better illuminated by a maximum stress failure criterion. For this reason, and since the interaction effects were found to be small, the series 2 data were compared to theory using the maximum stress failure criterion. It was found that the axial shear was the critical stress component. The theoretical results are compared with experimental data in Fig. 68. Based on the assumption that attainment of the maximum allowable shear stress is followed by failure, the material is achieving its potential. It should however be pointed out that the events which are expected to follow initial internal failures with a relatively brittle matrix are uncertain. Crack propagation to failure does not however appear to be unreasonable. Hence improvement in performance can be expected to require changes in material geometry, rather than improvements in processing parameters. This is discussed in the following section.

4.6 PARAMETRIC MATERIAL STUDIES

In view of the agreement between theoretical and experimental properties of the ADL-10, studies of the effect of variations in fiber orientation were undertaken to try to define improved performance materials. One set of such studies deserves attention in this report. This is the material in which θ_a and θ_t are equal and relatively small. For this case the material is defined adequately by the angle, θ , between any fiber direction and the weaving direction. All input parameters for fiber and matrix properties were retained as above and values of this angle, θ , between 10 and 30 degrees were

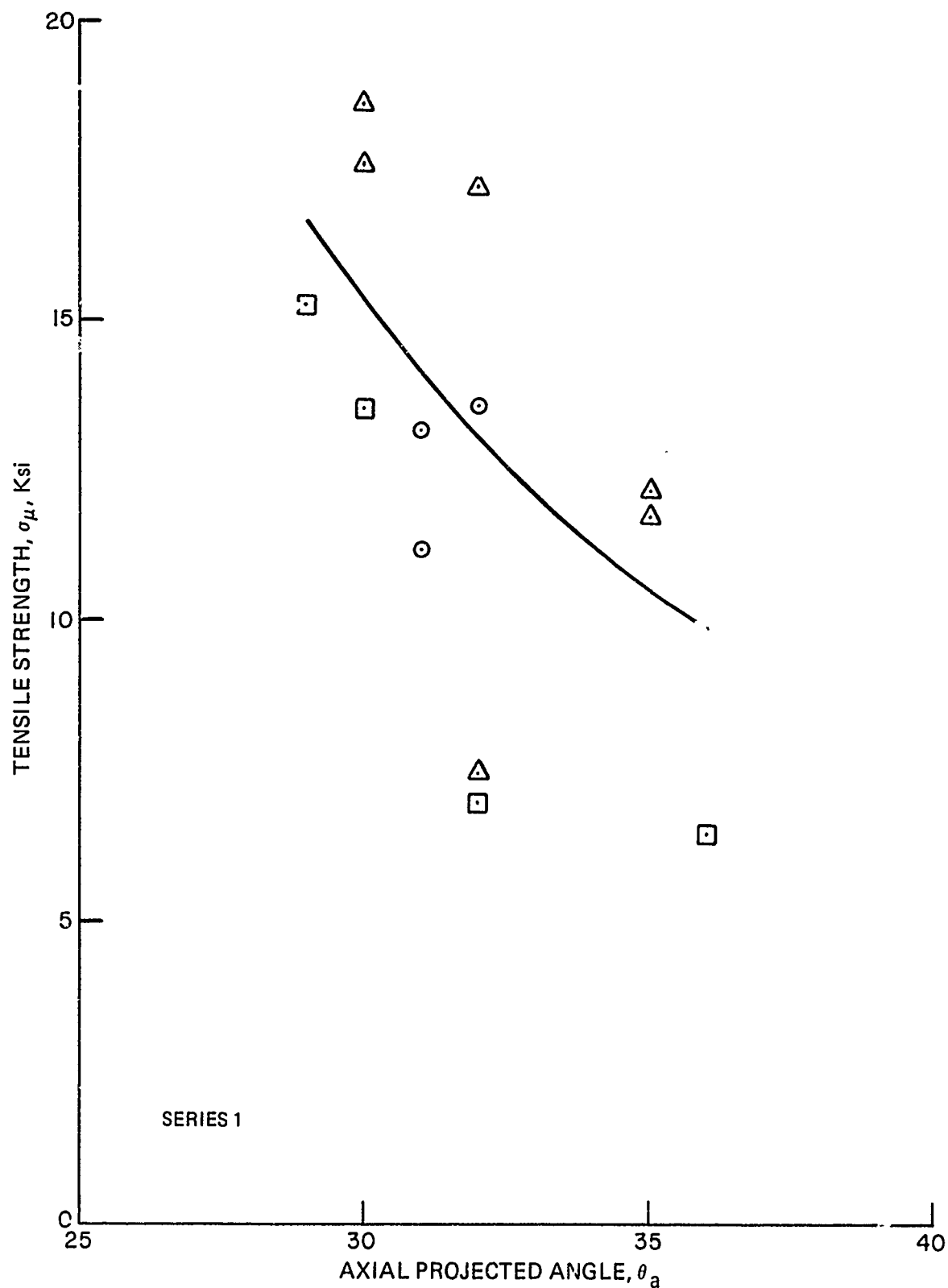


Fig. 67. Theoretical and Experimental Strength Values for ADL-10 Series 1 Specimens

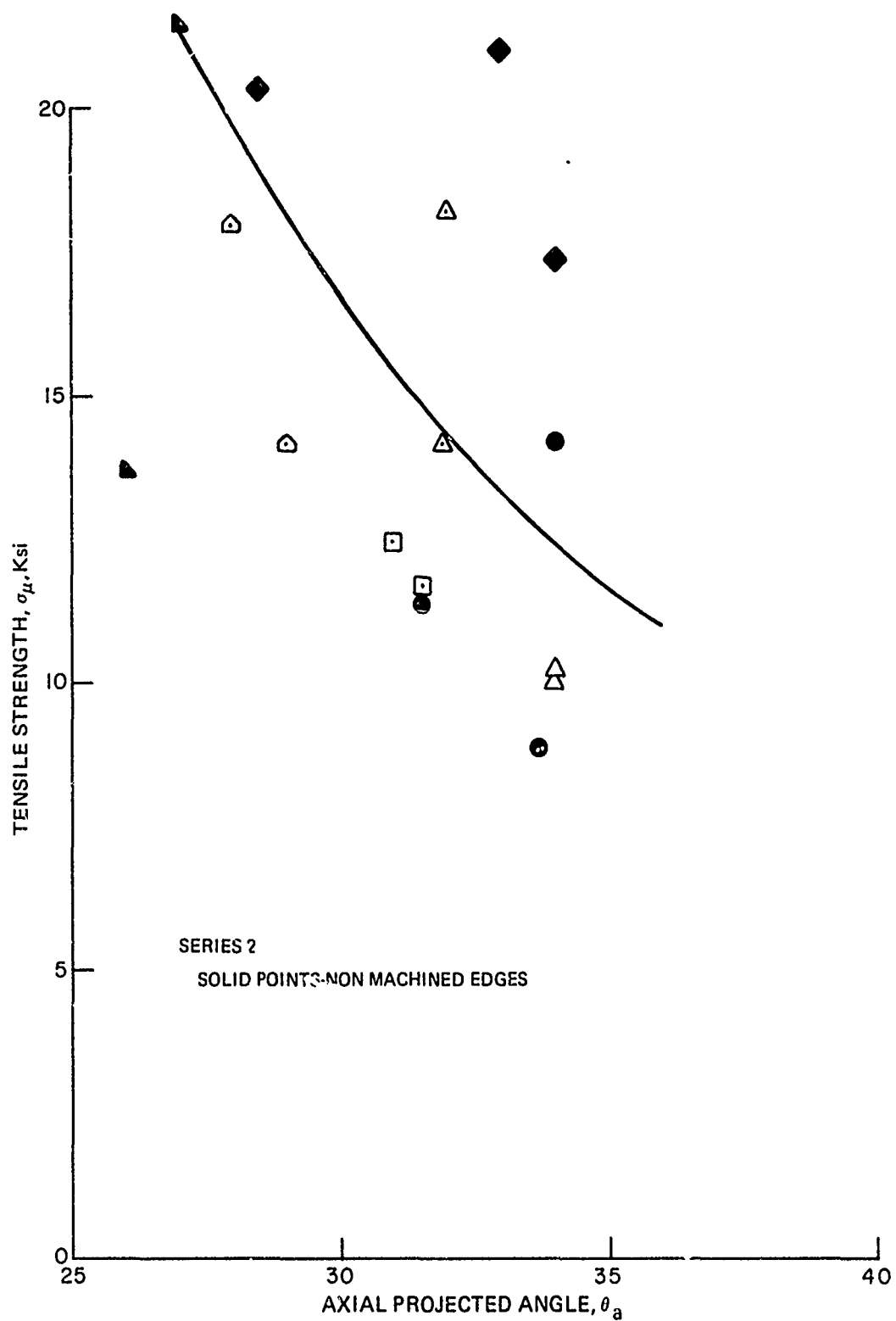


Fig. 68. Theoretical and Experimental Strength Values of ADL-10 Series 2 Specimens

explored. The results for axial stiffness are presented in Fig. 69 and for axial strength in Fig. 70. Substantial improvements over the values discussed in the preceding section are evident, for small values of θ . The usefulness of these materials cannot be assessed without examining strength in other directions. As discussed earlier, the directions of interest are those parallel to the face diagonals and body diagonals of the basic Omniweave element shown in Fig. 56.

The face diagonal direction is a measure of possible enhancement of through the thickness strength. Thus axial strength could be maintained while through-the-thickness strength is enhanced, by rotating the entire material 45 degrees about the axial direction. This would require some changes in the Omniweave mechanism, (with, however, little change in the concept or execution of the weaving process). The result of such an orientation change is illustrated by the results of computations carried out for the 30 degree material of Figs. 69 and 70. The through the thickness strength is computed as 6.1 Ksi for the normal configuration and as 8.5 Ksi for the improved orientation. A 40 percent improvement is indicated.

The question of maximum strength potential for the Omniweave in any single direction is assessed by considering loads applied in the direction of one of the four sets of fibers. For this case, tensile strengths of 25 Ksi are predicted based upon the properties cited earlier (namely, a unidirectional tensile strength of 100 Ksi). It is this type of loading which should be considered in comparing this 4-D material to an existing 3-D material, as this is the case in which shear strength values are minimal. It should be noted however that shear strengths for 4-D composites will always be larger than the shear strength in the principal directions of an orthogonal 3-D composite.

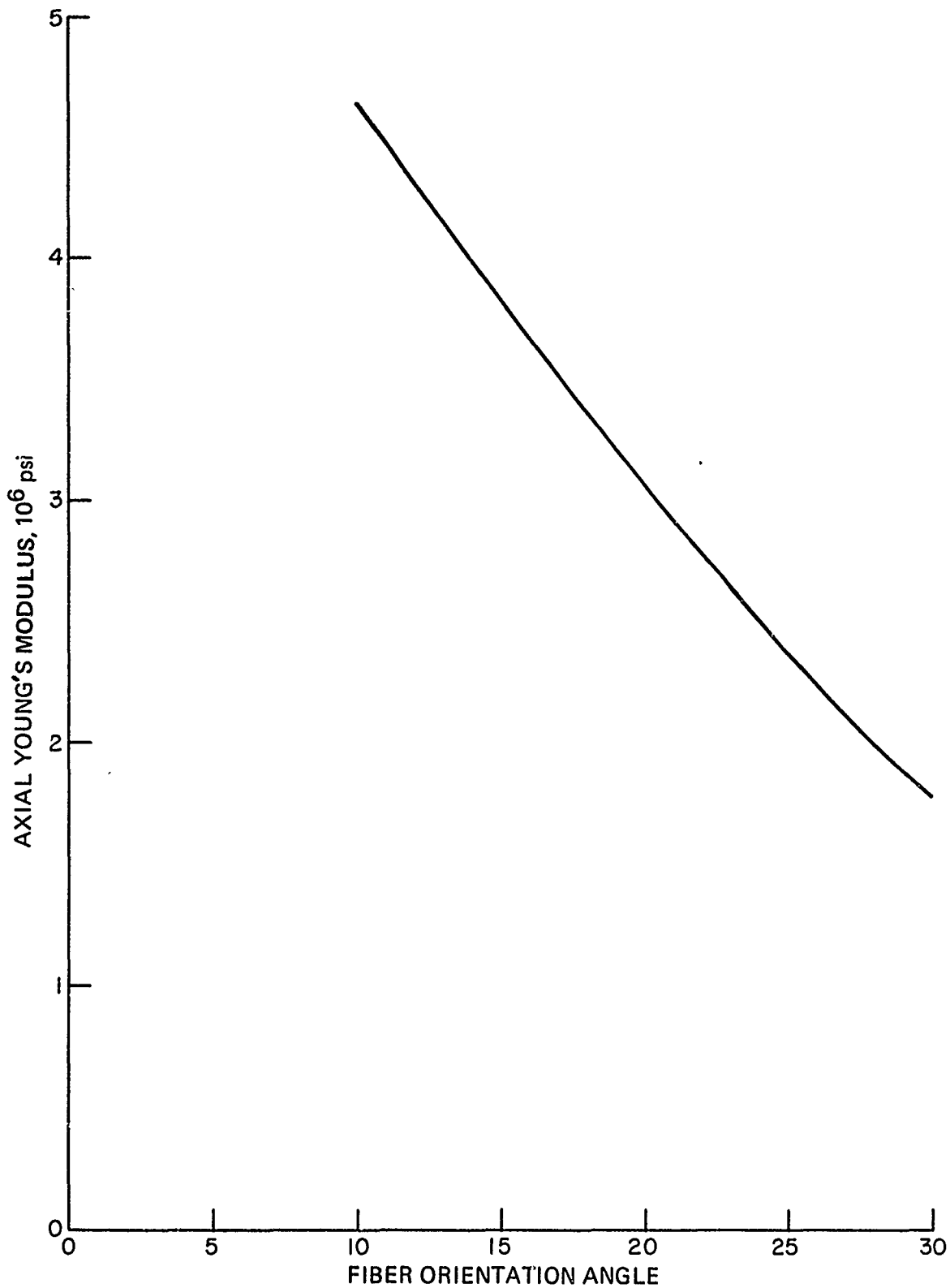


Fig. 69. Extensional Modulus as a Function of Angle Between Fibers and Load for Symmetric 4-D Configurations

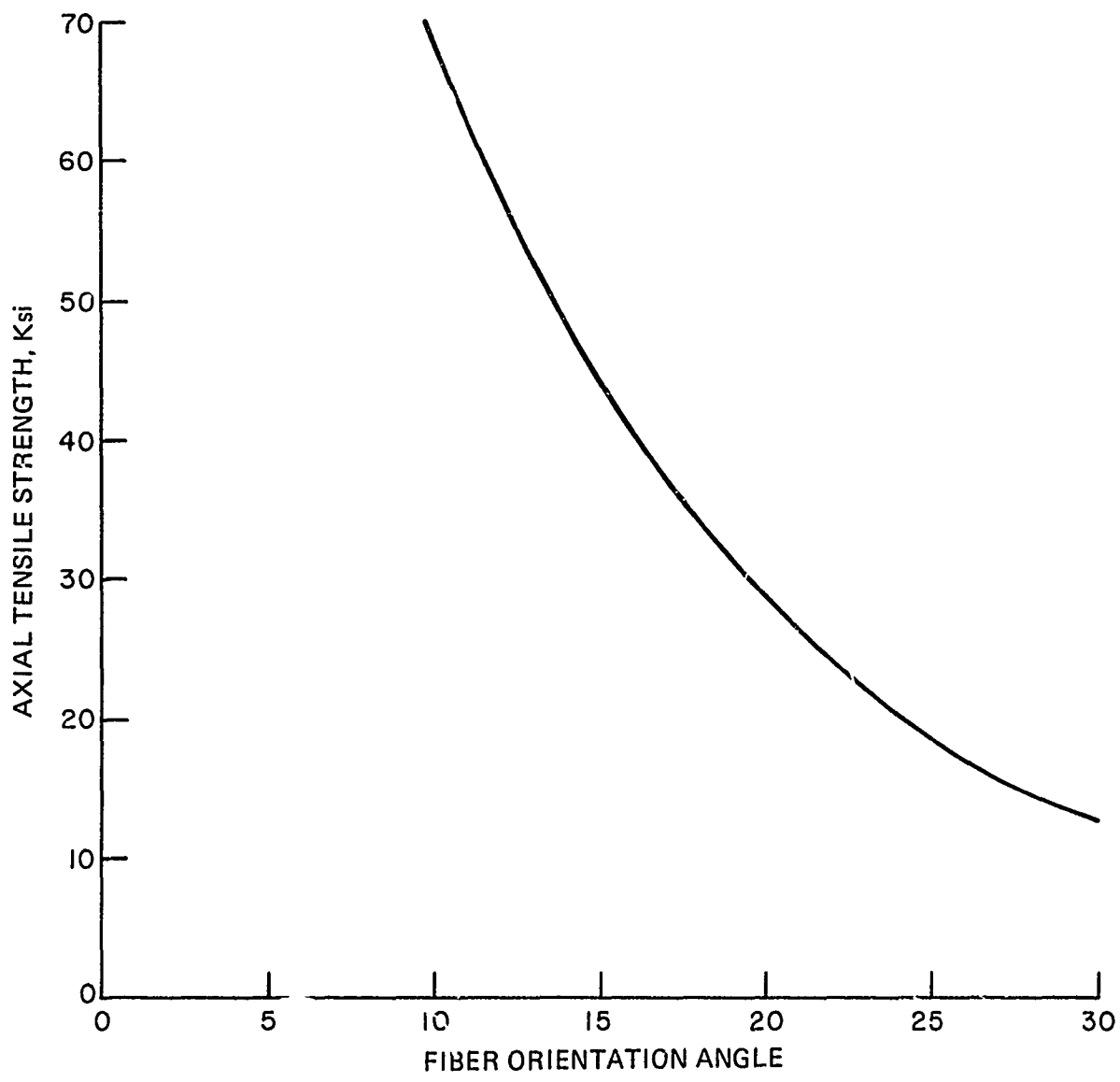


Fig. 70. Axial Strength as a Function of Angle Between Fibers and Load for Symmetric 4-D Configurations

4.7 ANALYSIS OF "MARKITE"

An approximate analysis of Markite was performed in order to assess anticipated strength levels for the material. Effects of fiber orientation and phase volume fractions were assessed on the basis of the assumption that the matrix formed predominantly along the fiber bundles, leaving voids in the interstices between these fiber pencils. On this basis, the material is highly structured and offers the potential of carrying higher stresses than a continuous ceramic, which is likely to be notch-sensitive.

It later became apparent (e. g., Fig. 71) that the matrix filled the regions between fiber bundles and that the void volume was distributed throughout the material. On this basis, it appears that Markite should be unable to resist crack propagation and will have a low strength level. Possibilities for crack arrest, by creating a weak interface between fiber and matrix, warrant consideration, especially in view of the high tensile strength retained by the plate-slapped ADL-10 specimens (section 3.2.1).

In view of the state of affairs, the following analysis should be regarded as assessing the potential of a material which has yet to be fabricated. It is a material which may be modeled as a space frame. As such, it would be expected to show improved performance with the addition of other members, particularly with "stuffing" fibers added during the Omni-weaving process. This improvement is also assessed in the following study.

The basic frame element is shown in Figs. 56 and 72. The body diagonals of the rectangular parallelepiped represent the fibers in a basic Omniweave material. If we consider a vertical plane containing the diagonals we find that the fibers contained in this plane form a parallelogram such as DOGO'. It is considered that the material is loaded parallel to the sides of the figure labeled "C". It is also assumed that the matrix material concentrated at the fiber intersections, such as D, O, G, O', etc. produces rigid joints.

Under these assumptions, a space frame resists an applied load P by both axial and bending stresses in the diagonal members. The addition of horizontal fibers along the face diagonals AF, BE, CH and DG reduces the bending stresses in the diagonal members, and improves material strength. The expressions for axial stress, f_a , and bending stress, f_b , in the diagonal frame members have been obtained in Reference 15.

The ultimate stress that a frame can carry is determined by setting $f_a + f_b = f_u$, where f_u is the fiber tensile strength. This equation defines the ultimate load on a single frame which yields the failure strength of the material, p_u .


Reproduced from
best available copy. 



Fig. 71. Photomicrograph of Markite Fracture Surface Structure Showing Characteristic Fiber Spacing (Plate 209-3, 21X)

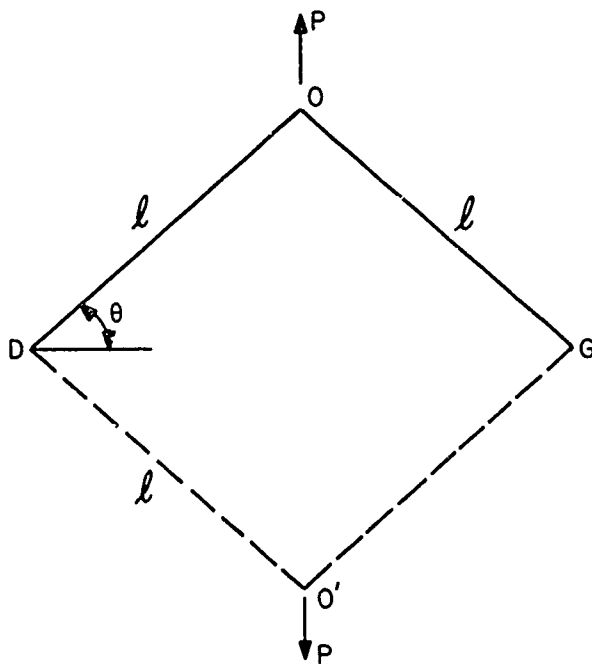
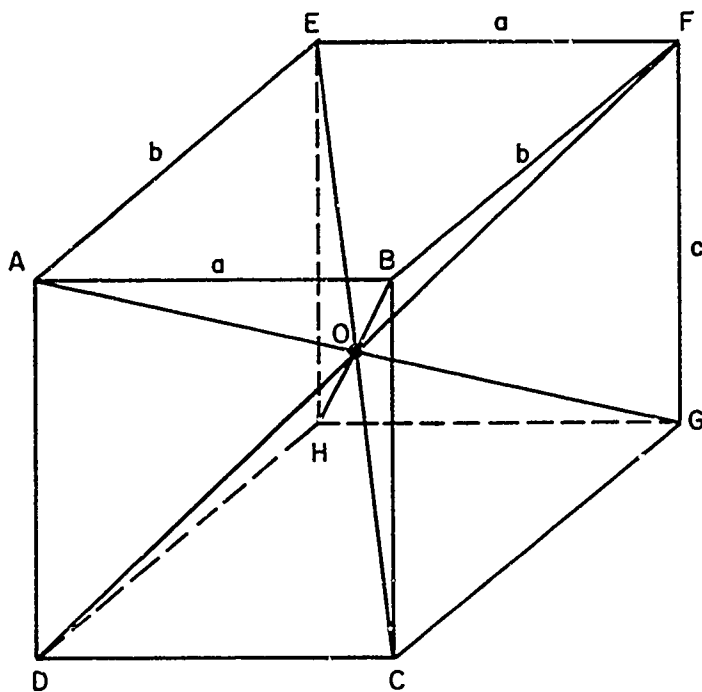


Fig. 72. Frame Model

The ultimate strength depends on the allowable fiber strength, f_u , the fiber orientation angle, θ , and the fiber aspect ratio l/d . In order to find l/d it was assumed that the fiber volume fraction was between 0.50 - 0.60. This corresponds to an l/d ratio of the order of 1.5. In order to account for flattening of the fibers during processing an l/d of 5 was used. Table 33 shows the ultimate strengths of materials without and with horizontal fibers for a range of θ - values. The factor R is the ratio of strengths with and without the horizontal member. A value of fiber strength, f_u , of 100,000 psi is used.

The results clearly show that for a material that can be represented by the model used, a significant enhancement in strength can be obtained. However, it must be pointed out, again, that this model is not representative of a high density Markite material which, it is believed, behaves more like a continuum with voids than a structured material.

TABLE 33. COMPARISON OF PREDICTED STRENGTH OF LOW-DENSITY MARKITE WITHOUT AND WITH THE ADDITION OF HORIZONTAL FIBERS

| ($l/d = 5, f_u = 100,000$ psi) | | | |
|---------------------------------|---------------------------------|--------------------------------|-------------------------------------|
| θ | Ultimate Strength (psi) | | Ratio of Strengths $R = p'_u / p_u$ |
| | Without Horizontal Fibers p_u | With Horizontal Fibers, p'_u | |
| 40 | 340 | 1390 | 4.1 |
| 50 | 560 | 2740 | 4.9 |
| 60 | 1160 | 6630 | 5.7 |

4.8 MODES OF FAILURE

Fiber composite materials have gained prominence in many engineering applications because of their high tensile strength. This strength results from a combination of two factors of importance. These are: 1) the very high strength of individual filaments of glass and various advanced fiber materials, and 2) the ability of the matrix to arrest cracks originating from a broken filament. Thus, tensile failure in a practical, high-strength, fiber composite material occurs as a cumulative process, wherein dispersed regions of damage initiate, grow and coalesce or propagate to fracture. On the other hand, there are combinations of fiber and matrix materials in which an initial crack in a fiber will propagate through both phases and result in

composite fracture at relatively low stresses. These brittle, notch-sensitive materials tend to show a weakest link type of failure and generally are not desirable engineering materials.

The desirable ability of a composite to prevent fiber breaks from propagating can be achieved by the use of an appropriate matrix. In the case of Markite, the brittle matrix is not suitable for this purpose and the material may fracture due to crack propagation at low stress levels. Indeed, with the matrix and fiber having similar properties, the material approximates a ceramic with voids. Two approaches to overcoming this are suggested. They are both based upon the concept of isolating internal fractures.

In the first approach, attempts would be made to form the material into a space frame type configuration on the microscale. Thus, breaks in individual frame members would not propagate to others. In the second approach, interlocking bundles of fibers would be isolated to prevent propagation. Resistance to fracture would be provided by the "Chinese finger puzzle" effect as in the ADL-10 specimens which had been plate-slapped. Omniweave provides a natural method of approaching either of these two methods of enhancing strength. The previous section showed that for the space frame approach, additional fiber directions would be required. These are subjects for future research.

4.9 CONCLUDING REMARKS

The behaviour of a multidirectionally reinforced material can be extremely complex. However, in the case of Omniweave reinforcement, the regular orientation and the fact that the fibers are straight between surface points, makes it feasible to obtain an analytical understanding of the composite behavior. This fiber straightness is a vital aspect of the Omniweave concept. The fact that a high fiber volume fraction can be achieved even with rigid fibers (see Fig. 57) is a characteristic which is unique among the existing reinforcement concepts offering four or more fiber reinforcement directions. This highly structured geometry is responsible for good performance and care must be taken in the molding process to retain this geometry. It should be noted that this fiber straightness and high volume fraction can be obtained for a wide range of axial and transverse projected fiber angles.

The analytical model incorporated into the present MSC* MULTI computer program appears to utilize a reasonable definition of geometry, of effective elastic stiffnesses and thermal expansion coefficients, and of the failure criteria. Possible shortcomings in the model may result if the actual material has fibers which are not straight due to the molding process. This could account for the experimental modulus values being lower than theoretical. It is also possible that the admissible displacement field approach is causing the theoretical results to be higher than they should.

*Materials Sciences Corporation

Failure predictions indicate that the present ADL-10 material is not falling short of its potential for strength in the weaving direction. However, studies of loads applied in other directions indicate that higher unidirectional strength values are available depending upon the orientation of the finished material with respect to the load directions. The material, as presently used, has a high shear strength capability. Tests to confirm these expectations appear to be warranted.

Further improvements in the strength properties of ADL-10 are indicated if the Omniweave reinforcement is supplemented by additional fiber directions. Studies of the geometry have indicated the important fact that 5 and 6 directional configurations could be obtained by addition of fibers in a plane perpendicular to the weaving direction and at 45-degree angles to the surface of the woven material. Fibers introduced in these directions can yield high volume fractions without affecting fiber straightness. In contrast, introduction of radial fibers may result in either lower fiber volume fraction or a high degree of local fiber curvature.

A brief investigation of an all silica design suggests that reasonable strength values may be obtained from either a highly structured material or a material with weak interfaces. The former could be achieved by localization of the silica formed in situ, such that it is along the fiber bundles, leaving intermediate void regions. The latter would require keeping a weak coating material on the fiber surfaces. These suggestions are somewhat speculative, but it does appear that the concept of a ceramic matrix with voids is not a promising one.

In summary, the understanding of the material geometry and its influence upon mechanical properties has been enhanced. A reliable method of computing stiffness and strength is available. Suggested changes in internal geometry, as well as in the relative orientation of the material axes with respect to the load directions, appear to offer potential for improved performance of silica Omniweave materials with either plastic or ceramic matrices.

5.0 CONCLUSIONS AND RECOMMENDATIONS

5.1 CONCLUSIONS

1. A processing study has been completed to determine the effect of such variables as fiber etching, silane coupling and molding pressure on strength improvements of ADL-10, Omniweave silica/SR-350 silicone resin composite. The results are:
 - a. Ultimate tensile strengths on the level of 10,000 to 20,000 psi;
 - b. Hardening levels well in excess of 4000 taps for 1/4 to 3/8-inch nominal thickness as determined by magnetic flyer testing,
 - c. Unattenuated RF transmission at heat flux levels below 100 Btu/ft² sec.
2. The use of Teflon coated fibers and improvements in weaving methods have resulted in an increase of silica Omniweave fabric density to 1.10 gm/cc in the present study, as compared to densities as low as 0.4 in the previous work, described in Reference 1. Through the thickness fiber pitch angles of 45° have been realized in the woven fabric, resulting in nominal through thickness fiber pitch angles of 20 to 25° in the molded composite.
3. The Markite silica/silica Omniweave composites based on repeated pyrolysis and reimpregnation of the optimized ADL-10 system have failed to yield the desired improvements in mechanical strength and shock resistance. Although marginal (20 percent) improvements have been made in the strength of the fully pyrolyzed versions as a result of significant Omniweave fabric density increases, it is concluded that the present matrix/fiber interaction offers little promise of significant Markite strength and hardening improvements.
4. The approach to a possible near term improvement is suggested by results on a hybrid form of Markite, which is reimpregnated with a low density and viscosity SR-350 in a final treatment to give improved strength.
5. A capability analysis of the ADL-10 system, using the experimental results of this program and its predecessor, has concluded that the Omniweave composite fully realizes its theoretical capability level. In support of this analysis, measurements of the flexural and shear moduli and strength of the cured and molded resin were made. A set of filament wound unidirectional composites was also prepared and tested, verifying the ultimate strength level of the ADL-10 composite.

6. The Omniweave processing studies conducted on ADL-10 have shown that molding pressures must be chosen in accord with the woven fabric density so that the fibers are not crimped, making them unable to bear loads in the true composite mode. The analysis of Section 4 states a maximum optimum fiber volume fraction of 68 percent for conventional 4-D Omniweave. Fiber volume fractions as high as 78.7 percent were measured for 1000 psi molding pressure specimens which had lower strength than 60 - 70 percent fiber volume specimens produced at 125 psi. However ADL-10 produced from higher density silica Omniweave achieved higher strength levels for 1000 psi than for 125 psi molding pressure. The 1000 psi molding had 67 percent fiber volume fraction, compared to 60 percent for 125 psi.

The immediate conclusion is that multidirectionally reinforced composites must be produced with careful regard to maximum useful fiber volume fractions and density. Neither of these composite properties is a monotonic indication of composite strength.

5.2 RECOMMENDATIONS

1. Application of the ADL-10 hardened antenna window material to existing and developmental systems should be investigated in the near future. This effort must include careful preparation of a specification for the manufacturing process and a cost analysis.
2. Further development of ADL-10 is recommended in specialized geometries corresponding to the principal stress directions or reinforcement directions or ratios required by specific applications. Specifically, it is possible to weave standard 45-degree fiber axis angle Omniweave with a fiber projecting in the axial or length direction of the conventional flat "scarf". Seven dimensional constructions can also be made.
3. The near-term potential for a hybrid, reimpregnated Markite should be explored. This material would differ from the previous process in that a higher pyrolysis temperature would be used to completely remove lossy resin residue and increase the permeability to a final, low viscosity resin impregnation.
4. A basic study of the silica matrix-silica fiber interaction is required for improvement of the mechanical and hardening performance of Markite. The current GE-RESD studies of silica-silica and mullite-silica composites under NASA's Space Shuttle program and the availability of the scanning electron microscope facilities at GE/RADC used for the fiber studies described in this report give this approach an excellent outlook for success.

Silica CVD techniques also offer a versatile method for introduction of the silica matrix, although this method will probably be specialized to an early infiltration of the low density structure or a final surface deposition treatment.

5. The Omniweave processing studies conducted on ADL-10, specifically the molding pressure studies and subsequent investigation of the relationship to maximum useful fiber volume fractions, suggest that additional Omniweave composites should be examined for other applications in the light of this new process technology.

6.0 REFERENCES

1. Brazel, J. P. , "Hardened Antenna Window Materials -- Final Report", GE-RESD Report TIS 70SD713, September 1970
2. Markowitz, L. , "The Development of a Multidirectional Silica-Silicone Antenna Window", GE-RESD Report TDM 9131-006, August 24, 1970
3. Markowitz, L. , et al, "RF Transparent, Ablative Silica-Silicone Composite", Proceedings of the 10th Symposium on Electromagnetic Windows, Georgia Institute of Technology, July 29, 1970
4. Silane Coupling Agents, Brochure 03-028, Dow Corning Corporation
5. Place, T. M. , and Bridges, D. W. , "Fused Quartz-Reinforced Silica Composites for Radomes", Proceedings of the 10th Symposium on Electromagnetic Windows, Georgia Institute of Technology, July 29, 1970
6. Markowitz, L. , "Proposed Action Plan for the Development of a Hardened Antenna Window", GE-RESD Report, PIR 9131-455, January 8, 1971
7. Brazel, J. P. , "Advanced Hardened Antenna Window Material Study", Progress Report, General Electric Co. , 8 June 1971
8. "Ceramic Processing", Publication 1576, National Academy of Sciences, 1968
9. Natrella, M. G. , "Experimental Statistics", NBS Handbook #91, 1963
10. General Electric Co. Technical Information Series Document TIS 64SD252
11. Dow, N. F. and Rosen, B. W. , "Zero Thermal Expansion Composites of High Strength and Stiffness", NASA CR-1324, May 1969.
12. Stover, E. R. , "Improved Graphite Materials for Re-entry Vehicles", Technical Report AFML-TR-69-67, Vol. III. General Electric Company, April, 1970.
13. Edighoffer, H. H. , "Thermoelastic Analysis of Fibrous Composites with Fibers in Four Directions Symmetric with the Composite Coordinate System (Orniweave) using the OMNI Computer Code, GE TM 9335-RF3-0017, 1969
14. Hashin, Z. and Rosen, B. W. , "Elastic Moduli of Fiber Reinforced Materials", J. of Appl. Mech. , June 1964.
15. Tanzilli, R. , "Development of An External Ceramic Insulation for the Space Shuttle Orbiter", NASA CR-112038, Contract Number 1-10533, April 1972

APPENDIX: INDEX OF TABULATED CHARACTERIZATION AND MECHANICAL
PROPERTIES, ADL-10 AND MARKITE

| Material | Characterization Table | Sampling Plan | Mechanical Properties |
|---|--|------------------------------------|-------------------------------------|
| Phase I - woven silica Omniweave "fingers" | Table 1, pg. 2-10 Table 2, pg. 2-10 | Figure 12, pg. 3-2 | ----- |
| Series 1, ADL-10 | Table 3, pg. 2-12 | Table 3, pg. 2-12 | Table 16, pg. 3-33 |
| Series 2, ADL-10 | Table 5, pg. 2-22 | Table 6, pg. 2-25 | Table 17, pg. 3-36 |
| Phase II - silica Omni- weave "scarves" | Table 8, pg. 2-29 | Figure 13, pg. 3-4 | ----- |
| ADL-10 panel 331-1 | Table 9, pg. 2-30 | Figure 22, pg. 3-15 | Table 18 and 19, pgs. 3-36 and 3-43 |
| 331-2 | Table 9, pg. 2-30 | Figure 24, pg. 3-17 | Table 18 and 19, pgs. 3-36 and 3-43 |
| 331-3 | Table 9, pg. 2-30 | (Full panel submitted to AMMRC) | No mechanical testing |
| Markite panel 318-1 | Table 10, pg. 2-33 | ----- | No mechanical testing |
| 318-2 | Table 10, pg. 2-33 | Figure 28, pg. 3-22 | Table 24, pg. 3-51 |
| 318-3 | Table 10, pg. 2-33 | Figure 30, pg. 3-24 | Table 23, 24, pg. 3-50, 51, |
| 318-4 | Table 10, pg. 2-33 | Figure 32, pg. 3-26 | Table 24, pg. 3-51 |
| Markite panel 319-1 | Table 11, pg. 2-37 | Figure 34, pg. 3-28 | Tables 23, 24, pg. 3-50, 51 |
| 319-2 | Table 11, pg. 2-37 | Figure 35, pg. 3-29 | Tables 23, 24, pgs. 3-50, 51 |
| Markite panel 209-3 | Table 14, pg. 2-41 | Figure 36, pg. 3-30 | Table 25, pg. 3-53 |
| ADL-10 Unidirectional Composite | Table 13, pg. 2-44 | ----- | Table 22, pg. 3-47 |
| SR-350 Molded, Cured | Section 2.5,6, pg. 2-41 | Figure 12, pg. 3-2 | Table 20, pg. 3-45 |